Investigating Mechanisms of Pain in Alzheimer's Disease

Aman, Yahyah

Awarding institution:
King's College London

INVESTIGATING MECHANISMS OF PAIN IN ALZHEIMER'S DISEASE

Yahyah Aman

Thesis submitted for the degree of
Doctor of Philosophy at King's College London

2017

Wolfson Centre for Age Related Diseases
Institute of Psychiatry, Psychology and Neuroscience
King's College London

Declaration

I hereby declare that all the work presented in this thesis is a result of my own research and has not been accepted for any other degree. Contributions from anyone else have been clearly stated throughout the text.

Abstract

Experience of pain is a key contributor to challenge of care in Alzheimer's disease (AD) individuals and is often associated with age-related medical comorbidities, commonly musculoskeletal conditions such as osteoarthritis (OA). Significant alteration in perception of pain is an important clinical issue in patients with AD and its effective treatment is increasingly recognised as a critical unmet clinical need. Currently, management of pain has been hindered by difficulties in the assessment of pain partly due to the impaired ability to communicate sensations as well as the inadequate understanding of the underlying mechanisms of pain in this susceptible patient group. Animal models of AD recapitulate many of the clinical and pathological features of the human AD and thereby offer to be a powerful tool in order to delineate mechanisms in AD. This thesis aims to investigate possible alterations of nociceptive sensitivity, in acute and chronic pain models, using the transgenic double-mutant APPswe×PS1.M146V (TASTPM) mouse model of AD. Furthermore, it aims to elucidate the associated plastic changes along the pain pathway (i.e. spinal cord and thalamus) of the preclinical TASTPM model and evaluate its translational implication using human post-mortem tissue obtained from AD patients with chronic pain conditions.

This thesis provides preclinical evidence for alterations in nocifensive behaviour that are associated with dysfunction of the opioidergic system in TASTPM mice compared to age- and gender-matched wild-type (WT) controls. Specifically, TASTPM mice display reduced sensitivity to acute noxious thermal stimulation and impaired persistent pain-like behaviour in a model of OA induced by an intra-articular administration of monosodium iodoacetate (MIA). These changes coincide with impairment of cognition, development of amyloid plaques in the brain, and intraneuronal accumulation of amyloid precursor protein/β-amyloid (APP/Aβ) in the spinal cord of TASTPM mice. Increase in expression of endogenous inhibitory peptides: enkephalins in the dorsal horn and β-endorphins in plasma correlate with the attenuated nociceptive sensitivity to noxious thermal stimulation and persistent pain, respectively, in TASTPM mice. Administration of naloxone, an opioid antagonist, re-establishes normal sensory thermal thresholds and unmasks the reduced MIA-induced mechanical allodynia exhibited by the

TASTPM mice. Subsequent administration of the analgesic morphine, an opioid agonist, induces heightened responsiveness in the TASTPM mice compared to WT controls. Together, these findings implicate the disruption of the opioidergic system as a common mechanism underlying the reduced acute nocifensive and impaired persistent pain-like behaviour in TASTPM model of AD.

In parallel to these observations, alteration in the neuro-immune plasticity along the pain pathway is also identified as a possible mechanism that underlies impaired persistent pain-like behaviour exhibited by AD mice. In particular, diminished spinal microgliosis in response MIA administration in the periphery coupled to inability of gabapentin to induce analgesia were evident in TASTPM. These data indicate blunted central sensitisation in the model of AD.

Intriguingly, increase in the extent of neuroinflammation is observed in the thalamus of TASTPM mice compared to WT, in the model of OA. However, no change in APP/Aβ pathology was detected in both the spinal cord and brain of TASTPM mice.

Analyses of human post-mortem tissue obtained from AD individuals lend support to preclinical observations in TASTPM mice of intraneuronal accumulation of APP/Aβ and amyloid plaque deposition in the spinal cord. The other pathological hallmark of AD, neurofibrillary tangles (NFT), was not detected in the spinal cord of AD patients. Assessment of supraspinal structures involved in pain processing, including the thalamus, reveal presence of both amyloid plaques and NFT, which increased in abundance with progression of AD. Moreover, evaluation of AD-associated pathology in AD individuals with a clinical history of chronic pain and/or persistent analgesic use displays no alteration in deposition of amyloid plaques and NFT. However, increase in microglial activation was observed in both the spinal cord and supraspinal regions compared to AD subjects with no clinical pain record. These data provide additional support for the exacerbation of ongoing neuroinflammation identified in the preclinical TASTPM mice in a model of OA. Such observations from human post-mortem tissue reinforce the advantage of utilising the TASTPM model of AD in order to delineate mechanisms of pain in AD as it recapitulates some of the key features that are observed in human AD patients.

Taken together, the findings of this thesis have important clinical implications for the care of patients with AD who have deteriorating cognitive function along with reduced sensitivity to pain.

Altered pain sensitivity could be considered in assessing clinical risk as it may be associated with neuropsychiatric symptoms as well as an increased risk of injury during daily routine activities. Finally, these data highlight the need to re-evaluate current treatments, such as opioids, or develop novel therapeutic strategies for management of pain in individuals with AD.

Acknowledgements

Firstly, I would like to thank my primary supervisor Professor Marzia Malcangio for providing me with the opportunity to take on this exciting project and for her generous support, guidance and encouragement throughout the past four years. I am truly honoured and privileged to have worked under her supervision. I also greatly appreciate the invaluable additional support, guidance and input of my secondary supervisor Professor Clive Ballard throughout the PhD.

I am also thankful to Professor Paul Francis for his keen interest in the project proceeding and guidance with human post-mortem tissue application. I'd also like to thank the King's College London Brain Bank, Dr. Claire Troakes and acknowledge the donors and their families for their generosity, which has made this project possible. Thank you also to Dr. David Howlett for his help and advice on human brain tissue histology, Professor Lawrence Bannister for his guidance with identification of human thalamic nuclei and Mary Johnson for carrying out semi-quantitative neuropathological analysis.

I would like to thank all members of the Malcangio Lab, past and present, for providing an enjoyable research environment as well as contributing to my learning experience in the laboratory. A special thanks to Thomas Pitcher for his patience and guidance with mouse behavioural tests, injections, and perfusions; and Dr. Raffaele Simeoli for his much appreciated guidance with RT-PCR and western-blots. I am greatly thankful to Dr. Anna Clark, Dr. Rie Rikki Hansen, Dr. Elizabeth Old, and Dr. Francisco Nieto who have expertly guided me through most of techniques in the lab. I am also very grateful for the friendly research environment and support provided by Dr. João Sousa-Valente, Dr. Karli Montague, Keshi Chung, Kelly Wood and Benjamin Allen.

I must also thank the past and present members of the Wolfson CARD who have made this journey a great experience. Sincere thanks to Carl Hobbs for his expert advice and guidance with histological techniques and Clive Gentry for the intra-articular injection demonstrations. I am also very grateful to Dr. Martin Broadstock and Dr. Alyma Somani for providing guidance with TASTPM genotyping.

I would also like to thank Medical Research Council (MRC) for funding this PhD; GlaxoSmithKline (GSK) for kindly providing the TASTPM mice; and Alzheimer's Research United Kingdom (ARUK) King's College Network Centre for financially supporting the human post-mortem study.

Finally, I would like to thank my family for their unconditional support and encouragement to achieve my career and life goals. Without the prayers and blessing of my parents this may not have been possible. Last but most importantly, I would like to thank God for His grace blessings in every aspect of life.

Table of Contents

Table of Figures

Table of Tables

Abbreviations

5-HT	5-Hydroxytryptamine or Serotonin
ACC	Anterior Cingulate Cortex
ACh	Acetylcholine
AD	Alzheimer's disease
AICD	Amyloid Precursor Protein Intracellular Domain
AMG	Amygdala
AMPA	α-Amino-3-Hydroxy-5-Methyl-4-Isoxazole Propionic Acid
Aph-1	Anterior Pharynx Defective 1
ApoE	Apolipoprotein E
APP	Amyloid Precursor Protein
APS	Abbey Pain Scale
ATF-3	Activating Transcription Factor-3
ATP	Adenosine Triphosphate
AUC	Area Under Curve
Aβ	β-Amyloid
BBB	Blood Brain Barrier
BDNF	Brain Derived Neurotrophic Factor
BPSD	Behavioural and Psychological Symptoms of Dementia
BSA	Bovine Serum Albumin
Ca^{2+}	Calcium Ion
CAA	Cerebral Amyloid Angiopathy
cAMP	Cyclic Adenosine Monophosphate
Cat(D or S)	Cathepsin (D or S)
CCI	Chronic Constriction Injury
CDK-5	Cyclin-Dependent Kinase 5

CERAD	Consortium to Establish a Registry for Alzheimer's disease
CFA	Complete Freud's Adjuvant
CGRP	Calcitonin Gene Related Peptide
ChAT	Choline Acetyltransferase
CMAI	Cohen-Mansfield Agitation Inventory
CNS	Central Nervous System
COX	Cyclooxygenase
CRH	Corticotroponin-Releasing Hormone
CSF	Cerebrospinal Fluid
CSF1(R)	Colony Stimulating Factor 1 (Receptor)
CTF	C-Terminus Fragment
DAB	3, 3'-Diaminobenzidine
DAPI	4',6-Diamidino-2-Phenylindole·2HCl
DNIC	Diffuse Noxious Inhibitory Control
DPX	Dibutylphthalate Xylene
DRG	Dorsal Root Ganglion
DRN	Dorsal Raphe Nucleus
D-ser	D-Serine
DSM-IV	Diagnostic and Statistical Manual of Mental Disorders-IV
EGF	Epidermal Growth Factor
EIA	Enzyme Immuno-Assay
ENK	Enkephalins
EOAD	Early-Onset Alzheimer's disease
EPSP	Excitatory Post-Synaptic Potentials
ERK	Extracellular Signal-Related Kinase
FDG	Fluorodeoxyglucose

FKN	Fraktalkine
fMRI	Functional Magnetic Resonance Imaging
FTD	Frontotemporal Lobe Dementia
GABA	Gamma-Amino Butyric Acid
GAD	Glutamate Decarboxylase
GDNF	Glial Derived Neurotrophic Factor
GFAP	Glial Fibrillary Acidic Protein
GlyT	Glycine Transporter
GPCR	G Protein-Coupled Receptor
GSH	Glutathione
GSK-3	Glycogen Synthase Kinase 3
H&E	Haematoxylin and Eosin
H^+	Proton
H_2O_2	Hydrogen Peroxide
hAPP	Human Amyloid Precursor Protein
HIER	Heat-Induced Epitope Retrieval
HRP	Horseradish Peroxidase
IASP	International Association for the Study of Pain
IB4	Isolectin B4
IBA1	Ionized Calcium-Binding Adaptor Molecule-1
IDE	Insulin-Degrading Enzyme
IL	Interleukin
iNOS	Inducible Nitric Oxide Synthase
INS	Insula
JNK	Jun N-terminal Kinase
KCC2	Potassium Chloride Co-Transporter 2

KCN	Potassium Ion Channel
LB&E	Luxol Fast Blue and Eosin
LC	Locus Coeruleus
LDCV	Large Dense Core Vesicles
LOAD	Late-Onset Alzheimer’s disease
LTP	Long Term Potentiation
MAO	Monoamine Oxidase
MAPK	Mitogen-Activated Protein Kinase
MAPT	Microtubule-Associated Protein Tau
MCI	Mild Cognitive Impairment
Mg^{2+}	Magnesium Ion
mGluR	Metabotropic Glutamate Receptor
MHC II	Major Histocompatibility Complex II
MHPG	3-Methoxy-4-Hydroxyphenylgycol
MIA	Monosodium Iodoacetate
MMP	Matrix Metalloproteinases
MMSE	Mini Mental State Examination
MrgD	Mas-Related G protein-Coupled Receptor Subtype D
MRI	Magnetic Resonance Imaging
NA	Noradrenaline
NBM	Nucleus Basalis of Meynert
NF200	Neurofilament 200
NFT	Neurofibrillary Tangle
NGF	Nerve growth factor
NIA-AA	National Institute on Aging-Alzheimer's Association
NINCDS-ADRDA	National Institute of Neurological and Communicative Disorders and Stroke/AD and Related Disorders Association

NK1(R)	Neurokinin 1 (Receptor)
NMDA	N-Methyl-D Aspartate
NO	Nitric Oxide
NP	Neuritic/Senile Plaque
NPI	Neuropsychiatric Inventory
NRM	Nucleus Raphe Magnus
NSAID	Non-Steroidal Anti-Inflammatory Drugs
OA	Osteoarthritis
OCT	Optimum Cutting Temperature
OR	Opioid Receptor
PAG	Periaqueductal Grey
PAINAD	Pain Assessment In Advanced Dementia Scale
PB	Phosphate Buffer
PbN	Parabrachial Nucleus
PBS	Phosphate-Buffered Saline
PCR	Polymerase Chain Reaction
Pen-2	Presenilin Enhancer 2
PENK	Proenkephalin
PET	Positron Emission Tomography
PFA	Paraformaldehyde
PFC	Prefrontal Cortex
PG	Prostaglandin
PHF	Paired Helical Filaments
PI3K	Phosphoinositol-3-Kinase
PK(A or C)	Protein Kinase (A or C)
PMD	Post-Mortem Delay

PNL	Partial Nerve Ligation
POMC	Proopiomelanocortin
P-p38	Phosphorylated p38 MAPK
pPENK	Pre-Proenkephalin
PS	Presenilin
PWT	Paw Withdrawal Threshold
ROS	Reactive Oxygen Species
RVM	Rostral Ventromedial Medulla
S1	Primary Somatosensory Cortex
S100β	S100 Calcium-Binding Protein β
sAPP	Soluble APP
SD	Standard Deviation
SDS-PAGE	Sodium Dodecyl Sulfate Polyacrylamide Gel Electrophoresis
SEM	Standard Error Mean
SNI	Spared Nerve Injury
SNL	Spinal Nerve Ligation
SNpc	Substantia Nigra Pars Compacta
SP	Substance P
SSV	Small Synaptic Vesicle
TBS	Tris-Buffered Saline
TBS-T	TBS-Tween 20
TGFβ	Transforming Growth Factor β
TH	Thalamus
Thy-1	Thymocyte Differentiation Antigen 1
TLR	Toll-Like Receptor
TNFα	Tumour Necrosis Factor α

TrK(A or B)	Tropomyosin Receptor Kinase (A or B)
TRP	Transient Receptor Potential Ion Channel
TSPO	Mitochondrial Translocator Protein
VGAT	Vesicular GABA Transporter
VGLUT	Vesicular Glutamate Transporter
VL	Ventral Lateral Nucleus of the Thalamus
VPL	Ventral Posterior Lateral Nucleus of the Thalamus
WDR	Wide Dynamic Range
WOMAC	Western Ontario and McMaster Universities Osteoarthritis Index
WT	Wild-type

Publications Arising from this Thesis

Published Abstracts

Aman Y, Ballard C, Malcangio M. (2015). The development of osteoarthritis pain in a model of Alzheimer's disease. 9th Congress of the European Pain Federation, EFIC 2015, Vienna, Austria, 2-5 September 2015; EFIC5-1228.

Published Papers

Aman Y, Pitcher T, Simeoli R, Ballard C, Malcangio M. (2016). Reduced thermal sensitivity and increased opioidergic tone in the TASTPM mouse model of Alzheimer's disease. Pain 157: 2285-96.

Chapter 1 General Introduction

1.1 Chapter Overview

The present chapter is set out to initially provide an overview of the current theories and mechanisms of pain, starting with a description of what pain is and how it can be defined. For this purpose, the structure of the nervous system is outlined with respect to detection and transmission of painful sensations. The integration and processing of sensory input within the central nervous system (CNS), including the modulation of pain within the spinal cord and the brain, is described. Chronic pain is a persistent debilitating condition. The theories of pain that propose mechanisms by which processing of pain may be altered during this maladaptive pathophysiological state are explored.

In the quest to investigate the perception of pain in Alzheimer's disease (AD), an outline of key principles and concepts of AD are subsequently provided, including a description of the major clinical features and cardinal pathological hallmarks of the disease. In turn, the impact of these clinical manifestations on the prevalence and diagnosis of pain in this patient group, is highlighted. Furthermore, a literature review is conducted for the clinical experimental evidence of pain in patients with AD. Finally, an overview of the impact of AD-associated neuropathology on processing of pain in AD is provided, which leads to the hypothesis and key aims of the work presented in this thesis.

1.2 Pain - An In-Built Biological Warning System

Pain is a subjective and multidimensional sensory and emotional experience in response to an actual or potential threat to the integrity of the body. It is a result of complex interactions between physiological, psychological (emotional and cognitive) and social processes (Wall 1979). The International Association for the Study of Pain (IASP) defines pain as "an unpleasant sensory and emotional experience associated with actual or potential tissue damage, or described in terms of such damage" (www.iasp-pain.org). This definition incorporates some key aspects of nature of pain in the form of psychological emotional (unpleasant) responses to the physiological sensation of noxious or potentially noxious stimuli.

Pain often acts as a protective mechanism that promotes survival in a hostile and dangerous environment, which can be described as nociceptive, inflammatory or neuropathic in nature

(Woolf 2010). It encourages recuperative behaviours that persist as long as the noxious stimuli or tissue damage is present and resolves with healing of the injury or damage. However, in some cases, following repair of injury, pain persists and becomes chronic in the absence of tissue damage stimuli, understanding of which remains elusive (Basbaum et al 2009). Pain is a personal experience that is influenced by cultural values, appraisal of situation, attention/awareness and other psychological components. Therefore, the pain process does not simply arise following sensory noxious stimulation eliciting a neural response; but it is a multifaceted experience whereby the disease/injury induced neural signals that enter the nervous system with learned behaviours concerning the experience of pain, culture, and a host of environmental and personal factors (Melzack & Katz 2013). The active nervous system influences the integration and interpretation of the sensory neural input, which results in a subjective and multidimensional experience of pain.

1.2.1 Physiological Pain

The somatosensory system conveys sensory information, in response to stimuli from the periphery, to the CNS where pain is perceived. Physiological pain is a useful adaptive response of an organism, which acts as an early-warning system for self-protection that promotes survival in a hostile and dangerous environment and encourages recuperative behaviours in response to pain (Woolf 2000, Woolf 2010). Loss of this protective mechanism, in individuals suffering from a congenital inability to perceive pain, has a considerable physical consequence and interferes with the quality of life. Under physiological conditions, nociception provides a critical protective mechanism that will only persist as long as the noxious stimulus or tissue damage is present, which resolves with healing of the injury or damage. Therefore despite the unpleasant nature of pain sensation, an intact pain system is important for the survival and wellbeing of the individual (Basbaum et al 2009, Kwon et al 2014).

1.2.1.1 **Pain Signalling**

The sensory messages arising from the detection of sensory signals/stimuli in the periphery are transmitted to the spinal cord by primary afferent fibres of highly specialised pseudo-unipolar sensory neurons with cell bodies located within the dorsal root ganglion (DRG) (Cordero-Erausquin et al 2016). Sensory neurons extend one axon to innervate a peripheral target (i.e.

skin, muscle and joint), whilst the second axon is projected towards the CNS in order to innervate second order neurons in the dorsal horn of the spinal cord (Dubin & Patapoutian 2010). The peripheral terminals of the sensory neurons represent the site of transduction in response to innocuous (i.e. light touch) and noxious (i.e. mechanical, thermal, chemical and electrical) stimuli. In order to convey this broad range of sensory information, the primary afferent fibres represent a heterogeneous population that can broadly be classified based on their anatomical and electrophysiological characteristics into three populations: A-beta fibres, A-delta (Aδ) fibres and C-fibres. Nociceptive information is conveyed from the periphery to the CNS via activation of specialised sensory neurons, known as nociceptors, in response to noxious stimuli that may potentially induce tissue damage. These primary afferent populations are constituted of thinly myelinated Aδ and unmyelinated C-fibres free nerve endings. This system works in parallel to the input of innocuous information transmitted by myelinated A-beta fibres. Sensory input to the spinal cord is integrated, modified and amplified before it is propagated to specific brain regions via various ascending pathways, as illustrated in Figure 1.1A (Basbaum et al 2009, Le Pichon & Chesler 2014, Todd 2017).

1.2.1.2 **Primary Afferent Fibres and Sensory Neurons**

A-beta primary afferent are large in diameter (> 10 μm) that predominantly possess thickly myelinated fibres which exhibit rapid conduction velocities (30 - 100 ms^{-1} in rodents) and low activation thresholds. These fibres are characterised by encapsulated peripheral nerve-endings, which principally respond to low-threshold innocuous mechanical stimuli (i.e. light touch), thereby these neurons are known as low-threshold mechanoreceptors. In comparison Aδ primary afferents are relatively smaller in size (> 2 - 6 μm) with fibres that are thinly myelinated which underlies the slower conduction velocities (5 - 30 ms^{-1} in rodents, cats and monkeys), and also possess a high activation threshold; thereby expanding their capacity to convey non-nociceptive but predominantly transduce noxious nociceptive sensory information (Abraira & Ginty 2013, Dubin & Patapoutian 2010, Le Pichon & Chesler 2014, Millan 1999, Rindos et al 1984). Aδ fibres convey well localised first and/or fast pain; and can broadly be classified as Type I and Type II which transduce first pain provoked by pinprick (noxious mechanical stimulation) and noxious heat, respectively (Basbaum et al 2009). All A-fibres can be

immunohistochemically identified using neurofilament 200 (NF200) as a marker. Whilst both A-beta and Aδ fibres terminate in deep dorsal horn laminae (III - VI), a sub-population of Aδ fibres have terminations in the superficial dorsal horn (laminae I - II) (D'Mello & Dickenson 2008, Le Pichon & Chesler 2014, Todd 2002). Finally, C-fibres represent the small-diameter unmyelinated fibres (0.2 - 1.4 µm) that display very slow conduction velocities (0.5 - 2 ms^{-1} in rodents, cats, monkeys and human) and possess high activation thresholds that respond predominantly to noxious stimuli (Dubin & Patapoutian 2010, Le Pichon & Chesler 2014, Millan 1999, Rindos et al 1984). Overview of the primary afferent fibres and their central terminals are illustrated in Figure 1.1B and C.

High-threshold C-fibres can be further classified into peptidergic and non-peptidergic based on their expression of neuropeptides. Peptidergic C-fibres express neuropeptides (i.e. substance P (SP) and calcitonin gene related peptide (CGRP)), ion channels (i.e. transient receptor potential cation channel subfamily V member 1 (TRPV1)), as well as tropomyosin receptor kinase A (TrkA) receptor that respond to nerve growth factor (NGF); and project to lamina I and the outer lamina II (IIo). In contrast, non-peptidergic C-fibres terminate in the inner lamina II (IIi) of the spinal cord dorsal horn and expresses cRET receptor that responds to glial derived neurotrophic factor (GDNF) which can be identified by the binding of isolectin B4 (IB4) and expresses Mas-related G protein-coupled receptor subtype D (MrgD); as well as the purinergic receptor subtype, $P2X_3$ (Basbaum et al 2009, Beaudry et al 2017, D'Mello & Dickenson 2008, Peirs & Seal 2016). Studies have delineated the functional outcome of the two sub-population of high-thresholds C-fibres, as selective ablation of MrgD reduced acute nocifensive behaviour and persistent mechanical hypersensitivity, whilst having no effect of thermal sensitivity, implicating the role of non-peptidergic fibres in mechanical sensitivity (Cavanaugh et al 2009). Similarly, ablation of CGRP-selective sub-population of C-fibres, which overlaps with TRPV1, resulted in pronounced loss of heat sensitivity but no alteration in mechanical sensations, indicating role of peptidergic sup-population of C-fibres in thermal sensitivity (McCoy et al 2013). Recent evidence from an optogenetic study further strengthens these functional activities through transdermal blue light stimulation of the hind paws of transgenic mice expressing opsin channelrhodopsin-2 in TRPV1 (peptidergic) or MrgD neurons (non-peptidergic), which

generated nocifensive behaviours consisting mainly of paw withdrawal and paw licking (thermal) in the former; with the latter displaying mostly withdrawal and lifting (mechanical) (Beaudry et al 2017).

Another distinct population is the non-nociceptive C-fibres, which respond to innocuous stimuli and can also be categorised into two groups, namely the low threshold mechanoreceptors and cold-sensitive fibres. Low threshold mechanoreceptors express vesicular glutamate transporter 3 (VGLUT3), cRet, as well as and the enzyme tyrosine hydroxylase, which terminate in lateral two-thirds of spinal dorsal horn lamina IIi (Li et al 2011, Seal et al 2009). This subset of C-fibres has been demonstrated to be important in the development and maintenance neuropathic and inflammatory pain (will be discussed below in Section 1.2.2), as demonstrated by profound and selective loss of mechanical hypersensitivity induced by nerve injury and inflammation in VGLUT3 knock-out mice. However, no alteration to acute nociceptive thresholds in response to thermal or mechanical stimulation were evident (Seal et al 2009). Whereas, the cold-sensitive fibres express TRPM8 channel, which can be activated by cooling and menthol; and project to lamina I of the spinal dorsal horn. TRPM8 has been demonstrated to a be critical transducer of innocuous cooling as genetic depletion of the channel resulted in partial avoidance of cold temperatures, whereas selective ablation of TRPM8-expressing cells completely prevented noxious cold sensitivity (Knowlton et al 2013).

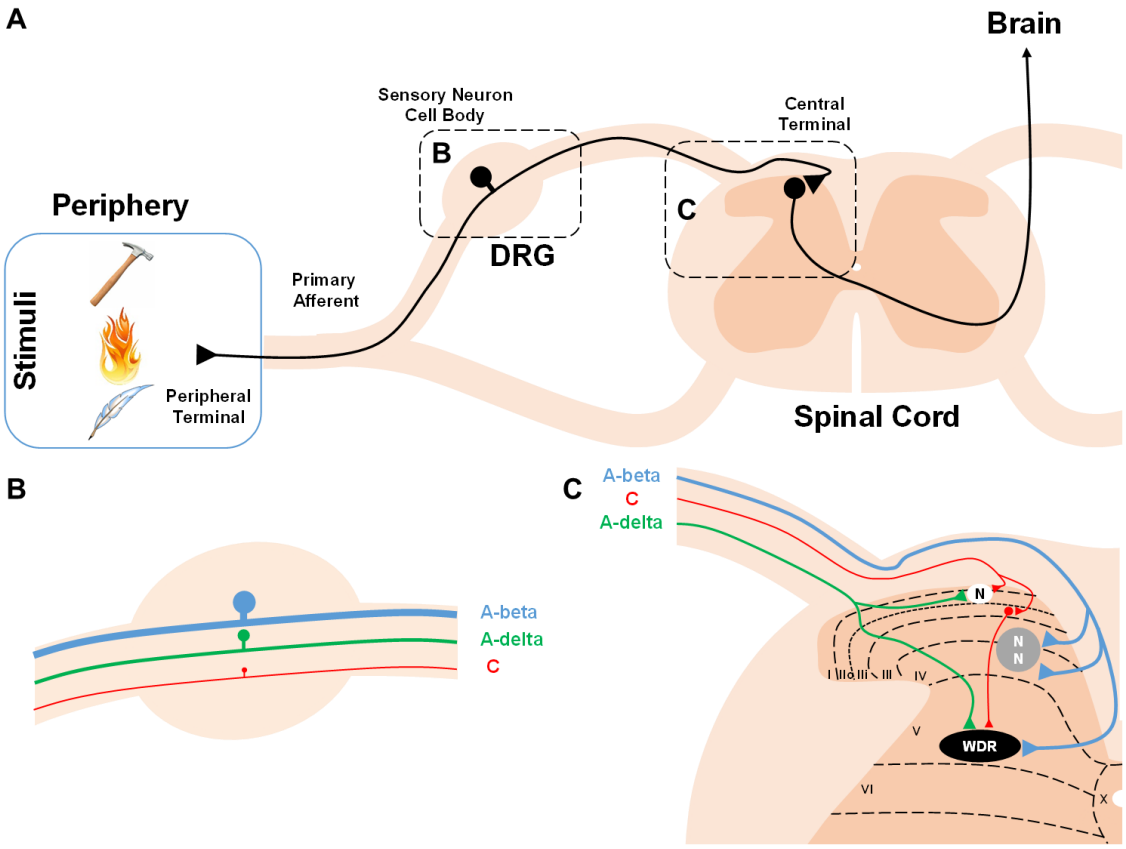

Figure 1.1: A Simplified Schematic of Primary Afferent Populations and their Central Terminals

(A) The primary afferent neurons are pseudo-unipolar in nature, with the cell body located within the dorsal root ganglion (DRG) that extends one axon to the periphery and the second directed towards the spinal cord in the central nervous system (CNS). Primary afferent fibres, in response to a stimulus, transmit signals from the periphery, through the DRG to the dorsal horn, which in turn propagates the sensory input to the supraspinal spinal structures via various ascending pathways. (B) Cell bodies of primary sensory fibres are located within the DRG. A-beta (blue) exhibit large-sized cell soma and thickly myelinated fibres; in comparison A-delta (green) are the medium-sized DRG neurons with thinly myelinated fibres; and finally, C-fibres (red) display the small-sized population of DRG neurons with unmyelinated fibres. (C) A-beta and A-delta fibres terminate in deep laminae (III - V) where they synapse onto wide-dynamic range (WDR) neurons and the former synapsing onto non-nociceptive (NN) neurons. A-delta fibres also have terminations in the superficial laminae (I - II), where along with C-fibres, they can synapse onto nociceptive-specific (N) neurons. Figure adapted from D'Mello and Dickenson (2008).

1.2.1.3 **Spinal Cord Processing of Sensory Input**

1.2.1.3.1 Sensory Input from Periphery to the Central Nervous System

Sensory information from the periphery is relayed to the spinal cord, via sensory neurons, where their central terminals synapse with second order dorsal horn neurons. The grey matter of the spinal cord is organised into ten laminae according to the size, density and pattern of

neurons (Rexed 1952). Neurons in the spinal cord are accompanied by non-neuronal glial cells (i.e. astrocytes and microglia). Under physiological conditions glial cells are involved in maintenance of homeostasis in the spinal cord, in principle by providing structural and metabolic support (astrocytes) and performing immune surveillance roles (microglia). However, mounting evidence have implicated a key role it may play in modulation of nociceptive signalling under pathophysiological conditions (Basbaum et al 2009, Ji et al 2013, Ji et al 2014).

The dorsal horn, which is involved in sensory processing, consists of laminae I-VI; with laminae VII-IX making up the ventral horn that is involved in motor signalling, and lamina X surrounding the central canal. Dorsal horn neurons can be divided into two major groups: those with axons ascending to the brain (projection neurons) and those with axons that remain in the dorsal horn (interneurons). The majority of intrinsic dorsal horn neurons are interneurons, with axons that remain in the spinal cord and branches that terminate locally (Todd 2017). Interneurons can be electrophysiologically and/or immunohistochemically classified as excitatory (glutamatergic) or inhibitory (mainly gamma-amino butyric acid (GABA)-ergic) in nature (Todd 2010, Todd 2017).

Neurons in lamina I (marginal layer) and II (substantia gelatinosa) predominantly receive sensory input from nociceptive primary afferent neurons, and therefore are characterised as nociceptive-specific cells (D'Mello & Dickenson 2008). Laminae I-II (superficial dorsal horn) consist of mainly local interneurons (virtually all neurons in lamina II and ~90% - 95% of lamina I neurons) with projection neurons only evident in the marginal layer. Approximately 25%- 55% of lamina I-II neurons in rodents belong to the inhibitory subpopulation of neurons, as illustrated by expression of GABAergic marker; based upon which it has been postulated the remaining population of neurons are glutamatergic (i.e. excitatory interneurons and projection neurons) within the superficial dorsal horn laminae (Todd 2017). Non-nociceptive primary input via A-beta fibres is directed towards neurons in the deeper laminae, III to VI, which mainly contain interneurons that are relatively larger in size to those located in in the superficial dorsal horn (Todd 2002). Finally, wide dynamic range (WDR) neurons located in deeper laminae (mainly lamina V) receive convergent innocuous and noxious sensory input from monosynaptic A-fibres and polysynaptic C-fibres enabling it to respond to a broad range of stimuli including mechanical, thermal, and chemical stimulation (D'Mello & Dickenson 2008).

1.2.1.3.2 Primary Afferent Terminals Cross-Talk in the Spinal Cord

In order to effectively communicate sensory nociceptive information, the action potential mediated electrical activity generated by the primary afferent terminal in response to a noxious stimulus in the periphery must be transferred to post-synaptic second-order dorsal horn neuron. The synaptic structures formed between pre-synaptic central terminals of primary afferent neurons and post-synaptic second-order dorsal horn neurons are specialised for intercellular communication. In the pre-synaptic neuron (primary afferent terminal) electrical activity is converted into the release of chemical signalling molecules (neurotransmitters) which in turn activate receptor proteins expressed by post-synaptic neuron (second-order dorsal horn neuron) in order to mediate a response. The primary afferent terminals contain a vast array of neurotransmitters including: amino acids (glutamate), neuropeptides (CGRP and SP), neurotrophic factors (brain-derived neurotrophic factor, BDNF) as well as small molecules such as adenosine triphosphate (ATP). The release of neurotransmitters into the synaptic cleft is mediated by exocytosis of vesicles from the pre-synaptic membrane (Dubin & Patapoutian 2010).

The amino acid glutamate is the predominant excitatory neurotransmitter in the CNS and is expressed in all primary afferent sensory neuron terminals. It is stored in small synaptic vesicles (SSVs) at the active zone of pre-synaptic terminals, and release via exocytosis mediated by an increase in intracellular calcium levels in response to membrane depolarisation (Merighi et al 1991, Niciu et al 2012). The excitatory effect of glutamate is exerted by activation of glutamate receptors expressed by post-synaptic neuronal membrane that include the ionotrophic N-methyl-D aspartate (NMDA), α-amino-3-hydroxy-5-methyl-4-isoxazole propionic acid (AMPA), and kainate receptors; as well as the metabotropic glutamate receptors (mGluR). AMPA and NMDA receptors predominantly contribute to the excitatory transmission in the spinal cord; with the AMPA receptors responsible for the majority of glutamate mediated monosynaptic rapid transmission; whilst NMDA receptors mainly play a role in synaptic plasticity (Larsson & Broman 2011, Osikowicz et al 2013). Electrical activity, in response to a noxious stimulus in the periphery, induces increase in calcium influx, which triggers rapid release of glutamate from the central pre-synaptic terminals of primary afferent neurons into the synaptic cleft; where it binds

to and activates AMPA receptors on the post-synaptic second-order dorsal horn neurons eliciting sodium influx-mediated depolarisation referred to as excitatory post-synaptic potentials (EPSPs). Although NMDA receptors are also present on the post-synaptic membrane, they contribute little to the generation of EPSPs as these receptors are tonically blocked by a magnesium (Mg^{2+}) ion under physiological conditions. Therefore, activation of the NMDA receptor requires sustained membrane depolarisation in order to remove the Mg^{2+} ion plug, which underlies the rare contribution of this receptor subset in basal neurotransmission. Upon NMDA receptor activation by glutamate, there is an influx of Ca^{2+} ions, which causes post-synaptic depolarisation as well as activation of signalling molecules such as calcium/calmodulin dependent intracellular signalling pathway which contributes to long term potentiation and central sensitisation (Bleakman et al 2006, Niciu et al 2012, Zhuo 2017).

A sub-population of C-fibres, the peptidergic, co-expresses a range of neuropeptides (i.e. SP and CGRP) with glutamate. These neuropeptides are packaged into large dense core vesicles (LDCVs) which are stored away from the pre-synaptic primary afferent active zone which underlies the delayed release in comparison to SSVs (Merighi et al 1991). Release of SP from cat primary afferent central terminals have been shown to be mediated in response to both noxious electrical and chemical (capsaicin) stimulation (Go & Yaksh 1987, Zhao et al 2004); as well as from dorsal horn slices following noxious-like electrical stimulation of the attached dorsal roots (Malcangio & Bowery 1993). SP exerts its effect via interaction with the neurokinin 1 receptor (NK1R) expressed on the membrane of second-order post-synaptic dorsal horn neuron, which is extensively expressed in lamina I and to a lesser extent in the deeper laminae IV - VI and X (Mantyh et al 1997). Moreover, despite absence of NK1R neurons in lamina II, NK1R immunoreactive dendrites that are thought to be derived from NK1R-expressing neurons in other laminae have been identified (Todd 2002, Todd et al 1998). Selective ablation of NK1R (chemical or genetic disruption) led to a significant attenuation of responses to highly noxious stimuli (capsaicin) as well as mechanical hyperalgesia (Laird et al 2001, Mantyh et al 1997); whilst resulted in diminished capacity to develop mechanical allodynia and spinal inflammation in a model of facet joint pain (Weisshaar & Winkelstein 2014). Altogether these findings

implicate the importance of NK1R-expressing cells in the development of hyperalgesia in models of neuropathic and inflammatory pain (Todd 2010).

Similar to SP, the second neuropeptide, CGRP, is also released into the spinal dorsal horn from primary afferent central terminals in an activity-dependent manner following noxious-like stimulation of dorsal roots ex-vivo (Malcangio & Bowery 1996). It contributes in nociceptive transmission directly via activation its CGRP receptor, a G-protein coupled receptor (GPCR) expressed by post-synaptic second order dorsal horn neurons, in response to a noxious stimuli; and by potentiating the actions of SP through: promoting release, inhibition of degradation, and regulating the expression of NK1R (Latremoliere & Woolf 2009). As a result, it is often considered to be an indicator for nociceptor activity. CGRP primary afferent terminals innervate dorsal horn neurons second-order neurons in predominantly in laminae I - II and to a lesser extent in lamina V. Dense immunoreactivity of CGRP receptors have been detected in laminae I and II of the spinal dorsal horn (Wiesenfeld-Hallin et al 1984). Furthermore CGRP receptor is also expressed on the C-fibres central terminals that may act as autoreceptors (Ye et al 1999). Activation of CGRP receptor induces a long-lasting EPSPs in the dorsal horn in response to a noxious stimulus in the periphery. Animals with CGRP deficiency in terms of genetic deficits and CGRP knockout exhibit reduced sensitivity to noxious thermal stimulation and impaired response to induction of knee joint arthritis, respectively (Mogil et al 2005, Zhang et al 2001).

In addition, other transmitter-like signalling molecules such as brain derived neurotrophic factor (BDNF) have been implicated to play an important role in nociceptive transmission. It is constitutively synthesised by the peptidergic subpopulation of nociceptive neurons, anterogradely transported and released from their central terminals in the spinal dorsal horn (mainly superficial laminae) upon burst of C-fibre stimulation which mimics C-fibre responses to intense noxious stimuli (Lever et al 2001, Pezet & McMahon 2006). BDNF exerts it effect through interaction with tropomyosin receptor kinase B (TrKB) expressed mainly on superficial spinal dorsal horn neurons, with only modest expression on the terminals of primary afferent terminals (Pezet et al 2002). Presynaptic BDNF interaction with TrKB facilitates glutamate and SP release from primary afferent terminals; whereas postsynaptic BDNF-TrKB interaction results in receptor dimerization and auto-phosphorylation that subsequently trigger several

intracellular transduction pathways including: phosphatidylinositol 3-kinase (PI3K), mitogen-activated protein kinase/extracellular signal-regulated kinase (MAPK/ERK), and phospholipase C/protein kinase C (PLC/PKC) cascades, which, in turn, determines synaptic facilitation (Luo et al 2014, Smith 2014).

1.2.1.3.3 Spinal Modulation of Primary Afferent Input

The transmission of pain can be modulated by a number of mechanisms at the level of the spinal cord, as vast majority of neurons in laminae I - III are intrinsic interneurons that receive input via primary afferent sensory fibres. These interneurons, as aforementioned, can broadly be classed as excitatory (glutamatergic) and inhibitory (mainly GABAergic and glycine). The latter cell population can be detected with antibodies against the amino acids with the dense plexus of inhibitory axons visible using antibodies against the vesicular GABA transporter (VGAT, which also transports glycine), glutamate decarboxylase (GAD, the GABA-synthesizing enzyme), or the neuronal glycine transporter (GlyT2) (Todd 2010, Todd 2017). However, at present there are no reliable immunohistochemcial markers for cell bodies of excitatory glutamate-containing neurons, which has led to postulating that neurons within the dorsal horn which do not express GABA or glycine amino acids are considered as glutamatergic. Although the network of excitatory axons can be identified using markers against vesicular glutamate transporters (VGLUTs), with the presumable population of dorsal horn excitatory interneurons expressing VGLUT2 (Todd 2010). Activation of their respective excitatory (glutamatergic) or inhibitory (GABAergic/glycine) receptors result in either increase or decrease in neuronal excitability in the spinal cord in response to primary afferent nociceptive input, respectively. Receptors for both excitatory and inhibitory neuromodulators are present on both pre-synaptic primary afferent terminals and post-synaptic second order projection neurons in the dorsal horn where they can regulate the primary afferent fibre neurotransmitter release and excitability of the of the projection neurons, respectively (Todd 2010).

In addition, immunohistochemical analysis reveal co-localisation of certain neuropeptides (i.e. SP) exclusively in glutamatergic interneurons, some neuropeptides (i.e. galanin) are confined to the GABAergic population, whereas other neuropeptide mediators (i.e. enkephalin and dynorphin) are present in both excitatory and inhibitory cell population. The opioid peptides are

distributed within the superficial laminae of the spinal dorsal horn and can dampen spinal hyper-excitability in response to a noxious stimulus via activation of their GPCR-inhibitory protein coupled receptors (Go/Gi) expressed mainly on primary nociceptive afferent terminals as well as on excitatory interneurons. The interaction between the opioid peptide and its receptor induces an inhibition of voltage-gated calcium channels or activation of the inwardly rectifying potassium channels which results in decrease in neuronal excitability. Therefore release of opioid peptides in the spinal cord dampens excitatory transmission mediated by intrinsic excitatory glutamatergic interneurons and inhibits neurotransmitter release form primary afferent nociceptive terminals (Todd 2010).

1.2.1.4 **Supraspinal Transmission and Modulation of Pain**

1.2.1.4.1 Ascending Pathways

Nociceptive information in response to tissue damage or noxious stimuli is propagated, via projection neurons, from the spinal dorsal horn to higher centres in the brain via multiple ascending pathways, as outlined in Figure 1.2A. The two main ascending pathways described in relation to relaying nociceptive information from the spinal dorsal horn to the higher brain areas include the spinoparabrachial pathway and spinothalamic pathway (Hunt & Mantyh 2001). Sub-population of projection neurons are distributed extensively in superficial lamina I and sparsely dispersed in the deeper laminae III-VI, with very few present within lamina II. Many of dorsal horn projection neurons travel rostrally into the contralateral white matter prior to ascending to various brainstem and thalamic nuclei. Quantitative retrograde tracing in rodents revealed approximately 5% for lamina I neurons located in the lumber segment 4 (L4) of the spinal cord are projection neurons of which 70-90% express NK1R (Baseer et al 2014, Cameron et al 2015, Todd 2010). These sub-population of lamina I dorsal horn projection neurons give rise to the spinoparabrachial pathway that mainly target the contralateral parabrachial nucleus as well as project towards the periaqueductal grey (PAG) and nuclei of the thalamus. Third order neurons originating in these regions project onwards to areas such as the hypothalamus and amygdala, which are involved in the autonomic-aversive and emotional-affective aspect associated with pain, respectively (Hunt & Mantyh 2001). Selective ablation of NK1R-expressing neurons using SP-conjugated neurotoxin, saporin, resulted in alteration in

chronic pain behaviour (Mantyh et al 1997, Nichols et al 1999, Weisshaar & Winkelstein 2014). The spinothalamic pathway initiates mainly from deeper (laminae III-VI) dorsal horn and terminates in the contralateral thalamic nuclei that in turn projects further in order to innervate the cortical regions, mainly the primary somatosensory cortex. This ascending pathway corresponds to the sensory-discriminative aspect of pain associated experience (Hunt & Mantyh 2001). In addition to the two main ascending pathways described, a third parallel pain pathway originating from lamina II interneurons that are in contact with non-peptidergic (IB4 expressing) C-fibres, synapse onto projection neurons located in lamina V which target the neurons in the amygdala, hypothalamus, and globus pallidus. This pathway differs from the previously identified projections from lamina I in that the motor areas are also targeted in addition to the regions involved in the autonomic-aversive and emotional-affective processing of pain (Braz et al 2005).

1.2.1.4.2 Descending Modulation

Input of nociceptive information to the supraspinal areas, which are involved in multi-dimensional processing of pain, give rise to a number of descending pathways in response that are involved in the modulation of pain transmission (outlined in Figure 1.2B). Descending pathways make contacts with spinal dorsal horn neurons and can influence nociceptive transmission in response to tissue damage or noxious stimulation. One of the major and best characterised descending pathways involves the PAG connected to the superficial dorsal horn of the spinal cord via the nucleus raphe magnus (NRM) in the rostral ventromedial medulla (RVM). The PAG receives input from the: spinal cord, anterior cingulate cortex via prefrontal cortex, insula via amygdala, and the hypothalamus. However the PAG itself has minimal direct projections to the spinal cord; therefore instead it projects to the RVM, which relays signal via monosynaptic connections with the superficial dorsal horn neurons (Schweinhardt & Bushnell 2010). In addition to PAG, the RVM also receives inputs from the thalamus, the parabrachial region , as well as the noradrenergic locus coeruleus (LC); and is considered to be the final common relay in descending modulation of pain (Ossipov et al 2014). Many of the descending projections from RVM are by serotonin or 5-hydroxytryptamine (5-HT) containing neurons which upon release in the dorsal horn of the spinal cord can facilitate and/or inhibit spinal neuronal

response to noxious stimulation (Ossipov et al 2014). Neurons from RVM project via the dorsolateral funiculus (DLF) to the spinal cord in order to mediate descending facilitation and/or descending inhibition (Schaible 2007). This ability of RVM to both facilitate and inhibit spinal cord pain transmission is owed to the heterogeneous cell population present in the region that orchestrate the descending modulation, namely the: on-cells, off-cells and neutral cells. Increased activity of the off-cell population is thought exert descending inhibition as decrease in their activity is correlated with pro-nociceptive transmission. On the contrary, the on-cells instead induce facilitation of nociceptive processing during activation (Ossipov et al 2014). The PAG and RVM contain large number of opioid peptide (i.e. enkephalin) and opioid sensitive neurons, respectively. Therefore, application of an exogenous opioid agonist, morphine, to either region as well as to the spinal cord is anti-nociceptive. In particular, the on-cell population in the RVM is opioid-sensitive thus application of an exogenous opioid induces descending inhibition of nociceptive transmission via direct inhibition of on-cells and indirect facilitation of off-cells via disinhibition (Lau & Vaughan 2014). Moreover, as aforementioned, a subpopulation of spinal cord interneurons contain endogenous opioid peptide that elicit inhibitory responses on primary afferent terminals and/or dorsal horn neurons (Todd 2010). Ultimately, the spinal-bulbo-spinal loops are key in setting the level of nociceptive transmission. Taken together these evidence indicate an important serotonergic role for bidirectional modulation of pain transmission (Ossipov et al 2014).

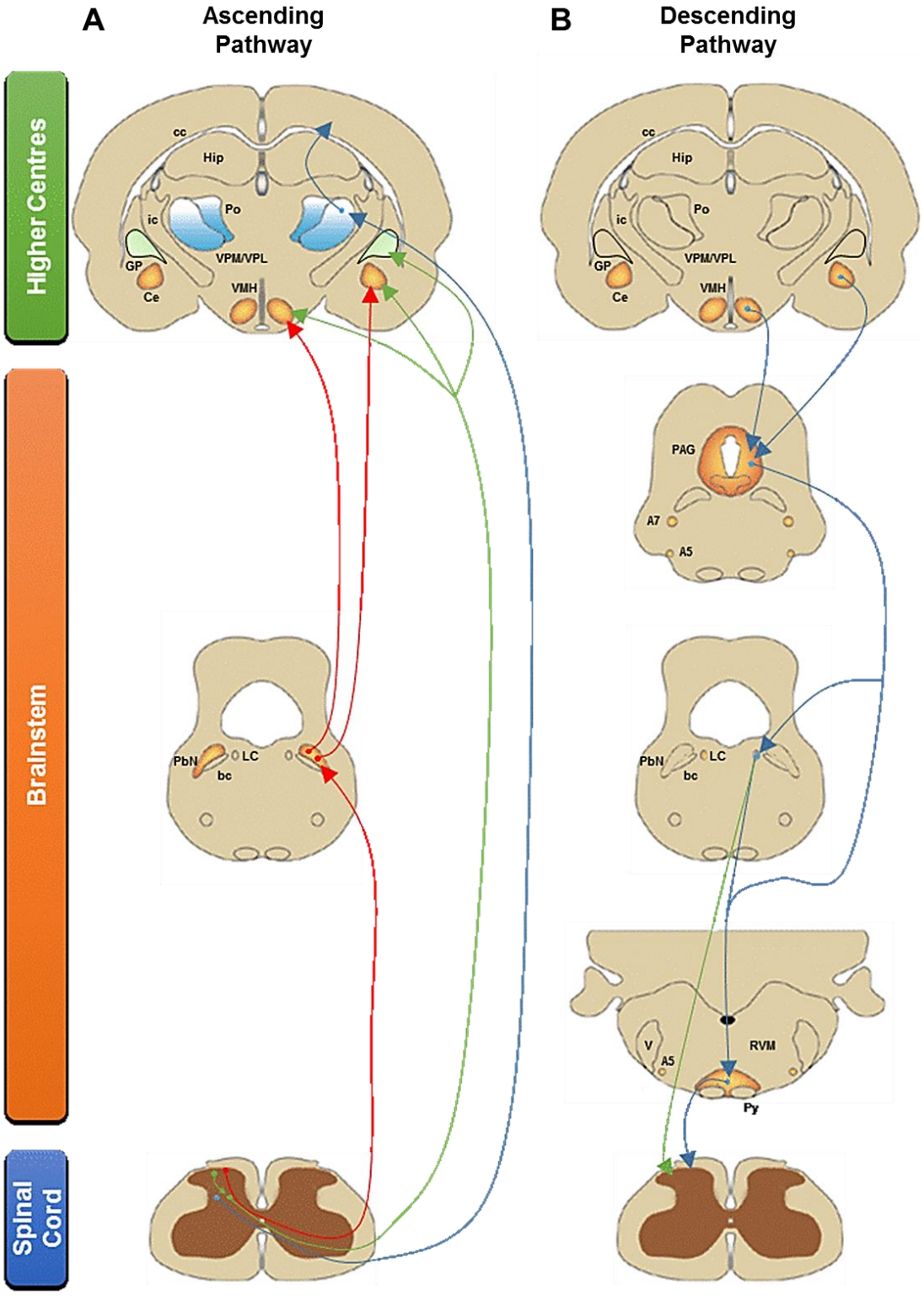

Figure 1.2: A Schematic of the Main Ascending and Descending Pain Pathways

The main ascending pain pathways are the spinothalamic (blue), spinoparabrachial (red), and the non-peptidegic (green) pathways (A). The spinoparabrachial pathway originates from the superficial dorsal horn and projects to areas of the brain that are concerned with emotional-affective component of pain. The spinothalamic pathway originates in deeper dorsal horn laminae which probably distributes

nociceptive information to areas of the cortex, via thalamus, that are concerned with both sensory-discrimination and emotional-affective aspect of pain. A third parallel non-peptidergic ascending pathway originates from lamina II neurons which projects to higher brain centres involved in autonomic-aversive and emotional-affective as well as motor processing of pain. The descending pathway (B) originates from the amygdala and hypothalamus and terminates in the periaqueductal grey (PAG). PAG neurons in turn project to the lower brainstem (locus coeruleus and rostroventral medulla) which control many of the antinociceptive and autonomic responses that follow noxious stimulation. Abbreviations: A, adrenergic nucleus; bc, brachium conjunctivum; cc, corpus callosum; Ce, central nucleus of the amygdala; Hip, hippocampus; GP, globus pallidus; ic, internal capsule; LC, locus coeruleus; PbN, parabrachial area; Po, posterior group of thalamic nuclei; Py, pyramidal tract; RVM, rostroventral medulla; V, ventricle; VMH, ventral medial nucleus of the hypothalamus; VPL, ventral posteriolateral nucleus of the thalamus; and VPM; ventral posteriomedial nucleus of the thalamus. Figure modified from Hunt and Mantyh (2001).

Another branch of descending modulation mediated by noradrenaline (NA) originates primarily from LC. Retrograde tracing of NA-projecting neurons in the rat dorsal horn (L4/L5) using adenoviral vector with catecholaminergic-selective promoter (AVV-PRS) coupled to fluorescent protein revealed approximately 80% of descending fibres originating from LC. It was further illustrated that administration of formalin in the hind paw resulted in activation of subpopulation of neurons in the LC. This implicates a possible role of descending pontospinal neurons in modulating nociceptive transmission (Howorth et al 2009). In fact, electrical and chemical stimulation of the LC has been demonstrated to increase nociceptive thresholds, which was blocked by administration of spinal α2-adrenergic receptor antagonists or a microinjection of lidocaine into the dorsolateral pons (Janss & Gebhart 1988, Ossipov et al 2014, Pertovaara 2006). Thus, indicating a descending inhibitory role mediated by noradrenergic pontine nuclei via its action of spinal α2-adrenergic receptor that are expressed by dorsal horn neurons as well as primary afferent terminals (Ossipov et al 2014).

However, recent evidence from optogenetic stimulation of LC delineated heterogeneous subpopulation of neurons in the LC, divided into ventral and dorsal NA-neurons. It was demonstrated that stimulation of the ventral sub-population neurons in LC resulted in anti-nociceptive effect whilst dorsal neuronal population stimulations induced pro-nociception in response to noxious thermal stimulation. This would suggest a bidirectional modulation of pain transmission mediated by NA containing neurons in the LC (Hickey et al 2014). Moreover, an intrathecal injection of α2-adrenergic receptor antagonist (atipamezole) failed to attenuate LC-evoked anti-nociception. These findings implicate that the mechanism of action of the

descending NA-pathway is not exclusively mediated by the spinal α2-adrenergic receptor (Hickey et al 2014, Llorca-Torralba et al 2016).

A particular form of descending inhibition of WDR neurons is the diffuse noxious inhibitory control (DNIC), whereby response of WDR neuron to stimulation from one location of the body may be inhibited by a noxious stimulus applied to another body location that is spatially distinct. The underlying mechanism is postulated to be that when a noxious stimulus is applied to the a given body region, nociceptive neurons transmitting the input send impulses to structures in the caudal medulla (caudal to RVM) which in turn triggers efferent inhibition of nociceptive WDR neurons located throughout the neuraxis (Le Bars et al 1979a, Le Bars et al 1979b).

1.2.2 Pathophysiology of Pain: Chronic Pain

Under normal conditions pain is a necessary self-protective mechanism that will only persist for the duration of noxious stimulus or tissue damage, and would resolve with removal of stimuli and healing of the injury or damage, respectively. However, under some circumstances pain can persist even after removal of stimuli or healing of tissue damage/injury, hence outlasting its physiological role, and developing into a maladaptive pathological state known as chronic pain. Chronic pain states can broadly be characterised into two groups, namely neuropathic pain and inflammatory pain, based upon their cause of persistence. In both cases, pathophysiologically it is characterised by a combination of mechanisms that result in enhanced and/or persistent nociceptive transmission due to induction of neuroplastic changes in both the periphery and CNS referred to as peripheral sensitisation and central sensitisation, respectively (Woolf 2010). Despite variability in its aetiology, chronic pain manifests clinically and pre-clinically as emergence of hyperalgesia (an exacerbated response to a normally noxious stimulus) and allodynia (a painful response to a normally innocuous stimulus) (www.iasp-pain.org). In addition to hyperalgesia at the site of injury/damage (primary hyperalgesia), hypersensitivity to a noxious stimulus that spreads to adjacent body locations (otherwise healthy) which are spatially distinct, a phenomenon known as referred pain (secondary hyperalgesia). A recent meta-analysis study revealed approximately 43% of the UK population is affected by a chronic pain condition. It has further been demonstrated that age is a major risk factor as the prevalence of chronic pain increases with age, affecting approximately 30% of individuals under the age of 40 years old increasing to 62% in the elderly population over the age of 75 years old. Thus highlighting these conditions as a major socio-economic burden that affects approximately 28 million people in the UK alone (Fayaz et al 2016).

1.2.2.1 **Neuropathic Pain**

Neuropathic pain arises from a primary lesion or dysfunction in the somatosensory nervous system, and may be a result of physical trauma or disease (www.iasp-pain.org). Neuropathy is typically associated with direct trauma to the nervous system in the form of crush or stretch of a peripheral nerve, or damage to the CNS following spinal cord injury, as examples. In addition, disease conditions such as diabetes mellitus, viral infections, and tumour growth may result in

clinical presentation of neuropathic pain symptoms. Furthermore, neuropathy can also occur following insults induced by direct exposure to certain toxins (i.e. acrylamide and arsenic), or an indirect side effect of anti-retroviral drugs and chemotherapy agents. Clinically it is characterised by sensory loss, abnormal sensation, ongoing/spontaneous pain, hyperalgesia, and allodynia (Baron et al 2010, Costigan et al 2009). Owing to the heterogeneity of the condition individuals with neuropathic pain also present with psychological changes, which range from mood disorders, anxiety, and altered sleep patterns. Neuropathic pain is a significant clinical problem as 6% - 10% of the general population present with clinical symptoms of the condition (Colloca et al 2017, Smith & Torrance 2012). However, at present there is no cure, with current treatments having limited effect and most undesirable side effects, making management of this pain state inadequate; largely due to an incomplete understanding of the underlying mechanisms (Colloca et al 2017).

1.2.2.2 **Inflammatory Pain**

Under physiological circumstances inflammation is a critical protective mechanism in response to injury, infection, and irritation in order to allow removal or repair of damaged tissue. It is characterised by five defining components: redness, heat, swelling, loss of function, and pain. Redness and heat are due increased blood flow; whilst swelling is a result of increased vascular permeability (Ji et al 2016). Pain occurs as a result of sensitisation and activation of peripheral sensory neurons by pro-nociceptive mediators, also known as inflammatory mediators/soup, (i.e. bradykinin, ATP, prostaglandin, growth factors, cytokines, and chemokines) released from damaged cells or infiltrating immune cells at the site of damage. In addition, inflammation can be modulated by the nervous system as nociceptor activation at site of insult triggers local release of neuropeptides (SP and CGRP) and a variety pro-inflammatory mediators, which in turn induce vasodilatation, plasma extravasation, and attraction of macrophages or degranulation of mast cells; a phenomenon known as neurogenic inflammation. Altogether inflammation entails a complex cascade of events that involve a variety of immune cells and associated plethora of inflammatory mediators, which can act by sensitising primary afferent terminals either indirectly, via attracting immune cells to site of injury, or directly, through activation of nerve fibres. Under these conditions inflammatory pain is protective as it limits use

of the affected area and prevents further damage during the healing process; which resolves following recovery of tissue (Ji et al 2014, Kidd & Urban 2001, Xu & Yaksh 2011). However, in patients with chronic inflammatory conditions, such as arthritis, prolonged hyperalgesia is commonly reported, as well as complaints of allodynia and spontaneous pain. It is thought this may be due to an impairment in the resolution of inflammation that is characterised by constant presence of algogenic mediators, which appear to result in sensitisation of both the peripheral and central nervous systems (Schaible 2007, Schaible 2012).

1.2.2.3 **Animal Models of Chronic Pain**

As clinical pain conditions cannot be reproduced in human volunteers in order to characterise the underlying chronic pain mechanisms, animal models have been developed in order to aid research in this field. To understand how animal models recapitulate the human pain condition, it is necessary to establish behavioural outcome measure for pain experience. Pain in itself is a subjective and multidimensional individual experience. Thus, assessment of pain in human subjects in terms of severity of pain can be conducted by questioning, which is not possible in animal models. Therefore, most animal studies do not measure pain directly, but instead use nociceptive thresholds in response to noxious stimulation as a surrogate measure for pain. The term “nociception”, which is typically described in animal studies, is defined by the IASP as “the neural process of encoding noxious stimuli” (www.iasp-pain.org). Thus, it is an aversive sensory behaviour in response to the noxious stimulus or injury, which is a protective function to avoid further injury/damage and promote healing and recovery.

Typically, the development of chronic pain in these animal models can be behaviourally determined via assessment of pain hypersensitivity, which can be measured in animals by studying the spinal reflex withdrawal thresholds in response to noxious mechanical, thermal, cold, chemical, and pressure stimulation. The reflex withdrawals are spinally mediated which are initiated by the activation of primary nociceptors and under the control of the descending control of the supraspinal structures (i.e. brainstem) (Gregory et al 2013). Many of the classical models of neuropathy involve traumatic surgical injury of a peripheral nerve (see Table 1.1), usually the sciatic nerve or branch thereof, which induces sustained pain behaviours illustrated by reduction in nociceptive thresholds in the hind paw of the affected rodent, with the

contralateral (unaffected) hind paw serving as an internal control. Likewise, a number of models of inflammatory pain have been developed in order to elucidate the underlying mechanisms by which inflammation becomes chronic, in pathological conditions, which result in persistent pain. Many of these models involve direct administration of exogenous algogenic substances (i.e. chemical irritants or inflammatory mediators; see Table 1.2) that result in inflammation in the area of administration accompanied by development of pain as a consequence.

Table 1.1: Surgical Models of Neuropathic Pain

Model	Surgical Paradigm	Reference
Chronic Constriction Injury (CCI)	Loose ligation of the sciatic nerve	Bennett and Xie (1988)
Partial Nerve Ligation (PNL)	Tight ligation of 1/3 - 1/2 of the sciatic nerve	Seltzer et al (1990)
Spinal Nerve Ligation (SNL)	Ligation of the L5 and/or L6 spinal nerve	Kim and Chung (1992)
Spared Nerve Injury (SNI)	Transection of the common tibial and common perineal nerves, leaving the sural nerve intact	Decosterd and Woolf (2000)

Table 1.2: Inflammatory Models of Chronic Pain

Model	Inflammation Agent	Reference
Complete Freud's Adjuvant (CFA)	Mineral oil containing *Mycobacterium tuberculosis*	Freund (1947)
Zymosan	Components of yeast cell wall	Pillemer and Ecker (1941)
Carrageenan	Seaweed extract	Vinegar et al (1976)
Formalin	Formalin solution	Dubuisson and Dennis (1977)

Although the use of these models has helped in identification and understanding of some of the underlying chronic pain mechanisms, they display little resemblance to most clinical pain conditions. Therefore, a number of models have been developed in order to recapitulate and thereby more closely mimic disease states, such as osteoarthritis (OA), which are associated with the development of chronic pain. Further review of OA and its animal models will be presented in Chapter 3.

1.2.2.4 **Chronic Pain Mechanisms**

The study of animal models of neuropathic and chronic pain has led to a vast increase in our understanding of the mechanisms which may contribute to the development of these pathological pain states. Plasticity in both the periphery and the CNS has been identified to underlie pathogenic mechanisms resulting in persistent pain. These can generally be categorised in one of the following, which are discussed below:

1. Peripheral sensitisation and changes in peripheral nerves
2. Central sensitisation and immune response in the spinal cord
3. Higher centre modulation

1.2.2.4.1 Peripheral Sensitisation

Under normal circumstances, nociceptors only respond to high intensity stimulation. However, in conditions of injury and or inflammation, nociceptive sensitivity is increased such that a normally innocuous stimulation result in pain and a noxious stimulus produces an exaggerated pain response. These changes are broadly due to a reduction in the nociceptor activation threshold as well as an increase in responsiveness to a suprathreshold stimulation of their receptive field, known as peripheral sensitisation (Gold & Gebhart 2010).

Peripheral sensitisation is typically a result of the dramatic change in the composition of the chemical milieu surrounding the primary afferents in the periphery. Tissue damage or injury causes a local inflammatory response whereby damaged cells as well as the infiltrating immune cells release plethora of inflammatory mediators around the site of nerve/tissue damage or inflammation (Ji et al 2014, Verma et al 2015). These mediators are referred to as the ‘inflammatory soup’ that includes: neuropeptides (i.e. bradykinin, CGRP and SP), ATP,

prostaglandin, growth factors (i.e. NGF), cytokines, and chemokines as well as extracellular proteases and protons (i.e. H^+). The primary afferent terminals express receptors/ion channels for all these inflammatory mediators, which interact with their respective receptors on peripheral free nerve ending. These receptors include ionotropic receptors (i.e. ATP $P2X_3$ receptor), GPCRs (i.e. receptors for prostaglandins, and neuropeptides), and tropomyosin receptor kinases (i.e. growth factor receptors); and their activation induces generation of intracellular second messengers such as Ca^{2+} and cAMP, which in turn activates several kinases, including: protein kinase A (PKA), protein kinase C (PKC), phosphoinositol-3-kinase (PI3K), and mitogen-activated protein kinase (MAPK; i.e. jun N-terminal kinase (JNK), extracellular signal-related kinase (ERK), and p38) (Gold & Gebhart 2010, Ji et al 2014, Woolf & Ma 2007). Activation of these kinases trigger phosphorylation of various proteins and a substantial increase in transcription of neuropeptides, growth factors, and key transduction (i.e. transient receptor potential ion channel A1 and V1 (TRPA1 and TRPV1)) as well as conduction ion channels (i.e. voltage gated sodium channels) (Linley et al 2010, Schaible et al 2011). These mechanisms are summarised in Figure 1.3.

In addition, during inflammation, the inflammatory soup can also recruit a host of silent nociceptor which further exacerbates the inflammatory nociceptive input to the spinal cord. Thus basal discharges may be induced or increased in nociceptors owing to inflammation, which consequently results in continuous afferent barrage into the spinal cord (Schaible et al 2009). Whereas, neuropathy induces a number of changes in the activity, properties, and transmitter content in the nociceptor neurons. Peripheral nerve injury generates spontaneous ectopic neuronal discharge at site of nerve injury or in the cell body located in the DRG, which in turn results in increased input to the spinal cord that may underlie spontaneous pain. Alteration in the expression, trafficking, and distribution of voltage gated sodium ion channels at the site of nerve injury accompanied by the process of Wallerian degeneration influencing intact fibres in close vicinity of injured nerve fibres contribute to spontaneous action potential discharge in afferent fibres. Ectopic discharges can be generated in nociceptive Aδ and C-fibres as well as the low threshold A-beta fibres (Schaible 2007, Scholz & Woolf 2007). Altogether driving a

functional plasticity of the nociceptors, which results in hypersensitivity and hyperexcitability of the nociceptor neurons.

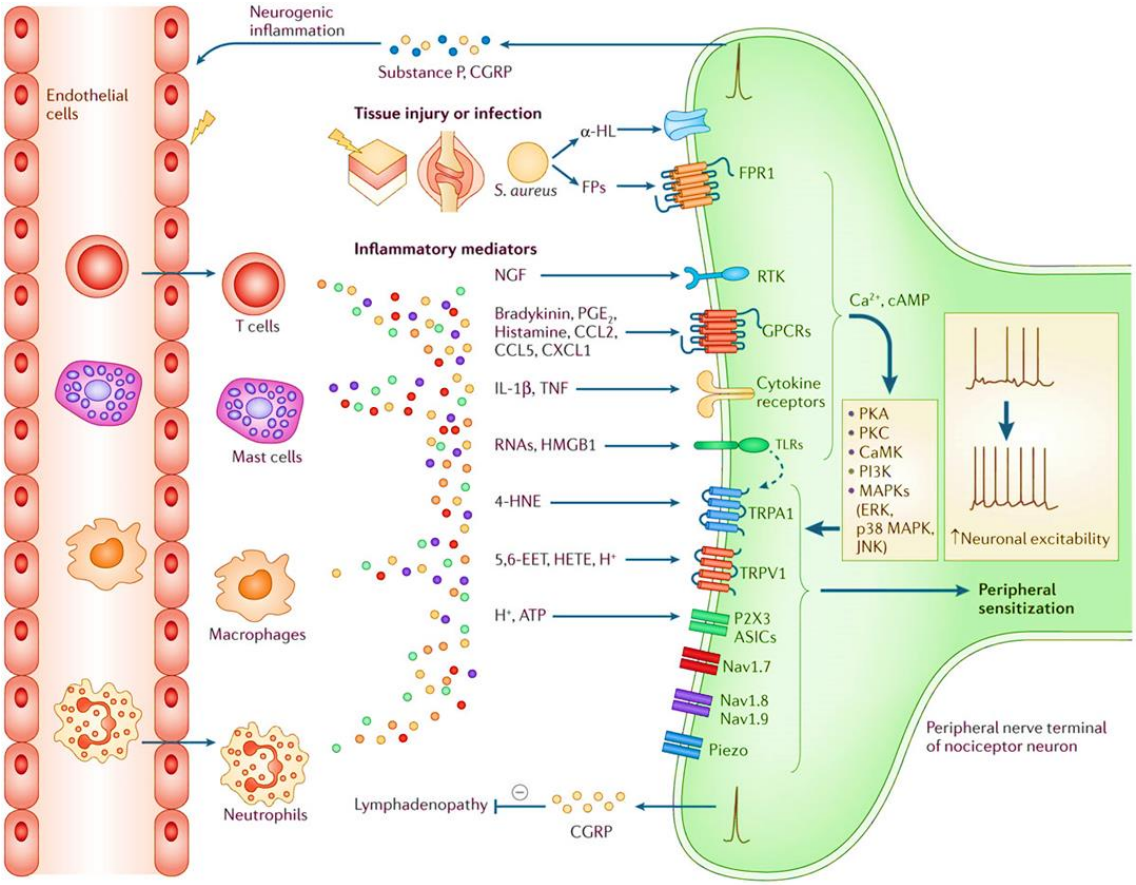

Figure 1.3: A Simplified Schematic of Key Components Involved in Peripheral Sensitisation

Following tissue injury/damage induces infiltration of immune cells (i.e. T-cells, mast cells, macrophages, and neutrophils) in vicinity of damaged tissue. Both the infiltrating immune cells and resident cells including mast cells, macrophages and keratinocytes, release a plethora of inflammatory mediators such as bradykinin, prostaglandins, protons (H^+), adenosine triphosphate (ATP), nerve growth factors (NGF), pro-inflammatory cytokines (tumour necrosis factor (TNFα), interleukin-1β (IL-1β) and IL-6) and pro-inflammatory chemokines (CC-chemokine ligand 2 (CCL2), CXC-chemokine ligand 1 (CXCL1) and CXCL5). Nociceptor peripheral terminals express receptors/ion channels for all these inflammatory mediators. These receptors include ionotropic receptors (i.e. ATP P2X3 receptor), GPCRs (i.e. receptors for prostaglandins, and neuropeptides), and tyrosine kinase receptors (i.e. growth factor receptors); and their activation induces generation of intracellular second messengers such as Ca2+ and cAMP, which in turn activates several kinases, including: protein kinase A (PKA), protein kinase C (PKC), phosphoinositol-3-kinase (PI3K), jun N-terminal kinase (JNK), extracellular signal-related kinase (ERK) and p38 mitogen-activated protein kinase (p38 MAPK). Activation of these kinases trigger phosphorylation of various proteins and a substantial increase in transcription of neuropeptides, growth factors, and key transduction (i.e. transient receptor potential ion channel A1 and V1 (TRPA1 and TRPV1)) as well as conduction ion channels (i.e. voltage gated sodium channels). Sensitisation of nociceptor peripheral terminal induces release of neuropeptides (i.e. substance P (SP) and calcitonin gene related peptide (CGRP)) that contribute to neurogenic inflammation. Altogether driving a functional plasticity of the nociceptors, which results in hypersensitivity and hyperexcitability of the nociceptor neurons. Figure taken from Ji et al (2014).

1.2.2.4.2 Central Sensitisation

Hyperactivity of primary sensory neurons in response to tissue damage and/or nerve injury in the periphery results in increased release of neurotransmitter (i.e. glutamate) and neuromodulator (i.e. SP, CGRP, BDNF, and ATP) from their central terminals in the spinal cord, inducing hyperactivity of second-order nociceptive neurons, a phenomenon referred to as central sensitisation (Ji et al 2014).

It is characterised by elevation in spontaneous activity; increased responsiveness of nociceptive neurons in the CNS to their normal or sub-threshold afferent input resulting in hyperalgesia (primary) and allodynia, respectively; and expansion of the receptive field, that enables input from non-injured tissue to generate pain (secondary hyperalgesia) (Latremoliere & Woolf 2009, Woolf 2011). The mechanisms contributing to the induction and maintenance of central sensitisation include NMDA-mediated glutamatergic neurotransmission and interneuron disinhibition; accompanied by glial-neuronal interactions and involvement from the descending modulation that are discussed in sections 1.2.2.4.3 and 1.2.2.4.4, respectively.

Input from the periphery is transmitted to second order dorsal horn neurons via the excitatory neurotransmitter, glutamate. The increased persistent release of glutamate and neuromodulators from the central terminals of hyperactive primary afferent neurons in response to tissue damage and/or nerve injury results in temporal summation of post-synaptic second-order neuron EPSPs that is sufficient to remove the Mg^{2+} ion block. Upon NMDA receptor activation by glutamate, there is an influx of Ca^{2+} ions, which causes post-synaptic depolarisation as well as activation of signalling molecules such as calcium/calmodulin dependent intracellular signalling pathway (i.e. MAPK, PKA, PKC, PI3K, and Src) which facilitate neuronal hyperexcitability in dorsal horn neurons (Basbaum et al 2009, D'Mello & Dickenson 2008, Latremoliere & Woolf 2009). These Ca^{2+} ion-dependent protein kinases contribute to phosphorylation-dependent modifications of NMDA and AMPA receptors, as well as numerous other receptors and ion channels; resulting in increased density in the post-synaptic membrane caused by enhanced synthesis and trafficking of ion channels and scaffold proteins. Moreover, long-lasting changes can be mediated by calcium/calmodulin dependent intracellular signalling pathway following NMDA receptor activation via inducing alteration in

transcription regulation, which drive expression of genes including: c-Fos, NK1, cyclooxygenase 2 (COX-2) and TrkB. Altogether these post-translational modifications strengthen nociceptive transmission by increasing membrane excitability and synaptic efficacy; whilst the transcriptional changes contribute to altered protein and/or molecules expression; collectively playing an important role in the induction and maintenance of central sensitisation, respectively (Costigan et al 2009, Latremoliere & Woolf 2009).

In addition, another mechanism that contributes to spinal neuronal hyperexcitability is the loss of the inhibitory control, referred to as disinhibition. As aforementioned, GABA and glycine containing interneurons represent the major subpopulation of intrinsic inhibitory neurons in the spinal cord. Administration of GABA or glycine receptor antagonist results in presentation of behavioural hypersensitivities resembling that illustrated following peripheral nerve injury (Sivilotti & Woolf 1994). Further evidence supporting this notion stems from model of peripheral nerve injury which demonstrates loss of GABAergic transmission in dorsal horn, possibly due to an activity-dependent excitotoxic cell death of dorsal horn inhibitory interneurons (Moore et al 2002). Moreover, BDNF released from microglial after peripheral nerve injury downregulates the expression of potassium chloride co-transporter 2 (KCC2) which in turn results in the diminished inhibitory efficacy of GABA owed to an alteration in the neuronal anion gradient (Coull et al 2005, Coull et al 2003, Peirs & Seal 2016). Altogether, resulting in an increase in neuronal excitability due to attenuation of the intrinsic inhibitory modulation in the spinal cord.

1.2.2.4.3 Role of Glial Cells in Chronic Pain

Glial cells represent the most abundant cell population of the nervous system. In the peripheral nervous system glial cells are present in the form of satellite glial cells in the DRG, with trigeminal glia and Schwann cells representing the glial cells in the peripheral nerves; whilst the CNS consist of three major types of glia, namely astrocytes, microglia and oligodendrocytes (Ji et al 2013). Notwithstanding the importance and relevance of other glial cell population and their role in pain regulation; we focused in the present set of studies mainly on two glial cell types, namely microglia and astrocytes, which have commonly been associated, as illustrated by change in morphology and functional activity, in the spinal cord of models of chronic pain conditions (Gosselin et al 2010).

1.2.2.4.3.1 Microglia

Microglia are the resident innate immune cells, originally identified by Rio-Hortega in 1919, which represent approximately 5% - 20% of the glial cell population in the CNS. The microglial cell population is derived from primitive myeloid precursors arising in the extra embryonic yolk sac in a limited time frame between embryonic day E7 and E9. These cells can be differentiated from macrophages in other tissues based on its ability to self-renew and resistance to ionised radiation (Arcuri et al 2017, Ransohoff & Cardona 2010). Under physiological conditions these cells were considered to be in a “resting” state for decades, in order to distinguish them from activated state. However, the advancement in research tools and techniques have helped to unveil microglial cells examining the environment repeatedly using two-photon imaging in a transgenic mouse harbouring overexpression of GFP in the Cx3cr1 locus (Nimmerjahn et al 2005). Morphologically they are characterised by a small cell soma with ramified processes and functionally perform immune surveillance role in the CNS, ranging from removal of metabolic products and deteriorated tissue components to the ability to recognise changes in neuronal activity and structures in order to maintain homeostasis. Moreover, it was demonstrated that it is the microglia processes that possess the dynamic ability to undergo cycles of formation and withdrawal and directly contacts with astrocytes, neurons, and blood vessels, whilst the somata of these cells remains bound to the same position, in order to monitor changes in their local microenvironment (Arcuri et al 2017, Nimmerjahn et al 2005). Thus, the term that has been proposed to describe microglial cells actively and continuously monitoring the CNS is “surveillant” (Ransohoff & Cardona 2010).

However, under pathological conditions, in response to injury or insult, microglia transform from their ramified “surveillance” state to become “activated”, a process referred to as microgliosis. During this process, microglial cells proliferate and undergo a series of changes in morphology, from ramified to amoeboid, characterised by enlargement of soma accompanied by retracted and shortened processes, in activated state; and function, as a consequence of altered expression of cell surface proteins and transcription of inflammatory mediators (Gehrmann et al 1995, Gosselin et al 2010). It has been extensively reported that in response to a CNS insult, activated microglia proliferate, migrate to and surround damaged or dead cells, where they clear

cellular debris via a process similar to the phagocytic activity of macrophages in the periphery; secrete cytotoxic molecules; and stimulate repair (Cagnin et al 2007, Gao & Hong 2008).

Microgliosis in the spinal dorsal horn has been extensively reported in models of both neuropathic and inflammatory chronic pain conditions (Clark et al 2007, Echeverry et al 2008, Staniland et al 2010). Following peripheral nerve injury or inflammation increased and persistent release of transmitters (i.e. neuropeptides and ATP) in the superficial dorsal horn from neighbouring and affected primary afferent fibres, respectively, induce recruitment and subsequent microglial activation via interaction with their respective receptors expressed. Upon activation microglia undergo morphological changes, as illustrated by increase in cell soma size, retraction of ramified processes, alteration to an amoeboid shape, accompanied by upregulation of microglial markers (i.e. major histocompatibility complex II (MHC II) and ionized calcium-binding adaptor molecule-1 (IBA1)); as well as a functional shift that is characterised by increase in expression of cell surface receptors (i.e. CX3CR1 and $P2X_4$ receptor), proteases (i.e. cathepsin S (CatS)), and release of various pro-inflammatory cytokine (i.e.IL1β and TNFα) and mediators (i.e. nitric oxide (NO), BDNF, and prostaglandins (PG)), which are induced via activation of the MAPK (i.e. p-38 and extracellular signal-regulated kinases (ERK)) pathways (Clark et al 2007, Clark et al 2009, Gosselin et al 2010, Ji et al 2013, Ji & Suter 2007, McMahon & Malcangio 2009, Tsuda et al 2005). The release of pro-inflammatory mediators can in turn increase the dorsal horn neuronal excitability thus contributing to central sensitisation.

Increase in spinal microglia has been demonstrated to play an important role in central sensitisation, as attenuation of microglial activation, via administration of glial inhibitors (i.e. minocycline), have been shown to correlate with reduced pain-like behaviours in the neuropathic and inflammatory models of chronic pain. Furthermore, evidence from CX3CR1, receptor for fraktalkine (FKN) (exclusively expressed on microglia), knockout mice revealed diminished microgliosis in models of neuropathic and inflammatory pain associated with attenuation of thermal hyperalgesia and mechanical allodynia, respectively (Clark et al 2007, Staniland et al 2010). The underlying source for this increase in microglial frequency in chronic pain conditions was not fully understood. Studies using bone-marrow chimeric mice reported increase in spinal microglia postulated to be a result of resident microglial undergoing

proliferation as well as infiltration of bone-marrow derived immune cells (macrophages) into the spinal dorsal horn parenchyma, presumably via peripheral blood circulation, that could differentiate into microglial-like cells. Thus, indicating a possible heterogeneous population of spinal microglia in neuropathic pain conditions (Isami et al 2013, Zhang et al 2007). However, recent study conducted by Tashima et al (2016) demonstrated little contribution of circulating bone-marrow derived cells to the population of spinal microglia after peripheral nerve injury using milder and split doses of irradiation (5 Gy × 2) rather than a single dose of 10 Gy used by previous studies. Although, the level of circulating blood leukocytes and spinal microgliosis were similar. As a result, indicating that spinal infiltration of bone-marrow derived cells may not be necessary for spinal microgliosis after peripheral nerve injury and that a stronger irradiation may induce changes in the blood brain barrier (BBB) that may cause cellular infiltration (Tashima et al 2016). Furthermore, upregulated expression of colony stimulating factor 1 (CSF1) has been shown in sensory neurons after peripheral nerve injury that is transported anterogradely to the spinal cord where it targets the CSF1 receptor (CSF1R) that is exclusively expressed by microglia, which in turn induces microglial activation and/or proliferation. Advillin-Cre-mediated CSF1 deletion from sensory neurons prevented nerve injury induced mechanical allodynia, implicating the important role of microgliosis in the development of chronic pain-like behaviour (Guan et al 2016).

Moreover, evidence from clinical studies have revealed increased binding of 18kDa mitochondrial translocator protein (TSPO) positron emission tomography (PET) tracer [11C] PBR28 in the spinal cord of individuals with sciatica, a low back originating from spinal nerve roots, and in the thalamus of individuals with lower back pain compared to healthy controls (Albrecht et al 2015, Loggia et al 2015). TSPO is a nuclear encoded mitochondrial protein, which is abundantly expressed in the peripheral organs but is present at low levels in the normal CNS as the microglia are in their “surveillant” state. Upregulation of mitochondrial TSPO expression is an early marker for microglial activation (Cagnin et al 2001b, Cagnin et al 2004). Therefore, these findings would suggest a role of spinal microgliosis in the development and maintenance of central sensitisation chronic pain state.

Recent advancements have implicated that the role of microglia in pain may be sexually dimorphic in animal models of chronic pain (Mapplebeck et al 2016). Selective ablation of microglia and pharmacological disruption of glial function (i.e. minocycline) in models of inflammatory and neuropathic pain specifically attenuated mechanical hypersensitivity in male mice only (Chen et al 2017, Sorge et al 2015). Evidence stemming from microglial-specific BDNF deletion and inhibition of spinal $P2X_4$ receptor were shown to prevent mechanical allodynia post SNI and/or reverse mechanical thresholds in male but not female mice (Sorge et al 2015). However, spinal NMDA receptor antagonist alleviated SNI-induced mechanical hypersensitivity in both sexes. Thus, suggesting a microglial-independent pathway in mediating mechanical hypersensitivity in females.

Further experimentation indicates the adaptive immune cells, in particular T-cells, which can infiltrate into the spinal cord following peripheral nerve injury, may contribute mechanical hypersensitivity in female mice. Sexually dimorphic expression of peroxisome proliferator activated receptors (PPARs) α and γ in mouse and human T-cells have been reported. The PPARα and PPARγ have been shown to be expressed differently based upon testosterone levels, with higher levels of PPARα in male and PPARγ in females. Administration of PPARα and PPARγ agonists selectively alleviated mechanical hypersensitivity in male and female mice, respectively (Sorge et al 2015). In addition to the different T-cell phenotype, female mice also exhibit a greater frequency of peripheral and central T-cells in comparison to males. Altogether, these data indicate a sexually dimorphic involvement of T-cells in pain processing. However, in female mice loss adaptive immune cells were demonstrated to develop mechanical hypersensitivity in a model of peripheral nerve injury via a microglial-dependent pathway; whilst reconstitution of the adaptive immune cells activates the switch towards the microglial-independent pathway (Sorge et al 2015). This indicates that a T-cell driven mechanism could possibly supress microglia-dependent pathway. Thus, these data support the role of T-cells in mediating pain hypersensitivity in female mice (Mapplebeck et al 2016, Mapplebeck et al 2017).

1.2.2.4.3.2 Astrocytes

Astrocytes belong to the macroglia subpopulation of glial cells that were first described as star-shaped cells by von Lenhossek in 1895; and constitute to approximately 30% of the cells in the

CNS (Liddelow & Barres 2017). Differentiated from neural stem cells, astrocytes have a similar developmental path to neurons and are native to the CNS (Zuchero & Barres 2015). These cells can broadly be subdivided into two main categories, namely protoplasmic and fibrous, on the basis of location and morphology. Protoplasmic astrocytes are distributed throughout the grey matter that are morphologically characterised by a globular cell soma from which several branches of ramified processes stem. Whereas, fibrous astrocytes which exhibit fewer but longer fibre-like processes and is localised to the white matter (Garcia-Marin et al 2007, Sofroniew & Vinters 2010).

Astrocytes are the most abundant glial cell population in the CNS which under physiological conditions maintain homeostasis by performing essential supportive roles for daily functioning of neurons in the CNS (Fuller et al 2009, Ricci et al 2009, Sofroniew 2005). The morphology of these cells allows them to enwrap neurons as well as blood vessels with their fine processes enabling them to play an important role in: neuronal development (Sofroniew & Vinters 2010); homeostatic maintenance of extracellular ionic environment and pH; modulation of synaptic functions via clearance and release of extracellular glutamate (Mazzanti et al 2001); replenishment of neuronal glutamate (Maragakis & Rothstein 2006); provision of metabolic substrates for neurons (Magistretti & Pellerin 1999); induction and maintenance of the blood-brain barrier (Barres 2008); coupling of cerebral blood flow to neuronal activity (Maragakis & Rothstein 2006, Mulligan & MacVicar 2004); and possibly sculpting and maintenance of synapses (Ullian et al 2001). In addition, astrocytes synthesise and release the anti-oxidant, glutathione (GSH), which protects cells against oxidative stress (Fuller et al 2009). Astrocytes are shown to be key mediators of inflammatory response as in response to CNS insult they can secrete both anti- and pro-inflammatory cytokines and chemokines (Farina et al 2007). Furthermore, some studies have indicated the role of astrocytes in memory formation via release of the gliotransmitter D-serine (D-ser), a co-agonist of the NMDA receptor, which promotes long term potentiation (LTP) establishment when glutamate is released from presynaptic terminal (Henneberger et al 2010, Santello & Volterra 2010).

In response to a CNS insult the astrocytes transform from their “active” housekeeping state to become “reactive” via a process known as astrocytosis. During this process, they undergo

hypertrophy, upregulate expression of intermediate filaments (nestin; vimentin; and glial fibrillary acidic protein, GFAP), and proliferate (Buffo et al 2010). The proliferating astrocytes migrate towards the CNS insult, where they form a glial “scar”, repair the blood brain barrier (BBB), and release a plethora of factors which mediate tissue inflammatory responses (i.e. cytokines, chemokines, and neurotoxic molecules) and trophic factors for remodelling after lesion (Buffo et al 2010, Ridet et al 1997, Silver & Miller 2004).

Likewise to microgliosis, spinal astrocytosis has been illustrated, in the form of upregulation of intermediate filament expression, in a number of models of both neuropathic pain (Coyle 1998, Cui et al 2014, Vega-Avelaira et al 2007) and inflammatory chronic pain states (Hui et al 2013, Raghavendra et al 2004, Sweitzer et al 1999). This sub-population of glial cells also possesses receptors for neurotransmitters released by primary afferent terminals in the spinal cord. Increased and persistent neurotransmitter release from primary afferent fibres, in response to injury or insult, interacts with its respective membrane receptor expressed by astrocytes, resulting in activation of astrocytes via inducing activation of JNK and ERK MAPK pathways; leading to release of pro-inflammatory cytokines and mediators (i.e. NO and PG). These mediators can either directly and/or indirectly contribute to sensitising of spinal neuronal activity; thereby increasing spinal neuronal hyper-excitability (Falsig et al 2004, Gosselin et al 2010, Ji et al 2013, McMahon & Malcangio 2009). In addition, pro-inflammatory cytokines released by activated microglia, such as TNFα, can also potentiate and drive astroglial activation, which implies that microgliosis in chronic pain conditions may precede the process of astrogliosis. Indeed astrocytic activation in a model of neuropathic pain appeared four days post-surgery in comparison microgliosis observed at earlier time point (McMahon & Malcangio 2009, Tanga et al 2004).

Astrocytes have been illustrated to play a role in the induction and subsequent maintenance of chronic pain condition as astroglial toxins (i.e. flurocitrate and a-aminoadipate), astroglial aconitase inhibitor (sodium fluoroacetate), or inhibitors of the astroglial enzyme glutamine synthetase (i.e. methionine sulfoximine) are effective in attenuation of pain-like behaviours (Ji et al 2013). Further evidence from GFAP-null mice revealed that SNL resulted in normal development of behavioural hypersensitivity however a shortened maintenance of pain-like

behaviour. In addition, administration of GFAP antisense oligonucleotide reversed injury-induced behavioural hypersensitivity as well as attenuating upregulation of GFAP in DRG and spinal cord (Kim et al 2009). Moreover, inhibition of astrocyte-related JNK activation in the spinal cord of neuropathic rats with a JNK inhibitor peptide (D-JNKI-1) has been demonstrated to prevent and reverse the development of allodynia, suggesting a key role played by astrocytic JNK in the induction and maintenance of neuropathic pain (Zhuang et al 2006). Finally, proliferation of spinal astrocytes has been observed in SNL model of neuropathic pain, which has been implicated to be associated with maintenance of chronic pain, as inhibition of astroglial proliferation resulted in reduced level of mechanical allodynia (Tsuda et al 2011). The overview of glial response has been outlined in Figure 1.4.

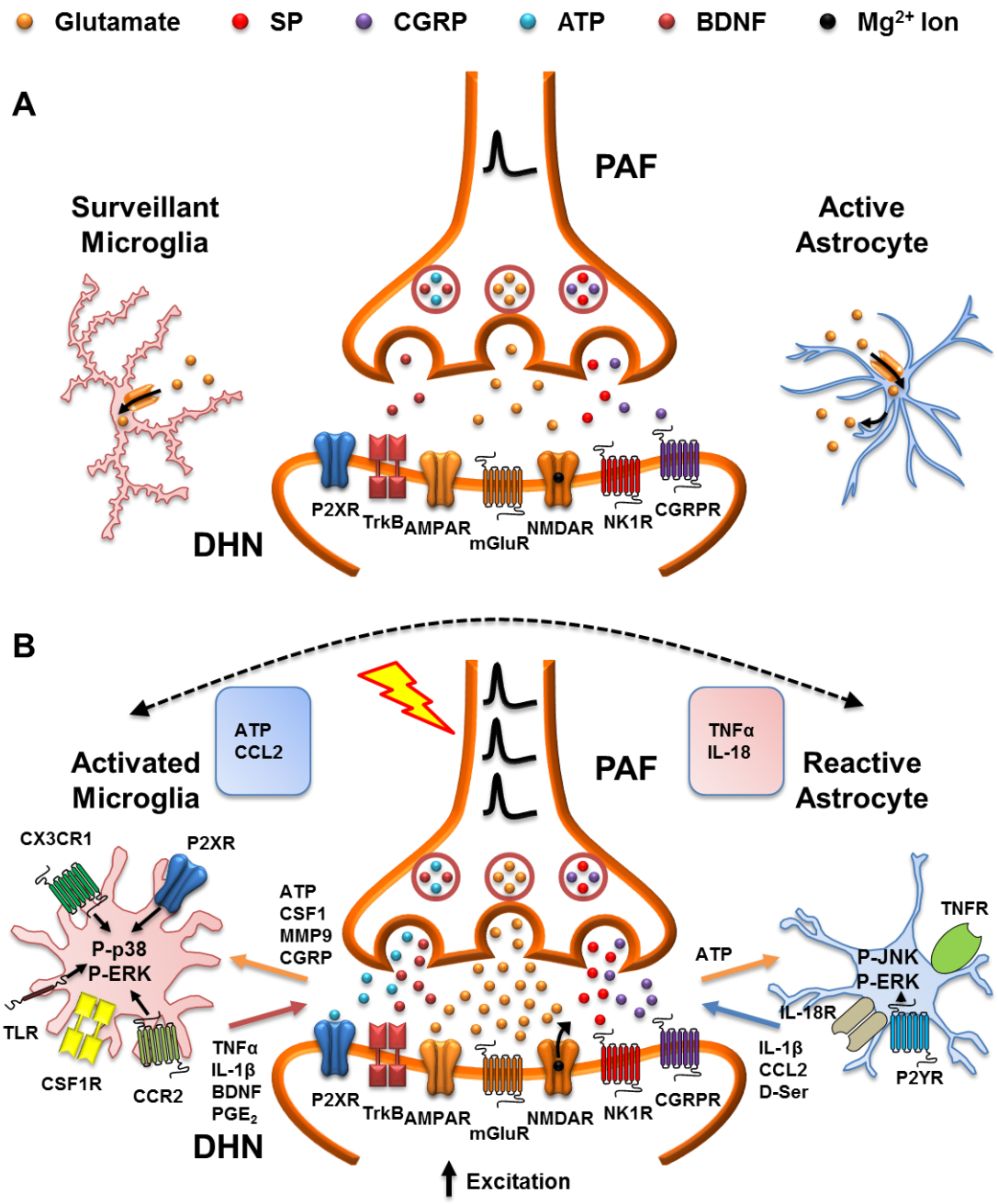

Figure 1.4: Simplified Schematic of Neuronal-Glial and Glial-Glial Interaction in Nociceptive and Chronic Pain

Under physiological conditions both microglia and astrocytes perform housekeeping roles in maintenance of homeostasis and modulation of synaptic function (i.e. via glutamate uptake) (A). Tissue damage or nerve injury results in increased release of neurotransmitter (i.e. adenosine triphosphate (ATP), neuropeptides, and brain derived neurotrophic factor (BDNF)) from primary afferent fibres presynaptic terminal (PAF) leading to activation of microglia and astrocytes (B). In concomitance to increased presynaptic neuronal neurotransmitter release, the glial cells act to enhance synaptic transmission via release of inflammatory mediators and neurotransmitters; inducing neuronal plasticity. Abbreviations: DHN, dorsal horn second-order postsynaptic neuron. Figure adapted from Ji et al (2013) and Malcangio (2016).

1.2.2.4.4 Higher Centre Modulation

Sensory output from the dorsal horn is relayed to higher processing centres in the brain via various ascending pathways, which in response give rise to a number of descending pathways from these supraspinal regions that are involved in modulation of pain transmission. Many of the areas receiving sensory input as well as those involved in pain transmission modulation have been demonstrated to be involved in the development and/or the maintenance of chronic pain state. Of these areas, the regions of the brainstem involved in descending modulation of spinal cord nociceptive signal transmission, namely the PAG, RVM and LC, exhibit an imbalance between descending facilitation or inhibition, which may underlie pathological pain states (Ossipov et al 2014). Injury or inflammation have been shown to decrease descending inhibition mediated by PAG and increase activity of on-cells in the RVM, which is pro-nociceptive; collectively shifting the balance of descending modulation towards facilitation of nociceptive transmission. Pharmacological, neurochemical, or physical disruption of descending facilitation mediated by the RVM, have been demonstrated to attenuate increased behavioural responses to evoked stimulation (Ossipov et al 2014). Moreover, administration of local anaesthetic in the RVM resulted in reversal of ongoing pain in models of neuropathic and arthritic pain (Allen et al 2017, King et al 2009). In addition, clinical neuroimaging studies have shown activation of the RVM in chronic pain conditions (Lee et al 2008). Furthermore, the activity of descending inhibitory LC is supressed by neurochemical changes in the amygdala in neuropathic pain state, which result in an increase in spinal nociceptive transmission owed to diminished descending inhibitory control (Viisanen & Pertovaara 2007). Altogether, implicating a role of an imbalance of descending modulation of pain transmission contributing to the induction and maintenance of central sensitisation (Ossipov et al 2014).

1.3 Alzheimer's disease

Alzheimer's disease (AD) is a progressive and irreversible age-related neurodegenerative disease of CNS. It was first described by a psychiatrist and neuropathologist Alois Alzheimer as a "peculiar severe disease process of the cerebral cortex" at the 37th Meeting of South-West German Psychiatrists in 1906 (George et al 2012). He had been clinically interacting with a 51 year old demented patient, Auguste D. (Deter, Figure 1.5A) since 1901; who presented with symptoms that included progressive memory loss, unfounded suspicions about her family as well as worsening psychological changes (i.e. sleep disturbance and persecutory delusions) (Maurer et al 1997). Histopathological assessment of brain autopsy upon her death in 1906 revealed severe cortical atrophy that was accompanied by senile plaques (Figure 1.5B) and neurofibrillary tangles (NFT, Figure 1.5C) (Alzheimer 1911). These histopathological observations are today recognised as the pathological hallmarks of the disease.

1.3.1 Epidemiology of Alzheimer's disease - A Socio-Economic Burden

AD is the most common cause of dementia (accounting for > 60% of dementia cases) in the elderly population, affecting over 45 million people worldwide and ~850,000 people in the United Kingdom (UK) (Prince et al 2016, Prince et al 2014). The prevalence of AD is approximately 5% in people over the age of 65 years, increasing to approximately 30% by the age of 85 years (Kamer et al 2008). Given the increase in life expectancy of the population, the frequency of individuals with AD is expected to increase dramatically and is estimated to be triple by 2050 (Brookmeyer et al 2007, Lopez 2011, Reitz et al 2011). As a result AD is considered to be a major public health issue in the UK where the cost of dementia care is over £26 billion a year (Prince et al 2014).

The aetiology of the disease is complex due to the heterogeneity of the disorder. Age is a well-known risk factor for all forms of dementia, and the majority of individuals (~95%) who develop AD are over the age of 65 years old, referred to as late-onset AD (LOAD); with approximately 1-5% of AD cases exhibiting an early onset, typically over the age of 40 years old, known as the early-onset AD (EOAD). The LOAD and EOAD are indistinguishable in terms of presentation of clinical symptoms; however, the latter is generally more clinically severe and has a greater rate

of progression in comparison to the former. EOAD is commonly associated with familial gene mutations; whereas LOAD occurs sporadically (i.e. idiopathic), but epidemiological studies have indicated the lipid-binding apolipoprotein E (APOE) ε4 variant as a susceptibility gene for LOAD (Reitz et al 2011).

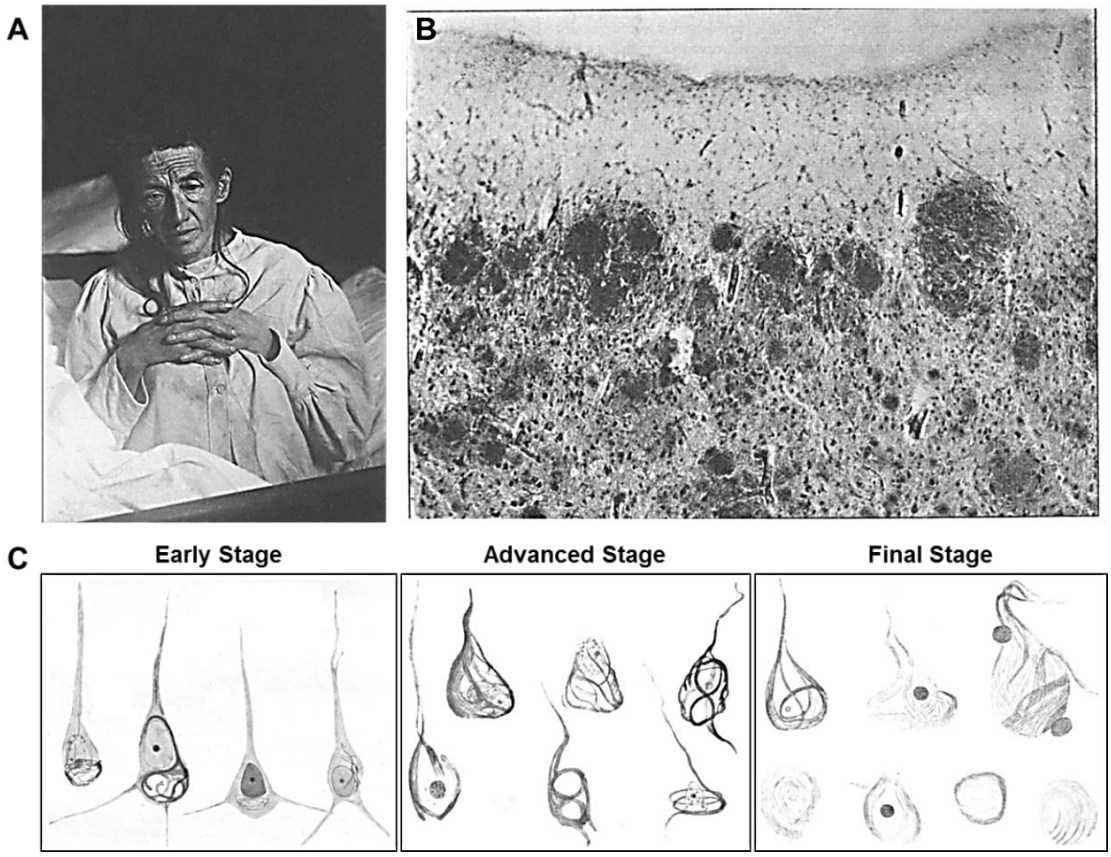

Figure 1.5: Alzheimer's Pathological Observations

A photograph of August Deter (D.) in November 1902, who presented with clinical symptoms as well as cortical pathological features of AD (A). Bielschowsky silver staining in the cerebral cortex of Auguste D. revealed senile plaques (B); accompanied by changes in neurofibrillary tangles characteristics with the progression of the disease (C). Figure adapted from Alzheimer (1911) and Maurer et al (1997).

1.3.2 Clinical Features and Diagnosis of Alzheimer's disease

Clinically, AD is characterised by a global deficit in cognition ranging from loss of memory to impaired judgement and reasoning (Tanzi & Bertram 2001). The revised clinical criteria for the diagnosis of AD is an update on the National Institute of Neurological and Communicative Disorders and Stroke/AD and Related Disorders Association (NINCDS-ADRDA) (McKhann et al

1984) and the Diagnostic and Statistical Manual of Mental Disorders-IV (DSM-IV). According to NINCDS-ADRDA criteria, the cardinal features to make a diagnosis of probable AD are dementia established by: (1) an insidious onset with gradual onset of symptoms over months to years; (2) clear-cut history of worsening of cognition by clinical examination and documented by neuropsychological tests; (3) evident amnestic (progressive worsening of episodic memory) and non-amnestic presentation (i.e. language deterioration, visuospatial deficits and executive dysfunctions); and (4) absence of systemic disorders or other brain diseases (i.e. vascular disease, frontotemporal lobe dementia, or Lewy body dementia) that in and of themselves could account for the progressive deficits in memory and cognition. The definitive diagnosis is based on the clinical diagnosis of probable AD accompanied by neuropathological demonstration of amyloid plaques and NFT in the brain at autopsy.

Owing to the advancements in the current understanding and of the diagnostic tools, the research criteria for the diagnosis of AD have been revised recently in order to include imaging and cerebrospinal fluid (CSF) biomarkers (Dubois et al 2010, Dubois et al 2007, Jack et al 2011). It was argued that the NINCDS-ADRDA and DSM-IV-TR criteria for the diagnosis of AD may have fallen behind as new reliable biomarkers have been developed, which could be assessed by structural magnetic resonance imaging (MRI), neuroimaging with PET and CSF analysis (Dubois et al 2010).

The latest revised diagnostic criterion has recently been established by the National Institute on Aging-Alzheimer's Association (NIA-AA) criteria (McKhann et al 2011). According to this criterion, diagnosis of AD dementia has been divided into four distinct descriptions: pathologically proven AD dementia, probable AD dementia, possible AD dementia and Not AD dementia. These were assessed by clinical and cognitive tests accompanied by evidence provided by AD biomarkers (McKhann et al 2011).

1.3.3 Alzheimer’s disease Associated Pathology

At macroscopic level, AD brains typically present with severe cortical atrophy, enlargement of the lateral ventricles, and shrinkage of the hippocampi. The major microscopic neuropathological hallmarks of AD are as defined by Alzheimer in 1911, extracellular senile/neuritic plaques and intracellular NFT (Alzheimer 1911). These hallmarks are

accompanied by neuronal loss, synaptic dysfunction, and neuroinflammation (Serrano-Pozo et al 2011).

1.3.3.1 **Amyloid Plaques**

Amyloid plaques are extracellular spherical insoluble accumulations of β-amyloid (Aβ), a product of proteolytic cleavage of the transmembrane amyloid precursor protein (APP), with a beta-pleated configuration. They are divided into two types: diffuse and senile/neuritic (NP) plaques (Figure 1.6A-B). The NP are characterised by a focal round central core composed of aggregates of filamentous Aβ (ranging from 10 µm – 120 µm in cross-sectional diameter) surrounded by dystrophic neurites consisting of enlarged lysosomes, degenerating mitochondria and paired helical filaments (PHF) in its close vicinity; and associated with inflammation (i.e. gliosis). In contrast, diffuse plaques exhibit spherical deposition of Aβ aggregates with no central core nor dystrophic neurites (Selkoe 2001). Such plaques are also detected in the brain of non-demented aged-individuals at autopsy and therefore may represent the precursor to neuritic plaque generation, which have led to the suggestion that the NP form of amyloid plaques are associated with AD. Thus, the Consortium to Establish a Registry for AD (CERAD) have developed a grading criteria in order to rank the density of NP as a neuropathological assessment of AD (Hyman et al 2012, Montine et al 2012).

Braak and Braak in 1991 provided a distribution pattern in a typical AD brain at autopsy with progression of AD (Figure 1.6C). In accordance to this criterion, initial Aβ deposits appear in the basal isocortex (Stage A), progressing to virtually all isocortical regions and mildly affecting the hippocampal formation (Stage B), prior to affecting all areas of the isocortex, involving sensory and motor core fields, in the terminal stages (Stage C) (Braak & Braak 1991b). More recently Thal and colleagues have described the spatiotemporal pattern of amyloid plaque distribution that can be classified in three stages, initially affecting the isocortical region (Stage 1), progressing to the limbic region (Stage 2), and finally affecting the subcortical structures as well as the cerebellar cortex in the final stages (Stage 3) (Thal et al 2002). However, deposition of amyloid plaques (diffuse and/or NP) do not correlate with the severity and duration of dementia (Serrano-Pozo et al 2011).

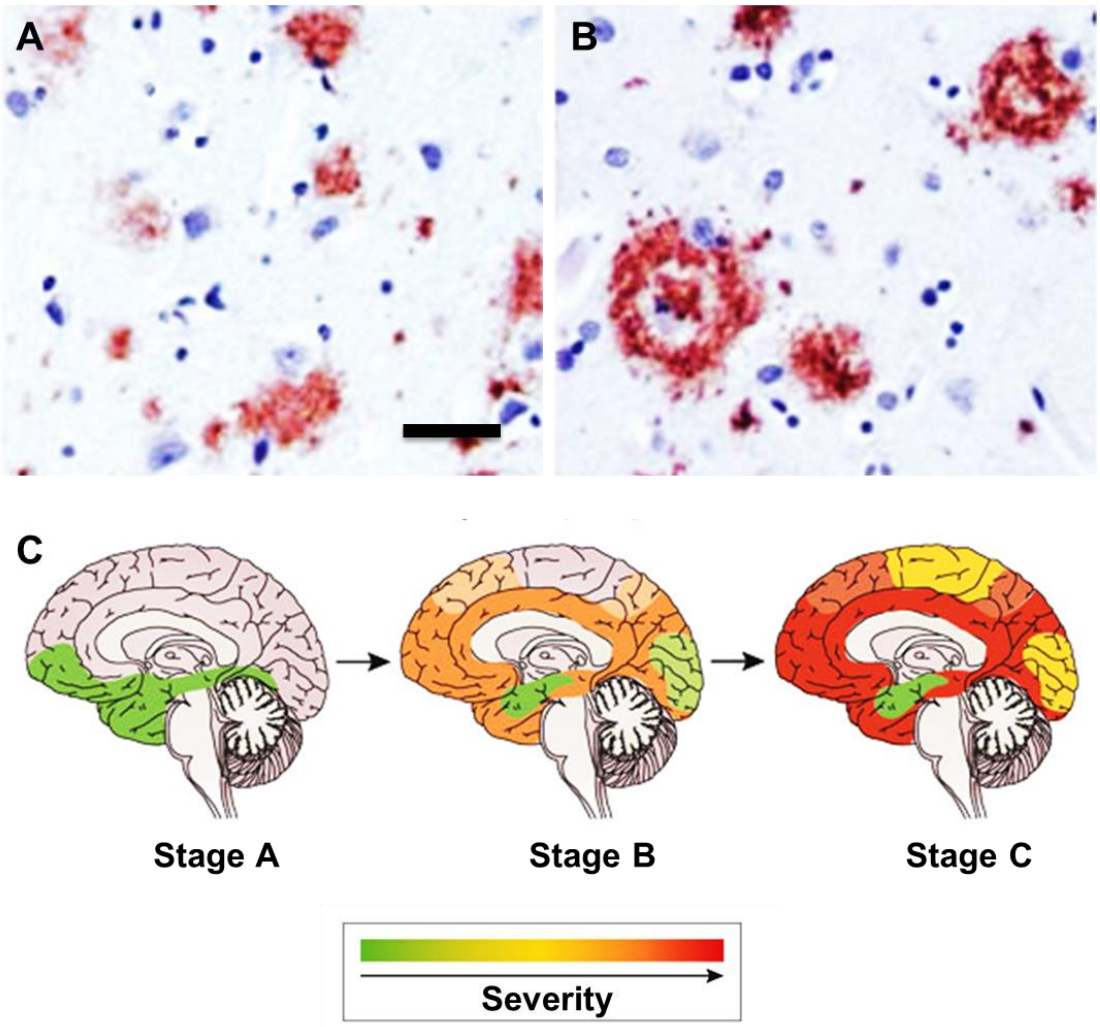

Figure 1.6: Amyloid Plaques and their Distribution with Progression of Alzheimer's disease

A representation of diffuse (A) and neuritic plaques (B) in a typical AD brain at autopsy (scale bar represents 10 µm). Amyloid deposits initially appear in the basal isocortex (Stage A), progressing to virtually all isocortical regions and mildly affecting the hippocampal formation (Stage B), prior to affecting all areas of the isocortex, involving sensory and motor core fields, in the terminal stages (Stage C) (Braak & Braak 1991b). Figures A and B were modified from Alafuzoff et al (2009); and C was modified from Masters et al (2015).

1.3.3.1.1 Amyloid Precursor Protein

APP is a member of the glycosylated transmembrane protein family which is ubiquitously expressed. The APP gene is mapped on chromosome 21 and contains 19 exons, which undergoes alternative splicing that gives rise to three major isoforms of human APP: 695, 751, and 770 amino acids; of which APP 695 is the most abundant isoform in neuronal cells (O'Brien & Wong 2011). The cellular function of APP remains elusive although it has been postulated to

have neurotropic properties and may play a role in neuronal growth (Oh et al 2009). APP knockout mice have shown reactive gliosis and locomotor deficits, accompanied by abnormal neuronal morphology, impairments in LTP and cognitive deficits (Senechal et al 2008, Zheng et al 1995). Furthermore there is evidence to support the role of APP in regulation of synaptic formation and activity as illustrated by: reduced density and length spines exhibited APP knockout mice in cultured hippocampal neurons; interaction with Ca^{2+} ion channel that in turn regulate in GABAergic short term plasticity in neuronal cultures obtained from the mouse striatum and hippocampus; and by promotion of NMDA receptor activity via increased membrane trafficking and decreased internalisation in APP transfected primary neurons (Hoe et al 2009, Tyan et al 2012, Yang et al 2009). Moreover, APP has been proposed to play a role in cell adhesion owing to a heparin binding domain it possesses, which allows binding to the proteoglycan in the extracellular matrix (Zheng & Koo 2011).

1.3.3.1.1.1 Processing of APP

APP undergoes a two-step process known as regulated intermembrane proteolysis, with an extracellular N-terminal cleavage step followed by a cleavage of the transmembrane domain of the protein and the release of an intracellular C-terminal fragment. The processing of APP can be either non-amyloidogenic or amyloidogenic based upon the cleavage by the initial secretase enzyme (as illustrated in Figure 1.7) (LaFerla et al 2007). However, the underlying reason for the cellular choice between the two pathways is not fully understood. In familial form of AD, it has been shown that the levels of Aβ peptide are elevated owing to the shift toward that amyloidogenic proteolysis of APP (LaFerla et al 2007, Zhang et al 2011).

The non-amyloidogenic processing of APP is initiated by the enzyme α-secretase (ADAM and zinc metaloproteases) which releases an extracellular fragment, soluble APPα (sAPPα), and a membrane-bound C-terminus fragment α (CTFα; also known as C83). The sAPPα cooperates with the epidermal growth factor (EGF) receptor and also directly or indirectly interacts and activates potassium ion channel (KCN) in order to promote cell proliferation and neuroprotection, respectively. The membrane-bound C-terminus fragments can interact with multiple adaptor and signalling molecules that are involved in cellular differentiation. Subsequent proteolytic cleavage of CTFα by the γ-secretase complex releasing p3 into the

extracellular space and a soluble intracellular domain of APP (AICD) which can act as transcriptional regulator in the nucleus. The γ-secretase complex is composed of a four-protein complex that includes: nicastrin, presenilin enhancer 2 (Pen-2), anterior pharynx defective 1 (Aph-1), presenilin (PS1 or PS2), from which both presenilins represent the catalytic site of the enzymatic complex (Willnow et al 2008, Zhang et al 2011).

In contrast, the amyloidogenic pathway is initiated by the proteolytic cleavage of APP by the enzyme aspartic-acid protease β-secretase (BACE1) which generates a soluble fragment from the N-terminal domain, soluble APPβ (sAPPβ), as well as a membrane-bound C-terminus fragment β (CTFβ; also known as C99). The membrane-bound CTFβ undergoes a subsequent cleavage by the γ-secretase complex yielding Aβ peptides and AICD. Aβ is proposed play a role in neuroprotection, when released in lower amounts in normal brains, via modulation of synaptic transmission as demonstrated by impaired hippocampal synaptic plasticity and memory in BACE1 knockout mice (Laird et al 2005). On the contrary, high yielding of Aβ in pathological conditions leads to loss of synapses as a result of impairments in LTP and facilitation of LTD in the hippocampus synapses; trigger cell death via direct interaction with the p75 neurotrophin receptor (p75NTR), a low affinity receptor transmembrane receptor that binds all neurotrophins (i.e. NGF and BDNF); and forms neurotoxic oligomers and plaques (Koffie et al 2011, Pezet & McMahon 2006, Willnow et al 2008, Zhang et al 2011).

Dependant on the cleavage site several forms of Aβ can be generated ranging from 39-43 amino acids in length (Aβ39-43). The most common isoforms of Aβ peptide produced contain 40 amino acids (Aβ40). The longer 42 amino acid Aβ (Aβ42) is more toxic and prone to aggregate more readily into protofibrils and fibrils in comparison to Aβ40 and therefore it is the major component of the human amyloid plaques. Under physiological conditions the ratio of Aβ42/Aβ40 is equal. However environmental and genetic influences (i.e. APP, PS1 and PS2 mutations) cause abnormal proteolytic cleavage of APP, leading to an elevation of the Aβ42/ Aβ40 ratio which is the insoluble and neurotoxic form of Aβ (Raskin et al 2015). The elevation of this ratio is as a result of either an increase in Aβ42 and/or a decrease in Aβ40 as outlined by some PS1 mutations. Mutations in APP, PS1 and PS2 gene are familial mutations that are associated with EOAD (Qiu et al 2015, Raskin et al 2015).

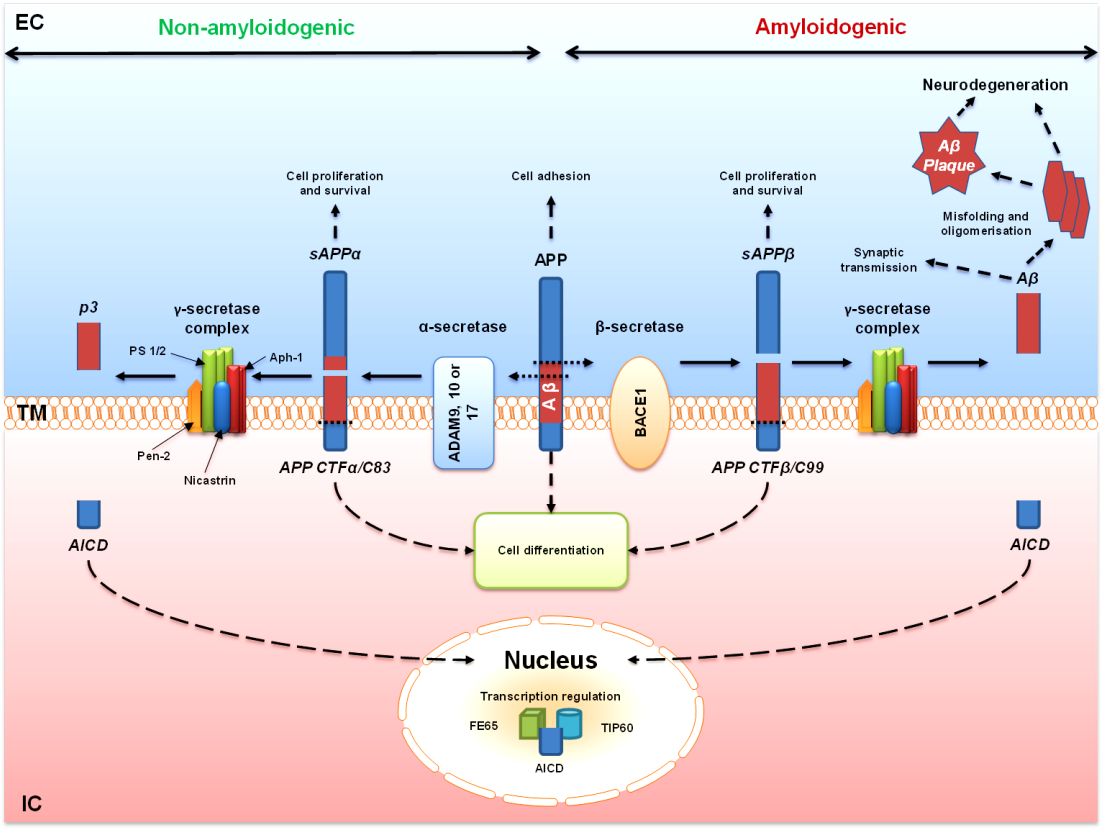

Figure 1.7: A Simplified Schematic of APP Processing

A representation of APP processing and the downstream signalling leading to neuronal survival or cell death. The non-amyloidogenic APP processing is characterised by initial cleavage by the α-secretase followed by a subsequent cleavage by the γ-secretase complex composed of: nicastrin, presenilin enhancer 2 (Pen-2), anterior pharynx defective 1 (Aph-1), presenilin (PS1 or PS2) leading to cell survival. Whereas, the amyloidogenic pathway of APP processioning involves initial cleavage by the β-secretase enzyme prior to processing by the γ-secretase complex that lead to generation of Aβ, which can accumulate and aggregate resulting in neurodegeneration. Figure modified from Willnow et al (2008).

1.3.3.2 **Neurofibrillary Tangles**

Intracellular NFTs consist of PHF of aberrantly hyperphosphorylated microtubule-associated protein tau (MAPT), which under physiological conditions is expressed in both neuronal and non-neuronal (glial) cells (Couchie et al 1988, Gu et al 1996, Muller et al 1997). In the adult human brain, through alternative splicing of mRNA of the *MAPT* gene located on chromosome 17q21, six different isoforms of tau are generated (van Herpen et al 2003). The inclusion or exclusion of exon 10, results in tau isoforms with four repeats (4R) or three repeats (3R) microtubule binding sites, respectively. Under physiological conditions, the levels of 3R and 4R tau are approximately equal (de Silva et al 2003, van Herpen et al 2003). Physiological tau is

bound to microtubules, performing an important role in regulating the assembly and stabilisation of microtubules, which is essential for intra-neuronal vesicle and organelle transport (Hirokawa 1994, Stamelou et al 2010, Wang & Mandelkow 2016).

However, in pathological conditions, tau undergoes abnormal hyperphosphorylated and accumulates as aggregates in the somatodendritic compartment of neurons in the form of NFT, neuropil threads and dystrophic neurites (Figure 1.8A) (Ballatore et al 2007). Phosphorylation of tau mainly takes place post-translation and mainly at the serine and threonine residue of the protein. Several candidate kinases have been identified that can potentially be involved in this phosphorylation which include glycogen synthase kinase 3 (GSK-3), cyclin-dependent kinase 5 (CDK-5) and mitogen-activated protein kinase (MAPK) (Wang & Mandelkow 2016). NFT are initially observed in the transentorhinal region which spreads to the limbic and the associated cortical regions with the progression of AD (Braak & Braak 1991b).

In addition, NFT have been shown to demonstrate a stereotypical spatiotemporal progression which correlates with the severity of cognitive decline. Therefore, the topographic staging of NFT is used for the pathological diagnosis of AD, referred to as the Braak's NFT staging of AD. According to this criterion the distribution pattern of neurofibrillary (NF) changes (i.e. NFT and neuropil threads) in the brain of a typical AD subject is classified in six stages (I-VI) which can be further distinguished as the: (1) Transentorhinal (Stages I-II), which display NF alterations confined to a single layer of the transentorhinal cortex; (2) Limbic (Stages III-IV) that is characterised by the severe NF changes in the entorhinal and transentorhinal layer; and (3) Isocortical (Stages V-VI) which is marked by isocortical involvement, with NF changes appearing in the associated cortical regions, as illustrated in Figure 1.8B (Braak & Braak 1991b).

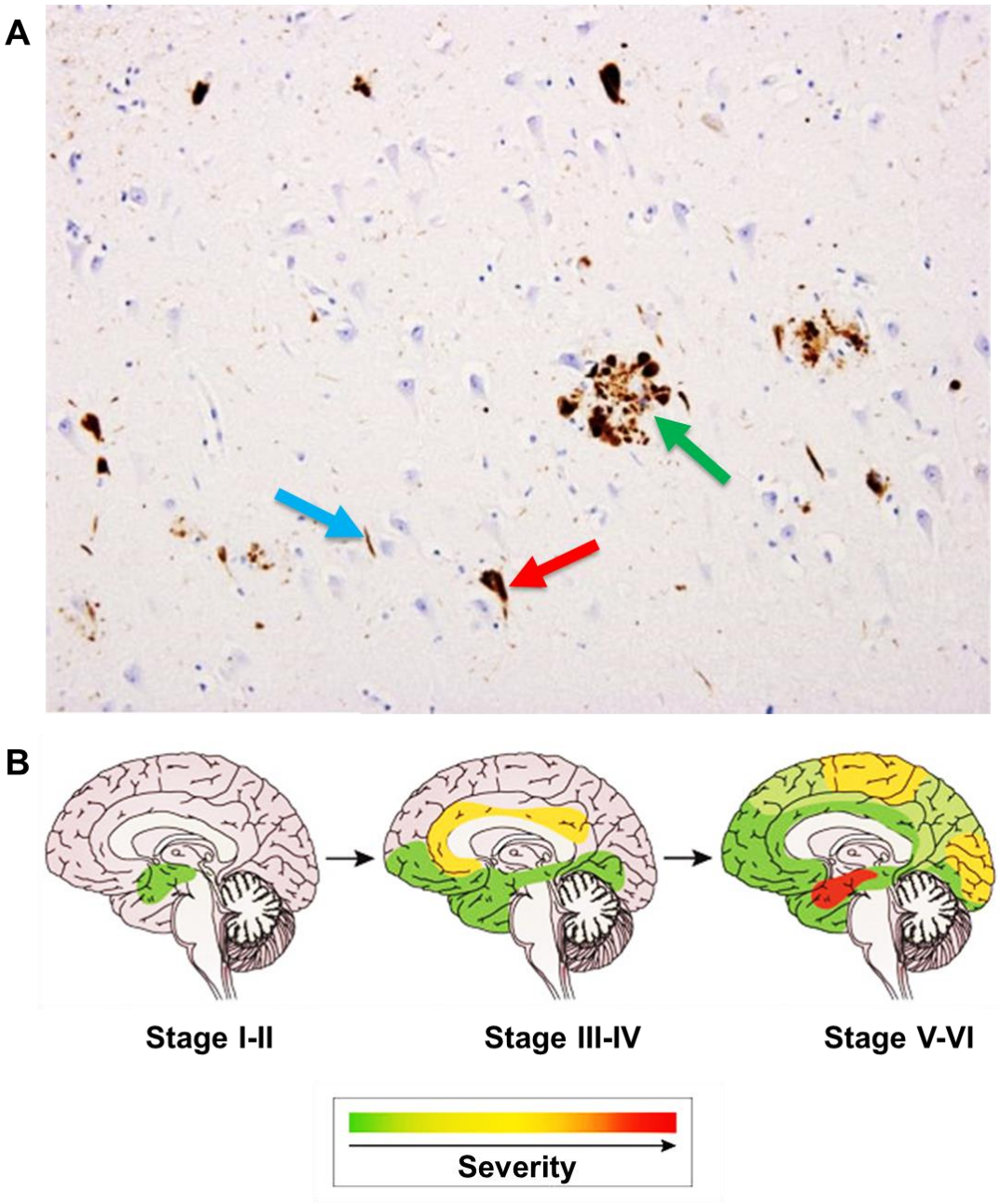

Figure 1.8: Tau Pathology and their Distribution with Progression of Alzheimer's disease

A representation of tau lesions detected in the temporal cortex of an AD patient at autopsy. Immunohistochemical staining against abnormally phosphorylated tau (TG-3) identified tau pathology in the form of neuropil threads (blue arrow), neurofibrillary tangles (red arrow), and dystrophic neurites (green arrow). Neurofibrillary (NF) changes (i.e. neurofibrillary tangles and neuropil threads) are initially confined to a single layer of the transentorhinal cortex (Transentorhinal; Stages I-II); progressively affecting the entorhinal and transentorhinal layer (Limbic; Stages III-IV); prior to marked isocortical involvement, with NF changes appearing in the associated cortical regions (Isocortical, Stages V-VI). (Braak & Braak 1991b). Figures A was modified from Perl (2010); and B was modified from Masters et al (2015).

1.3.3.3 **Cerebral Amyloid Angiopathy**

In addition to aggregation of Aβ in the form of amyloid plaques, patients with AD also show accumulation of Aβ in the cerebral and cerebellar blood vessels, known as cerebral amyloid angiopathy (CAA). Although CAA is evident in the brains of elderly individuals; the prevalence in AD brains is significantly higher in comparison (Serrano-Pozo et al 2011). Amongst the blood vessels affected by CAA include: meningeal and cerebral arteries, and to a lesser degree capillaries and veins; whilst the white matter blood vessels are usually spared. Deposition of vascular amyloid may result in cerebral blood flow dysregulation, breakdown of the blood-brain barrier (BBB) and microhemorrhages (Perl 2010).

1.3.3.4 **Inflammation**

Inflammation in the form of reactive gliosis has also been noted by Alzheimer as a prominent cellular feature that is close in vicinity of amyloid plaques in the form of a barrier surrounding the pathological lesion (Figure 1.9A), which may also interact with the amyloid plaques (Alzheimer et al 1991). Both microglia and astrocytes cluster around amyloid plaques forming a barrier and display a shift in phenotype from physiological housekeeping role to an activated or reactive form, respectively, in pathological conditions; whereby they undergo a series of changes in morphology and function (Figure 1.9B) (Serrano-Pozo et al 2013).

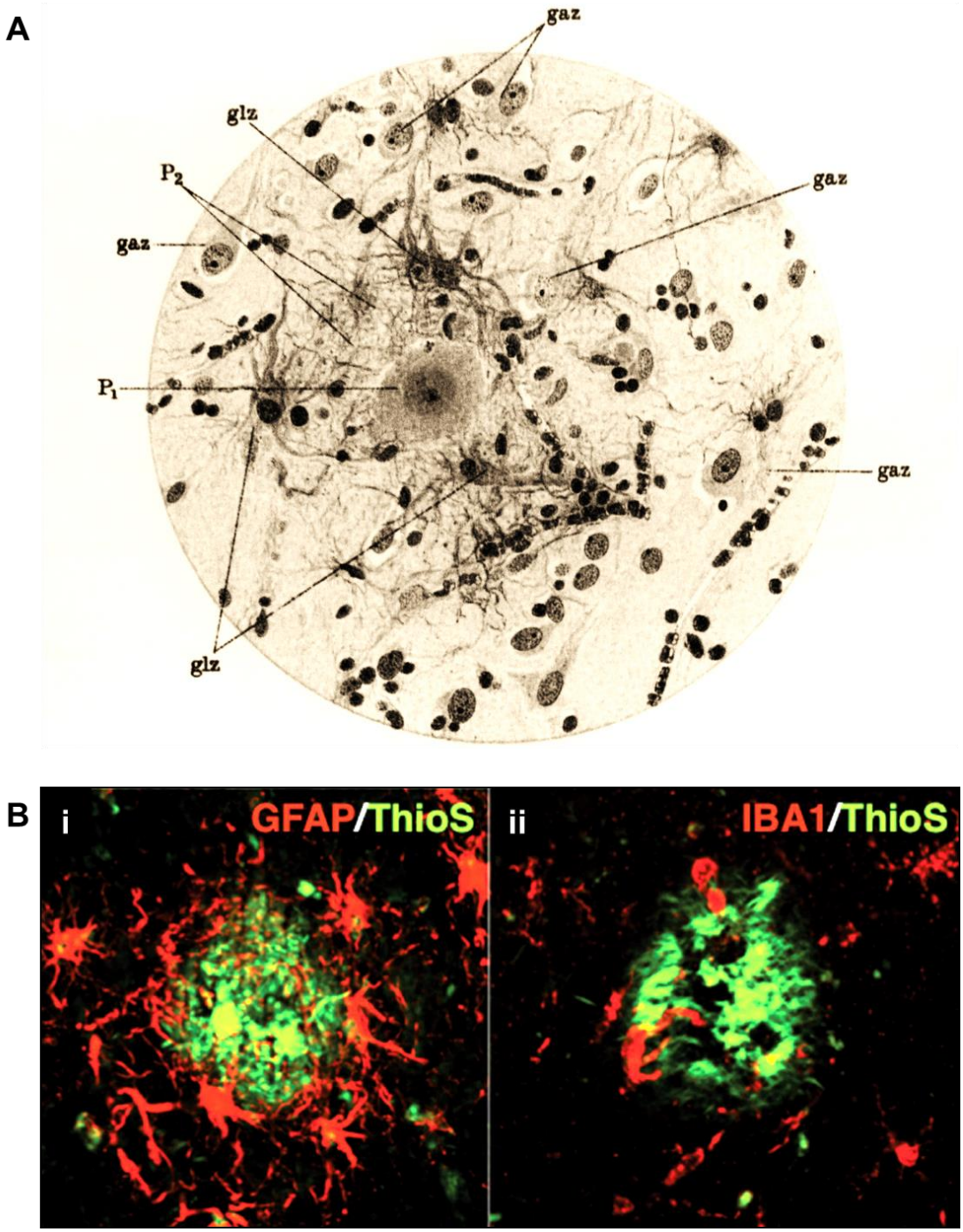

Figure 1.9: Amyloid Plaque Associated Reactive Gliosis

A representation of glial cells (glz) surrounding the central amyloid plaque (P1). Abbreviations: gaz, neuron; glz, glial cell; P1, central core of plaque; P2, peripheral part (halo) of plaque (A). Immunohistochemical representation (B) of amyloid plaque labelled with Thioflavin-S (ThioS) surrounded astrocytes labelled with antibody against glial fibrillary acidic protein (GFAP, i); and ionized calcium binding adaptor molecule 1 (IBA1) immunoreactuive microglia (ii). Figure A was taken from Alzheimer et al (1991) and Figure B adapted from Serrano-Pozo et al (2013).

1.3.3.4.1 Microglia

Microglia have been shown to accumulate in the vicinity of amyloid plaques in brains of AD individuals at autopsy and animal models of AD (Malm et al 2015). The role of microglia in progression of AD is controversial; but over the years it has been suggested that this cell population may play a dual role in the pathogenesis of AD. One being degradation and clearance of Aβ via phagocytosis (beneficial); and the other, an inflammatory response whereby these cells release cytokines and chemokines which can trigger detrimental signalling pathways in other glial cells and neurons leading to further disease progression (Bagyinszky et al 2017, Heneka et al 2015, Wyss-Coray 2006). It has been illustrated that in AD, microglia are attracted and subsequently activated by Aβ (Streit 2004). Aβ oligomers or fibrils can bind to a number of cell-surface receptors expressed by microglia, including: triggering receptor expressed on myeloid cells 2 (TREM2), receptor for advanced glycosylation end products (RAGE), class A scavenger receptor (SCARA), CD36, CD14, α6β1 integrin, CD47, and Toll-like receptors (TLR2, TLR4, TLR6, and TLR9). Stimulation of these receptors by Aβ induces activation of multiple parallel signal transduction cascades which in turn stimulates the nuclear factor kappa B (NFκB)-dependent transcription of pro-inflammatory cytokines, generation of reactive oxygen species (ROS), and phagocytosis (Heneka et al 2015, Malm et al 2015, Ramirez et al 2017).

In-vivo two-photon imaging in double-transgenic APP reporter mice (PDAPP;CX3CR1/GFP) revealed recruitment of microglia to the site of a newly formed plaques within a day (Meyer-Luehmann et al 2008). Aβ deposits attract and activate microglia via MCP-1, MIP-1α, MIP-1β, IL-8, and M-CSF, which may mediate microglial attraction to plaques (Mosher & Wyss-Coray 2014). A large body of evidence supports the role of microglia in degradation and clearance of Aβ via the process of phagocytosis. It is thought to be mediated by binding of Aβ oligomers or fibrils to microglial cell surface expressed receptors, namely TREM2, CD36 and TLR, which induce internalisation of the Aβ-receptor complex (phagosome) that is subsequently trafficked to the lysosomal compartment where it is degraded by a host of proteases including cathepsin B (CatB) (Arcuri et al 2017, Malm et al 2015). In addition to phagocytosis, activation of TREM2 receptor has also been associated with suppressing the secretion of pro-inflammatory cytokines and ROS (Arcuri et al 2017). Evidence form TREM2 deficient mice in the 5XFAD mouse model

of AD revealed lack of microgliosis, diminished capacity of microglia to accumulate in vicinity of amyloid plaques, increased concentration of toxic Aβ42 accompanied by reduced nuclear density in the hippocampus and cortex in comparison to 5XFAD control. This would indicate a role of TREM2 in microglial activation and migration to site of amyloid deposition as well as clearance of Aβ, which collectively in important for neuronal integrity (Wang et al 2015). Furthermore, mutations in TREM2 have been associated with increased risk of developing AD (Jonsson et al 2013). Finally, besides phagocytosis, microglia have been shown be involved in clearance and degradation of Aβ via secretion of Aβ-degrading proteases neprilysin and insulin-degrading enzyme (IDE) (Heneka et al 2015). Collectively these findings implicate a potential beneficial role of microglia in hindering the progression of AD via degradation and clearance of AD-associated pathological hallmarks.

However, there is also mounting evidence that in contrast argues the detrimental role of microglia in pathogenesis of AD; as demonstrated by secretion of pro-inflammatory cytokines and chemokines accompanied by ROS in response to Aβ deposition. Aβ deposits have been illustrated to act as chronic stimuli for microglial activation through interaction with CD36, TLR4, and TLR6 cell surface receptors. Chronic activation of microglial cells has been implicated to induce neuronal damage via release of cytotoxic chemical substances through an uncontrolled amplification of self-propagating cycle (Gao & Hong 2008, Heneka et al 2015, Streit et al 2004). Evidence from genetic deletion of CD36, TLR4, or TLR6 in-vitro have demonstrated reduction in Aβ- induced production of cytokines as well as prevention of intracellular accumulation of Aβ (Heneka et al 2015).

In addition, it has been proposed that sustained exposure to Aβ, cytokine and chemokines may result in microglial cells dysfunction that consequently leads to failure to perform their functional role of restoring homeostatic environment in the CNS, which subsequently leads to neuronal dysfunction and death (Heneka et al 2015, Streit 2004). As aforementioned, Aβ can attract and activate microglia that results in recruitment and proliferation of microglia around the plaques, which may serve as a first line of defence restricting the spread of amyloid pathology. However, in AD it seems that despite formation of microglial barrier around the amyloid plaques, there is an inability to degrade and clear the pathology with microglial senescence (Heneka et al 2015,

Krabbe et al 2013, Mosher & Wyss-Coray 2014, Ramirez et al 2017). Further evidence in support of this notion arises from in-vitro studies using cultured adult microglia, which demonstrated reduced ability of microglia to internalise Aβ peptide in comparison to young microglial cells (Floden & Combs 2011, Njie et al 2012). Age dependent decline of microglial cell surface Aβ-binding receptors as well as Aβ-degrading enzymes in the APP/PS1 transgenic mouse model of AD were reported (Hickman et al 2008). The underlying reasons for such changes are not fully understood, although it has been suggested that microglial-specific genetic alteration may play a role in microglial dysfunction. Of particular interest upon which microglial phagocytosis is reliant on is beclin 1, a protein that is often associated with autophagy. Beclin 1 may promote phagocytic clearance of Aβ via retromer-mediated recycling of the phagocytic receptors CD36 and TREM2 in microglia. Beclin 1 deficiency has been shown impair recycling of these receptors thereby disrupting the process of microglial mediated phagocytosis. Individuals with AD have been reported to have reduced levels of beclin 1 in the brain, which may be responsible for the inability of these cells to phagocytose amyloid deposits efficiently (Lucin et al 2013, Malm et al 2015, Mosher & Wyss-Coray 2014). Amongst the recent pathways that have been described for intracellular signalling upon Aβ interaction with microglial cells is the NLRP3 inflammasome. NLRP3 inflammasome is an intracellular protein complex that upon activation can regulate activity of caspase-1, which in turn catalyses the cleavage, activation and subsequent release of pro-inflammatory cytokines (i.e. IL-1β) that can induce neuronal degeneration. Moreover, the NLRP3 inflammasome activation reduces Aβ phagocytosis via interaction with beclin 1, thus increasing Aβ deposition and contributing towards the pathogenesis of AD (Malm et al 2015, Mosher & Wyss-Coray 2014, Ramirez et al 2017).

1.3.3.4.2 Astrocytes

Likewise to microglia, in the brains of AD patients and animal models of this disease, reactive astrocytes have been illustrated to be closely associated with amyloid plaques (Verkhratsky et al 2010). Further evidence shows that reactive astrocytes are present in high concentration, forming scar-like barriers around the perimeter of Aβ deposits (Fuller et al 2009, Heneka et al 2015). Moreover, tissue levels of the protein S100β, a marker of astrocytes, have been shown

to correlate with the number of neuritic plaques (Farfara et al 2008, Marshak et al 1992, Sheng et al 1994). Collectively, these evidences indicate that astrocytes are involved in the progression of AD, although their role is unclear.

Increasing evidence is debating on the potential beneficial or detrimental role of astrocytes in AD. Several studies have shown that astrocytes are involved in the clearance and degradation of Aβ plaques (Guenette 2003, Kurt et al 1999, Nicoll & Weller 2003, Pihlaja et al 2011, Verkhratsky et al 2010, Wegiel et al 2000) and are attracted to Aβ plaques where they can potentially internalise and degrade Aβ deposits in human brain sections in-vitro (Koistinaho et al 2004, Nagele et al 2003, Wyss-Coray et al 2003). In addition, green fluorescent protein (GFP)-expressing astrocytes transplanted in an AD mouse model, were shown to migrate toward the amyloid plaques, where they internalised Aβ peptides (Pihlaja et al 2008). Although the mechanism underlying this notion is still unclear, some studies suggest the potential role of ApoE, which is primarily synthesised and secreted by astrocytes in the brain and is proposed to be responsible for internalisation and subsequent degradation of Aβ peptides (Fagan & Holtzman 2000, Farfara et al 2008, Koistinaho et al 2004). Furthermore, astrocytes that are in the close vicinity to amyloid plaques were shown to have a higher expression of Aβ degrading enzymes such as neprilysin and IDE (Verkhratsky et al 2010).

Moreover, astrocytes have been demonstrated exert protective effects in AD via inhibition of activated microglia (Sidoryk-Wegrzynowicz et al 2011). It has been shown that Aβ peptides induce secretion of transforming growth factor β (TGFβ) from astrocytes. This in turn inhibits inducible nitric oxide synthase (iNOS) activity in microglia; thereby inhibiting the neurotoxic effects of NO exerted on neurons (Sidoryk-Wegrzynowicz et al 2011, Vincent et al 1997). In addition, astrocytes have been shown to form a halo or scar around the Aβ plaque and therefore demarcating the damaged area and restricting the spread of inflammation (Rodriguez et al 2009, Sidoryk-Wegrzynowicz et al 2011).

However, other studies argue to the detrimental role of astrocytes and its contribution in accelerating the progression of AD; as Aβ interaction with astrocytes induces loss of physiological homeostatic functions of astrocytes, which include disturbance of glucose metabolism and impaired regulation of glutamate thus leading to impairment of neuronal viability

and excitotoxicity respectively (Allaman et al 2010, Fuller et al 2009, Sidoryk-Wegrzynowicz et al 2011, Tian et al 2010). Additionally, it has been reported that Aβ-induced activation of astrocytes leads to secretion of pro-inflammatory mediators, such as TNFα and IL-1β, which can cause neuronal injury (Heneka et al 2010, McGeer & McGeer 2002, Rossi & Volterra 2009).

Therefore, the role of both microglia and astrocytes in AD is still elusive as it is not clear if their reactions to AD-associated pathology are beneficial or detrimental in the pathogenesis of AD.

1.3.3.5 **Neuronal Loss and Synaptic Dysfunction**

Synaptic dysfunction and neurodegeneration are key features underlying memory dysfunction in individuals with AD. Loss of synapses is an early feature of AD which may precede neuronal loss. Earlier studies reported decrease in synaptic density in the frontal, temporal, and the dentate gyrus of the hippocampus using electron microscopy and immunohistochemical techniques. It is one of the strongest pathological correlate to dementia as illustrated by significant correlation between decrease in synaptic number and Mini Mental State Examination (MMSE), a surrogate marker of cognitive ability; whilst less association was considered to be with AD-associated neuropathological hallmarks, despite both Aβ and tau pathologies contributing to this loss (DeKosky & Scheff 1990, Spires-Jones & Hyman 2014, Terry et al 1991). Furthermore, individuals with mild cognitive impairment (MCI), a transitional stage between healthy control and AD, exhibited synaptic dysfunction prior to deposition of amyloid plaques and NFT; indicating synaptic loss as a key early characteristic of AD. Moreover, the same study reported progressive decrease in synaptic density, as demonstrated by 18% in MCI increasing to 55% in individuals with mild AD at autopsy, compared to healthy controls (Scheff et al 2007). Altogether implicating that synapses may play a key role in both the initiation and the spread of disease processes throughout the brain (Spires-Jones & Hyman 2014).

Neuronal loss in AD is the main pathological substrate underlying cortical atrophy at autopsy which also correlates to cognitive deficits in the disease. It has been made evident that neuronal cell death closely follows the spatiotemporal regional and laminar pattern of that exhibited by NFT in the entorhinal cortex and superior temporal gyrus. Although, the level of neuronal loss has been demonstrated to be relatively greater than NFT containing cells, which implicates that not only cellular accumulation of AD-associated aggregates but other factors may also

contribute in neuronal dysfunction and eventual death (GomezIsla 1997, GomezIsla et al 1996). Indeed, a quantitative stereological assessment of the prefrontal cortex, entorhinal cortex and hippocampus revealed that intracellular NFT can last up to two decades indicating that these cells remain viable throughout this period despite the presence of intracellular NFT inclusions; although whether they remained functional was debatable. Therefore, leading to a suggestion that there may be two dissociate pathways that may underlie the greater neuronal loss in comparison to NFT-containing cells within the same region: one affecting NFT-containing neurons that will eventually become dysfunctional and degenerate to appear as extracellular ghost tangles; and another affecting NFT-free neurons, possibly owed to their presence in close vicinity of tangle containing neurons and thus exposure to the neurotoxic molecules secreted by glial cells in the inflammatory process (Bussiere et al 2003, Hof et al 2003, Serrano-Pozo et al 2011).

Moreover, evidence provided by PET imaging display synaptic dysfunction and neuronal loss in AD by a corresponding progressive decline in brain cerebral metabolic rate for glucose, using fluorodeoxyglucose, [18F] FDG, as a marker, which precede the onset of clinical symptoms by several years and correlates with dementia severity and pathological diagnosis of AD (Mosconi et al 2009, Raskin et al 2015). As a result, number of systems (i.e. cholinergic, opioidergic and monoaminergic) are affected, which, collectively, are responsible for the broad and profound clinical presentation of AD (Cai & Ratka 2012, Ferreira-Vieira et al 2016, Simic et al 2017). Detailed overviews of these systems are beyond the scope of this thesis and therefore a brief outline highlighting the changes and regions affected will be described. One of the most prominent neurochemical dysfunction associated with AD is the development of cholinergic hypofunction, demonstrated by marked reduction in the enzyme choline acetyltransferase (ChAT) responsible for acetylcholine (ACh) synthesis thereby decrease in ACh neurotransmitter accompanied by reduced ACh receptors (Bowen et al 1976, Ferreira-Vieira et al 2016, Perry et al 1978). Amongst the earlier observation in the brain autopsy of AD individuals were reduced cholinergic projections from the basal forebrain, in particular the nucleus basalis of Meynert (NBM), to the cortex and hippocampus accompanied by loss of ChAT activity. The underlying reason can be explained by the severe loss of cholinergic neurons in the NBM (Whitehouse et

al 1981). These cholinergic deficits (i.e. ChAT reduction) progress with the severity of disease which have been closely correlated with the impairment of attention and memory and amyloid pathology observed in patients with mild to moderate AD using PET imaging (Ferreira-Vieira et al 2016, Kuhl et al 1999, Raskin et al 2015). Further evidence from MRI imaging demonstrated exacerbation of age-related atrophy in NBM in individuals with AD that were detected at the earliest stage of cognitive impairment; and also associated with severity of cognitive impairments with the progression of AD (Grothe et al 2012, Grothe et al 2010, Teipel et al 2011).

Another system that appears to be dysfunctional in AD is the monoaminergic system, which can be further sub-divided into the serotoninergic, noradrenergic, dopaminergic and histaminergic systems; contributes to AD-associated oxidative stress via increased activity of the monoamine oxidase enzymes A and B (MAO-A and MAO-B).The MAO enzymes are involved in catalysis of various biogenic and xenobiotic amines, including monoamine neurotransmitters, such as 5-HT, NA and dopamine; leading to generation of aldehydes and hydrogen peroxide (H_2O_2). Therefore, increased activity of these enzymes result in decrease in CNS monoamines in individuals with AD (Weinreb et al 2016). Moreover, results from AD human post-mortem tissue have provided additional evidence for diminished monoamines, their metabolites and receptors, in a number of brain regions, due to the loss of neurons owed to AD-associated NFT pathology (Simic et al 2017). Amongst the component of monoaminergic system and the regions affected include the: serotoninergic dorsal raphe nucleus (DRN), noradrenergic LC (up to 80% neuronal loss), dopaminergic substantia nigra pars compacta (SNpc), and histamine containing neuronal population in tuberomammillary nucleus of the hypothalamus (Attems et al 2012, Bondareff et al 1982, Braak et al 1993, Simic et al 2017). Collectively these deficits in the monoaminergic system have been indicated to be associated with the impairment in cognitive functions (i.e. responsiveness to novel stimuli, vigilance, learning through reinforcement), as well as the behavioural and psychological symptoms of dementia (BPSD) that include mood disorder, agitation, and disrupted sleep-wake cycle (Simic et al 2017). In addition, the noradrenergic projections innervate cerebral vasculature and regulate neurovascular coupling, which is shown to be diminished in AD, which results in reduced ability to couple blood volume to cellular

oxygen demand and thereby may contribute directly to the pathogenesis of AD (Bekar et al 2012).

Finally, alterations in the opioidergic system have been suggested to be involved in pathogenesis of AD via dysregulation of a number of neurotransmitters (i.e. glutamate, GABA, ACh, and monoamines), promoting Aβ production, abnormal tau hyperphosphorylation, and neuroinflammation, which eventually leads to presentation of cognitive impairment (Cai & Ratka 2012). Alterations in the opioidergic system in AD have been reported in the form of expression of the opioid peptides (i.e. enkephalins (ENK)) in a few NFT containing neurons in the subiculum and hippocampus of AD individuals at autopsy, with additional evidence indicated abnormal ENK labelling of axons/fibres and neurites within the amygdala and globus pallidus (Kulmala 1985, Matsumoto et al 1990, Struble et al 1987). Furthermore, increased immunoreactivity of ENK in the hippocampus as well as elevated levels in the cerebrospinal fluid (CSF) were reported in this disease group cohort; implicating a change in the opioidergic content in AD (Muhlbauer et al 1986, Risser et al 1996, Yew et al 1999). Reports of AD individuals with high use of opiates outlined an increase in abnormal hyperphosphorylation of tau, in the form of NT, in the frontal, temporal and LC (Anthony et al 2010). Moreover, evidence from transgenic mouse models of AD have illustrated increased ENK brain content (especially in the hippocampus), which correlated with Aβ-associated neuronal and behavioural changes, and may play a role in cognitive impairment (Meilandt et al 2008). In addition, alterations in opioidergic receptor expression have also been demonstrated with the most prominent being reduced mu (μ) and delta (δ) opioid receptor immunoreactivity or binding within the amygdala, hippocampus, and subiculum; whilst increases in the kappa (κ) opioid receptors in the striatum, temporal and frontal cortical and sub-cortical regions (Hiller et al 1987, Mathieu-Kia et al 2001). Altogether, these alterations in the opioid peptides and their respective receptor have been implicated to be involved in the pathogenesis of AD and contributing to cognitive impairment in the disease (Cai & Ratka 2012).

1.3.4 The Amyloid Cascade Hypothesis

There are a number of hypothesis postulated in relation to pathogenesis of AD; however, a detailed overview of these theories is beyond the scope of this work. The leading theory of the

progression of AD is the amyloid hypothesis based on evidence supporting altered processing of the APP due mutations in APP and/or PS1/2 as one of the early events in the pathogenesis of AD (Hardy & Allsop 1991). Broadly the most recent revision of the theory, on the basis of advancement in the field, proposes that, whether due to a genetic mutation in APP or PS1/2 (in familial EOAD cases) or through another cause (i.e. ApoE4 in sporadic LOAD cases), toxic forms of Aβ are produced. An imbalance in in the production and/or clearance of Aβ results in accumulation of Aβ, which in turn triggers a cascade of events leading to aberrant phosphorylation of tau, impairing tau function and initiating its aggregation into PHF and NFT that causes neurodegeneration. Altogether the progressive cascade of neurotoxic events manifests clinically as impairment of memory and other symptoms associated with dementia (Hardy & Selkoe 2002, Selkoe & Hardy 2016). The overview of the hypothesis is illustrated in Figure 1.10.

The hypothesis has gained support over the years due to several observations suggesting that tau hyperphosphorylation may be a downstream process induced by Aβ. Firstly, familial mutations in APP as well as PS1/2 (rare) are a cause for EOAD that is associated with neuropathological and clinical manifestations of AD. Such mutations in mouse models of AD result in increase of the Aβ42/ Aβ40 ratio, which is the insoluble and neurotoxic form of Aβ; either owed to an increase in Aβ42 and/or a decrease in Aβ40; leading to subsequent increase in plaque formation which coincide with cognitive deficits (Citron et al 1997, Duff et al 1996, Singh et al 2016). Secondly, evidence from transgenic mice overexpressing mutant human APP and mutant human tau revealed increased formation of tau tangles compared to transgenic mice only harbouring the tau mutations (Lewis et al 2001). In support of this notion, evidence from hippocampal cell culture demonstrated that Aβ-induced toxicity is dependent on tau as illustrated by lack of neurodegeneration in tau-depleted neurons in the presence of Aβ (Rapoport et al 2002). Thirdly, crossing ApoE knockout mice with a transgenic mouse overexpressing the human mutant APP gene (PDAPP) revealed a dramatic decrease in amyloid deposits within the hippocampus and cortex in comparison to PDAPP mice. Thus, implicating a possible role of ApoE in plaque formation and supporting the ApoE genotype as a relative risk factor for developing LOAD, with increased Aβ being a chief source; although it was not

determined whether the three isoforms of ApoE (ApoE2, ApoE3, or ApoE4) had different impact on Aβ depositions (Bales et al 1997). Finally, observations of low levels of Aβ42 in CSF and positive increased amyloid PET radio-ligand retention prior to detection of other changes associated with AD (i.e. increase in CSF tau concentration, decreased cerebral glucose metabolism, brain atrophy, and clinical dementia) indicate Aβ as an upstream mediator that may initiate and drive the cascade of events (Craig-Schapiro et al 2009). The emergence of this theory led to development of several models of AD harbouring mutations in the APP and/or PS1/2 that recapitulated several but not complete pathological and behavioural characteristic of AD. These transgenic mouse models were termed as amyloidogenic modelling of AD, which have played an important role in delineating key mechanisms involved in the pathogenesis and behavioural phenotype in relation to AD (Elder et al 2010). A general overview of animal models of AD will be discussed in Chapter 2.

Due to the simplicity of the amyloid cascade hypothesis many have raised criticism in relation to the linearity of the theory. A large body of evidence suggest that there may be multiple pathways involved at many stages of the cascade and also dispute the role of Aβ as an initiator (De Strooper & Karran 2016). Firstly, deposition of Aβ has been observed in cognitively-intact individuals. Furthermore, there is a weak of correlation evident between the load of amyloid plaques and the progression of the disease, in the form of cognitive deficits (Morris et al 2014). Secondly, the revised amyloid hypothesis in principle is attempting to integrate the common factor of both EOAD and LOAD characteristics, namely the pathological hallmarks of AD; but at the same time fails to take into account the heterogeneity in nature. Both EOAD and LOAD exhibit differences in: (1) age of onset (2) temporal progression of disease; and (3) variability and severity of cognitive deficits. As a result it would implicate possibly different mechanisms underlying variability in pathological progression and clinical presentation of AD in EOAD and LOAD (Morris et al 2014). Thirdly, clinical evidence from anti-Aβ immunotherapy till date has provided little success as the human monoclonal antibodies were either: poorly tolerated giving rise to adverse side effect; or were able to reduce Aβ but failing to improve cognition (Rygiel 2016). Finally, the causative link between Aβ and tau hyperphosphorylation remains largely elusive, as illustrated by amyloidogenic animal models of AD that fail develop tau pathology;

with mutations in both APP and MAPT required in order to fully resemble the pathological aspect of AD (Elder et al 2010). Despite these inconsistencies, the genetic cause of AD is indisputable, the amyloid cascade hypothesis is still a valuable starting point for research in the field of AD (Selkoe & Hardy 2016).

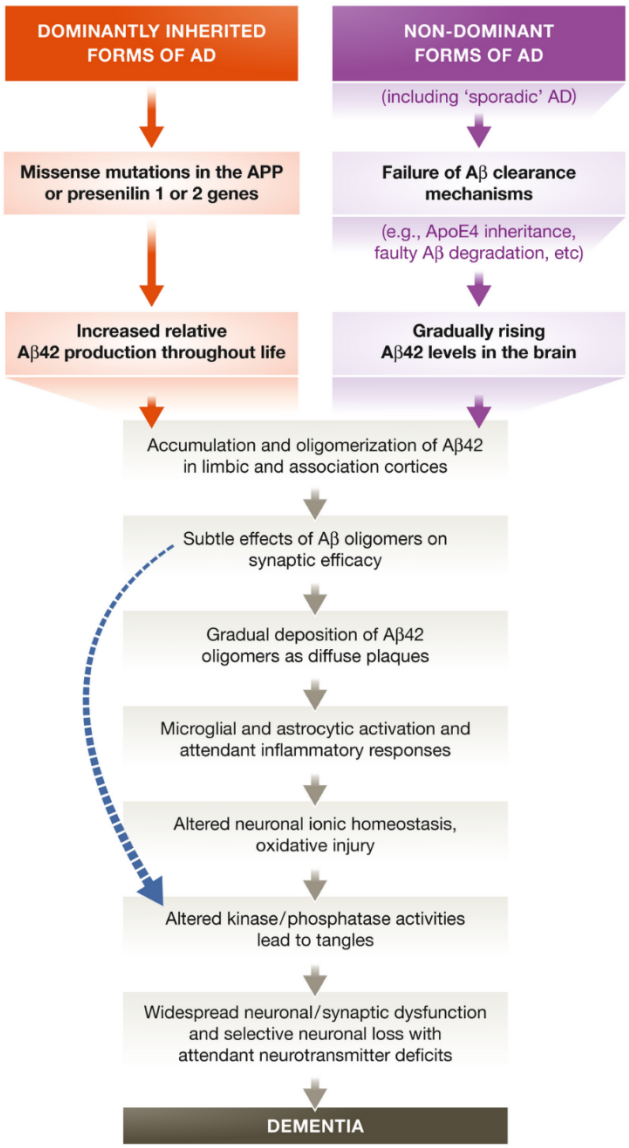

Figure 1.10: The Amyloid Cascade Hypothesis

A representation of sequence of pathogenic events leading to AD, identifying the increased level of Aβ as the chief causative factor. Increase in levels of Aβ1-42 in both: autosomal dominant inheritance due of mutations in APP and presenilins (PS1/2) (red arrows); and sporadic AD owed to ApoE (purple arrows), due to an imbalance in the production and/or clearance of Aβ peptide results in accumulation of Aβ which in turn can either directly (blue arrow) or indirectly via a cascade of events (i.e. neuroinflammation) trigger the formation of tau NFT, which eventually results in synaptic and neuronal dysfunction. Figure taken from Selkoe and Hardy (2016).

1.4 Pain: A Clinical Issue in Alzheimer's disease

Pain is as common in individuals with AD as in the general elderly population. In particular, over one-third of individuals with dementia are estimated to reside in care homes (Knapp & Prince 2007). These individuals often have moderate to severe dementia associated with medical health symptoms, medical comorbidity, and communication difficulties that requires highly complex treatment and care needs. Pain is an important clinical issue in patients with AD, which is a major contributor to challenge of care and is often associated with medical comorbidities, particularly musculoskeletal conditions and long-term neuropathic pain conditions such as diabetes. Despite availability of pain treatment options, assessment and treatment of pain in AD is often difficult, thereby having a negative impact on the quality of life (Ballard et al 2009, Corbett et al 2012, Corbett et al 2014, Rajkumar et al 2017). In fact, prevalence of pain in dementia has been estimated to be ~30% - 80%, and the presence of pain is associated with distress and neuropsychiatric symptoms (Corbett et al 2012, Husebo et al 2011, Rajkumar et al 2017). Recent studies suggest that patients with AD do not report pain as often and are prescribed analgesics less frequently compared to age-matched individuals without AD (Cohen-Mansfield 2008, Scherder 2000). Under-treated and inappropriate prescribing in this patient group results in reduced mobility, muscle weakness and falls, which consequently has a major detrimental impact on quality of life.

The major difficulty in assessment and treatment of pain in individuals with dementia is the deteriorating ability to communicate, which hinders their capacity to describe their suffering and self-report the location and duration of pain (Corbett et al 2012). Thus behaviour observational tools have been developed in order to assess pain in people with advanced stages of dementia. Typical signs that can be considered as perception of pain in individuals with dementia include: repetitive verbal complaints, negative vocalizations, restlessness, agitation, grimacing, inappropriate verbal speech, and aggression. However, in people with cognitive impairment, these signs may be taken as BPSD, which makes assessment of pain in people with dementia difficult (Husebo et al 2016, Malara et al 2016). Therefore, pain is considered as a key trigger for BPSD such as agitation and mood disorders, which are a major treatment challenge and can

result in overprescribing of harmful anti-psychotic medications (Ballard et al 2014, Rajkumar et al 2017).

1.4.1 Aetiology and Prevalence of Pain in Cognitively Impaired Individuals

Accumulating evidence reveal the existence of pain in individuals with cognitive deficits. In general, the aetiology of pain in people with cognitive impairment is not different from cognitively-intact individuals. The most common causes of pain in individuals with cognitive impairment include: musculoskeletal pain (i.e. OA), post-surgery/fractures, neuropathic pain (i.e. diabetic neuropathy), cancer, genitourinary infection (i.e. peptic ulcers), and fall-related injuries (Corbett et al 2012, Pickering et al 2006, Proctor & Hirdes 2001).

Evidence from earlier studies that conducted interviews, nurse observations, pain experience scales, and review of medical records of nursing home residents and geriatric outpatients revealed approximately 32% - 62% of individuals with cognitive deficits experienced some form (acute or persistent) of pain (Ferrell et al 1995, Shega et al 2004). However, the limitations of these studies were exclusion of subjects with cognitive deficits who were unable communicate and also those individuals that were not capable of attending the outpatient clinic. Therefore, the figures reported may not completely reflect the prevalence of pain in individuals with cognitive deficits.

More recent studies have reported pain affecting approximately 30% - 80% of individuals with dementia. One of which is a longitudinal Dutch End of Life in Dementia observational study, which assessed frequency of pain, prevalence of agitation/aggression, and the use of analgesic medications in 372 nursing home residents with variable stages of dementia. Prevalence of pain was reported to vary from 47% to 68% in individuals with dementia over the course of the study that increased to 78% in individuals during their terminal stage of life. The pharmacological intervention most frequently used was paracetamol (ranging from 34% - 52%), and at the end of life with parenteral opioids (44%). Agitation was commonly observed in up to 70% of individuals that persists but to a lesser extent in the final weeks of patient life (~35%), which indicates a possible association with pain in individuals with dementia (Hendriks et al 2015).

Further evidence from Malara and co-workers in a cross-sectional study evaluated the prevalence of pain in individuals with progressively deteriorating cognitive abilities in 233 long term care facilities residents. They utilised the MMSE as an assessment of cognitive ability; with pain assessments conducted using self-reporting of numeric rating scale (NPS) in individuals with no or mild cognitive deficits (MMSE score = 21 - 23) and Pain Assessment In Advanced Dementia Scale (PAINAD) for individuals of MMSE scores less than 20; and behavioural examination performed using the Neuropsychiatric Inventory (NPI) and Cohen-Mansfield Agitation Inventory (CMAI). Their results demonstrate prevalence of pain detected (ICD-9 diagnosed) in 46.4% of individuals with mild cognitive deficits of which 97% were taking analgesic medications. PAINAD revealed 51.8% of moderate-severe cognitively impaired individuals (MMSE score < 20) experiencing some form of pain or chronic pain condition of which only 47% received analgesic medication (mainly paracetamol accounting for 48.3% of analgesic use) and musculoskeletal pain represented the most prevalent source (36.5%). Pain in moderate-severe cognitively impaired individuals was associated with BPSD including increased agitation (Malara et al 2016).

Studies conducted in the UK on pain in individuals with dementia showed that 27% of patients with cognitive deficits admitted in hospital (n = 270) self-reported an experience of some form of pain, with PAINAD determining pain in 19% of the subjects at rest increasing to 57% during movement. Pain experiences in these individuals were also reported to be associated with BPSD, which mainly included aggression and anxiety. Hence implicating the negative distressing impact pain may have on patient's quality of life in individuals with cognitive deficits (Sampson et al 2015). In addition, evidence from 967 individuals with dementia residing in 67 care homes in London revealed pain, assessed using the Abbey pain scale (APS), in 35.3% of the participants of which only 58.1% were treated with analgesics. Moreover, the severity painful experience was generally demonstrated to be correlated with BPSD using measures including CMAI and NPI (Rajkumar et al 2017). These findings further reinforce the notion that pain experience in dementia leads to the development of BPSD, which have a negative impact on the quality of life of an individual.

Altogether these studies collectively suggest that pain is an important clinical issue in the elderly population with cognitive deficits. However, there are certain limitations in terms of the different parameter utilised by individual groups in order to assess level of cognitive deficit, presence of pain, and assessment of BPSD that makes it difficult to make direct comparison between observations in different populations. Furthermore, all assessments in most studies were conducted by a single physician or research assistant, which raises curiosity on the reproducibility of data within a given population. Therefore, future work is required in order to establish a validated 'gold-standard' criterion for assessment of pain in individuals with cognitive impairment, which would allow identification and as result potentially improved management of pain in these elderly individuals.

1.4.2 Management of Pain in Individuals with Cognitive Deficits

Despite pain being a prevalent issue in individuals with cognitive deficits, assessment and management of pain is often difficult, which in consequence results in a negative impact on the individuals' quality of life (Ballard et al 2009, Corbett et al 2012). Amongst the earlier studies that compared the prescription of analgesics in nursing home residents with cognitive impairment and cognitively-intact controls, with diagnosis of a pain condition (i.e. cancer, chronic pain, and musculoskeletal conditions), revealed less likelihood of cognitively impaired individuals diagnosed for musculoskeletal condition and significantly fewer analgesics prescribed to cognitively impaired individuals than their cognitively intact peers. Moreover, it was evident that the more withdrawn and disorientated residents were prescribed significantly less analgesics (Horgas & Tsai 1998). However, evidence for the level of cognitive impairment associated with reduction in prescription of analgesics was not provided by this study as data was presented for only two groups: with or without diagnosis of cognitive impairment.

Further evidence from patients recovering from hip fracture surgery demonstrated the individuals with cognitive impairment received three times less opioid analgesics in comparison to their cognitively intact counterparts (Morrison & Siu 2000). In addition, a study conducted by Feldt et al (1998) demonstrated significantly lower administration of opioids analgesics during the first four days post hip fracture surgery in cognitively impaired individuals despite scoring significantly higher on Checklist of Nonverbal Pain Indicators observed with movement (CNPI-

m) compared to cognitively-intact controls. These observations indicate that undertreatment of pain in individuals with cognitive impairments may be due to either inability to report pain in this population and/or altered perception of pain. This can consequently result in distress and neuropsychiatric symptoms including agitation, aggression, and depression in these individuals.

Indeed, a cross-sectional evaluation of pain treatment, in a collection of twelve Austrian nursing homes, in accordance to individual's cognitive ability demonstrated that despite higher prevalence of pain in cognitively impaired individuals (~80% compared to ~66% in cognitively intact), significantly less analgesics were prescribed in comparison to cognitively intact group. Cognitively impaired individuals were typically prescribed fewer non-steroidal anti-inflammatory drugs (NSAID). Moreover, it was highlighted that cognitively impaired individuals are more susceptible of not getting analgesics prescribed when in pain, with those unable to verbally communicate affected the most, in comparison to cognitively intact residents. Finally, it was also reported that more anti-psychotic drugs were prescribed in the cognitively impaired group; further reinforcing the notion that pain is inappropriately managed in individuals with cognitive deficits and may be associated BPSD (Bauer et al 2016).

However, conflicting evidence stemming from studies conducted mainly in Scandinavia reveal either unaltered or increased prescription of analgesics in individuals with dementia. Sandvik et al (2016) provide evidence for in trend for prescription of analgesics between 2000 and 2011 in Norwegian nursing home individuals, as illustrated by 65% increase in prescription. In particular increase in prescription of paracetamol (113% increase) and strong opioids (increased from 1.9% in 2000 to 17.9% in 2011), whist the decrease in use of NSAID (decreased from 6.8 in 2000 to 3.2%.in 2011) and weak opioids (~26% decrease) were observed. It was reported that in earlier years of 2000, 2004, and 2009, individuals with cognitive impairment were prescribed relatively fewer analgesics in comparison to cognitively intact group; however in 2011, no differences in overall analgesic drug use was observed between the groups were found in 2011. Thus implicating equal prescription of analgesic drugs in individuals with dementia compared to non-dementia control residents.

Further evidence from Swedish home and institutionalised residents revealed increased use of analgesics in individuals with dementia (46%) in comparison to non-demented controls (25%)

despite infrequent self-reporting of pain in the former group. Moreover, individuals with dementia were more likely to use paracetamol as analgesics as well as anti-psychotic drugs (Haasum et al 2011). Thus, implicating that pain may be associated with BPSD in individuals with cognitive impairment. A notion further reinforced by a study analysing the use of analgesics in the elderly Swedish and Finish population, as demonstrated by more common use of analgesics, in particular paracetamol, and anti-psychotic as well as anti-depressants, despite unaltered experience of pain, among individuals with dementia compared to cognitively intact cohort (Lovheim et al 2008).

Whereas in a Danish study comprising of home-dwelling and nursing home residents demonstrated increased use of opioids with age; and most frequent use amongst nursing home resident as well as home-dwelling individuals with dementia (Jensen-Dahm et al 2015). Collectively, the discrepancies in the prescription of analgesics in individuals with cognitive deficits implicate the lack of understanding of pain mechanisms and/or assessment underlying in this susceptible patient group. Evidence for prescription and use of analgesics in the cognitively impaired population is not sufficient to deduce the effectiveness of these drugs in relieving pain. Thus, pharmacological studies have been conducted in order to evaluate the effectiveness of these drugs in inducing analgesia.

Evidence from parallel-group randomised control trials conducted to evaluate treatment of pain in 352 individuals with moderate to severe dementia residing in 18 Norwegian nursing homes using stepwise analgesic treatment for a period of 8-weeks with an additional follow-up 4-weeks post termination of treatment or to usual treatment (controls). Participants in the treatment group received individual daily treatment of pain for eight weeks according to the stepwise protocol, with paracetamol, morphine, buprenorphine transdermal patch, or pregabalin; whilst the control group received usual treatment and care. It was noteworthy that majority of the subjects (~63%) in the treatment group received paracetamol as treatment. Parameters assessed as measure of improvement were agitation (CMAI), aggression (neuropsychiatric inventory-nursing home version (NPI-NH)), pain (mobilisation-observation-behaviour-intensity-dementia-2 (MOBID-2)), daily functional activity, and cognitive status (MMSE). Results from this study revealed improvement in the agitation (CMAI), aggression (NPI-NH), and pain (MOBID-2) in the

treatment group compared to the control cohort evident as early as two weeks post initiation of study and lasted up to the eighth week. However, no alteration in daily functional activity nor in the cognitive status was reported throughout the course of the study. Moreover, during the four-week withdrawal phase (week 12), individuals the treatment group starting to display worsening of agitation during the withdrawal phase in comparison to the control group; despite the improvement in pain and aggression maintained in treatment group four weeks post termination of the step-wise treatment (week 12) (Husebo et al 2011).

Additional evidence evaluating the impact of the different levels of pharmacological intervention in individuals with dementia revealed that all administration of paracetamol, morphine/buprenorphine transdermal patch, or pregabalin resulted in progressive decline in MOBID-2 scores up to the eighth week; with pregabalin administration resulting in the greatest reduction in pain (61.7%) compared to its respective baseline. However, despite the analgesic effect of pregabalin, it resulted in progressive deterioration of daily functional activity till the end to treatment; with paracetamol identified as the only drug treatment which improved daily functional activity in this population over the period of eight-week (Sandvik et al 2014). Altogether implicating the benefit of step-wise protocols in treatment of pain in individuals with moderate to severe dementia in nursing homes, as well as highlighting that it is not necessary that the drug which induces the greatest level of analgesia would also improve or restore patients' quality of life as illustrated by the daily functional activity measure. Thus, demanding standardised approaches in nursing homes for assessment and treatment of pain in individuals with dementia (Sandvik et al 2014).

1.4.3 Perception of Pain in Alzheimer's disease - Experimental Studies Evidence

Experimental pain studies have provided conflicting evidence on noxious pain thresholds and tolerance in individuals with AD. Earlier studies by Benedetti and co-workers assessed pain thresholds and pain tolerance via application of electrical stimuli and the tourniquet technique to the non-dominant wrist and arm, respectively. The results from this study revealed that patients with AD manifest increased tolerance to ischemic pain and noxious electrical stimulation; but no change in the sensory detection of stimulus or pain thresholds compared to healthy controls. Furthermore, it was reported that the pain tolerance increased with the progression of the

disease using MMSE and electroencephalogram (EEG) as assessment measures of cognitive deficits. Collectively suggesting an alteration in the emotional dimension of pain, whilst preservation of the sensory-discriminative aspect of pain in AD (Benedetti et al 1999).

Further evidence from a study examining autonomic responses, (i.e. assessment of heart rate using electrocardiogram (ECG) and systolic blood pressure) and pain perception in response to an application of a noxious electrical stimulus to the non-dominant arm revealed blunted autonomic responses, as demonstrated by minimal increase in heart rate and systolic blood pressure, to electrical noxious stimulation in individuals with AD compared to healthy controls. Therefore, indicating elevation of autonomic threshold which implicates that only strong/severe pain can only induce an emotional and/or autonomic reaction in patients with dementia. It was also noteworthy, that a mild stimulus induced a normal pain experience whilst a strong pain stimulation which is twice the pain threshold resulted in reduced pain experience in AD patients, which was associated with comparable increase in blood pressure but diminished heart increase in comparison to healthy controls. Hence, further reinforces the notion that there is an increased pain tolerance exhibited by AD patients whilst sensory discriminative aspect of pain is preserved (Rainero et al 2000).

In addition, assessment of heart rate using ECG in order to examine level anticipation following a warning 15 seconds prior to application of a noxious electrical stimulus to the non-dominant arm. This study demonstrated the deteriorating ability to anticipate a noxious stimulus, reflected by the diminished change in heart rate, with the progression of the disease reflected by lower MMSE scores; although no alteration in both stimulus detection and pain thresholds. Thus providing additional evidence for changes in the autonomic reactivity to pain may underlie the lack of anticipation in AD subjects with progressive cognitive decline (Benedetti et al 2004).

A more recent study examined electrical and thermal pain thresholds via application of noxious electrical stimulus to the non-dominant wrist delivered by two electrodes, and placing the palm of the hand onto a hot plate (temperature ranging between 40°C and 65°C), respectively. Results from this study show that AD individuals retain the capacity to detect noxious electrical and thermal stimulation as demonstrated by similar pain thresholds exhibited to cognitively-intact control subjects (Limongi et al 2013). These findings reinforce the notion that the sensory-

discriminative aspect of pain is unaltered in response to electrical stimulation as well as demonstrating similar findings in response to noxious thermal stimuli application in AD.

Furthermore, a study conducted by Jensen-Dahm carried out assessment of pressure pain thresholds/tolerance using a manual pressure algometer with a felt-tipped probe with circular surface applied to the index finger, thermal detection/thresholds using a thermode applied to skin with a firm but gentle pressure (cut-off temperature at 50°C), and cold thresholds/tolerance in which the subject submerged their right hand into a recirculating water cooler (thermostatically controlled at 10°C). The principle findings of this study were comparable detection and thresholds of pressure, thermal, and cold stimulation; however significantly reduced tolerance to pressure in individuals with AD compared to healthy controls. Therefore, despite confirming pain thresholds as previous reports, this study in contrast argues reduced pain tolerance in AD subjects and suggests that the reduced pain tolerance in AD cannot be explained by reduced processing of painful stimuli (Jensen-Dahm et al 2014).

In contrast, a functional magnetic resonance imaging (fMRI) study highlighted that the perception and processing of moderate pain were not diminished in individuals with AD; although higher pain sensitivity thresholds for just noticeable-weak pain, in response to application of mechanical pressure stimuli, were reported by AD patients compared to healthy controls. However, fMRI observation did not reveal any reduction in pain processing in these patient group in comparison to healthy controls; but on the contrary AD subjects exhibited greater amplitude and duration of pain-related activity in regions involved sensory, emotional and cognitive aspect of pain (Cole et al 2006). Therefore, suggesting a possible alteration in the sensory component of pain perception in AD and that pain processing may not underlie this alteration in individuals with cognitive deficits.

In addition, a study conducted by Monroe and group indicates that patients with AD exhibit reduced sensitivity to thermal stimulation, as demonstrated by higher temperatures required in order to report warmth sensation, mild pain, and moderate pain in response to a noxious thermal stimulus applied using thermode (ramp up at 1°C/second) on the hand in comparison to healthy controls. However, comparable affective responses in terms of the unpleasant nature of

the pain experience were recorded in AD individuals (Monroe et al 2016). Thus, indicating that there may also be an alteration in the sensory-discriminative aspect of pain.

Collectively, these studies highlight the notion that although patients with AD may still perceive the presence of pain, they may experience its intensity (sensory-discriminative) and/or affective (emotional-affective) aspects to a lesser extent compared to the healthy controls. As a result, making it difficult to understand the meaning of the sensory experience and the associated emotional context in patients with dementia; which may underlie the atypical behavioural responses (i.e. agitation and mood disorders) in this population (Scherder et al 2005).

1.4.4 Alzheimer's disease Associated Neuropathology in Pain Pathway

A possible explanation for altered perception of pain in AD could be the presence of amyloid deposits and NFT in key regions involved in pain processing, namely the spinal cord and thalamus, of AD patient at autopsy. Both the spinal cord and the thalamus are key regions in the pain pathway which are involved in processing and relaying nociceptive inputs to supraspinal structures (Rub et al 2002, Schmidt et al 2001). These pathological lesions are accompanied by neurodegeneration in the form of atrophy of cortical areas (i.e. anterior cingulate cortex, prefrontal cortex, insula, and primary somatosensory cortex) which involved in decoding the interpretation of multiple dimensions of nociceptive input (Hyman et al 1984). Thus, presence of AD-associated pathological hallmarks and associated cortical atrophy of regions involved in pain processing could possibly contribute to the altered perception of pain in individuals with AD. An in-depth review of AD-associated pathology in regions involved in pain processing is presented in Chapter 4.

1.4.5 Overview of Pain in Alzheimer's disease

Collectively, evidence suggesting elevation in pain tolerance and reduced sensitivity to noxious stimulation exhibited by AD patients has made it difficult to understand whether decreased pain complaints are related to altered pain processing or the deteriorating ability of these patients to communicate which hinders their capacity to report pain (Scherder & Bouma 2000). Therefore, a better understanding of the pathophysiological mechanisms underlying alterations in sensory transmission is essential for improving the clinical management of pain in patients with AD.

1.5 General Aims and Hypothesis

The aim of this thesis is to test the hypothesis that AD-related pathology and neuroinflammation occurring at key regions of the pain pathways, namely the spinal cord and thalamus, may alter the sensitivity to pain in individuals with AD. In order to test this hypothesis, we have:

1. Assessed nociceptive thresholds in response to acute noxious mechanical and thermal stimulation in the TASTPM transgenic mouse model of AD compared to age-and gender-matched controls. – Chapter 2
2. Examined the development of OA pain and the characteristic plastic changes in the pain pathways in TASTPM mice compared to age-and gender-matched controls. – Chapter 3
3. Conducted a human post-mortem case-control study in order to assess whether individuals with AD display AD-associated pathology and neuroinflammation in key pain processing regions (spinal cord and brain); and whether that is altered in chronic pain conditions (i.e. OA). – Chapter 4

Chapter 2 Sensitivity to Acute Noxious Stimuli in TASTPM Model of Alzheimer's disease

2.1 Introduction

Pain is a subjective and complex multidimensional sensory and emotional experience in response to an actual or potential threat to the integrity of the body. It acts as an early-warning system for self-protection that promotes survival in a hostile and dangerous environment and encourages recuperative behaviours in response to pain (Woolf 2010). Loss of this protective mechanism, in individuals suffering from a congenital inability to perceive pain, has a considerable physical consequence and interferes with the quality of life. Nociception, under physiological conditions, provides a critical protective mechanism that will only persist as long as the noxious stimulus or tissue damage is present, which resolves with healing of the injury or damage (Basbaum et al 2009). Therefore, despite the unpleasant nature of pain sensation, an intact pain system is important for the survival and wellbeing of the individual.

However, in individuals with Alzheimer's disease (AD) this self-protective mechanism seems to be compromised, as illustrated by elevation in pain tolerance and reduced sensitivity to noxious stimulation accompanied by infrequent reporting of pain (outlined in Chapter 1). Clinically, AD is characterised is by deterioration of memory and cognitive function, progressive impairment of activities of daily living, and neuropsychiatric symptoms, which has made the assessment and management of pain challenging in this subject population (Burns & Iliffe 2009). As a result it is difficult to understand whether decreased pain complaints are related to altered pain processing or the deteriorating ability of these patients to communicate which hinders their capacity to report pain (Scherder & Bouma 2000). In addition, neuropathological evidence obtained from AD post-mortem tissue have reported the presence of AD-associated neuropathological hallmarks, namely extracellular amyloid plaques composed of aggregated β-amyloid (Aβ) deposition and intracellular neurofibrillary tangles (NFT) consisting of aberrantly hyperphosphorylated microtubule associated protein tau (MAPT), in regions involved in pain processing, such as the spinal cord and thalamus. Based upon which it was postulated that alteration in the perception of pain may be due to the microenvironment changes in the regions involved in pain processing, as AD pathological hallmarks are associated with gliosis, synaptic dysfunction and neuronal loss (Rub et al 2002, Schmidt et al 2001, Serrano-Pozo et al 2011). Therefore a better understanding of the pathophysiological mechanisms underlying alterations

in sensory transmission is essential for improving the clinical management of pain in patients with AD.

2.1.1 Animal Models of Alzheimer's disease

As it is difficult to depict the underlying mechanism of AD pathogenesis leading clinical manifestations in human subjects, animal models of the disease have been developed in order to aid research in this field. Identification of familial mutations in human genes (i.e. amyloid precursor protein (APP) and presenelin-1/2 (PS1/2)) in individuals with early-onset AD (EOAD) have led to the development of transgenic mouse models in order to explore pathogenesis of AD via incorporating the mutant forms of the identified genes (Onos et al 2016). Despite differences in initiators of AD, with EOAD (representing 1-5% AD cases) associated with familial gene mutations and late-onset AD (LOAD; representing ~95% AD cases) that occurs sporadically (i.e. idiopathic), the clinical presentation and sequence of pathological events are indistinguishable (Reitz et al 2011, Selkoe & Hardy 2016). Therefore, these mouse models provide powerful tools to help elucidate and study the intricate pathophysiological mechanism underlying the development and progression of AD as well as identifying therapeutic targets for future treatment.

To date, none of the existing transgenic mouse models of AD fully recapitulate the wide spectrum of AD associated pathological and behavioural changes as observed in human. Nevertheless, these "incomplete" animal models exhibit some critical aspects of AD, which enable the identification of mechanisms and pathways underlying the development and progression of the disease (Elder et al 2010).

The majority of the transgenic animal models of AD can be classified as follows:

1. Amyloidogenic models (Baptists) of AD expressing human APP and/or PS1/2: The initial models of AD were generated via overexpression of mutation(s) in the APP gene (outlined in Table 2.1), whilst the double-mutant (APP + PS1/2) models (displayed in Table 2.2) were developed with improvement in our understanding. Mutations in human APP and/or PS1/2 generally resulted in development of substantial Aβ pathology associated with gliosis, synaptic dysfunction, impairment

in cognition (memory and learning), with minimal, if any, neurodegeneration (Elder et al 2010, Kitazawa et al 2012). Moreover, these mice displayed only subtle increase in tau phosphorylation that was apparent in the form of dystrophic neurites surrounding amyloid plaque, without any NFT formation (Howlett et al 2008, Kitazawa et al 2012, Sturchler-Pierrat et al 1997). Furthermore, accelerated disease progression was evident in multiple mutant transgenes (i.e. 5 × FAD) in comparison to expression of a single transgene (Elder et al 2010).

Table 2.1: APP Transgenic Mouse Models of AD

Model	PDAPP	APP23	CRND8
Background	C57BL/6;DBA2	C57BL/6	C57BL/6;C3H
APP Mutation	IND: V717F	SWE: KM670/671NL	SWE: KM670/671NL IND: V717F
Promoter	PDGF	Thy-1	Hm-Prnp
Cognitive Deficits	3 months old	3 months old	3 months old
Plaques	8 months old	6 months old	5 months old
Tangles	Absent	Absent	Absent
Neuronal Loss	Absent	14 months old	6 months old
Gliosis	6 months old	6 months old	3 months old
Reference	Games et al (1995)	Sturchler-Pierrat et al (1997)	Chishti et al (2001)

Abbreviations: APP, amyloid precursor protein; Hm-Prnp, hamster prion protein; IND, Indiana; PDGF, platelet-derived growth factor β; SWE, Swedish; Thy-1, thymocyte differentiation antigen 1

Table 2.2: APP and PS Transgenic Mouse Models of AD

Model	APP/PS1DE9	TASTPM	5×FAD
Background	C57BL/6;C3H	C57BL/6	C57BL/6;SJL
APP Mutation	SWE: KM670/671NL	SWE: KM670/671NL	SWE: KM670/671NL FLO: I716V LON: V717I
PS Mutation	PS1: deltaE9	PS1: M146V	PS1: M146L PS1: L286V
Promoter	Ms-Prnp	Thy-1	Thy-1
Cognitive Deficits	12 months old	6 months old	4 months old
Plaques	6 months old	6 months old	2 months old
Tangles	Absent	Absent	Absent
Neuronal Loss	8 months old	Absent	9 months old
Gliosis	6 months old	6 months old	2 months old
Reference	Jankowsky et al (2004)	Howlett et al (2004)	Oakley et al (2006)

Abbreviations: APP, amyloid precursor protein; FLO, Florida; LON, London; Ms-Prnp, mouse prion protein; SWE, Swedish; PS, presenilin; Thy-1, thymocyte differentiation antigen 1

2. Tau Models (Tauists) of AD expressing human MAPT: These mouse models harbouring mutations in MAPT were generated in order to understand changes in tau in a number of taupathies; but also serve as a useful tool to understand tau-related changes in AD (Table 2.3). In general, mutations in tau are associated with frontotemporal lobe dementia (FTD) (Goedert et al 2012), which exhibit AD-like tau changes such as development of NFT accompanied by gliosis, synaptic dysfunction, substantial neurodegeneration, as well as impairment in learning and

memory (Allen et al 2002, Kitazawa et al 2012). However, no amyloid plaques are evident in these models, which proposes an argument against and thereby challenges the amyloid cascade hypothesis (described in Chapter 1) according to which Aβ initiates the cascade of events leading to formation of NFT and subsequent neurodegeneration resulting in cognitive deficits (Selkoe & Hardy 2016).

Table 2.3: Tau Transgenic Mouse Models of AD

Model	P301S-htau	rTg4510	PS19
Background	C57BL/6;CBA	FVB/N	C57BL/6;C3H
MAPT Mutation	P301S	P301L	P301S
Promoter	Thy-1	Tet-O	Ms-Prnp
Cognitive Deficits	3 months old	3 months old	6 months old
Plaques	Absent	Absent	Absent
Tangles	4 months old	4 months old	6 months old
Neuronal Loss	3 months old	6 months old	9 months old
Gliosis	5 months old	Unknown	3 months old
Reference	Allen et al (2002)	Santacruz et al (2005)	Yoshiyama et al (2007)

Abbreviations: MAPT, microtubule-associated protein tau; Ms-Prnp, mouse prion protein; Thy-1, thymocyte differentiation antigen 1; Tet-O, tetracycline operator

3. Baptised Tauist expressing APP or APP + PS1/2 and MAPT: Development of models of amyloid and tau pathological changes in AD led to attempts to generate animal models converging the amyloidogenic and tau models of AD in order to develop a more comprehensive model of AD (Table 2.4) (Kitazawa et al 2012).These mice express mutations in multiple transgenes which generally show

progressive development of changes in Aβ and deposition of extracellular plaques, followed by changes in tau as illustrated by increased tau phosphorylation and formation of NFT accompanied by impairment in cognition (Oddo et al 2003). In addition, these mice also exhibited synaptic dysfunction and can display neuronal loss. As with amyloidogenic models, increasing the number of transgenes accelerated the progression of disease phenotype (Saul et al 2013).

Table 2.4: Triple Transgenic Mouse Models of AD

Model	3×Tg	5×FAD/PS19
Background	C57BL/6;129SvJ	C57BL/6
APP Mutation	SWE: KM670/671NL via Thy-1	5×FAD Oakley et al (2006)
PS Mutation	M146V via Knock-in	
MAPT Mutation	P301L via Thy-1	PS19 Yoshiyama et al (2007)
Cognitive Deficits	4 months old	Unknown
Plaques	6 months old	3 months old
Tangles	12 months old	3 months old
Neuronal Loss	Unknown	9 months old
Gliosis	7 months old	3 months old
Reference	Oddo et al (2003)	Saul et al (2013)

Abbreviations: APP, amyloid precursor protein; MAPT, microtubule-associated protein tau; PS, presenilin; Thy-1, thymocyte differentiation antigen 1 promoter

Altogether, these transgenic mouse models of AD have enabled insight into multiple aspects of human AD pathogenesis and clinical manifestations. Therefore, utilisation of such models to evaluate nociceptive thresholds provides a powerful tool in order to depict perception of pain in AD. Preclinical studies using transgenic AD mice have provided variable evidence in relation to

nociceptive thresholds in response to acute noxious stimulation as well as in models of chronic pain.

2.1.2 Nociceptive Sensitivity in Models of Alzheimer's disease

So far, there is little, though variable, evidence for nociceptive sensitivity to noxious stimulation in mouse models of AD; as many of these studies are in principle characterising the non-cognitive aspects of such models of AD amongst which nociception is one aspect. Specifically, unaltered nociceptive thresholds in response to noxious thermal stimulation, demonstrated by similar paw withdrawal latencies using the hot-plate test, was reported in twelve to fourteen months old 3×Tg compared to their wild-type (WT) control littermates (Filali et al 2012). In addition, comparable tail-flick latencies in response to noxious cold were exhibited by the young (7 months old) and aged (11 months old) triple transgenic, 3×Tg, when compared to age-matched WT littermates (Baeta-Corral et al 2015). These findings suggest preservation of sensory discriminative component of thermal and cold sensitivity in the triple transgenic mouse model of AD.

In contrast, tau models of AD display variable nociceptive sensitivity. In particular, the P301-htau mice exhibited reduced paw withdrawal latencies on the hot-plate test, implicating an increased thermal sensitivity, at the age of six months old. This thermal hypersensitivity was suggested to be associated with the hyperactivity displayed by these transgenic mice (Takeuchi et al 2011). On the other hand, another tau model of AD, P301S-htau, exhibited no alteration in the thermal sensitivity, demonstrated by similar paw withdrawal thresholds using the Hargreaves's test. Further nociceptive assessments revealed an age-dependent reduction in P301S-htau mechanical sensitivity, as illustrated by increased force required in order to elicit hind paw withdrawal using the paw pressure test, which becomes apparent at the age of three months old. These behavioural changes coincided with aggregation and deposition of hyperphosphorylated tau in dorsal root ganglia (DRG) neurons, which may underlie the altered nocifensive behaviour exhibited by the P301S-htau mice (Mellone et al 2013).

In general, the amyloidogenic models of AD have been reported to display reduced nociceptive sensitivity. Especially, the APP over-expressing CRND8 transgenic mice that demonstrated reduced sensitivity to noxious thermal and mechanical stimulation in comparison to WT control

littermates at the age of three and six months old, respectively. Elevated thermal thresholds concurred with lower expression of neuropeptides substance P (SP) and calcitonin-gene related peptide (CGRP) as well as pain-related ion channel transient receptor potential vallinoid-1 (TRPV1) in the DRG, which represent the peptidergic C-fibre population (Shukla et al 2013). In addition, the CRND8 mice developed similar thermal hyperalgesia as exhibited by WT controls in the complete Freud's adjuvant (CFA) model of inflammatory pain, in both young (3 months old) and aged mice (12 months old); however, the latter age-group (12 months old) recovered faster in comparison to age-matched WT controls. Together, these findings implicate a blunted age-dependent acute nociception and chronic inflammatory pain in the CRND8 transgenic model of AD possibly due to alterations in primary afferent neurons as well as AD-associated amyloid pathology and cognitive impairment (Shukla et al 2013). Furthermore, evidence from hAPP over-expressing FVB/N strain of mice indicates less severe neuropathic pain development following complete sciatic nerve axotomy which coincides with reduced motor neuron death, neuroma formation and swelling at the site of injury (Kotulska et al 2010). Overexpression of APP was indicated to be protective in persistent pain condition owed to its role in promoting wound healing (Kummer et al 2002).

Besides the transgenic mouse models, the use of chemically induced models of AD and knockout mice have also provided valuable understanding in nociceptive sensitivity. Evidence from three months old Swiss mice 30-days after a single intracerebroventricular (i.c.v.) injection of Aβ1-40 peptide reveals unaltered nociceptive thermal and mechanical thresholds in the hot-plate test and electrical foot-shock-sensitivity test, respectively. Furthermore, these mice were shown to display an increased tolerance to noxious stimulation, reflected by the jumping response upon application of foot-shock. The nocifensive behavioural changes correlated with impairment of cognition, illustrated by greater escape latency and less time spent on target quadrant in the Morris water-maze test; and altered emotionality, demonstrated by increased emotional responses in the elevated plus-maze and forced-swim tests, reflecting anxiety-like and depressive-like states, respectively, resembling the emotional disturbances observed in AD. These findings suggest that Aβ1–40 peptide increases pain tolerance, but not pain sensitivity in

mice, which seems to be linked to alterations in cognitive/emotional components of pain processing (Pamplona et al 2010).

Moreover, administration of Aβ1-40 and Aβ1-42 peptides into the rat hippocampus results in no change in acute nociceptive thermal and mechanical sensitivity using the Hargreaves's test and von-Frey test, respectively. Further behavioural assessment in an inflammatory CFA model of chronic pain demonstrated attenuated persistent nociception in Aβ-injected rats. This was illustrated by similar development but faster recovery of thermal hyperalgesia and mechanical allodynia evident on day three post CFA administration in the ankle joint in comparison to persistent thermal hyperalgesia lasting up to two-weeks in control rats. These behaviours were concomitant to impairment of learning and memory functions as well as increased Aβ immunoreactivity in the hippocampus. Similarly, chemically induced memory and learning impairments by a single bilateral administration of cycloheximide into the hippocampus, five days post CFA-induced development of thermal hyperalgesia and mechanical allodynia, caused faster recovery from these pain-like behaviours in comparison to vehicle controls. Collectively these data implicate that impairment in cognition may underlie altered perception of chronic pain in the Aβ-induced model of AD (Ma et al 2013).

Finally, tau-null mice exhibit reduced thermal sensitivity, as illustrated by increased paw withdrawal response latency in response to noxious thermal stimulus applied using the Hargreaves's test, but unaltered mechanical thresholds observed using the von-Frey test. In addition, behavioural assessment in an inflammatory model, the formalin test, resulted in less time in engaging in pain-like behaviour (i.e. paw protection/licking periods and paw jerks) in the acute phase exhibited by the tau-null mice compared to WT controls; whereas increased pain-related behaviour in the tonic phase. Ultrastructural and biochemical analysis revealed the underlying mechanism as reduction in unmyelinated C-fibres and the hypomyelination of Aδ-fibres in the sciatic nerves responsible for the acute phase; whilst increased excitability of second order spinal cord nociceptive neurons, demonstrated by increased c-fos immunoreactivity in the dorsal horn, correlating with heightened pain-like behaviours in the tonic phase of formalin test (Sotiropoulos et al 2014).

An overview of nociceptive thresholds in response acute noxious thermal and mechanical stimulation is presented in Table 2.5. Altogether, these preclinical data suggest alterations in nociceptive sensitivity, in both sensory and emotional dimension, in preclinical rodent models of AD. However, it is still elusive whether there are changes within the spinal cord of transgenic mouse models of AD over expressing the mutant APP, which may be responsible and/or involved in the alteration in the nociceptive processing.

Table 2.5: Overview of Acute Nociceptive Sensitivity in Models of AD

Model	Thermal	Mechanical	Reference
3×Tg	↔	N.D.	Filali et al (2012)
P301-hTau	↑	N.D.	Takeuchi et al (2011)
P301S-hTau	↔	↓	Mellone et al (2013)
CRND8	↓	↓	Shukla et al (2013)
Aβ1-40 [1]	↔	↔	Pamplona et al (2010)
Aβ1-40 + Aβ1-42 [2]	↔	↔	Ma et al (2013)
Tau-null	↓	↔	Sotiropoulos et al (2014)

[1] Injection of Aβ1-40 peptide - intracerebroventricular

[2] Injection of Aβ1-40 and Aβ1-42 peptides – into the hippocampus

Abbreviations: N.D., not determined; ↔, no change; ↑, increased sensitivity; ↓, reduced sensitivity.

2.1.3 Chapter Aims

Therefore in order to investigate the mechanisms of nociceptive pain in AD, in the present chapter, we assessed nociceptive behaviour and explored AD-related pathology in the spinal cord of a double-mutant transgenic TASTPM mouse model of AD that carries mutant versions of the APP (APPswe) and PS1 (PS1.M146V) associated with familial forms of AD (Howlett et al

2004). Histological and behavioural analysis of these animals has identified pathological characteristics and cognitive alterations in the form amyloid deposits evident at the age of 3 months developing into amyloid plaques at 6 months old, when cognitive deficits also appear, which reflect some aspects of the pathological changes and cognitive defects observed in people with AD (Howlett et al 2008, Howlett et al 2004).

In addition, disturbances in non-cognitive and unconditioned behaviours have also been described in the TASTPM mice. Firstly, in male TASTPM mice, a high level of aggression has been characterised as demonstrated by increased irritability and vigorous escape response; as well as greater tendency to attack territory intruder. They also exhibit weight loss despite a greater level of food intake, and premature mortality particularly evident in female mice. Moreover, a reduction in anxiety-like behaviour is exhibited by the TASTPM mice have been described using the elevated-maze test. Furthermore, they show alterations in circadian rhythms and locomotor hypoactivity; although no alteration in motor co-ordination and balance is evident (Pugh et al 2007). These behavioural characteristics recapitulate some aspects of the neuropsychiatric behavioural alterations observed in people with AD, such as a fragmented sleep-wake cycle and personality changes that include irritability and aggression.

Altogether, the TASTPM model recapitulates some of the pathological and cognitive features observed in AD and bears a resemblance to certain neuropsychiatric characteristics associated with the disease. Therefore, it offers to be a powerful tool in order to delineate mechanisms in AD.

As a result, the aims of the present chapter were to:

1. Validate characteristic behavioural and pathological features of TASTPM model of AD.
2. Examine if AD-related pathology is present in the TASTPM spinal cord, and if so, explore how it may affect the nociceptive processing.
3. Assess if nociceptive thresholds in response to acute noxious thermal and mechanical stimulation are altered in the transgenic TASTPM mouse model of AD. If so, to investigate the possible underlying mechanisms.

The majority of the work presented in this chapter was published as a part of the following peer-reviewed article (Aman et al 2016):

Aman Y, Pitcher T, Simeoli R, Ballard C, Malcangio M. (2016). Reduced thermal sensitivity and increased opioidergic tone in the TASTPM mouse model of Alzheimer's disease. Pain 157: 2285-96.

2.2 Materials and Methods

2.2.1 Animals

All experiments were carried out in accordance with United Kingdom Home Office Regulations (Animal Scientific Procedures Act, 1986). Experiments were performed on 4-12 months old adult male and female heterozygous double-mutant TASTPM transgenic mouse model of AD obtained from GlaxoSmithKline (GSK). Age and gender-matched C57BL/6J (WT) obtained from Charles River were used as controls. All animals were housed in the Biological Services Unit, King's College London; maintained in 12 hours day/night cycle with *ad libitum* access to food and water; and were allowed acclimatisation for 7 days prior to behavioural experiments. All procedures were performed under personal licence code PIL 70/26010 and project licence 70/7629.

2.2.1.1 **Generation of TASTPM Mouse Model of AD**

The transgenic TASTPM mouse model of AD were generated at GSK using TAS10 transgenic mice expressing the Swedish mutant human amyloid precursor protein (APP) (695-aa isoform) under the control of the murine Thy-1 promoter and transgenic mice over expressing presenilin-1 (PS1) M146V mutation (TPM) driven through the murine Thy-1 promoter (Howlett et al 2004, Richardson et al 2003). Briefly, the 5' end of the APP coding sequence is preceded by a blunted *Hind*III site and a strong Kozak translation initiation sequence. The 5' end of the human PS1 coding sequence is preceded by a blunted *Xba*I site and a strong Kozak translation initiation sequence. All modifications were made using standard cloning methods and PCR-based site-directed mutagenesis. Thy-1.APP and Thy1-PS1 gene fusions were dissolved in 10mM Tris and 1mM EDTA (pH 8) to a final concentration of 10 μg/ml prior to injection. Transgenic lines were generated by pronuclear microinjection of this fragment, after removal of backbone plasmid sequence, into fertilised oocytes from either C57BL/6;C3H mice in the case of Thy-1.APP transgene, or into fertilised oocytes from pure C57BL/6 mice in the case of Thy1-PS1 transgene. TAS10 (Thy-1.APP695swe) mice were generated and backcrossed onto a pure C57BL/6 background before being crossed with TPM (Thy-1.PS-1.M146V) mice to produce heterozygous double mutant TASTPM mice (Figure 2.1A) (Howlett et al 2004).

2.2.1.2 **Breeding Strategy**

Double homozygous mutant TASTPM mice were obtained from GSK. In order to generate heterozygous TASTPM litter, homozygous TASTPM female were bred with non-transgenic WT male. Upon birth, animals were marked with an ear notch and given a unique identifier code. The skin excised during the ear notch procedure was utilised for genotyping with polymerase chain reaction (PCR). Offspring were weaned at 3 weeks of age and placed into single sex cages, with up to 5 littermates housed in one cage. Age- and sex-matched WT controls were also group housed in single sex cages (Figure 2.1B).

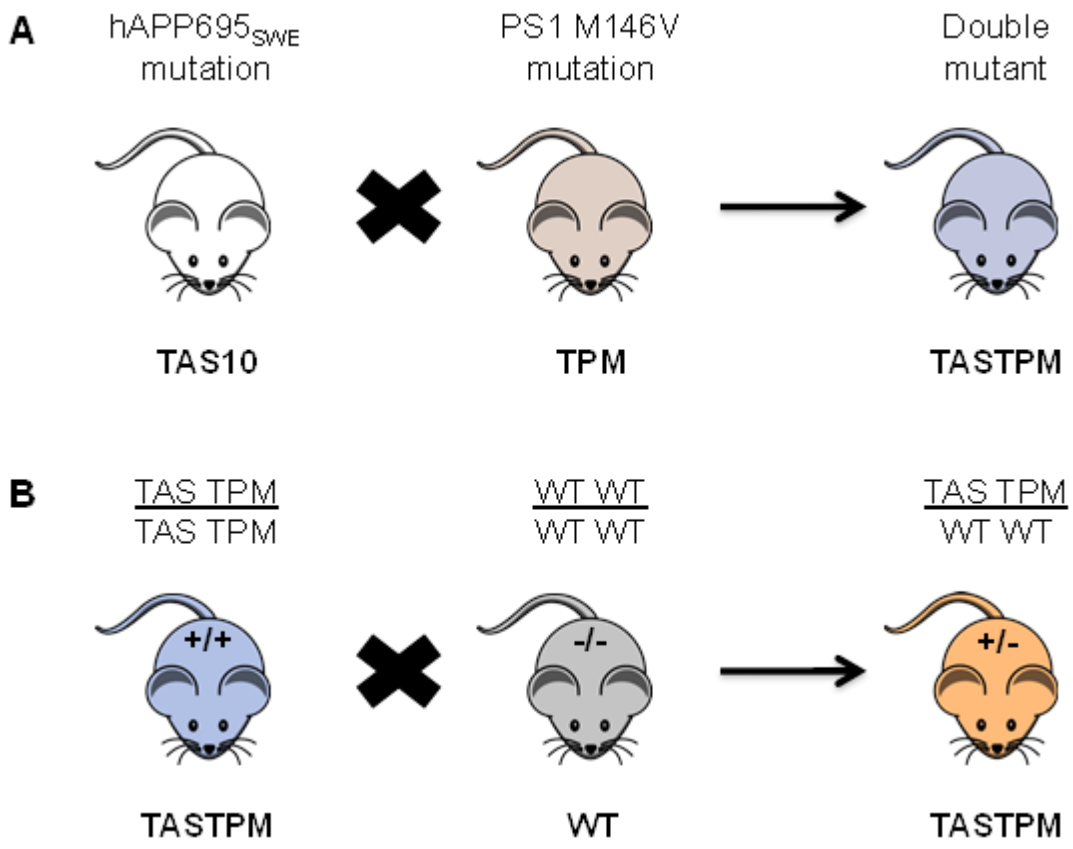

Figure 2.1: Generation and Breeding of TASTPM Model of AD

The TASTPM double-mutant transgenic model of AD were generated by mating TAS10 mouse carrying the Swedish mutant human amyloid precursor protein (APP) (695-aa isoform) and TPM transgenic mice over expressing presenilin-1 M146V mutation (Howlett et al 2004, Richardson et al 2003) (A). Homozygous TASTPM female were bred with non-transgenic WT male in order to generate heterozygous litter (B).

2.2.2 Genotyping

2.2.2.1 **Genomic DNA Extraction**

Prior to any experimental procedures carried out in TASTPM mice, verification that the animals were carrying both the $hAPP695_{SWE}$ (TAS10) and presenilin-1 M146V (TPM) transgenes was performed by genotyping. Ear notch skin samples were incubated with 30µl lysis buffer (nuclease-free water (ddH_2O) containing 150mM Tris-HCl (pH 8.8); 100mM $(Na_4)_2SO_4$; 100mM $MgCl_2$; 0.5% (v/v) Triton X-100; 0.1% (v/v) β-mercaptoethanol; and 0.04 mg/ml Proteinase K) for 60 minutes at 55°C which was followed by a 5 minutes heat inactivation step at 95°C. Samples were subsequently vortexed for 30 seconds prior to being centrifuged at 12,000 rpm for 1 minute. The DNA containing supernatant was collected and DNA concentration of each sample was determined using the NanoDrop spectrometer. Samples were subsequently diluted in ddH_2O to give a final concentration of 25ng/µl and stored at -20°C until use.

2.2.2.2 **TASTPM Polymerase Chain Reaction (PCR)**

PCR was performed for each DNA sample to amplify genomic DNA. The PCR reaction was conducted using the Taq DNA polymerase kit (Qiagen). Individual PCR reactions were performed for TAS primers and TPM primers for each DNA sample. PCR amplification was carried out in reaction volumes of 25µl of PCR mixture containing 2µl of template DNA (25ng/µl) added to 23µl master mix consisting of 10% (v/v) 10× Coral Load PCR Buffer, 200µM of dNTP Mix, 0.625 units/reaction of Taq polymerase and 1µM of each of the oligonucleotide primers (Sigma) in ddH_2O. Amplification was performed using the Applied Biosystems PCR System 9700 using the following primers: TAS (CAGCTGGTTGACCTGTAGCTTT and GTGTGCCAGTGAAGATGA) and TPM (CAGCTGGTTGACCTGTAGCTTT and ATGCTTGGCGCCATATTTCAATG). The reaction conditions were as follows: initial denaturation at 95°C for 10 minutes followed by 10 cycles of 95°C for 15 seconds (denaturation), 68°C for 15 seconds (annealing: temperature reduced by 1°C/cycle) and 72°C for 30 seconds (extension). Subsequently, samples were subjected to a final set of 25 cycles of 95°C for 15 seconds (denaturation), 58°C for 15 seconds (annealing) and 72°C for 30 seconds (extension).

2.2.2.3 **Electrophoresis of PCR Products**

To visualize the PCR products a gel electrophoresis was conducted. Following the PCR, samples were loaded onto a 1.5% agarose gel (Sigma) containing 100µg/ml ethidium bromide (Sigma). A 1kB DNA ladder (Promega, UK) was also loaded onto each gel in order to allow the identification of the product sizes. Gels were run at 100V for 60 minutes using the Power Pac 200. DNA fragments were visualised using a GeneGenius (Syngene, UK) UV transilluminator and pictures captured using GeneSnap software (Syngene, UK). The expected sizes of the end-products were 500bp for the TAS transgene and 350bp for the TPM transgene.

2.2.3 Behavioural Testing

All behavioural testing was conducted blind to experimental groups.

2.2.3.1 **Locomotor Function (RotoRod)**

Locomotor function was assessed using an accelerating RotoRod (Series 8, IITC, USA) with rubber drums set to accelerate from 4 to 40 rpm over a period of 300 seconds. Any mice remaining on the apparatus after 300 seconds were removed and their time was recorded as 300 seconds. Three separate trials were performed for each animal, separated by at least 15 minutes.

2.2.3.2 **Novel Object Recognition Test**

Animals were placed in the neutral test arena, circular open maze (diameter: 60cm; height: 50cm) obtained from Ugo Basile, and allowed to freely explore it 3 times (10 minutes each) in order to habituate to both the arena and experimenter prior to the beginning of the experiment. After each exploration, animals were removed from the arena, which was then cleaned with 70% ethanol. After the habituation period, two identical objects (2 × black cube, F) were placed inside the arena, at equal distance from the walls. Mice were placed in the arena at the furthest distance from the objects and allowed to freely explore the objects for 10 minutes (Figure 2.2). Subsequently, following a retention period of 24 hours, mice were placed back into the arena with one of the familiar objects (F) replaced by one novel object (white sphere, N) in the same location with N being different in colour, shape and texture. The mice were then allowed to freely explore both objects for 10 minutes. The objects and the arena were thoroughly cleaned

with 70% ethanol between each animal in order to avoid any odour recognition. The mouse was considered to be exploring the object when its head was facing the object at a distance of 2 cm or less. Mice were individually observed and the time taken to explore each object was recorded to the nearest 0.01 s. The time difference in exploring each object was calculated:

$$Difference = N - F$$

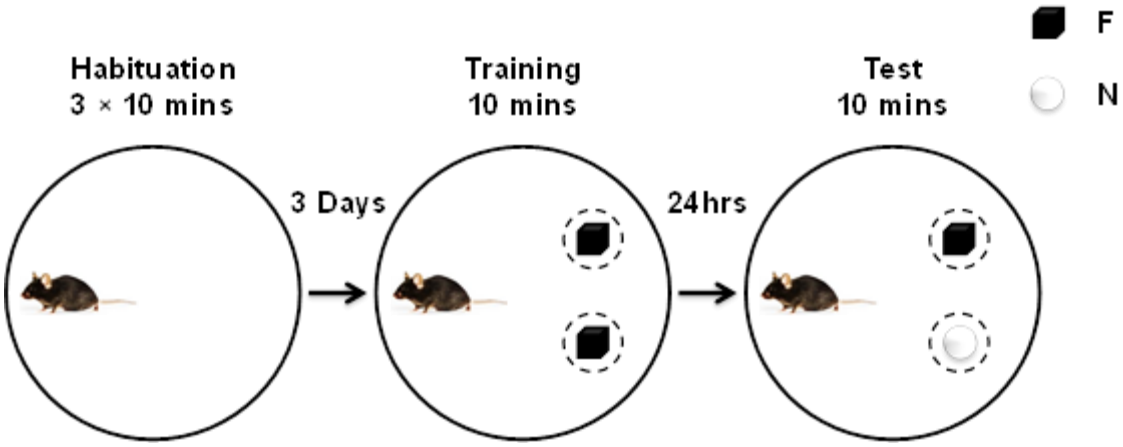

Figure 2.2: A Schematic Representation of the Novel Object Recognition Test

Individual mouse was placed in the arena facing the opposite direction to where the objects were due to be placed. Animals were allowed to habituate (3 × 10 minutes each) in the arena before two identical objects were introduced for a period of 10 minutes. Subsequently, 24 hours later one of the object was replaced by a novel object in the arena the time spent exploring the familiar (F) and novel (N) object were recorded. The dotted lines encircling the objects represent the 2 cm area in which mouse facing the object was considered to be exploring the objects.

2.2.3.3 **Mechanical Thresholds**

2.2.3.3.1 von Frey Filaments

Static mechanical withdrawal thresholds were assessed by applying calibrated von Frey monofilaments (0.007g – 1.00g) to the plantar surface of the hind paw. The 50% paw withdrawal threshold (PWT) was determined by increasing or decreasing stimulus intensity, and estimated using Dixon's 'up-down' method (Chaplan et al 1994). Unrestrained mice were placed individually and acclimatised up to 60 minutes, prior testing, in acrylic cubicles (8 × 5 × 10 cm) on a wire mesh grid, providing access to the underside of the hind paw. Monofilaments were applied perpendicular to the plantar surface of the selected hind paw, and then held in this position with enough force to cause a slight bend in the filament for approximately 3 seconds or

until an abrupt withdrawal of the hind paw from the stimulus, the latter defining a positive response. Each test started with the application of 0.07g filament and each hind paw was assessed alternately with approximately 30 seconds gap between each application. Stimulus intensity was increased in a sequence until a positive response was achieved or the maximum strength stimulus of 1.00g filament failed to induce a positive response, in order to avoid tissue damage. If the mouse withdrew its hind paw upon application of a filament, the next lower force filament in the sequence was applied and vice versa until there was a change in response from the mouse. Following a positive response, four successive filaments were assessed according to the 'up-down' sequence, with no filament applied more than three times, in order to prevent sensitization. A 50% PWT (g) was determined using the 'up-down' procedure (Dixon 1980).

2.2.3.3.2 Paw Pressure

Response to noxious mechanical thresholds were examined in the hind paws of restrained and alert mice using an Analgesiometer (Ugo Basile, Italy) as described previously (Randall & Selitto 1957). Briefly, the plantar surface of the mouse hind paw was placed on a pedestal with the dorsal surface of the hind paw under a blunt probe connected to a sliding weigh scale and force was applied using a pedal-switch Increasing pressure was applied on the mouse hind paw using the pedal-switch either until the mouse flicks and withdraws or up to a maximum load of 250 g. The nociceptive paw withdrawal threshold (PWT) was defined as the force (g) at which the mouse withdrew its hind paw or reached the maximum cut-off (250g). The paw pressure test was conducted by Mr Thomas Pitcher.

2.2.3.4 **Thermal Thresholds**

2.2.3.4.1 Hot-plate Test

Response to noxious heat stimulation of the paws was assessed using the hot plate. Mice were placed on the hot plate device set at temperature ~52.5°C (± 0.2°C). The latency to respond (licking of hind paw or flicking of hind paw or jumping) was recorded to the nearest 0.01 seconds in order to obtain the withdrawal response latency. A cut off time of 45 seconds was used at which point the animals were removed to avoid tissue injury.

2.2.4 Pharmacological Drug Administration

Naloxone hydrochloride (1mg/kg) and morphine sulphate (6mg/kg) were obtained from Sigma and dissolved in sterile saline. Drugs or saline (vehicle) were administrated either: via an intraperitoneal (i.p.) injection (naloxone hydrochloride); or subcutaneously (s.c., morphine sulphate) in TASTPM and WT controls. Baseline paw withdrawal latencies were recorded prior to drug administration and on the day of testing the effect of the drug administrated were monitored over a period of 3 hours, with hot-plate tests carried out at 30 minutes, 90 minutes, and 180 minutes after administration.

2.2.5 Behavioural Testing Post Drug Administration

2.2.5.1 **Novel Object Recognition Test: Naloxone**

Naloxone hydrochloride (1mg/kg) was obtained from Sigma, dissolved in sterile saline, and was administrated i.p. in TASTPM and WT controls. Cognitive deficit in the TASTPM mice were determined prior to administration of naloxone. The subsequent week naloxone was administrated and the effect of drug on cognition was observed using the novel object recognition test 30 minutes post administration (Figure 2.3).

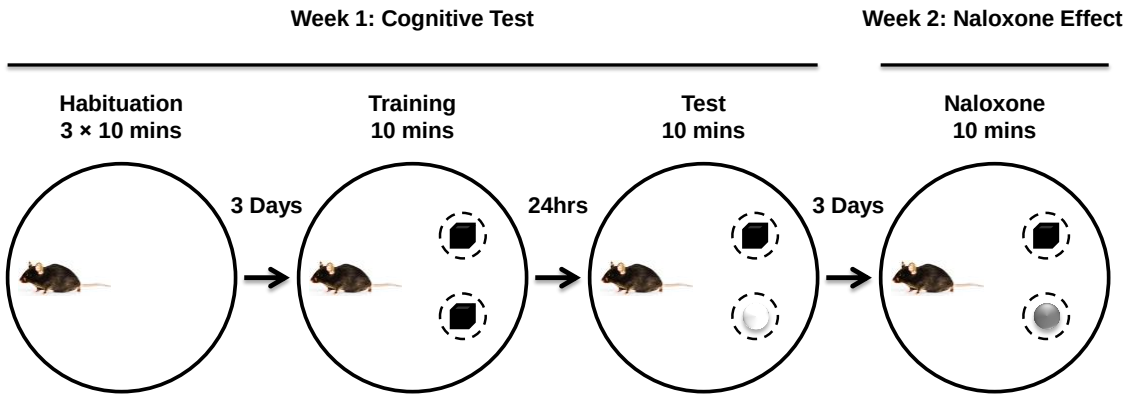

Figure 2.3: Representation of Experimental Design to Test the Effect of Naloxone on Cognition

During the first week the novel object recognition test was conducted as described in Figure 2.2. The following week both WT and TASTPM mice were administrated with naloxone (1 mg/kg, i.p.) and novel object recognition test was repeated 30 minutes post naloxone administration with introduction of another novel object, different to that shown to mice before; in order to assess the effect of naloxone on cognition.

2.2.5.2 **Conditioned Place Preference**

The conditioned place preference apparatus has three compartments composed of two large outer chambers and one small 'neutral' inner chamber. One outer chamber is a white-walled chamber with a rough floor whilst the other outer chamber is black-walled with a smooth floor. The neutral chamber is grey with a smooth floor. Each animal was placed in the central neutral chamber with access to both outer chambers and allowed to freely explore between the three chambers for 30 minutes (pre-conditioning). Time spent in the two outer chambers was recorded any animal showing a bias for one of the chambers (more than 80% of its time) was removed from the study. Subsequently animals were conditioned with either morphine sulphate (6mg/kg; Sigma) dissolved in sterile saline or saline (vehicle). Morphine or vehicle was injected s.c. in the morning and the animal was confined to an outer chamber for 30 minutes with access blocked to the neutral inner chamber. In the afternoon, the same animal receives the vehicle and was then confined to the opposite chamber for 30 minutes with access blocked to the neutral inner chamber (conditioning: repeated 3 times). Post conditioning animals were allowed to freely explore the chambers again for 30 minutes with access to both outer chambers and the time spent in each outer chamber was recorded (Figure 2.4). Data was expressed as the difference in time spent in the drug paired chamber. The conditioned place preference experiment was conducted by Mr Thomas Pitcher.

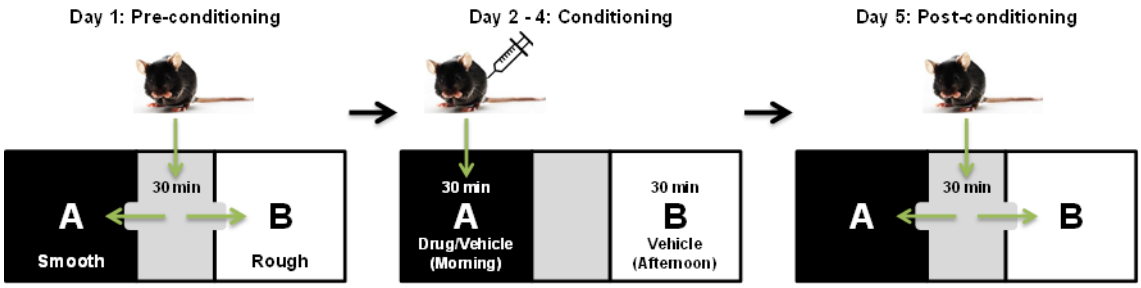

Figure 2.4: Representation of the Conditioned Place Preference Test

Individual mouse was placed in the central 'neutral' chamber with free access to the two outer chambers (A: black and smooth surface; B white and rough surface) for 30 minutes (pre-conditioning) prior to the conditioning phase (Day 2-4) in which mouse was confined to one selected chamber for 30 minutes post either morphine or vehicle drug administration, with blocked access to the neutral chamber. The same afternoon the mouse was injected with the vehicle drug and confined to opposite chamber with access blocked to the neutral chamber. Subsequently, individual mouse was placed in the neutral chamber with free access to both outer chambers and the time spent in each chamber was recorded (post-conditioning).

2.2.6 Histology and Immunohistology

2.2.6.1 **Perfusion, Tissue Preparation and Sectioning**

Naive WT (6 - 7 months old) and TASTPM (6 - 7 months and 12 months old) mice were terminally anaesthetised with an overdose of sodium pentobarbital (Euthatal®, ~150mg/kg body weight) and perfused transcardially with heparinised (1 U/ml) sterile saline (0.9% NaCl) followed by 4% paraformaldehyde fixative solution containing 1.5% picric acid (Sigma) in phosphate buffer (PB, 0.1M, pH 7.4). Spinal cords (L3-L6) and brains were removed and immersion-fixed in 4% paraformaldehyde fixative solution containing 1.5% picric acid for 24 hours at 4°C. Subsequently, spinal cords and brains were cryoprotected in a solution of 20% sucrose in PB at 4°C for at least 48 hours and subsequently embedded in optimum cutting temperature (OCT, BDH, UK) medium and then snap-frozen using liquid nitrogen and stored at -80°C.

Transverse spinal cord and coronal brain sections were cut (20µm thick) using a cryostat and thaw mounted onto Superfrost Plus microscope slides (BDH, UK). Free-floating spinal cord sections were cut at 30µm thickness and transferred to phosphate-buffered saline (PBS) in 24-well plates.

2.2.6.2 **Immunofluorescence**

Frozen slide-mounted sections were washed three times (5 minutes each) with PBS, blocked with 1% (w/v) bovine serum albumin (BSA, Sigma, UK) and 0.2% (w/v) sodium azide (Sigma, UK) in 0.1% Triton X-100 (BDH, UK) in PBS for 1 hour, and incubated overnight for single staining with rabbit anti-met enkephalin (ENK) and mouse anti-β-amyloid 1-16 (6E10) or with a combination of primary antibodies. Double staining was performed using rabbit anti-vesicular glutamate transporter 1 (VGLUT1) with guinea pig anti-vesicular glutamate transporter 2 (VGLUT2); and mouse anti-6E10 in combination with the following primary antibodies: rabbit anti-glial fibrillary acidic protein (GFAP), rabbit anti-ionized calcium binding adaptor molecule 1 (IBA1), rabbit anti-neuronal nuclei (NeuN), or sheep anti-calcitonin gene-related peptide (CGRP). Triple staining was performed using rabbit anti-VGLUT1, guinea pig anti-VGLUT2 and mouse anti-6E10. Details of the source and dilution of the primary antibodies are provided in Table 2.6. The following day sections were three times (5 minutes each) with PBS and were

subsequently incubated for two hours with the appropriate Alexa Fluor 488- or 546- or 647-conjugated antibody (Table 2.7). Sections were then washed three times with PBS (5 minutes each) and coverslipped with Vectashield Mounting Medium containing nuclear marker 4',6-diamidino-2-phenylindole·2HCl (DAPI; Vector Laboratories, UK). Where sections were stained with 6E10, pre-treatment with 70% formic acid (VWR) for 20 minutes was performed. All steps were conducted at room temperature and all antibody solutions were prepared in PBS with 1% BSA, 0.1% Triton X-100 and 0.2% sodium azide. Where spinal cord sections were stained with VGLUT1 and VGLUT2, 10% BSA was used in antibody solution instead of 1%.

Table 2.6: List of Primary Antibodies Used for Immunofluorescence and Immunohistochemistry

Antibody	Species	Dilution	Source
6E10	Mouse	1:400/1:1000*	Cambridge Biosciences
IBA1#	Rabbit	1:1000	Wako
GFAP#	Rabbit	1:1000	Dako
CGRP	Sheep	1:500	Enzo Life Sciences
NK1R	Rabbit	1:10,000*	Sigma
VGLUT1	Rabbit	1:5000	Synaptic Systems
VGLUT2	Guinea pig	1:250	Synaptic Systems
Met-ENK	Rabbit	1:1000	Peninsula Laboratories
NeuN	Rabbit	1:1000	Cell Signaling

* Dilutions for free floating sections; # Antibodies used for immunohistochemistry

Frozen free-floating spinal cord sections were washed three times (5 minutes each) with PBS, blocked with 1% BSA, 0.1% Triton X-100 and 0.2% sodium azide in PBS and incubated for 72 hours on a shaker at 4°C with the primary antibodies (Table 2.6): mouse anti-6E10 and rabbit anti-neurokinin 1 receptor (NK1R). Sections were then washed three times (5 minutes each)

with PBS, incubated with the appropriate Alexa Fluor 488- or 546-conjugated antibody (Table 2.7) overnight on a shaker at 4°C and then mounted onto microscope slides. All slides were coverslipped with Vectashield Mounting Medium containing DAPI. The specificity of immunoreactivity was confirmed by omitting the primary antibody and fluorescent staining was visualized using Zeiss LSM710 confocal microscope and the software ZEN (Zeiss, UK).

Table 2.7: List of Secondary Antibodies Used for Immunofluorescence

Secondary Antibody	Dilution	Source
Goat Anti-Mouse IgG-Conjugated Alexa Fluor 488™	1:500	Molecular Probes
Goat Anti-Rabbit IgG-Conjugated Alexa Fluor 488™	1:500	Molecular Probes
Goat Anti-Guinea-Pig IgG-Conjugated Alexa Fluor 488™	1:500	Molecular Probes
Goat Anti-Rabbit IgG-Conjugated Alexa Fluor 546™	1:500	Molecular Probes
Goat Anti-Guinea-Pig IgG-Conjugated Alexa Fluor 546™	1:500	Molecular Probes
Goat Anti-Rabbit IgG-Conjugated Alexa Fluor 647™	1:500	Molecular Probes
Donkey Anti-Mouse IgG-Conjugated Alexa Fluor 488™	1:500	Molecular Probes
Donkey Anti-Sheep IgG-Conjugated Alexa Fluor 546™	1:500	Molecular Probes

2.2.6.3 **Immunohistochemistry: Chromogenic**

Frozen slide-mounted 20µm coronal brain sections were washed three times with PBS (5 minutes each), incubated with 3% (v/v in methanol) hydrogen peroxide (H_2O_2, Sigma) in order to quench endogenous peroxidase activity and blocked with 1% BSA, 0.1% Triton X-100 and 0.2% sodium azide in PBS and incubated overnight with either primary antibodies: rabbit anti-GFAP or rabbit anti-IBA1. Details of the source and dilution of the primary antibodies are provided in Table 2.6. The following day sections were washed three times (5 minutes each) with PBS and incubated for 1 hour with the secondary antibody: biotinylated donkey anti-rabbit (1:400; Jackson ImmunoResearch). In order to remove excess secondary antibody, sections were washed three times (5 minutes each) with PBS prior to incubation with avidin-biotinylated

horseradish peroxidase complex (Vectastatin® ABC Kit, Vector) in PBS for 30 minutes. Sections were subsequently washed three times (5 minutes each) with PBS and peroxidase labelling was visualised with incubation (10 minutes) with 3, 3'-diaminobenzidine (DAB) Peroxidase (HRP) Substrate Kit (Vector). Sections were then washed for 5 minutes with distilled water (dH_2O) to terminate the DAB reaction and then 5 minutes in tap water. The sections were subsequently dehydrated in 60°C oven for 1 hour and immersed in xylene to clear for 20 minutes before being coverslipped with dibutylphthalate in xylene (DPX, Sigma) mounting medium (Sigma). All steps were conducted at room temperature and all antibody solutions were prepared in PBS with 1% BSA, 0.1% Triton X-100 and 0.2% sodium azide. The specificity of immunoreactivity was confirmed by omitting the primary antibody; immunostaining was visualised using Zeiss Axiovision light microscope and images were captured using Zeiss AxioCam MRc and the software Axiovision Release 4.6. (Zeiss, UK).

2.2.6.4 **Thioflavin-S Staining**

Staining for amyloid plaques in mice brain was performed on frozen slide-mounted 20µm coronal brain sections. Sections were washed three times with PBS (5 minutes each) and incubated with Thioflavin-S (1% w/v aqueous solution, Sigma) for 8 minutes. Sections were washed twice (3 minutes each) in 80% ethanol followed by a 3 minutes wash in 95% ethanol. Finally, sections were rinsed 3 times in PBS; coverslipped with Vectashield Mounting Medium containing DAPI and fluorescent staining was visualized using Zeiss microscope (Imager.Z1) and images were captured using Zeiss AxioCam MRm and the software Axiovision Release 4.8.2. (Zeiss, UK).

2.2.7 Quantification of Histological and Immunohistological Staining

2.2.7.1 **Quantitative Assessment of Fluorescence Intensity**

Quantitative assessment of VGLUT1, VGLUT2, CGRP and met-ENK immunoreactivity was calculated by determining immunofluorescence intensity within 1×10^4 μm^2 boxes placed onto areas of the lateral, central and medial dorsal horn laminae I-III and laminae IV-VI (VGLUT1 and VGLUT2 only) (Figure 2.5A) using Axiovision LE 4.8 software (Zeiss, UK). Background fluorescence intensity of each tissue section was also determined and subtracted from the

values obtained. Three L3-L5 sections (at least 160 µm apart) from each animal were randomly selected from at least four animals per experimental group.

2.2.7.2 **Quantitative Assessment of APP/Aβ in Projection Neurons**

Quantitative assessment of number of 6E10 positive neurons that also expressed NK1R immunoreactivity were calculated by counting the frequency of 6E10 immunopositive cells in a defined region of 6×10^4 μm^2 placed onto the deep laminae of the dorsal horn (laminae III-VI) (Figure 2.5B) using Axiovision LE 4.8 software. Three L3-L5 sections from each animal were randomly selected from at least three animals per experimental group.

2.2.7.3 **Quantification of GFAP, IBA1 and Thioflavin-S Staining**

Tissue sections stained with GFAP, IBA1, and Thioflavin-S were quantified by the percentage area occupied (immunoreactivity burden) using the ImageJ software (NIH). Three defined regions of 8×10^4 μm^2 were placed onto the cortex, hippocampus, and the thalamus. Images were converted to 8-bit greyscale, thresholded within a linear range (constant per stain), and the percentage of area covered by GFAP, IBA1, and Thioflavin-S immunoreactivity was calculated in each of the three regions of interest.

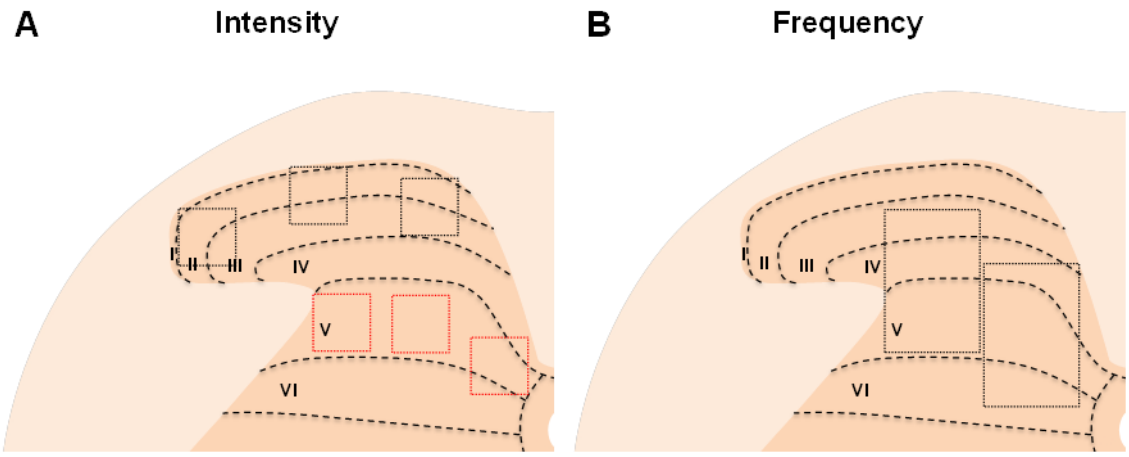

Figure 2.5: Schematic Representation of Immunofluorescence Quantification

Immunofluorescence intensities within three 1×10^4 μm^2 boxes placed onto areas of the lateral, central and medial dorsal horn laminae I-III (black) and laminae IV-VI (red; VGLUT1 and VGLUT2 only) (A). The frequency APP/Aβ positive neurons that also express NK1R in the spinal cord dorsal horn were examined in two 6×10^4 μm^2 boxes placed onto deep laminae of the dorsal horn (laminae III-VI) (B).

2.2.8 Western Blots

Lumbar spinal cord (L3–L5) tissue from 6-7 months old WT and TASTPM mice were homogenized on ice in lysis buffer (Tris-HCl, 20 mM pH 7.5, 10 mM NaF, 150 mM NaCl, 1% Nonidet P-40, 1 mM phenylmethylsulphonyl fluoride, 1 mM Na_3VO_4, 10 µg/ml leupeptin and trypsin inhibitor) with complete mini cocktail protease inhibitor (Roche). Tissue lysates were then centrifuged at 13,000 rpm for 20 min at 4°C. The protein concentration of the supernatant was determined using the NanoDrop spectrometer. Equal protein concentrations per sample (60µg protein) were added to Laemmli's sample buffer, boiled for 5 min, and subjected to 10% SDS-PAGE. Wet transfer was performed using the Bio-Rad Trans-Blot® Cell (Bio-Rad Laboratories, Hertfordshire, U.K.) for 1 hr at 4°C, and the membrane was then blocked with 5% non-fat dried milk in TBS-T (50 mM Tris-HCl, pH 7.6, 150 mM NaCl, 0.1% Tween 20) for 30 min at room temperature. The blot was probed with rabbit anti-VGLUT1 (1:1000, Cell Signaling, UK), rabbit anti-VGLUT2 (1:1000, Cell Signaling, UK), and mouse anti-amyloid 1-16 (1:1000, 6E10, Cambridge Biosciences, UK) antibodies. Results were visualised with horseradish peroxidase-coupled anti-mouse or anti-rabbit immunoglobulin (Dako) using enhanced chemiluminescence detection reagents ECL (EMD Millipore, UK) Western blotting detection system according to the manufacturer's instructions, and the immune complex visualized by the BioSpectrum® Imaging System. The protein bands were densitometrically analyzed with Quantity One (Bio-Rad Laboratories, UK). Western blot for β-actin (1:1000, Cell Signaling, UK) and α-tubulin (1:10000, Sigma, UK) were performed as loading controls. Data was expressed as protein expression relative to control.

2.2.9 Real-time Reverse Transcription Polymerase Chain Reaction (RT-PCR)

Lumbar segments (L3-L5) of the spinal cord were dissected and snap-frozen in liquid nitrogen and subsequently divided into dorsal and ventral horn. Total RNA was then isolated from minced dorsal horn tissue using the RNeasy mini-kit (Qiagen) according to the manufacturer's protocol. The total RNA concentration was determined using the NanoDrop spectrometer. Total RNA (50-100ng) was used to synthesize first strand cDNA, using Supersensitive III Reverse Transcriptase kit (Thermo Fisher Science) according to the manufacturer's protocol. Expression levels of the following genes were analysed: pre-pro-enkephalin (pPENK), pro-enkephalin

(PENK), and 18S rRNA was used a reference transcript. pPENK is the precursor for PENK which contains peptides with seven amino acid sequences and produces enkephalin peptide (Dickenson & Kieffer 2006). Amplification was performed with a Light Cycler 480 (Roche) using Syber Green I Master (Roche) using the primers: pPENK (TTCAGCAGATCGGAGGAGTTG and AGAAGCGAACGGAGGAGAGAT) (Denning et al 2008), PENK (ATGCAGCTACCGCCTGGTT and GTGTGCACGCCAGGAAATT) (Kurrikoff et al 2004), and 18S rRNA (GCTGGAATTACCGCGGCT and CGGCTACCACATCCAAGGAA) (Denning et al 2008). The instrument was programmed as follows: 95°C for 5 minutes and 45 cycles of three steps of 10 seconds each including denaturing at 95°C, annealing at 60°C and primer extending at 72°C. All samples were run as duplicates and the 18S rRNA was used as the housekeeping gene. The relative gene expression levels were calculated according to the $2^{-\Delta\Delta Ct}$ method, where Ct represents the threshold cycle.

2.2.10 Statistical Analysis

The data were analysed using SigmaPlot 12.5 (Systat Software, San Jose, CA). The statistical tests performed and the numbers of animals used are displayed in the results section and within the figure legends. Where data were not normally distributed, the appropriate non-parametric test was applied. Graphs were generated using GraphPad Prism 5 (Graphpad Software Inc., San Diego, USA). All data are presented as mean ± standard error mean (SEM) and a probability value less than 0.05 ($p < 0.05$) was considered statistically significant.

2.3 Results

In the quest to investigate and elucidate mechanisms of pain in AD, the present chapter aims to examine whether nociceptive thresholds in response to acute noxious stimuli are altered in the double-mutant TASTPM mouse model of AD. For this purpose, initially the characteristic features of TASTPM model of AD were validated in terms of demonstration of cognitive deficits accompanied by AD-associated neuropathology. Subsequently, we explored if AD-associated pathology is present in key regions of the pain pathway, namely the thalamus and spinal cord, before investigating the impact of AD-associated feature on nociceptive thresholds in response to acute noxious stimuli.

2.3.1 Characteristic Features of TASTPM Model of Alzheimer's disease

Prior to all experiments, mice were genotyped to confirm the expression of mutant human APP (TAS) and PS1 (TPM).

2.3.1.1 **TASTPM Mice Express Human Mutant APP and PS1**

Human mutant APP and PS1 are expressed in the TASTPM mouse model of AD (Howlett et al 2004, Richardson et al 2003). In order to confirm the presence of the mutant transgenes in our colony, DNA was extracted, amplified by PCR and visualised on agarose gels. Expectedly, mutant human APP (~500bp) and PS1 (~350bp) were detected in the TASTPM mice, but not in the WT controls as demonstrated in Figure 2.6.

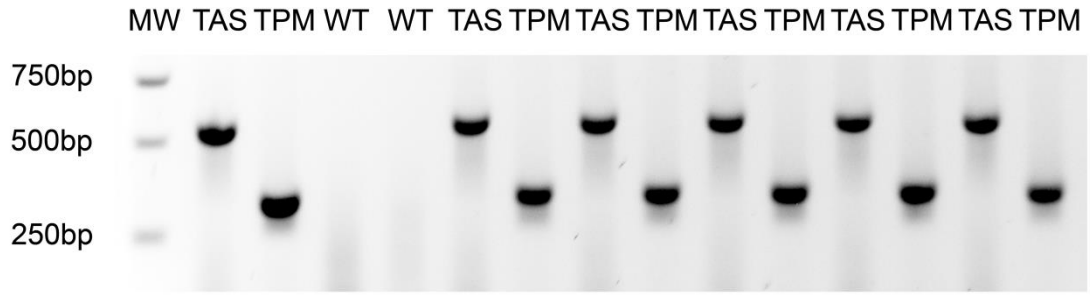

Figure 2.6: TASTPM Express Human Mutant APP and PS1

DNA from WT and TASTPM was extracted, amplified by PCR and the transcripts detected on agarose gel. Human APP (TAS, 500bp) and PS1 (TPM, 350bp) were detected only in TASTPM but not WT mice.

2.3.1.2 **Age-dependant Impairment of Cognition Exhibited by TASTPM Mice**

The transgenic TASTPM model recapitulates certain features of AD which includes memory impairment. Behavioural assessments in the double-mutant model of AD have identified cognitive deficits that become apparent at the age of 6 months old (Howlett et al 2004). Therefore, to examine and confirm the impairment of cognition in our colony, the novel object recognition test was utilised between the age of 4 months old to 7 months old TASTPM mice accompanied by age-and gender-matched WT controls. As expected, TASTPM mice displayed an age-dependant memory deficit in the novel object recognition test as they spent significantly less time exploring the novel object compared to WT mice at the age of 6 and 7 months, but not at the age of 4 and 5 months (Figure 2.7).

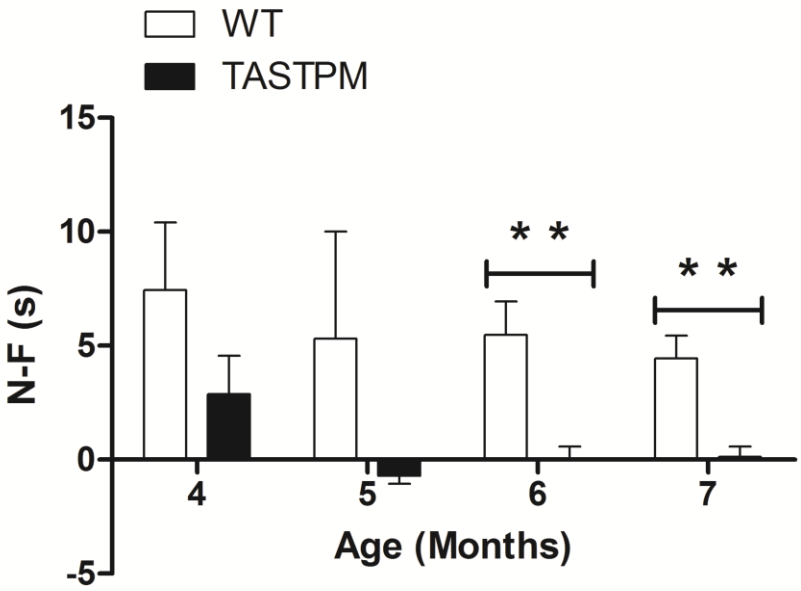

Figure 2.7: Age-dependant Cognitive Decline in the TASTPM Model of AD

TASTPM mice displayed an age-dependant memory deficits compared to WT mice that become apparent at the age of 6 months old (* * $p < 0.01$, Student's *t*-test or Mann-Whitney Rank Sum Test). Data values are expressed as mean ± SEM (n = 10-15 per experimental group). Abbreviations: N-F, difference in time spent exploring novel object (N) and familiar object (F); s, seconds.

2.3.1.3 **AD-associated Pathology in the Brain of 6 Months Old TASTPM**

TASTPM model exhibits many, although not all pathological features associated with AD. Amyloid deposits have been reported to appear in the brain at the age of 3 months old TASTPM mice, with amyloid plaques, the pathological hallmark of AD, developing at the age of 6 months old accompanied by neuroinflammation (Howlett et al 2004). Immunohistochemical staining revealed obvious extracellular amyloid plaques composed of aggregated Aβ in the brain of 6 months old TASTPM mice but not WT mice (Figure 2.8A-B). These plaques were located specifically in the cortex and hippocampus as well as in the thalamus (Figure 2.8B). Amyloid plaques in the brain were surrounded by barriers formed by astrocytes (GFAP, Figure 2.8C) and microglia (IBA1, Figure 2.8D).

Quantitative analysis of Aβ pathology and neuroinflammation in the brain has been summarised in Table 2.8. Amyloid plaques were only in the TASTPM cortex, hippocampus, and thalamus, whilst they were exclusively absent in the brain of age- and gender-matched WT controls. Using gliosis (astrocytosis, GFAP; and microgliosis, IBA1) as markers for neuroinflammation in the brain displayed significantly increased astroglial and microglial burden (percentage of area occupied respective immunoreactivity) in the cortex, hippocampus, and thalamus of TASTPM mice compared to WT controls.

Collectively, confirming that the 6 months old TASTPM model of AD recapitulates many the characteristic behavioural and pathological features associated with AD. Therefore, it offers to be a suitable model to assess nociceptive pain-like behaviour in order to elucidate mechanisms of pain in AD.

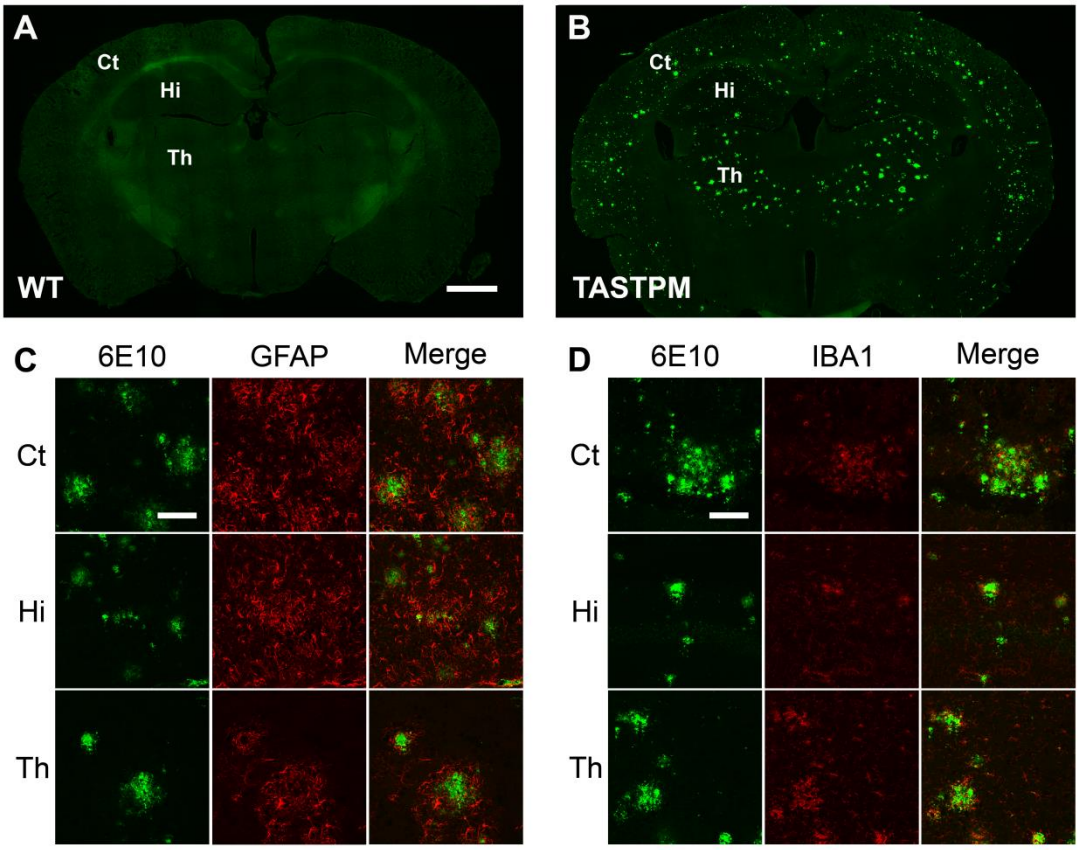

Figure 2.8: AD-associated Pathological Features in the Transgenic TASTPM Brain

Coronal brain sections from 6 months old TASTPM mice displayed AD-related pathological hallmark namely amyloid plaques composed of aggregated Aβ whilst no amyloid pathology was observed in age- and gender-matched WT controls (A-B). This amyloid pathology was accompanied by astrocytes (C) and microglia (D) forming a barrier around Aβ pathology. Abbreviation: Ct, cerebral cortex; Hi, hippocampus; Th, thalamus. The scale bar represents 1 mm (A-B) and 100 µm (C-D).

Table 2.8: Quantitative Analysis of Amyloid Pathology and Neuroinflammation in the Brain

	Region	WT	TASTPM	*t*-test (p-value)
β-amyloid	Cortex	0.00 ± 0.00	**0.31 ± 0.12**	-
	Hippocampus	0.00 ± 0.00	**0.38 ± 0.10**	-
	Thalamus	0.00 ± 0.00	**0.90 ± 0.21**	-
GFAP	Cortex	2.14 ± 0.58	29.30 ± 2.19	**< 0.001**
	Hippocampus	16.65 ± 3.99	29.41 ± 1.76	**0.026**
	Thalamus	0.80 ± 0.21	17.17± 3.63	**0.004**
IBA1	Cortex	1.64 ± 0.71	7.44 ± 1.20	**0.006**
	Hippocampus	0.91 ± 0.28	3.65 ± 0.81	**0.019**
	Thalamus	0.52 ± 0.17	5.70 ± 1.38	**0.010**

Values represent immunoreactivity burden (percentage of area occupied by immunopositive staining) and are expressed as mean ± SEM (n = 4 per experimental group).

2.3.2 Spinal Cord Characterisation of TASTPM Model of Alzheimer's disease

2.3.2.1 **APP/Aβ in Spinal Cord of 6 Months Old TASTPM Mice**

Following observation of cognitive deficit and presence of AD-associated pathological features in the brain of 6 months old TASTPM mice, the presence of AD-pathology in the spinal cord, site of first sensory synapse, was examined. In contrast to the brain, no amyloid plaque pathology was observed in the spinal cord of 6 months old TASTPM mice. However, in the spinal cords of 6 months old TASTPM, but not WT mice we observed APP/Aβ expression in the grey matter, both dorsal and ventral horns (Figure 2.9A-B). In addition, biochemical analysis displayed the expression of APP was present only in the TASTPM spinal cords (Figure 2.9C).

2.3.2.2 **Neuronal Expression of APP/Aβ in Spinal Cord of 6 Months Old TASTPM Mice**

In order to identify the cell population in which APP/Aβ is present in spinal cord, sections from TASTPM spinal cord were initially co-stained with antibodies against APP/Aβ (6E10) and neuronal nuclei marker (NeuN). It became apparent that APP/Aβ expression was mainly neuronal as it was observed exclusively in NeuN positive cells in the TASTPM mice (Figure 2.10A-C). APP/Aβ was evidently expressed in neurons in deep dorsal horn laminae (Figure 2.10D-F) as well as in motor neurons in the ventral horn (Figure 2.10G-I).

2.3.2.3 **Amyloid Plaques in the Spinal Cord of 12 Months Old TASTPM**

In contrast to spinal cord of 6 months old TASTPM, in the spinal cord, amyloid deposits were detected in 12 months old TASTPM mice (Figure 2.11). These deposits were accompanied by barriers formed by astrocytes (GFAP, Figure 2.11A-C) and microglia (IBA1, Figure 2.11D-F) similar to that observed in the brain of 6 months old TASTPM. In addition, lack of neuronal nuclei in the area occupied and close vicinity of the deposition was evident (NeuN, Figure 2.11G-I), indicative of extracellular plaques.

Collectively, these findings illustrate that intraneuronal accumulation of APP/Aβ in the spinal cord go onto develop and form extracellular amyloid plaques as AD progresses. Thus, indicating the former may be an early characteristic of AD which develops into the pathological hallmark, amyloid plaques, in the spinal cord of 12 months old TASTPM mice.

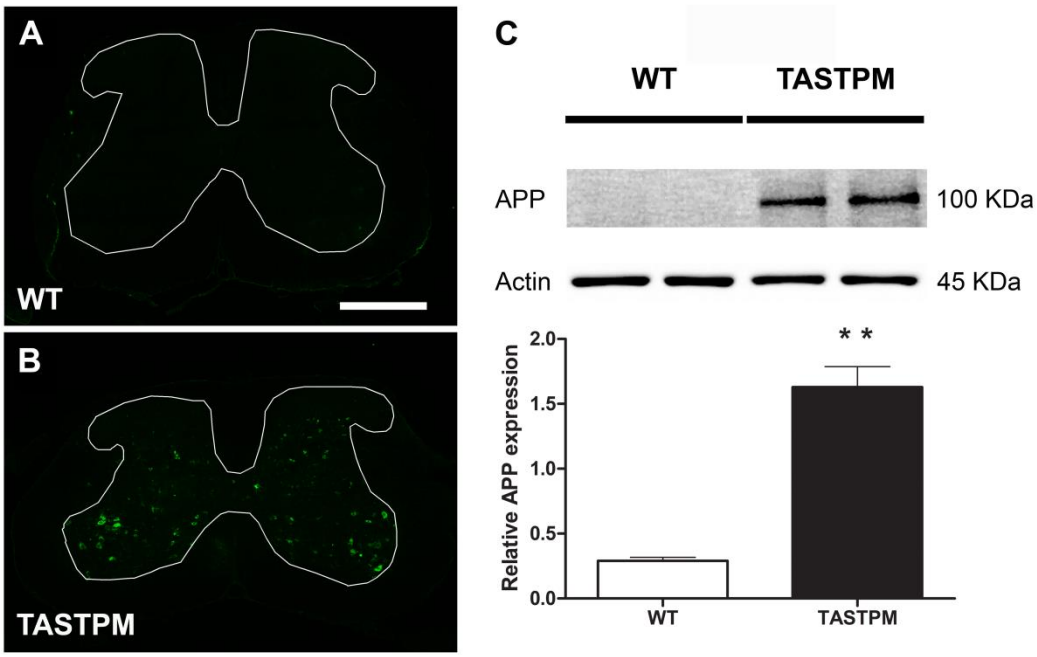

Figure 2.9: APP/Aβ Only Expressed in the 6 Months Old TASTPM Spinal Cord

Transverse lumbar spinal cord sections from 6-7 months old TASTPM and WT mice were stained with antibodies against β-amyloid 1-16 (6E10) (A-B). 6E10 staining was only detected in the spinal cord of the transgenic TASTPM mice which was distributed throughout the grey matter. Further quantitative analysis of APP/Aβ determined by western blot revealed significantly higher expression of APP/Aβ in the lumbar (L3-L5) spinal cord of TASTPM mice compared to WT controls (* * $p < 0.01$, Students' *t*-test) relative to β-actin (loading control). Data values are expressed as mean ± SEM (n = 3 per experimental group). The scale bar represents 500 µm (A-B).

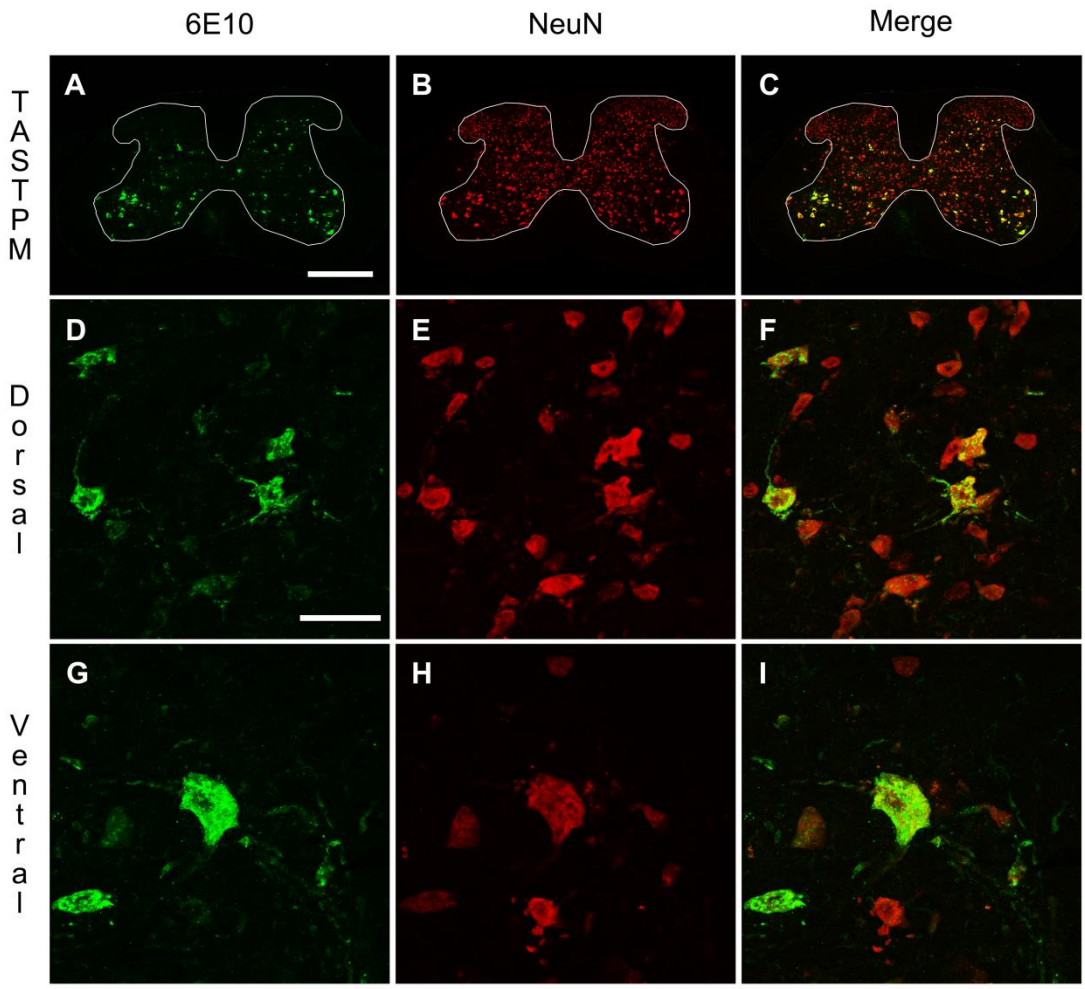

Figure 2.10: Intraneuronal Accumulation of APP/Aβ in the Spinal Cord of 6 Months Old TASTPM

Transverse lumbar spinal cord sections from TASTPM mice were stained with antibodies against β-amyloid 1-16 (6E10) (A, D, and G) and neuronal nuclei marker (NeuN) (B, E, and H). Merged images are shown for 6E10 and NeuN co-immunostaining in spinal cord of TASTPM (C) mice as well as TASTPM dorsal horn (F) and ventral horn (I). 6E10 staining was detected in the spinal cord of the transgenic TASTPM mice and was distributed throughout the grey matter. A high power magnification revealed co-localisation of 6E10 and NeuN in the dorsal horn laminae III-IV and motor neurons in the ventral horn of the transgenic TASTPM mice spinal cord. Scale bars: 500 µm (A-C) and 50 µm (D-I).

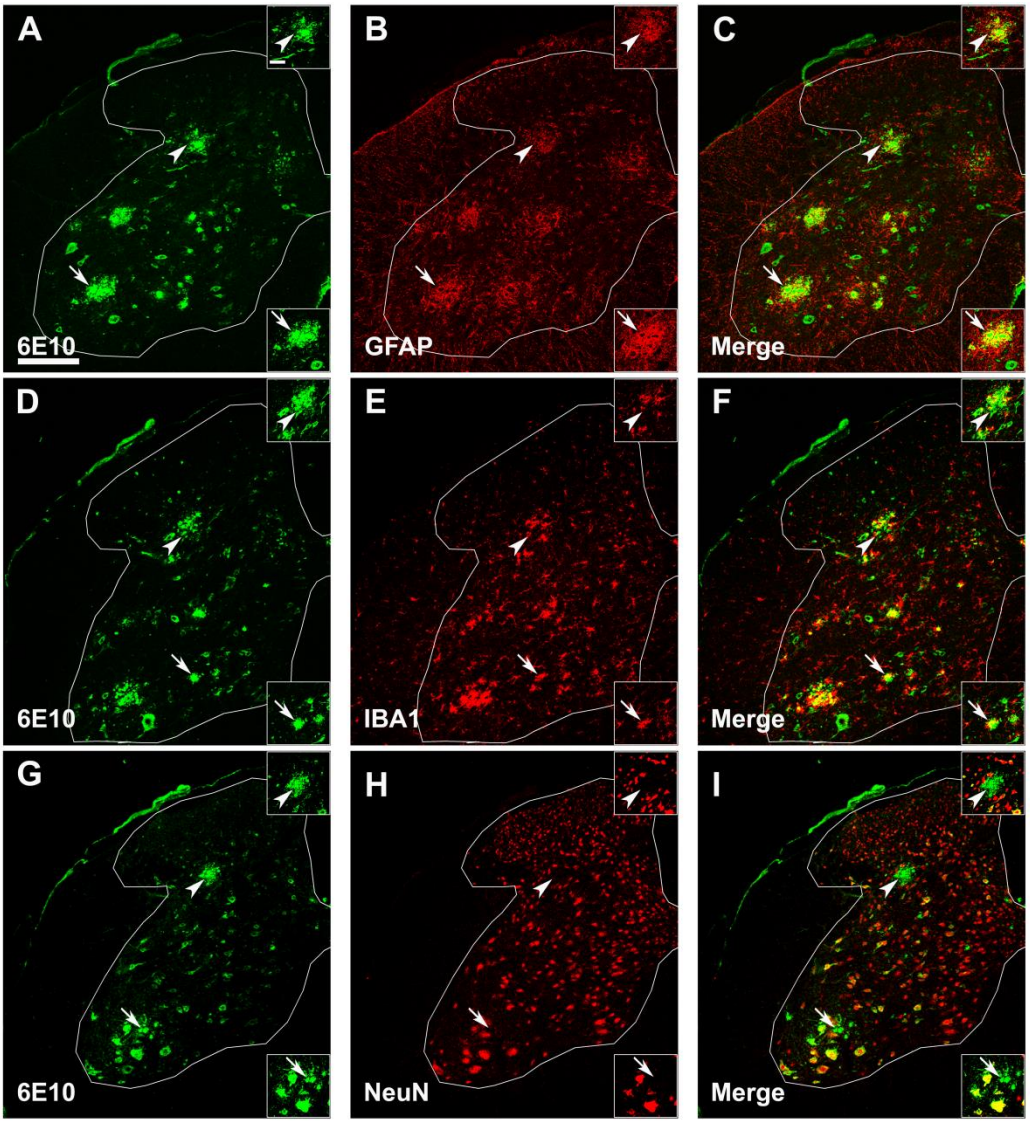

Figure 2.11: Aβ Deposits in the Spinal Cord of 12 Months Old TASTPM Mice

Transverse lumbar spinal cord sections from 12-month-old TASTPM mice were stained with antibodies against β-amyloid 1-16 (6E10) (A, D and G) with either glial fibrillary acidic protein (GFAP) (B); ionized calcium binding adaptor molecule 1 (IBA1) (E); or neuronal nuclei marker (NeuN) (H). Merged images are shown for 6E10 with GFAP (C) or IBA1 (F) or NeuN (I) co-immunostaining in the spinal cord. Pathological amyloid plaques composed of Aβ are evident in the dorsal (arrowheads) and ventral horns (arrows) of the spinal cord (A, D and G). A high-power magnification (insets) revealed GFAP (A-C) and IBA1 (D-F) immunoreactivity surrounding the 6E10-labelled amyloid plaques in the dorsal and ventral horns of the spinal cord; whilst NeuN co-staining (G-I) shows lack of neuronal cells within the vicinity of amyloid deposition. Scale bars: 200 µm (A–I) and 50 µm (insets).

2.3.2.4 **APP/Aβ Absent in CGRP-positive Primary Afferents**

Following the observation of intraneuronal accumulation of APP/Aβ in the dorsal and ventral horns of the TASTPM spinal cord, we assessed if APP/Aβ also co-localised with and/or affected a sub-population of primary afferent terminals. In the TASTPM dorsal horn, APP/Aβ was not co-expressed with the primary afferent marker CGRP in laminae I and II (Figure 2.12A-C). It was evident that APP/Aβ was mainly distributed in deeper dorsal horn laminae starting from lamina III onwards thereby justifying the absence in this subpopulation of peptidergic primary afferent terminals innervating the superficial laminae I and II. Subsequently, we assessed whether expression of APP/Aβ in the dorsal horn had an impact on the level and distribution of CGRP-positive sub-population primary afferent terminals. Immunohistochemical quantification of CGRP intensities in the superficial laminae of the spinal cord dorsal horn revealed no significant difference in the mean CGRP immunoreactivity intensities when comparing TASTPM to age- and gender-matched WT controls (Figure 2.12D-F). Therefore, these results indicate that the intraneuronal accumulation of APP/Aβ in the dorsal horn does not affect CGRP immunopositive sub-population of primary afferent terminals in the spinal cord.

2.3.2.5 **APP/Aβ Mainly Absent in NK1R-positive Projection Neurons**

Given the intraneuronal accumulation of APP/Aβ in deeper laminae of the dorsal horn, we examined whether APP/Aβ was expressed in projection neurons that are located in mainly in lamina I as well as deeper laminae of the spinal cord dorsal horn (Figure 2.13A-C) (Cameron et al 2015). Immunohistochemical quantification revealed that most APP/Aβ (>95%) did not co-localise with NK_1 receptor (NK1R) in neurons which are presumably a subpopulation of projection neurons in lamina III (Figure 2.13D-G). Similar to CGRP, we assessed if presence of APP/Aβ had an impact on the level of NK1R expression in the spinal cord. Western blot analysis revealed no significant change in the expression of NK1R in the spinal cord of TASTPM compared to age- and gender matched WT controls (Figure 2.13H). Thus APP/Aβ presence in the dorsal horn does not have an impact on the level of NK1R that is presumably expressed in projection neurons.

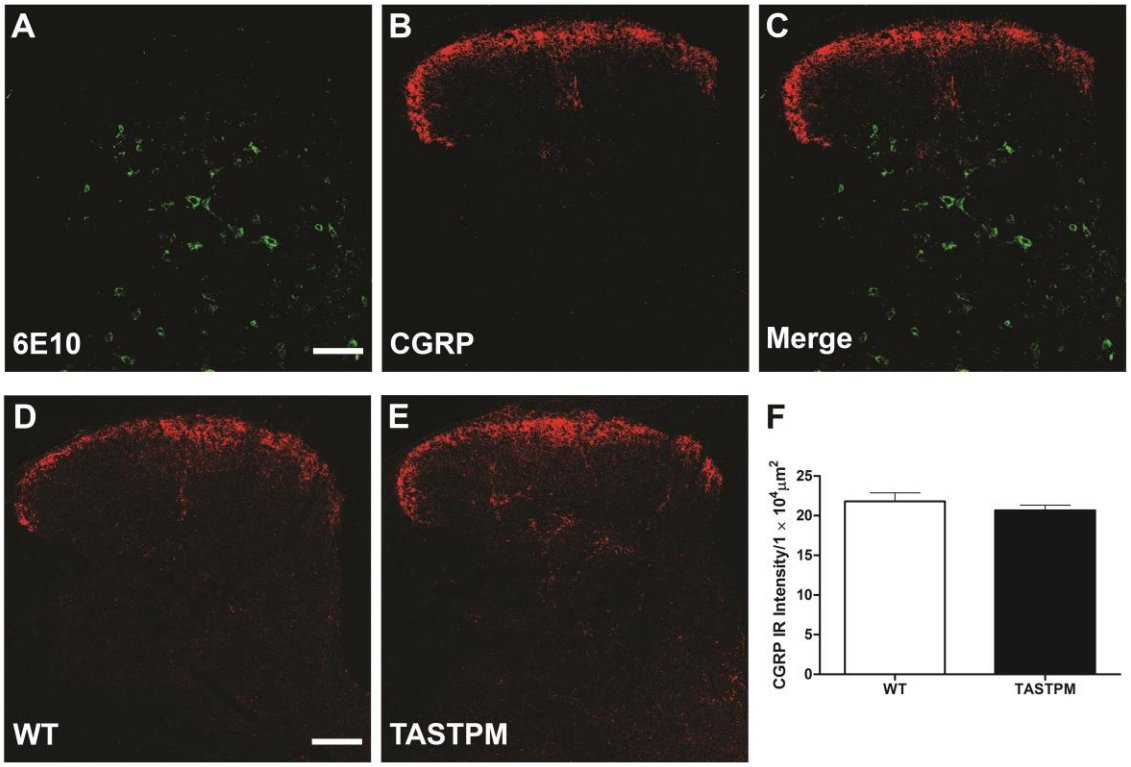

Figure 2.12: APP/Aβ Absent in a Subpopulation of Primary Afferent Terminals

Transverse spinal cord sections from 6 months old TASTPM were stained with antibodies against β-amyloid 1-16 (6E10) (A) and calcitonin gene-related peptide (CGRP), a marker for peptidergic primary afferent terminals (B). Merged images are shown for 6E10 co-stained with CGRP (C). β-amyloid 1-16 was absent in primary afferent CGRP immunopositive terminals. Transverse spinal cord sections from 6 months old TASTPM and WT mice were stained with an antibody against CGRP (D-E). Quantitative analysis of CGRP immunostaining intensity in the dorsal horn revealed no significant difference ($p > 0.05$, Student's *t*-test) in the CGRP intensity between TASTPM mice compared to WT controls (F). Scale bars: 100 µm.

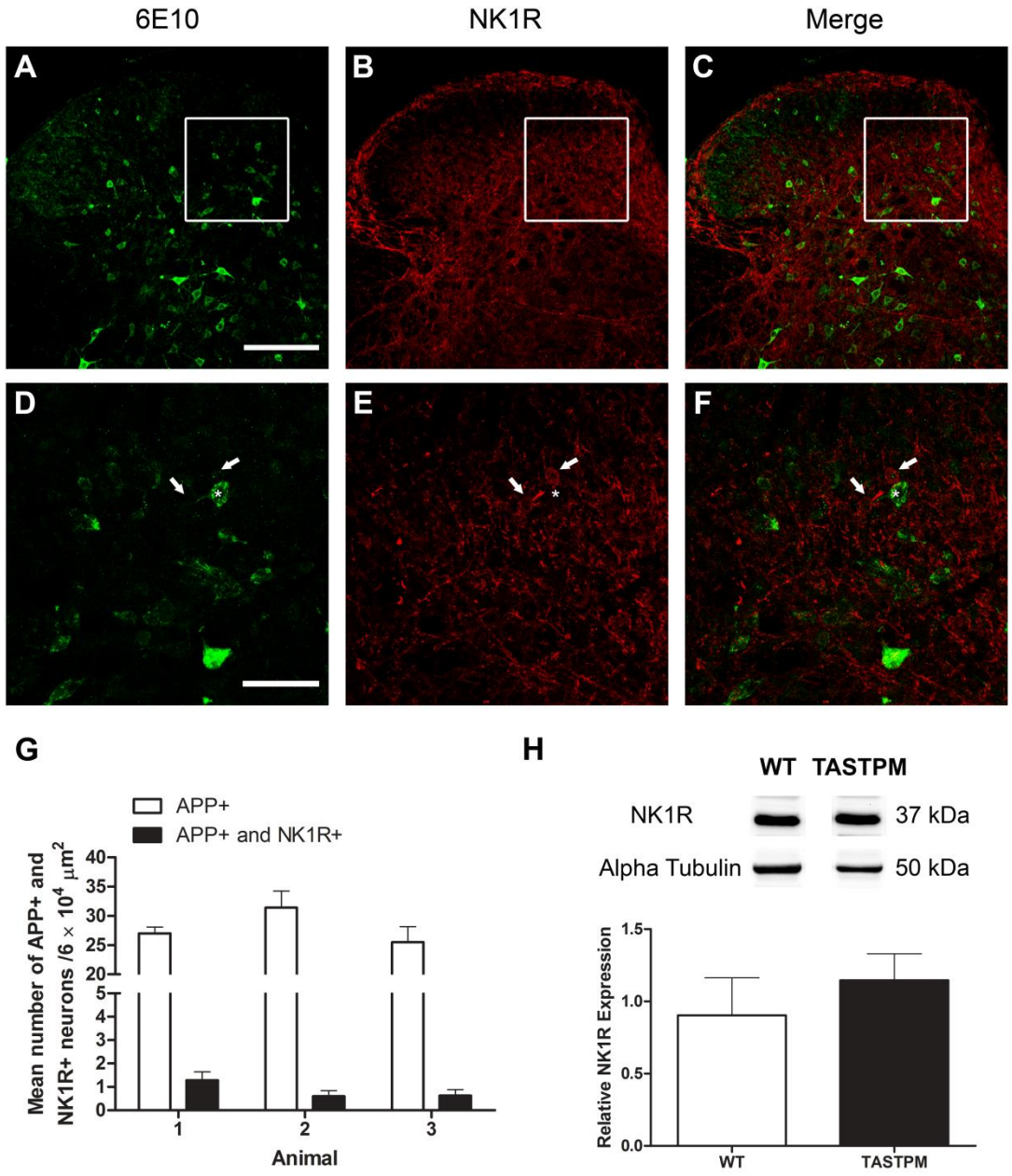

Figure 2.13: APP/Aβ Mostly Absent in a Subpopulation of NK1R-positive Projection Neurons

Transverse spinal cord sections from 6 months old TASTPM mice were stained with antibodies against β-amyloid 1-16 (6E10) (A and D) and neurokinin 1 receptor (NK1R) (B and E). Merged images are shown for 6E10 co-stained with NK1R (C and F). A high-power magnification image represented by the boxed-outline (A-C) is shown (D-F). Quantitative analysis of total number of APP/Aβ (APP+) and number of APP/Aβ that also express NK1R (APP+ and NK1R+) revealed β-amyloid 1-16 was mostly absent in NK1R-positive neurons (D-F: arrows, NK1R; *, APP/Aβ) in the dorsal horn of the TASTPM spinal cord (G). Scale bars: 150 µm (A-C) and 50 µm (D–F). Quantitative levels of NK1R determined by Western blot revealed no significant difference in the lumbar (L3-L5) spinal cord of 6 months old TASTPM mice compared to age- and gender-matched WT controls ($p > 0.05$, Student's *t*-test) relative to α-tubulin (loading control) (H).

2.3.2.6 **VGLUT Boutons Innervate APP/Aβ-containing Dorsal Horn Neurons**

As APP/Aβ was absent in the sub-population of primary afferent terminals and projection neurons, we explored further in order to examine which sub-population of neurons either expressed APP/Aβ or that may have been affected by the intraneuronal accumulation of APP/Aβ. In AD, the glutamatergic system has been identified to contribute to the synaptic dysfunction in the hippocampus (Parameshwaran et al 2008, Paula-Lima et al 2013, Ting et al 2007) therefore; we initially explored the excitatory transmission in the spinal cord using markers for vesicular glutamate transporter, namely, VGLUT1 and VGLUT2. APP/Aβ positive neurons received innervations by the excitatory VGLUT1 and VGLUT2 immunopositive boutons (Figure 2.14A-D). Triple staining (VGLUTs and 6E10), revealed that there was an exclusive sub-population of VGLUT1 and VGLUT2 innervating APP/Aβ positive neuron in the dorsal horn lamina IV, with little, if any, overlap (Figure 2.14E-H). As a result, we focused on assessing whether interaction of VGLUTs boutons with APP/Aβ containing neurons had an impact on the excitatory neuronal population innervating the TASTPM spinal cord.

2.3.2.7 **Reduced VGLUT2 Expression in the TASTPM Spinal Cord**

In order to evaluate possible changes in excitatory neuronal innervation in TASTPM spinal cord, we assessed the expression of vesicular glutamate transporters VGLUT1 and VGLUT2. As previously reported (Brumovsky et al 2007) the distribution of VGLUT1 profiles in WT spinal cord was mainly in the deeper dorsal horn laminae (III-V) (Figure 2.15A), and we observed that this was not altered in the spinal cords of TASTPM mice (Figure 2.15B). As reported, VGLUT2 immunoreactivity was found throughout the grey matter in WT spinal cords (Figure 2.15C), but we observed that VGLUT2 immunostaining was less prominent in the medial part of the deep dorsal horn in TASTPM spinal cord (Figure 2.15D). Quantitative analysis of VGLUT1 and VGLUT2 immunostaining intensity in the dorsal horn revealed significantly reduced VGLUT2 staining intensity in the dorsal horn of the TASTPM mice compared to WT mice whilst no difference in the expression of VGLUT1 was observed (Figure 2.15G-H). Furthermore, Western blot analysis of VGLUT1 and VGLUT2 proteins in lumbar spinal cord showed significantly lower expression of VGLUT2, but not VGLUT1 in TASTPM mouse tissue compared to WT mice

controls (Figure 2.15I-J). These data further reinforce that VGLUT2 expression in reduced in the spinal cord of 6 months old TASTPM mice compared to WT controls.

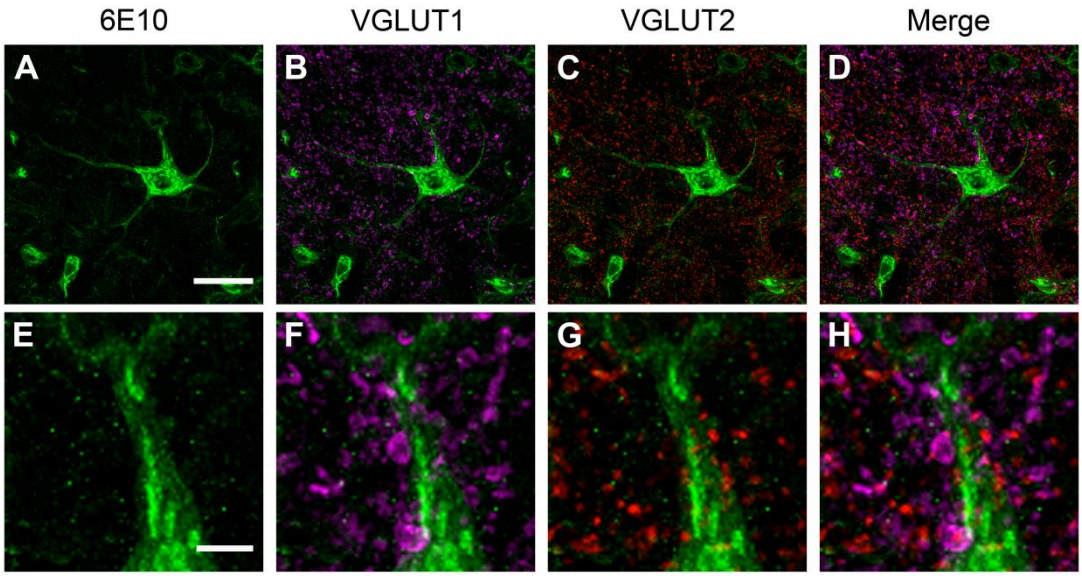

Figure 2.14: APP/Aβ Present in Neurons Innervated by Glutamatergic Inputs in the Dorsal Horn of the Spinal Cord

Transverse spinal cord sections from 6 months old TASTPM were triple stained with antibodies raised against β-amyloid 1-16 (6E10) (A and E), vesicular glutamate transporter 1 (VGLUT1) and vesicular glutamate transporter 2 (VGLUT2). Merged images are shown for 6E10 co-stained with VGLUT1 (B and F), VGLUT2 (C and G) and triple staining (D and H). β-amyloid 1-16 containing neurons in the dorsal horn of the spinal cord receive innervations from both VGLUT1 and VGLUT2 immunopositive boutons. VGLUT1 and VGLUT2 have been identified mainly to be expressed in different subpopulation of boutons due to lack of co-localisation. Scale bars: 30 µm (A-D) and 5 µm (E-H).

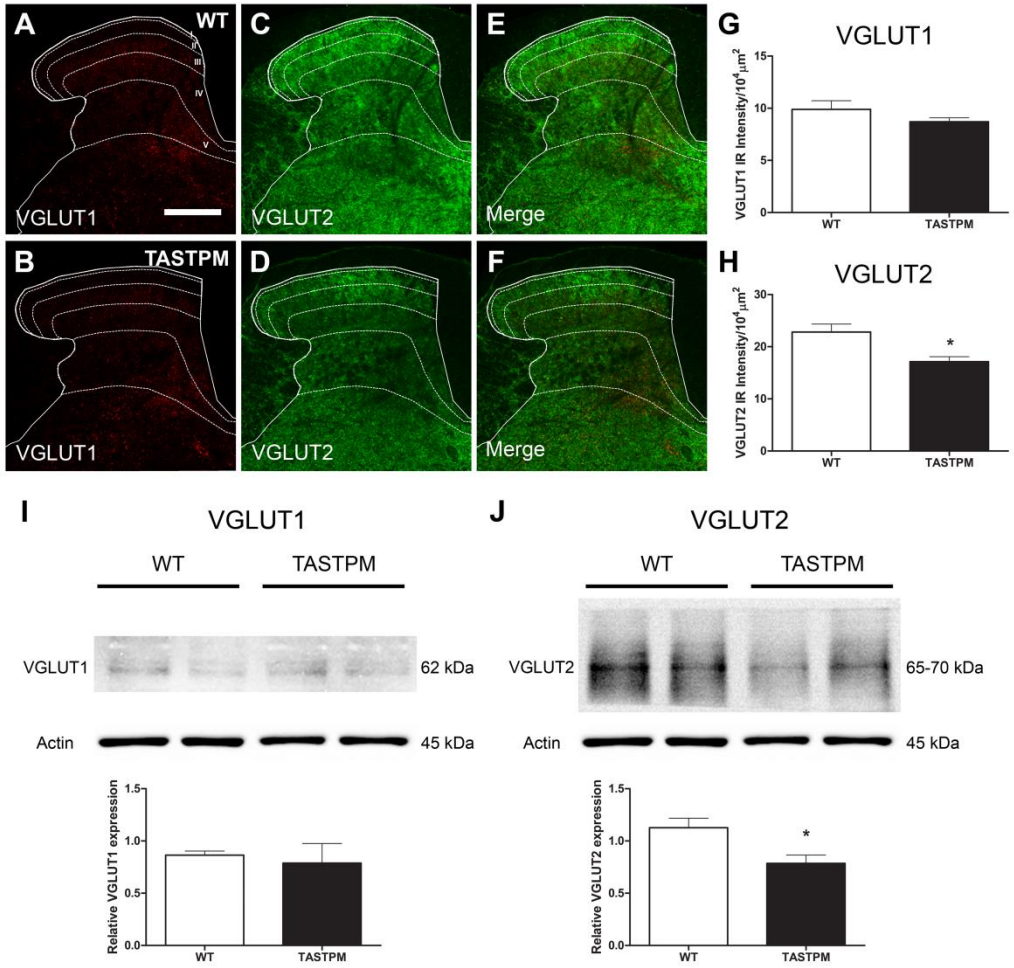

Figure 2.15: Reduced VGLUT2 Expression in the TASTPM Spinal Cord

Transverse spinal cord sections from 6 months old TASTPM and wild-type (WT) mice were stained with antibodies against vesicular glutamate transporter 1 (VGLUT1) (A and B) and vesicular glutamate transporter 2 (VGLUT2) (C and D). Merged images are shown for VGLUT1 co-staining with VGLUT2 (E and F). The distribution of VGLUT1 in TASTPM and WT spinal cord was mainly in the deeper dorsal horn laminae (III-VI) (A and B), while VGLUT2 was found throughout the grey matter but with less prominence in the medial part of the TASTPM deep dorsal horn (C and D). Quantitative analysis of VGLUT1 and VGLUT2 immunostaining intensity in the dorsal horn revealed significantly reduced VGLUT2 intensity in the dorsal horn of the TASTPM mice compared with WT controls (* $p < 0.05$, Student's *t*-test, H) but no difference in VGLUT1 intensity ($p > 0.05$, Student's *t*-test, G). Data values are expressed as mean ± SEM (n = 4 per experimental group). Scale bars: 200 mm (A–F). Quantitative levels of VGLUTs determined by Western blot revealed significantly reduced levels of VGLUT2 expression in the lumbar (L3-L5) spinal cord of 6 months old TASTPM mice compared with WT controls (* $p < 0.05$, Student's *t*-test) relative to β-actin (loading control), whilst no change in VGLUT1 was detected (I–J). Data values are expressed as mean ± SEM (n = 3 per experimental group).

2.3.3 Sensory and Motor Behaviour of TASTPM

As in 6 months old TASTPM mice the presence of APP/Aβ in the spinal cord is associated with a significant decrease in expression of VGLUT2, these data suggest possible alterations of the excitatory function. Many deep dorsal horn neurons respond to noxious input and also send their dorsal dendrites superficially into laminae I-III where they receive primary afferent input from unmyelinated sensory fibres which respond to noxious stimuli in the periphery (Willis Jr & Coggeshall 1991). Thus, although we observed no significant APP/Aβ expression in superficial laminae, we evaluated whether TASTPM mice display sensory changes compared to WT mice.

2.3.3.1 **Age-dependant Reduced Sensitivity to Acute Noxious Stimuli**

In order to investigate whether AD-associated changes observed in the TASTPM brain and spinal cord had an impact on acute nociceptive thresholds we carried out a set of behavioural assessments for responses to thermal (Figure 2.16A-C) and mechanical stimulations (Figure 2.16D-I) compared to age- and gender-matched WT controls. TASTPM mice displayed increased response latency to thermal stimulation compared to WT mice at the age of 6 and 12 months old, but not at the age of 4 months old (Figure 2.16A-C).

However, hind paw withdrawal thresholds to mechanical stimulation using von Frey monofilaments in the TASTPM mice were comparable to WT mice at the age of 4 and 6 months; with mechanical hyposensitivity only apparent in 12 months old TASTPM mice compared to WT control (Figure 2.16D-F). Similarly, using the paw pressure, another test for assessment of mechanical threshold, revealed an age-dependant reduced sensitivity to noxious mechanical threshold that had become evident in TASTPM mice at the age of 12 months old but not 6 months old compared to age- and gender-matched WT controls (Figure 2.16G-I). Thus, confirming reduced mechanical sensitivity which becomes evident at the age of 12 months old.

Collectively these data indicate an age-dependant reduced sensitivity to acute noxious thermal and mechanical stimulation with onset thermal hypoalgesia preceding the mechanical hyposensitivity.

2.3.3.2 **No Alteration in Locomotor Function**

Subsequent to sensory testing, motor function at the three age time points was examined using the accelerating RotoRod. Motor coordination was no different from WT mice in any age group (Figure 2.16J-L). Thus, indicative of no motor impairment at any time point in the TASTPM model of AD compared to age- and gender-matched WT controls.

Therefore, mice displaying amyloid plaques in the brain and cognitive deficits, which are both indicative of development of AD-like pathology in the brain, also display accumulation of APP/Aβ in spinal cord neurons and an age-dependant reduced sensitivity to acute noxious heat stimulation applied to the hind paw in the periphery. Whilst deposition of amyloid plaques in the spinal cord in older (12 months old) TASTPM mice coincided with the reduced sensitivity in response to acute noxious mechanical stimuli applied to the hind paw in the periphery.

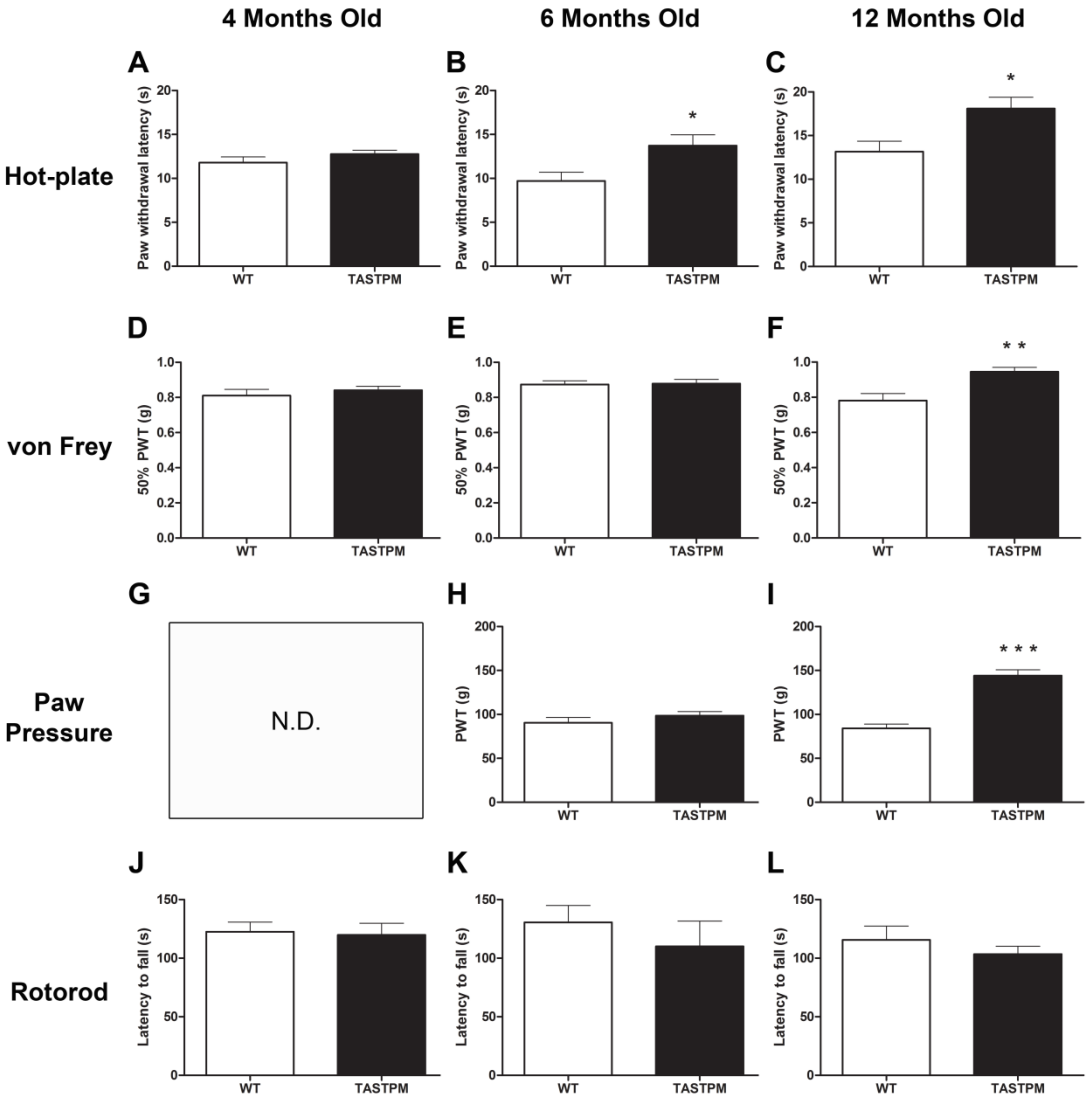

Figure 2.16: Age-related Reduced Sensitivity to Noxious Acute Stimuli

TASTPM mice displayed comparable nociceptive thresholds to wild-type (WT) mice in response to noxious thermal stimulation at the age of 4 months old (A); however, an increased paw withdrawal latency compared with WT mice at the age of 6 months old (B) and 12 months old (C) (* $p < 0.05$, Mann-Whitney Rank Sum test). TASTPM mice exhibited responses comparable with WT mice in response to noxious mechanical stimulation induced by von Frey filaments and at the age of 4 and 6 months old (D and E) whilst developed an age-dependant reduced sensitivity mechanical stimulation at the age of 12 months old (F) (* * $p < 0.01$, Student's *t*-test). Nociceptive responses to noxious mechanical stimulation induced by paw pressure test also displayed TASTPM mice comparable paw withdrawal threshold (PWT) to WT controls at the age of 6 months old (H), however an increased PWT compared to WT at the age of 12 months old (I) (* * * $p < 0.001$, Student's *t*-test). No motor deficit in the TASTPM mice at the age of 4, 6 and 12 months old, as no significant difference in the latency to fall from an accelerating RotoRod was observed when compared with WT controls (J-L) ($p > 0.05$, Student's *t*-test). Data are expressed as mean ± SEM (n = 5-16 per experimental group). Abbreviations: N.D., not determined. Paw pressure test was conducted by Mr Thomas Pitcher.

2.3.4 Involvement of Opioidergic System in Altered Nociceptive Thresholds

Notwithstanding the importance and relevance of the higher structures in the brain in the perception and modulation of pain, we focussed this study on the dorsal horn of the spinal cord which is the first relay station of noxious heat stimuli from the periphery, in order to delineate the mechanism underlying altered nociceptive thresholds exhibited by 6 months old TASTPM mice. In particular we tested the hypothesis that an increased inhibitory tone may underlie reduced thermal sensitivity in TASTPM mice. Specifically, we examined the expression of the enkephalins, in TASTPM mice, as elevated levels of opioid peptides in the CSF in AD patients have been reported (Muhlbauer et al 1986, Risser et al 1996).

2.3.4.1 **Increased Expression of Enkephalin in the 6 Months Old TASTPM Spinal Cord**

In order to test the hypothesis that there is an increased opioid level in spinal cord we carried out an immunohistochemical study in order to assess the expression of enkephalins in the TASTPM mice compared to WT controls. We observed a significant increase of enkephalin immunoreactivity in laminae I and II of the dorsal horn of 6 months old TASTPM mice compared to WT mice (Figure 2.17A-C). Furthermore, pre-pro enkephalin (pPENK) and pro-enkephalin (PENK) mRNA expression in TASTPM mice dorsal horn tissue extracts were significantly higher than in control tissue (Figure 2.17D-E). The pre-pro enkephalins and pro-enkephalins are processed to generate the enkephalin peptides (Dickenson & Kieffer 2006). These data suggest an increase opioidergic tone in TASTPM mice due to increased production and release of enkephalins in the spinal cord.

2.3.4.2 **Naloxone Re-Establishes Normal Thermal Sensitivity in TASTPM**

In order to test possibility of an increased opioidergic tone we administered the opioid receptor antagonist naloxone. We observed a significant reduction of TASTPM mice thermal thresholds at 30 minutes from injection compared to both baseline and its respective saline control values (Figure 2.18). Moreover, the effect of naloxone started to diminish 90 minutes post administration and returning to baseline levels 3 hours after administration in the TASTPM mice. However, administration of naloxone did not alter the nociceptive thresholds of WT mice in response to acute thermal stimulation throughout the course of the experiment. Therefore,

these data reinforce the notion that the increased opioidergic tone may underlie the reduced sensitivity to noxious thermal stimulation in the TASTPM mouse model of AD.

2.3.4.3 **Naloxone Fails to Improve TASTPM Cognitive Ability**

In order to test the possibility whether the altered opioidergic tone affected cognitive ability, we subsequently went on to explore whether the opioid antagonist had the potential to induce recovery of the cognitive impairment exhibited by the 6 months old TASTPM mice. A standard novel object recognition test was performed during the first week in order to confirm the presence cognitive deficits (as in section 2.3.1.2). An i.p. injection of naloxone, three days post confirmation of cognitive impairment, resulted in no significant change in the time spent in exploring the novel object relative to the familiar object by both WT and TASTPM mice (Figure 2.19). Thus, suggesting that naloxone was unable to improve cognitive impairment, which is may be reflective of the short-lived effect of naloxone with limited effect on cognition and/or suggest possibly different pathways involved in pain processing and those involved in learning and memory, an avenue that requires to be further scrutinised.

2.3.4.4 **Morphine: A Potent Analgesic**

Subsequently, we assessed the analgesic effect of the opioid agonist, morphine, in the TASTPM model of AD. As expected, morphine induced increased latency to respond in response to noxious thermal stimuli in WT mice 30 minutes post injection compared to its baseline. The effect of morphine started to reduce at 90 minutes with mice recovering back to their baseline values 180 minutes post morphine administration (Figure 2.20). A similar pattern of response was also observed in the TASTPM model of AD, with peak effect at 30 minutes exhibiting similar paw withdrawal latencies to those demonstrated by the WT mice. Therefore, suggesting an opioid agonist is still successful in inducing analgesia in a model with an increased opioidergic tone.

2.3.4.5 **Morphine Fails to Induce and/or Recall Reward in TASTPM**

Given that morphine was able to exhibit analgesia, we utilised the conditioned place preference test in order to determine whether the reward effect of morphine was altered in the TASTPM mice. Expectedly, repeated administration of morphine induced conditioned place preference in

WT mice as they spent significantly greater amount of time in morphine-paired chamber in comparison to the WT vehicle control group at the age of 6 months old and 12 months old. However, TASTPM mice did not exhibit the morphine induced conditioned place preference at any age group as there was no difference in the time spent in the morphine-paired chamber by TASTPM mice that were administrated with morphine compared vehicle TASTPM controls (Figure 2.21). Therefore, indicating that morphine fails to induce reward/motivation in the transgenic TASTPM model of AD.

Altogether these data suggest that there is an age-dependant alteration in thermal sensitivity at the age of 6 months old which coincides with the onset of cognitive deficits. Intracellular APP/Aβ expression was detected only in the spinal cords of TASTPM mice and was accompanied by alterations in both the glutamatergic and opioidergic systems in the spinal cord. In addition, mechanical hyposensitivity follows the reduced sensitivity to noxious heat at a later age of 12 months old which coincides with the presence of amyloid depositions in the spinal cord accompanied by neuroinflammation. Finally, diminished morphine-induced reward and/or inability to recognise reward was exhibited by the transgenic TASTPM mice.

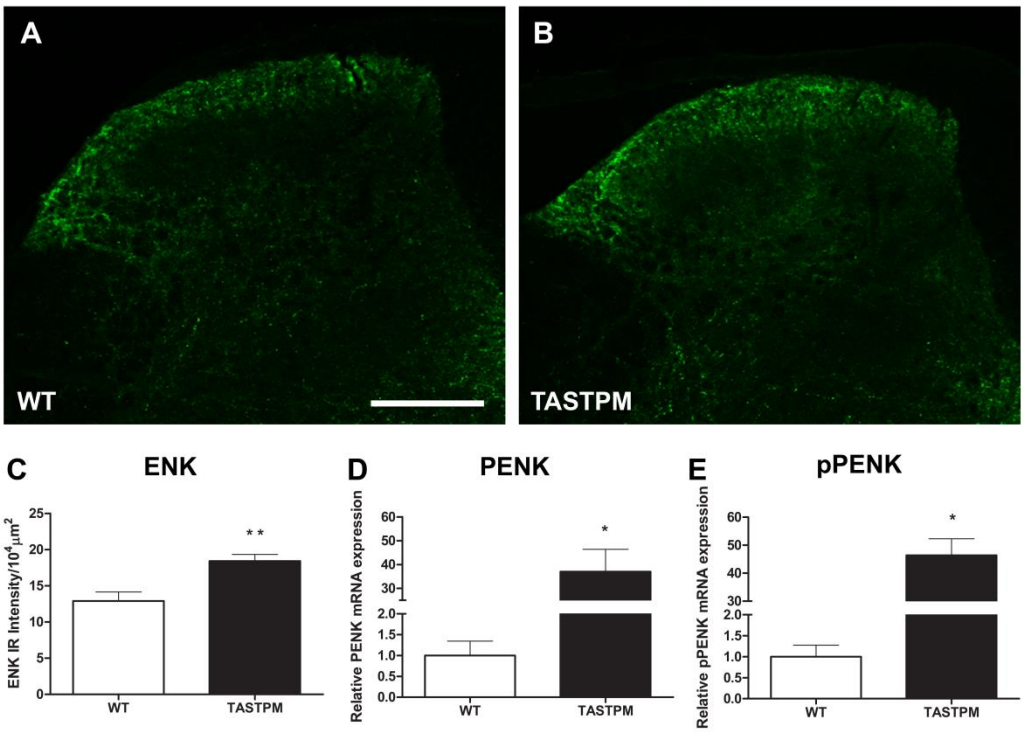

Figure 2.17: Increased Expression of Enkephalins in the TASTPM Spinal Cord

Transverse lumbar spinal cord sections from 6 months old TASTPM and wild-type (WT) mice were stained with met-enkephalin (ENK) (A and B). Quantitative analysis of met-ENK immunostaining in the dorsal horn revealed significantly higher met-ENK intensity in the dorsal horn of TASTPM compared with WT controls (* * $p < 0.01$, Mann-Whitney Rank Sum test, C). Values are expressed as mean ± SEM (n = 8-10 per experimental group) and scale bar represents 200 µm. In addition, RT-PCR displayed significantly higher mRNA expression of pre-proenkephalin (pPENK, D) and proenkephalin (PENK, E) in 6 months old TASTPM dorsal horn (L3-L5) compared age-matched WT controls (* $p < 0.05$, Mann-Whitney Rank Sum test). Data are expressed as mean ± SEM (n = 4 per experimental group).

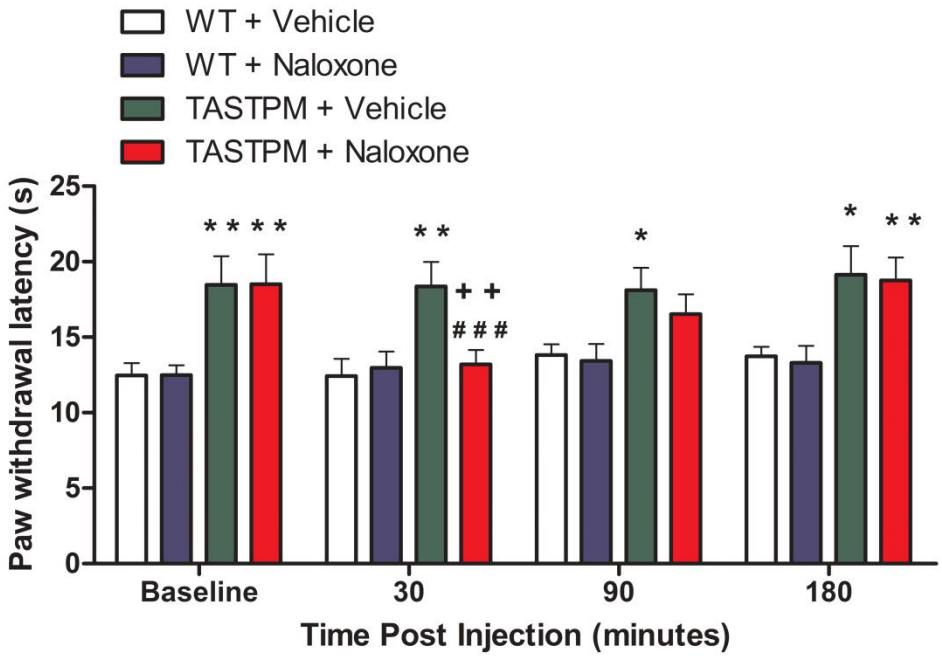

Figure 2.18: Naloxone Re-establishes Normal Thermal Sensitivity in 6 Months Old TASTPM Mice

Administration of naloxone (1mg/kg intraperitoneally), an opioid antagonist, reduced paw withdrawal latency in TASTPM mice compared with baseline ($^{\#\#\#}p < 0.001$) and TASTPM saline control ($^{++}p < 0.01$) after 30 minutes. However, there was no effect of naloxone observed in WT mice compared with their respective baseline and WT saline control. TASTPM mice exhibited significantly higher paw withdrawal latency compared with WT mice injected with saline at baseline and recovered back to baseline levels and significantly higher 3 hours after naloxone administration (* $p < 0.05$, * * $p < 0.01$) using two-way repeated-measures analysis of variance (ANOVA) followed by Tukey multiple comparison test. Data is presented as mean ± SEM (n = 9-10 per experimental group).

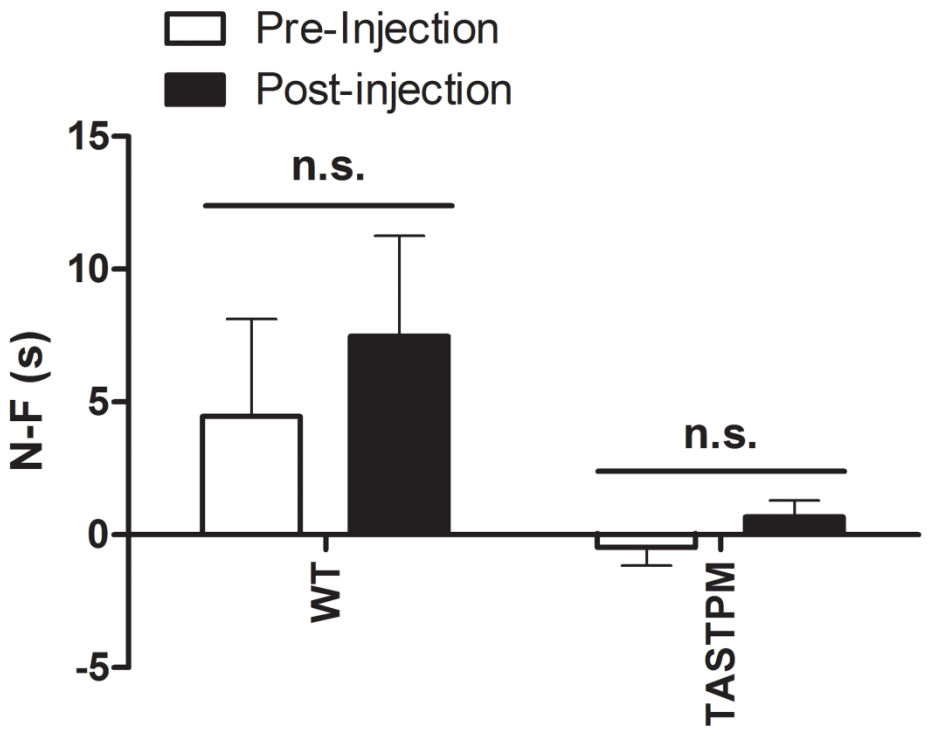

Figure 2.19: No Effect of Naloxone on Cognitive Recovery in 6 Months Old TASTPM Mice

Administration of naloxone (1mg/kg intraperitoneally), an opioid antagonist, failed to rescue AD-related cognitive deficit exhibited by the TASTPM mice ($p > 0.05$, Student's *t*-test). Data is expressed as mean ± SEM (n = 9 animals per experimental group). Abbreviations: F, familiar object; N, novel object; n.s. not significant.

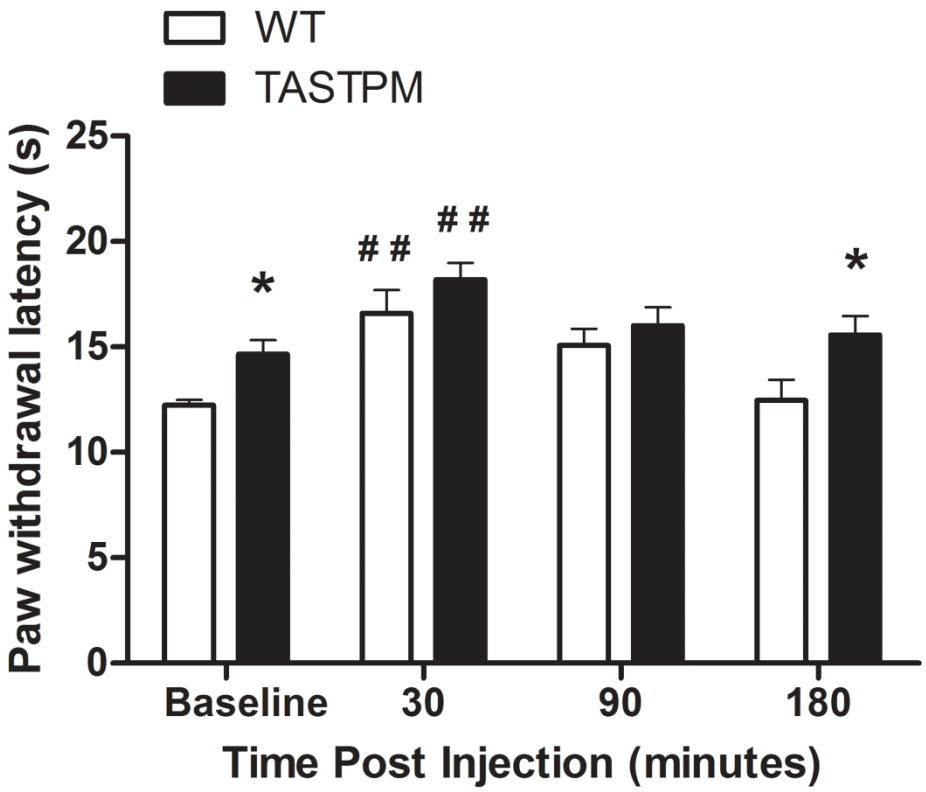

Figure 2.20: Morphine is a Potent Analgesic in both WT and TASTPM Mice

TASTPM mice exhibited significantly higher paw withdrawal latency compared to WT at baseline (* $p < 0.05$). Administration of morphine (6mg/kg subcutaneously), an opioid agonist, increased paw withdrawal latencies comparable level in both WT and TASTPM mice compared to their respective baselines ($^{\#\#} p < 0.01$) after 30 minutes. The effect of morphine reduced over time and recovering back to baseline levels at 180 minutes post administration in both genotypes. Statistical analysis was performed using two-way repeated-measures ANOVA followed by Tukey multiple comparison test. Data is presented as mean ± SEM (n = 5-6 per experimental group).

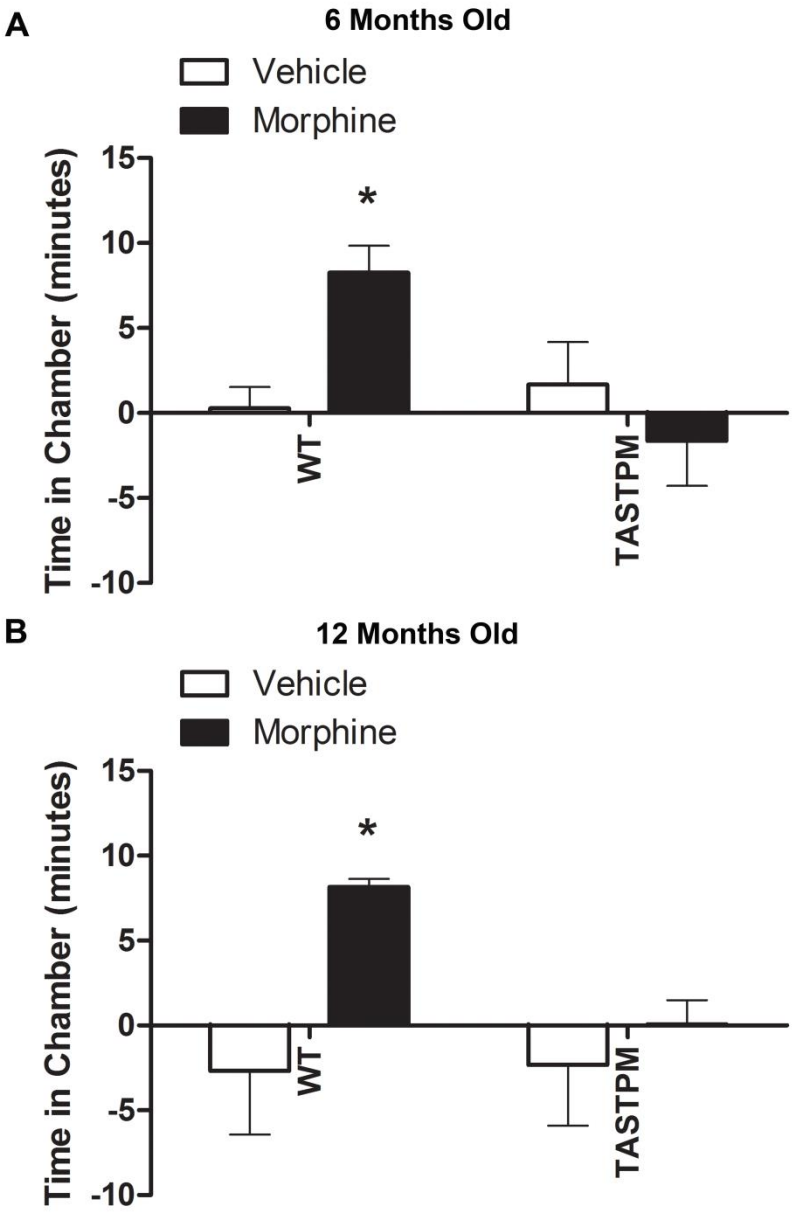

Figure 2.21: Lack of Morphine induced Motivational/Reward Behaviour in TASTPM Mice

Administration of morphine (6mg/kg subcutaneously), an opioid agonist, resulted in significantly greater time spent by WT mice in the morphine-paired chamber in comparison to the vehicle-paired control chamber at the age of 6 months old ($p < 0.05$, Student's *t*-test); whilst no significant difference was observed in the TASTPM mice (A). A similar behavioural pattern was observed even at the age of 12 months old in both genotypes (B). Data are presented as mean ± SEM (n = 5-7 per experimental group).

2.4 Discussion

The aim of the present chapter was to explore AD-associated pathology in the spinal cord of the transgenic TASTPM mouse model of AD; and to assess the impact it may have on nociceptive thresholds in response to acute noxious stimulation. In this chapter we initially validated AD-associated age-dependant cognitive decline and development of amyloid plaques in the brain of 6 months old transgenic TASTPM mouse model of AD (Howlett et al 2004). In addition, we provide evidence for intra-neuronal accumulation of APP/Aβ in the spinal cords of TASTPM mice, in both dorsal and ventral grey matter; thereby highlighting the presence of early AD-like pathology in the spinal cord of 6 months old TASTPM mice. Further analysis revealed a decrease of glutamatergic interneurons marker VGLUT2 in the dorsal horn of TASTPM mice compared to WT mice. The glutamatergic system has been identified to contribute to the synaptic dysfunction in AD hippocampus (Parameshwaran et al 2008, Paula-Lima et al 2013, Ting et al 2007); and glutamate is present in primary afferent terminals, projection neurons as well as excitatory interneurons in the spinal cord where it plays pro-nociceptive roles (Todd et al 2003).

In nociceptive behavioural studies, the transgenic mice exhibited an age-dependant decline in sensitivity to thermal stimulation which could be attributed to a reduced glutamatergic excitation and/or increased inhibition in the spinal cord. Indeed, we found higher levels of pre-pro and pro-enkephalin mRNA and enkephalin peptide expression in the dorsal horn of TASTPM mice suggesting that an increased synthesis and release of enkephalins in the spinal cord could result in elevated inhibitory tone. This likely possibility is strengthened by our finding of the recovery of normal thermal sensitivity following administration of the opioid antagonist naloxone in TASTPM mice. However, the anti-nociceptive effect of morphine, an opioid agonist, was preserved in the TASTPM mice that exhibited an elevated opioidergic tone.

We have also provided evidence in this chapter for age-related development of amyloid plaques in the spinal cord of aged 12 months old TASTPM mice, both in the dorsal and ventral horns. These amyloid plaques were accompanied by barriers formed by astroglial and microglial cells; whilst neuronal cells were absent at the site suggesting the extracellular deposition of amyloid

plaques accompanied by neuroinflammation. Further behavioural studies revealed reduced sensitivity of thermal and mechanical nociceptive thresholds in mice displaying spinal cord amyloid plaques. Therefore, indicating that AD-associated pathology in the spinal cord might have a deteriorating impact on acute nociceptive thresholds.

Cognitive deficits and amyloid plaques are among the major clinical and pathological hallmarks of AD in the brain, respectively. As expected, TASTPM mice displayed an age-dependant cognitive impairment in the object recognition test which becomes apparent at the age of 6 months. In addition, extracellular amyloid plaques accompanied by gliosis were present in the cerebral cortex and hippocampus as well as the thalamus, a key relay station in nociceptive signalling pathways (Howlett et al 2008). Further quantification of gliosis in the cerebral cortex, hippocampus and thalamus revealed significantly greater burden of glial cells in each of the regions examined in the 6 months old TASTPM mice compared to WT controls. Therefore, indicating the presence of neuroinflammation in the transgenic TASTPM mouse model of AD. Collectively, these findings are consistent with previous reports indicating that the TASTPM mouse model recapitulates some of the key features of AD clinically and pathologically (Howlett et al 2008, Howlett et al 2004).

The novelty of the present study was the identification of the presence of intra-neuronal accumulation of APP/Aβ in both the dorsal (lamina III and deeper) and ventral horns of the lumbar spinal cords of TASTPM mice whilst previous studies have primarily focused on the brain. Previous studies that have reported Aβ pathology in the 5×FAD and Tg2576 transgenic mouse models of AD, but have mainly focused on the dorsal column or the ventral horn and suggested an association between intra-neuronal Aβ and motor impairment (Jawhar et al 2012, Seo et al 2010, Wirths et al 2006). Differently, in the present study despite the accumulation of APP/Aβ in ventral horns, no gross motor deficits were detected in the TASTPM mice using the accelerating RotoRod test. However, this may have been due to the fact that the RotoRod may not have been a sensitive enough test to detect subtle motor deficits (Brooks & Dunnett 2009). Furthermore, our study highlights the presence of APP/Aβ accumulation in both dorsal and ventral horn neurons and assesses the impact on sensory and motor behaviour in the transgenic TASTPM mice compared to WT mice controls.

Intra-neuronal Aβ is associated with synaptic dysfunction and early cognitive impairments prior to the development of the AD pathological hallmark in the form of extracellular plaques (Iulita et al 2014, Oddo et al 2003). The intracellular pool of Aβ may act as a source for the formation of extracellular plaques and the intracellular Aβ intensity decreases as the AD core pathology develops (Leon et al 2010). Further evidence illustrates that intracellular Aβ accumulates in multivesicular bodies of neurons within the presynaptic and postsynaptic compartments and a study in 3xTg model of AD revealed synaptic dysfunction and long-term potentiating (LTP) deficit prior to the presence of amyloid plaques (Oddo et al 2003, Takahashi et al 2002). Therefore, we speculate that intra-neuronal accumulation of APP/Aβ in the spinal cord of 6 months old TASTPM mice is an early stage AD-like pathological feature which has the potential to induce synaptic dysfunction and contribute towards the development of amyloid plaques, as observed in the spinal cords of 12 months old TASTPM mice, with progression of the disease.

APP/Aβ were not found in primary afferent nociceptive terminals in the superficial (laminae I-II) and were at large absent in lamina I and laminae III-VI presumed projection neurons. Presence of APP/Aβ in the spinal cord did not affect the relative expression of CGRP and NK1R in TASTPM compared to non-transgenic WT controls. Following activation by noxious stimuli in the periphery, a subpopulation of primary afferent fibres release CGRP and substance P (SP) alongside glutamate from their central terminals in the dorsal horn and mediate nociceptive transmission via activation of CGRP and NK1R in projection neurons. Ablation of NK1R resulted in a significant attenuation of responses to highly noxious stimuli (capsaicin) as well as mechanical hyperalgesia (Laird et al 2001). Whilst, CGRP contributes in nociceptive transmission directly and indirectly by potentiating the actions of SP through: promoting release, inhibition of degradation, and regulating the expression of NK1R (Latremoliere & Woolf 2009). Therefore, the lack of APP/Aβ immunoreactivity in a NK1R labelled subpopulation of presumed projection neurons implies that APP/Aβ may not directly affect the neurons relaying nociceptive information to the supraspinal structures. Notably, recent evidence suggests there may be a species difference between the mouse and rat as many of the large lamina III anterolateral tract neurons in the mouse do not show NK1R immunoreactivity (Cameron et al 2015). We therefore

cannot completely rule out the possibility that lamina III anterolateral tract neurons that lack the NK1R may express APP/Aβ.

However, APP/Aβ immunoreactivity was present in deep dorsal horn neurons where we detected innervations from the excitatory VGLUT1 and VGLUT2 immunopositive boutons. We were able to confirm that VGLUT1 and VGLUT2 are mostly expressed in different sub-population of terminals (Todd et al 2003). Further analysis revealed a reduction in VGLUT2 expression in the lumbar segment of the spinal cord and especially in the dorsal horn laminae IV-V. This finding may suggest that the presence of APP/Aβ is associated with glutamatergic dysfunction. Many lamina IV neurons send their dorsal dendrites superficially into laminae I-III and can receive primary afferent input from unmyelinated sensory fibres which respond to noxious stimuli in the periphery (Willis Jr & Coggeshall 1991). Thus, the presence of APP/Aβ in the dorsal horn of the spinal cord may indicate an alteration of glutamatergic function that, in turn, could reduce nociceptive transmission and/or excitatory modulation.

In TASTPM mice, thresholds to noxious mechanical stimuli were increased to that of the WT controls at the age of 12 months old but not at the age of 4 and 6 months old. In addition, we provide evidence for an age-dependant decrease in sensitivity to noxious thermal stimulation in the hot-plate test that becomes apparent at the age of 6 months old and which also involves supraspinal integration of nociceptive signals (Gregory et al 2013). Consistent with these observations, reduced sensitivity to noxious thermal stimuli has been observed to occur prior to any changes in mechanical nociceptive thresholds in the CRND8 model of AD (Shukla et al 2013) and by us in the tail immersion test in TASTPM mice (Corbett et al 2012).

It was noteworthy that the onset of thermal hyposensitivity was evident with deposition of amyloid plaques in the brain; whilst, reduced sensitivity to noxious mechanical sensitivity coincided with presence of amyloid plaques in the supraspinal structures and spinal cord. Therefore, there may be a relationship between impaired nociceptive responses and deposition of amyloid plaques in the regions involved in the pain pathway, namely spinal cord and thalamus, along with cognitive impairment. Intriguingly, a longitudinal study found that patients with AD exhibit reduced pain intensity and affect when compared to individuals without

dementia; thereby, supporting the possibility that the pain experience is altered in AD (Scherder et al 2001) and that the spinal expression of APP/Aβ may be a contributing factor.

In order to explore the underlying reason for the increase of TASTPM thermal thresholds, the impact of opioid levels on nociceptive behavioural responses were assessed. This approach was based upon evidence that AD patients show increased CSF levels of opioid peptides and a reduction in opioid binding receptors in the dentate gyrus (Jansen et al 1990, Muhlbauer et al 1986, Risser et al 1996). Endogenous opioid peptides may block pain via multiple mechanisms including actions on the mu opioid receptors (μ-OR) located in the periphery, spinal cord, and the brain (cortical and sub-cortical regions) (Stein et al 2003). Evidence stemming from global μ-OR knockout mice suggest increased sensitivity to acute thermal and tactile mechanical stimulation in comparison to control littermates. Whereas, conditional μ-OR ablation specifically in Nav1.8 and TRPV1 expressing primary afferent neurons displayed comparable nociceptive sensitivity to thermal, mechanical, and chemical stimulation (Corder et al 2017, Weibel et al 2013). Altogether, indicating that the peripheral μ-OR expressed by Nav1.8 and TRPV1 neurons are not predominantly involved in determining basal nociceptive thresholds in models of acute pain. The opioid receptor antagonist, naloxone, induced recovery of thermal thresholds in TASTPM mice suggesting that increased opioidergic tone in the transgenic mice is responsible for the altered thermal thresholds. Furthermore, histological and quantitative mRNA expression analysis revealed increased expression of enkephalins in the dorsal horn of the spinal cords of TASTPM mice compared to WT controls. In a transgenic mouse model that over expresses the human APP (hAPP), increased levels of enkephalins have been found in the hippocampus and entorhinal cortex which are associated with neuronal and cognitive impairments (Meilandt et al 2008). In addition, in an APP/PS transgenic mouse model of AD, evidence reported in knockdown or antagonism of the delta opioid receptor has revealed reductions in Aβ accumulation, plaque formation and associated gliosis and behavioural deficits, a result that supports the role of opioid peptides in Aβ generation (Teng et al 2010).

Whilst naloxone affected thermal thresholds, it was not able to reverse the cognitive impairment exhibited by the TASTPM mice; thereby, suggesting different mechanisms involved in nociceptive processing and those that process learning and memory. Indeed, clinical

experimental study reported no significant effect of a range of naloxone doses in improving cognitive ability of patients with AD (Tariot et al 1986). Although, chronic administration of an irreversible opioid antagonist, β-funaltrexamine, in hAPP mouse model of AD induced reversal of cognitive impairment (Meilandt et al 2008). Therefore, use of naloxone, an opioid antagonist with a short half-life, in our experimental design may not have been an effective mean to examine the role of the opioidergic system in cognitive deficits in transgenic mouse model of AD. This may also be a possible explanation for lack of progress in using naloxone to evaluate efficacy to halt and/or recover cognitive impairments in the people with AD.

In addition, we explored whether the anti-nociceptive effect of opioid agonist morphine was affected in 6 months old TASTPM mice, a model which displays an elevated opioidergic tone. Studies conducted in μ-OR knockout mice have indicated that the peripheral μ-OR expressed by primary Nav1.8 and TRPV1 nociceptors are not predominantly implicated in morphine induced anti-nociception in models of acute pain. Specifically, conditional μ-OR knockout in Nav1.8-expressing primary afferent neurons displayed comparable analgesia and tolerance induced by systemic administration of morphine (Weibel et al 2013). Likewise, conditional μ-OR knockout selectively in TRPV1-expressing primary afferent nociceptors (mainly peptidergic nociceptors) displayed similar level of anti-nociception in response to systemic morphine administration compared to their respective littermate controls. Furthermore, intrathecal administration of morphine in conditional μ-OR knockout in TRPV1-expressing neurons resulted in lack of anti-nociception relative to littermate controls. Thus, indicating spinal opioid anti-nociception may primarily be mediated via presynaptic μ-OR signalling in nociceptors (Corder et al 2017). Our data demonstrates that morphine was as effective in inducing thermal analgesia in TASTPM as it was in WT controls. Indeed, anti-nociceptive effect of morphine has also been shown in the hAPP model of AD, although pre-treatment with an irreversible opioid antagonist attenuates morphine-induced analgesia (Meilandt et al 2008).

However, morphine was unable to induce reward or motivational dependant conditioned place preference in the transgenic mouse model of AD at the age of 6 and 12 months old. As a result, indicating different mechanisms involved in nociceptive processing and those that process reward and motivation. Morphine has been demonstrated to induce conditioned place

preference in a dose-dependent manner, peaking at a dose of 40mg/kg, as it is a receptor-mediated response (Sala et al 1992). However, doses as high as 40mg/kg have been reported to cause catalepsy and motor dysfunction in mice (Zarrindast et al 2002). Thus, it would be of great relevance in future studies to evaluate whether an increase in dose of morphine administration, which does not induce catalepsy and motor dysfunction, can induce reward dependant conditioned place preference in the TASTPM mice.

In addition, histological and neuroimaging data demonstrated severe amygdala atrophy in AD individuals, a region that has been identified to be directly involved in morphine-induced reward (Gadd et al 2003, Poulin et al 2011). In particular, the NK1R sub-population of amygdala neurons have been suggested to mediate opiate related reward behaviour as selective ablation of NK1R neurons in the amygdala resulted in attenuation of morphine-induced reward but not cocaine (Gadd et al 2003). Therefore, a possible future avenue in pursuit to understand the underlying mechanism of attenuated morphine reward behaviour exhibited by TASTPM mice would be to assess NK1R expressing neurons and level of neurodegeneration in relation to amyloid load in the amygdala. It would also be of a great interest to explore in future studies whether the reward-effect of cocaine is preserved in the TASTPM mice that exhibit attenuated morphine-induced reward in order to delineate the underlying mechanisms.

Altogether, these data in a transgenic mouse model of AD shows an age-dependant decline in sensitivity to acute noxious thermal stimulation in a model that includes both spinal and supraspinal-mediated components. Thermal hyposensitivity coincides with cognitive deficits and pathological amyloid plaques in the brain as well as histopathological Aβ plaques and intraneuronal accumulation of APP/Aβ in key regions involved in nociceptive processing, namely the thalamus and spinal cord, respectively. The accumulation of intraneuronal APP/Aβ in the spinal cord was associated with an alteration of excitatory neuronal markers especially in the deeper laminae coupled with an increased expression of endogenous opioid in superficial laminae of the dorsal horn of the spinal cord. An increased inhibitory tone mediated by endogenous opioid is likely to contribute significantly to thermal hyposensitivity in AD transgenic mice. Finally, AD-associated deposition of amyloid plaques accompanied by neuroinflammation in the spinal cord of aged 12 months old TASTPM mice result in impairment of nociceptive

thresholds to noxious mechanical stimuli. Therefore, suggesting that there may be a relationship between impaired nociceptive responses and deposition of amyloid plaques in the regions involved in the pain pathway, namely spinal cord and thalamus, along with cognitive impairment in the transgenic model of AD.

2.4.1 Chapter Key Findings

In this chapter, we provide preclinical evidence for:

- Age-dependent reduced sensitivity to acute thermal stimulation in TASTPM model of AD, which coincided with impairment of cognition and AD-related pathology in the form of deposition of amyloid plaques in the brain and intraneuronal accumulation of APP/Aβ in the spinal cord at the age of 6 months old.
- Increased inhibitory opioidergic tone in parallel to decrease in excitatory VGLUT2 expression in the 6 months old TASTPM mice which may underlie the altered nociceptive sensitivity.
- Impairment in mechanical thresholds, mechanical hyposensitivity, was associated with the formation of amyloid plaques in the spinal cord of 12 months old TASTPM mice.

The data suggests increased inhibition and decreased excitation in the spinal cord may be responsible for the reduced nociceptive sensitivity associated with AD-related pathology.

2.4.2 Future Direction Leading to Chapter 3

Experience of pain is often associated with age-related medical comorbidities namely, musculoskeletal conditions such as osteoarthritis (OA), which is a major contributor to the challenge of care in AD individuals. Despite availability of pain treatment options, it is inappropriately treated as assessment of pain in this susceptible population if often difficult. This could partly be explained by the impaired ability to communicate sensations and inadequate understanding of the underlying mechanisms of pain in this susceptible patient group. An effective strategy management of pain is increasingly recognised as a critical unmet clinical need. Thus, in the next chapter (Chapter 3), we pursued to determine whether AD-associated changes in the preclinical TASTPM model, identified in the present chapter, would have any impact on the development and treatment of OA chronic pain in a clinically relevant model.

Chapter 3 Development of Osteoarthritis Pain in TASTPM Model of Alzheimer's disease

3.1 Introduction

Osteoarthritis (OA) is the most common age-related and progressive degenerative joint disease affecting one or more joints of the body. Any joint can develop OA but knees, hips and small hand joints are the most commonly affected sites (Sofat et al 2011). It is a major cause of disability and morbidity in people over the age of 50 (Litwic et al 2013). The prevalence of OA increases with age, affecting approximately 8.5 million individuals in the United Kingdom (UK) (Neogi 2013). The cardinal pathological hallmarks of OA include: progressive deterioration of articular cartilage, synovial proliferation, bone remodelling observable as diminished joint space and bone overgrowth at the joint margins (osteophytes) (Dieppe & Lohmander 2005). Clinically, OA is diagnosed on the basis of the patients' history and physical examination; with individuals presenting with symptoms that include: loss of joint function, stiffness, disability and chronic pain, which have negative impact on the patients' quality of life (Hunter et al 2008). Despite extensive research conducted on understanding the pathophysiology of the joint degeneration in OA, it still remains elusive how joint pathology leads to the clinical symptoms in OA. Consequently, due to an incomplete understanding of the underlying mechanisms, there are no cure or disease modifying drugs, at present. Currently the best treatment options are physiotherapy, pain relief (i.e. paracetamol, NSAID, and opiates) and surgical joint replacement (Hunter & Felson 2006).

3.1.1 Mechanisms of Pain in Osteoarthritis

Pathologically OA is characterised by cartilage degradation accompanied by inflammation in the knee joint. Cartilage consists of chondrocytes and an extracellular matrix, which is composed of collagen and proteoglycans. Chondrocytes within the articular cartilage, under physiological conditions, help to maintain the extracellular matrix via regulating its production and degradation, which are critical for the functional properties of cartilage. However, the OA joint is characterised by increased expression of inflammatory mediators, elevated release of cartilage degradation proteinases, depletion of proteoglycans, and stress-induced intracellular signalling. The source of these inflammatory mediators (i.e. nerve growth factor (NGF), cytokines, chemokines and matrix metalloproteinases (MMP)) arises from the chondrocytes and the

peripheral immune cells (i.e. macrophages and lymphocytes) that infiltrate the synovial membrane in response to altered joint biomechanics, instability and/or damage (Bijlsma et al 2011, Dieppe & Lohmander 2005). Interleukin 1β (IL-1β) is amongst the plethora of pro-inflammatory cytokines released by chondrocytes and synovial cells, which induce the active form of MMP that in turn results in an increase in collagen degradation thereby compromising the integrity of the extracellular cartilage matrix. Moreover, tumour necrosis factor α (TNF- α) and IL-1β stimulate inflammation further via inducing the gene expression of cycloxygenase-2 (COX-2) and subsequent synthesis of prostaglandin-E2 (PGE_2) (Kapoor et al 2011). The articular cartilage itself has no nerve supply or blood vessels, implicating that it may not directly be the source of nociceptive input. However, the underling subchondral bone as well as structures in its close vicinity, namely the capsule, ligaments, periosteum, and menisci are densely innervated by myelinated Aβ, thinly myelinated Aδ- and the unmyelinated C- sensory fibres; whist the synovial membrane is innervated solely by small diameter unmyelinated and nociceptive C-fibres (Schaible & Grubb 1993). In the knee joints of rats and cats, approximately 60% - 80% of the sensory innervating fibres are nociceptive (Heppelmann 1997, McDougall 2006). Furthermore, estimated 15 - 35% nociceptive fibres innervating the knee joint in a cat are reported to be peptidergic, which upon activation release neuropeptides including substance P (SP) and calcitonin-gene related peptide (CGRP) into the knee joint that in turn contribute to the neurogenic inflammation in the periphery (Hanesch et al 1991, Schaible & Grubb 1993). Altogether, release of neuropeptides, growth factors, cytokines, chemokines, and proteases sensitise primary afferent peripheral free nerve endings that in turn result in enhanced response to pressure on joints by the proprioceptive terminals whilst the nociceptive fibres become responsive to light pressure and movement in the working range of the joint. Moreover, mechano-sensitive fibres, known as silent nociceptors also become responsive to mechanical stimulation of the joint which further increases the nociceptive input to the spinal cord (Schaible et al 2002). Thus, a reduction in threshold and an amplification in the responsiveness of nociceptors that occurs when the peripheral terminals of these high-threshold primary sensory neurons are exposed to inflammatory mediators and damaged joint (peripheral sensitisation) causes activation of the nociceptive system by normally innocuous (allodynia) and non-painful mechanical stimuli (hyperalgesia) (Latremoliere & Woolf 2009).

In addition to the nociceptive pain at the site of joint disease (primary hyperalgesia), individuals with OA complain of pain in areas adjacent to and remote from the affected joint, defined as referred pain (secondary hyperalgesia), such that hip OA may cause pain in the knee (Schaible et al 2009). Bajaj and co-workers (2001) have provided evidence for elevated local pain duration and intensity, larger pain areas as well as increased referred and radiating pain intensities following intra-muscular hypertonic saline infusion in OA subjects compared to controls. Moreover, a study of fifty-one subjects with knee OA that exhibited lower pain pressure thresholds in the forearm (i.e. greater widespread pain sensation) in comparison to healthy controls, alluding to the greater widespread of pain sensation. Furthermore, one year post total knee joint replacement these OA subjects were reported to still exhibit increased sensitivity to painful pressure (Wylde et al 2013). Evidence from quantitative sensory testing studies have demonstrated lower pressure pain thresholds at spatially distinct sites from the affected joint as well as higher suprathreshold heat pain rating in OA individuals (Farrell et al 2000, Lee et al 2011b). Also, randomised controlled trials evaluating the efficacy of drugs acting at the CNS have shown significant reduction of pain ratings and significant improvement in Western Ontario and McMaster Universities Osteoarthritis Index (WOMAC) scores following administration of duloxetine, a serotonin and norepinephrine reuptake inhibitor (SNRI) in subjects with knee OA compared to placebo-controls (Abou-Raya et al 2012, Chappell et al 2009). Finally, a neuroimaging positron emission tomography (PET) study demonstrated that arthritic patients with knee pain exhibited significantly increased neuronal and/or synaptic activity, using ^{18}F-fluorodeoxyglucose (FDG) as a marker, in the cingulate cortex, the thalamus, and the amygdala, regions that are involved in the processing of fear, emotions, aversive conditioning and motivational responses (Kulkarni et al 2007). Altogether, implicating that in addition to peripheral sensitisation, plasticity within the central nervous system (CNS) (central sensitisation) including: increased neuronal excitability the spinal cord to innocuous (allodynia) and noxious (hyperalgesia) stimuli; expansion of the neuronal receptive field such that stimulation from adjacent unaffected sites results in increased response (secondary hyperalgesia); and altered descending supraspinal inhibitory control may also underlie pain in OA individuals.

3.1.2 Monosodium Iodoacetate Model of Osteoarthritis Pain

Animal models of OA are a powerful tool to help elucidate and study the associated pathological changes and pain; as well as enable the pharmacological interventions in order to evaluate the efficacy of drugs in treatment of OA pain. Models of OA recapitulate most if not all clinical features of OA including development of hyperalgesia and allodynia accompanied by joint degradation and associated inflammation; and it can be induced: spontaneously, via genetic modification (transgenic), surgically, and chemically (Teeple et al 2013, Zhang et al 2013). The chemical monosodium iodoacetate (MIA) model of OA is amongst the most extensively characterised model, which is robust, reproducible, and characterised by immediate onset and rapid progression of OA associated pathological changes and behavioural phenotype. MIA is a metabolic inhibitor which causes joint pathology by disrupting chondrocyte glycolysis via inhibition of glyceraldehyde-3-phosphate dehydrogenase, leading to eventual cell death. The progressive loss of chondrocytes following MIA results in histological and morphological changes of the articular cartilage similar to pathology observed in OA patients (Bove et al 2003, Combe et al 2004, Fernihough et al 2004, Guzman et al 2003).

The MIA rodent model of OA displays immediate onset of mechanical allodynia and weight bearing deficit initiating from days 1 to 3 following intra-articular administration of 1 mg MIA (Bove et al 2003, Combe et al 2004, Fernihough et al 2004, Ogbonna et al 2013). The cartilage matrix appears to collapse by day seven as illustrated by loss of proteoglycans and the cellular detail (Bove et al 2003). Furthermore, joints of MIA-injected rodents exhibit alteration in both the surrounding synovium and to the articular cartilage. Robust inflammatory response in the synovium is characterised by expansion of the synovial membrane, by proteinaceous oedema fluid, and fibrin, with infiltrating immune cells (i.e. macrophages and lymphocytes), that is evident as early as day one post MIA administration. This inflammatory response starts to subside on day three before resolving by day seven after the initial MIA injection. Furthermore, coinciding with the early inflammatory response in the knee joint is the elevation of pro-inflammatory mediators such as TNF-α and IL-6 in the knee synovium and capsule. The level of TNF-α and IL-6 in the knee joint increases gradually, peaking at day four post MIA and remained elevated up to day 28 (Orita et al 2011). This initial inflammatory phase is proposed to

be a direct chemical reaction to MIA administration and it is sensitive to NSAIDs. Following resolution of inflammation in the knee joint, the pain-like behaviour still persists which is relatively insensitive to NSAIDs whilst efficacy for morphine and gabapentin have been demonstrated (Fernihough et al 2004).

Whilst the early major source of pain-like behaviour in the MIA model of OA may be inflammation, the late and established phase may share components of common central mechanisms associated with neuropathic pain (Harvey & Dickenson 2009). Cell bodies of the primary afferent terminals innervating the knee joint located in the dorsal root ganglion (DRG, L3 - L5) displayed a small but significant increase in activating transcription factor-3 (ATF-3) seven days post intra-articular administration of MIA, a marker for neuronal damage (Fernihough et al 2004, Orita et al 2011). Moreover, gabapentin, a drug used for treatment of neuropathic pain in human patients and efficacious in animal models of neuropathy, has been demonstrated to be effective in reversing pain-associated behaviour in the MIA model (Fernihough et al 2004). In addition, immunohistological studies have provided evidence for up-regulated CGRP expression in a subpopulation of primary afferent neurons in the DRG innervating the knee joint. CGRP is reported to be NGF-dependant and therefore increase in its immunoreactive neurons in the DRG following MIA injection into the knee joint may allude to the increase in peripheral NGF production owing to the local inflammation which induces stimulation of the primary afferent terminals (Ferreira-Gomes et al 2010, Orita et al 2011). Furthermore, in the spinal cord, activation of both neuronal and glial cells has been reported from day seven onwards following MIA administration (Lee et al 2011a, Ogbonna et al 2013, Sagar et al 2011). Also a behavioural and electrophysiological study provides evidence for increased A- and C-fibre inputs and responses; as well as wind-up in the spinal dorsal horn neurons, indicative of spinal hyperexcitability (central sensitisation) in the MIA model of OA (Harvey & Dickenson 2009). In addition, a recent functional MRI (fMRI) study has shown increased functional connectivity between the thalamus, hippocampus and globus pallidus following intra-articular administration of capsaicin into the MIA-injected knee joint when compared to responses from capsaicin injection into the knee joints of saline controls. These findings implicate that alteration

in the brain activation patterns may reflect the up-regulated nociceptive inputs due to either peripheral and/or central sensitisation mechanisms (Abaei et al 2016).

3.1.3 Osteoarthritis in Individuals with Alzheimer's disease

Currently there is variable evidence in the literature on the prevalence of arthritis/OA pain in AD ranging from 12%-70%; though largely comparable incidence in comparison to cognitively-intact controls (outlined in Table 3.1). The variability in the prevalence of pain in arthritis/OA is likely to be a result of the subject selection criterion and sample size, which ranges from nursing home sample to retrospective nationwide population-based cohort. In addition, different clinical inclusion criteria for arthritis/OA as a diagnosis, which varied in retrospective analysis medical reports ranging from within one week to one year, may have also contributed to such variability in prevalence in different studies (Huang et al 2015, Proctor & Hirdes 2001, Scherder & Bouma 2000).

Table 3.1: Prevalence of Arthritis/Osteoarthritis in Individuals with Cognitive Impairment

Reference	Cognitively Intact (n)	Cognitively Impaired (n)
Heyman et al (1984)	36.7% (80)	41.0% (40)
Scherder and Bouma (2000)	35.0% (20)	37.5% (40)
Proctor and Hirdes (2001)	21.8% (911)	12.9% (1009)
Pickering et al (2006)	65.0% (150)	70.0% (150)
Huang et al (2015)	33.3% (104,376)	39.3% (1,071)
Jensen-Dahm et al (2015)	16.1% (870,645)	19.7% (35,455)
Bauer et al (2016)	20.6% (243)	13.2% (182)

Abbreviation: n, sample size.

Earlier epidemiological studies reported comparable prevalence of arthritis in individuals clinically diagnosed with AD compared to their healthy control counterparts (Heyman et al 1984,

Pickering et al 2006). Further evidence suggested that although the number of individuals experiencing a chronic pain condition did not differ between healthy controls, early-stage AD, and mid-stage AD; the presence of arthritis was significantly lower in AD mid-stage subjects compared to healthy controls (Scherder & Bouma 2000). These findings are supported by evidence provided from a cohort of nursing home residents in Canada that indicates reduced prevalence of detecting pain amongst individuals with deteriorating cognitive deficits despite similar causes of pain compared to cognitively-intact control (Proctor & Hirdes 2001).

In addition, a study which was set out to evaluate the strengths and weaknesses of self-assessment in comparison to observational scales of pain in subjects with severe dementia recorded that 44% of individuals reported pain (over two thirds constituted OA of the joints); 40% of such cases were not receiving any analgesics (Pautex et al 2006). Moreover, Cornali et al (2006) reported lower prevalence of patients with severe cognitive decline admitted to Geriatric Evaluation and Rehabilitation Unit (GERU) for assessment and treatment of OA on referral of general practitioners and caregivers, highlighting the under-diagnosis of musculoskeletal pain in cognitively impaired subjects. On the other hand, examination by medical and nursing staff of GERU in the same cohort identified symptomatic OA in comparable percentages of subjects across the different degrees of cognitive impairment. However, despite the difference in prevalence of OA in cognitively impaired individuals reported, prescription of analgesics was lower in subjects with greater cognitive decline compared to the cognitively-intact cohort. These observations gain further support from studies carried out by Pickering et al (2006) and Bauer et al (2016), which also report lower equivalent dosage of analgesics prescribed to cognitively impaired individuals compared to cognitively-intact healthy controls for chronic pain treatment.

Altogether, these evidence suggest: (1) lower and/or comparable prevalence of OA in individuals with AD compared to cognitively-intact controls, which indicates either deteriorating capacity to report pain in such individuals and/or generally a reduced perception of chronic pain, owing to neuropathological lesions, accompanied by neuroinflammation, along the pain pathway that may affect nociceptive processing; and (2) lower prescription and/or consumption of

analgesics in AD individuals with OA that may reflect the under-treatment and/or inappropriate management of pain in such population (Scherder & Bouma 2000).

However, a recent Danish register-based cross-sectional nationwide study has indicated otherwise, such that individuals with dementia more frequently prescribed opioids compared to their cognitively-intact counterparts (Jensen-Dahm et al 2015). These results gain further support from evidence provided by Sandvik et al (2016) that have indicated a generally increasing trend of analgesic use, in particular opioids and paracetamol, in individuals with dementia from 2000-2011 in Norwegian nursing homes. Such that individuals with dementia were prescribed relatively similar level of analgesics in 2011 compared to cognitively-intact cohort. Collectively, indicating variability in analgesic prescription in individuals with cognitive impairments.

3.1.4 Chapter Aims

Therefore, it is of great relevance to initially evaluate pain-like behaviour in the transgenic TASTPM mice following intra-articular administration of MIA in order to examine any alterations in behavioural phenotype compared to age-matched controls and if so to explore and elucidate the underlying mechanisms. Furthermore, variable prescription of analgesics in AD individuals experiencing chronic pain questions the efficacy of these drugs in a possibly compromised system, which warrants further investigation into the pain-relief potency of commonly used drugs in OA in the transgenic mouse model of OA. As a result, the key aims of the present chapter were:

1. To assess whether the AD-related pathology occurring along the pain pathway changes the development of OA pain in TASTPM, a transgenic mouse model of AD.
2. To examine MIA-induced characteristic plastic changes in the key regions of the pain pathway, namely the spinal cord and thalamus, of TASTPM AD mice compared to age-matched controls.
3. To explore the effect of pharmacological agents in potentiating reversal of MIA-induced hypersensitivity in the TASTPM AD mice compared to age-matched controls.

3.2 Materials and Methods

3.2.1 Animals

All experiments were carried out in accordance with United Kingdom Home Office Regulations (Animal Scientific Procedures Act, 1986). Experiments were performed on 6-8 months old adult male and female heterozygous double-mutant TASTPM transgenic mouse model of AD obtained from GlaxoSmithKline (GSK). Age and gender-matched C57BL/6J (WT) obtained from Charles River were used as controls. All animals were housed in the Biological Services Unit, King's College London; maintained in 12 hours day/night cycle with *ad libitum* access to food and water; and were allowed acclimatisation for 7 days prior to behavioural experiments. All procedures were performed under personal licence code PIL 70/26010 and project licence 70/7629.

3.2.2 Monosodium Iodoacetate Model (MIA) of Osteoarthritis Pain

Unilateral knee joint osteoarthritis was induced by a single intra-articular injection of 10 µl sterile 0.9% saline containing 1 mg monosodium iodoacetate (MIA, Sigma, UK) into the left knee using a 28G needle and a Hamilton syringe, under isoflurane/O_2 inhalation anaesthesia as described previously (Ogbonna et al 2013, Pitcher et al 2016). Briefly, mice were anesthetized by 2-3% isoflurane-O_2 mixture (flow rate 1.5L/min), and subsequently area around left knee joint was trimmed and wiped making the patellar tendon visible. In order to stabilise the site of injection, the left leg was flexed and the MIA solution was injected using a 28G needle attached to the Hamilton syringe inserted through the patellar tendon into the left knee joint.

3.2.3 Behavioural Testing

Behaviour was assessed prior to (baseline observations) and at regular intervals: 3, 7, 10, 14, 17, 21, 24 and 28 days following MIA injection. All behavioural testing was conducted blind to experimental groups.

3.2.3.1 **Weight Bearing**

Changes in weight bearing were assessed as a measure of ongoing pain associated hypersensitivity. Weight bearing was assessed using an incapacitance tester (Linton

Instrumentation, UK). Mice were placed in a Perspex enclosure so that each hind paw is rested on separate transducer pads. Once the mice were settled and in correct position, the force exerted by each hind limb was measured over a period of 1 second. The first 3 sets of 1 second measurements were taken and then averaged. These values were then transformed to give the percentage of total hind limb weight borne on the ipsilateral side using the formula:

$$Weight\ Borne = \frac{Ipsilateral\ weight\ borne\ \times 100}{Ipsilteral\ weight\ borne + Contralateral\ weight\ borne}$$

A value of 50% represents equal weight distributed across both hind limbs, whereas a value of less than 50% was indicative of reduced weight borne on the ipsilateral hind limb.

3.2.3.2 **Mechanical Hypersensitivity**

Static mechanical withdrawal thresholds were assessed by applying calibrated von Frey monofilaments (0.007g – 1.00g) to the plantar surface of the hind paw. The 50% paw withdrawal threshold (PWT) was determined by increasing or decreasing stimulus intensity, and estimated using Dixon's 'up-down' method (Chaplan et al 1994). Unrestrained mice were placed individually and acclimatised up to 60 minutes, prior testing, in acrylic cubicles (8 × 5 × 10 cm) on a wire mesh grid, providing access to the underside of the hind paw. Monofilaments were applied perpendicular to the plantar surface of the selected hind paw, and then held in this position with enough force to cause a slight bend in the filament for approximately 3 seconds or until an abrupt withdrawal of the hind paw from the stimulus, the latter defining a positive response. Each test started with the application of 0.07g filament and each hind paw was assessed alternately with approximately 30 seconds gap between each application. Stimulus intensity was increased in a sequence until a positive response was achieved or the maximum strength stimulus of 1.00g filament failed to induce a positive response, in order to avoid tissue damage. If the mouse withdrew its hind paw upon application of a filament, the next lower force filament in the sequence was applied and vice versa until there was a change in response from the mouse. Following a positive response, four successive filaments were assessed according to the 'up-down' sequence, with no filament applied more than three times, in order to prevent sensitization. A 50% PWT (g) was determined using the 'up-down' procedure (Dixon 1980).

3.2.4 Pharmacological Drug Treatment

Pharmacological interventions were conducted during the early phase (up to day 7) and late phase (day 10 to day 28) post MIA administration considered to be the development and maintenance phase of OA respectively. On the day of testing pre-dose behavioural readings were recorded and the effect of the drugs administrated were monitored at regular intervals. The maximum percentage of mechanical hypersensitivity reversal induced by a drug was calculated using the following formula:

$$\%\, Reversal = 100 - [(\frac{Max\ Pre\ dose\ PWT\ - Ips\ Post\ dose\ PWT}{Max\ Pre\ dose\ PWT - Ips\ Pre\ dose\ PWT}) \times 100]$$

3.2.4.1 **Early Analgesic Interventions**

Celecoxib (30 mg/kg) was purchased from Sigma and dissolved in 1% (w/v) methyl cellulose solution. Sodium diclofenac (30 mg/kg) was obtained from Sigma and was dissolved in sterile saline. Drugs were administrated either subcutaneously (s.c.: sodium diclofenac) or orally (p.o.: celecoxib). Celecoxib was p.o. administrated 6 and 7 days following MIA injection (crossover). Sodium diclofenac was injected s.c. in the scruff of the back of the neck 7 and 9 days post MIA injection (crossover). On the day of testing pre-dose behavioural readings were recorded and the effect of the drugs administrated were monitored over a period of 6 hours, with mechanical hypersensitivity tests carried out at 1 hour, 3 hours, and 6 hours after administration. Oral administration of drugs was conducted by Mr Thomas Pitcher.

3.2.4.2 **Late Analgesic Interventions**

Gabapentin (60 mg/kg) was supplied by LKT Laboratories inc. and was dissolved in distilled water (dH_2O). Paracetamol (acetaminophen; 300 mg/kg) and morphine sulfate (6 mg/kg) were obtained from Sigma and were dissolved in sterile saline. Drugs were administrated either subcutaneously (morphine sulphate) or orally (paracetamol and gabapentin). Gabapentin was p.o. administrated 22 and 24 days following MIA injection (crossover). Whist paracetamol (p.o.) and morphine sulphate (s.c.) were administered on day 28 post MIA injection. On the day of testing pre-dose behavioural readings were recorded and the effect of the drug administrated was monitored over a period of 3 hours (paracetamol and morphine sulfate) or 6 hours

(gabapentin), with mechanical hypersensitivity tests carried out at regular intervals after administration. Oral administration of drugs was conducted by Mr Thomas Pitcher.

3.2.4.3 **Effect of Opioid Antagonist: Naloxone**

Naloxone hydrochloride (1mg/kg) and naloxone methiodide (1 mg/kg) were obtained from Sigma and dissolved in sterile saline. Both naloxone hydrochloride and naloxone methiodide were administered via an intra-peritoneal (i.p.) injection on day 24 post MIA injection. On the day of testing pre-dose behavioural readings were recorded and the effect of the drugs administrated were monitored over a period of 3 hours, with mechanical hypersensitivity tests carried out at 30 minutes, 90 minutes, and 180 minutes after administration.

3.2.5 Histology and Immunohistology

3.2.5.1 **Perfusion**

WT and TASTPM mice were terminally anaesthetised with an overdose of sodium pentobarbital (Euthatal®, ~150mg/kg body weight) 28 days post MIA injection and perfused transcardially with heparinised (1 U/ml) sterile saline (0.9% NaCl) followed by 4% paraformaldehyde fixative solution containing 1.5% picric acid (Sigma) in phosphate buffer (PB, 0.1M, pH 7.4).

3.2.5.2 **Knee Histology**

3.2.5.2.1 Knee Joint Processing

The knees were dissected out and the surrounding muscle was trimmed. Tissues were post-fixed 72 hours in 4% PFA and then placed in decalcifying solution containing 10% (w/v) formic acid (VWR) for 72 hours. The decalcified knee joints were washed thoroughly with dH_2O and placed in 70% (v/v) ethanol overnight prior to processing into paraffin wax. For histological analysis, 6µm thick tissue sagittal sections were cut using a microtome and mounted onto Superfrost Plus microscope slides (BDH, UK). Sections were then placed in 60°C oven overnight to dry.

3.2.5.2.2 Toluidine Blue Staining

Slide mounted paraffin-embedded knee joint sections were de-waxed in xylene (2 × 10 minutes each) and rehydrated in 100 % ethanol (4 × 3 minutes each) before being washed with dH_2O

and subsequently immersed in 0.05% (v/v) toluidine blue dye (pH 4) for 6 minutes in order to visualise proteoglycans in the articular cartilage. Finally sections were air dried, dehydrated in 60°C oven for 1 hour and cleared in xylene (20 minutes) before being coverslipped using dibutylphthalate in xylene (DPX, Sigma) mounting medium (Sigma). The knee joint histology was visualised using Zeiss microscope (Axioskop) and images were captured using Zeiss Axiocam MRc and the software Axiovision Release 4.6.

3.2.5.2.3 Haematoxylin and Eosin (H&E) Staining

Slide mounted paraffin-embedded knee joint sections were de-waxed in xylene (2 × 10 minutes each) and rehydrated in 100 % ethanol (4 × 3 minutes each) before being washed with dH_2O and subsequently immersed in Gill's (2) haematoxylin solution (Sigma) for 5 minutes. Sections were then rinsed until clear under running tap water, differentiated in acid-alcohol solution (5 seconds) and rinsed again until clear under running tap water (5 minutes) to blue. Following haematoxylin, sections were placed in eosin solution for 10 minutes. Sections were rinsed with tap water followed by dH_2O in order to remove excess eosin before being placed in an oven at 60°C (1 hour) to dehydrate. Finally, sections were cleared in xylene (20 minutes) and coverslipped with DPX mounting medium. The knee joint histology was visualised using Zeiss microscope (Axioskop) and images were captured using Zeiss Axiocam MRc and the software Axiovision Release 4.6.

3.2.5.3 **Immunohistology: Tissue Preparation and Sectioning**

Spinal cords (L3-L6) and brains were removed and immersion-fixed in 4% paraformaldehyde fixative solution containing 1.5% picric acid for 24 hours at 4°C. Subsequently, spinal cords and brains were cryoprotected in a solution of 20% sucrose in PB at 4°C for at least 48 hours and subsequently embedded in optimum cutting temperature (OCT, BDH, UK) medium and then snap-frozen using liquid nitrogen and stored at -80°C.

Transverse spinal cord and coronal brain sections were cut (20µm thick) using a cryostat and thaw mounted onto Superfrost Plus microscope slides.

3.2.5.4 **Immunohistochemistry: Chromogenic**

Frozen slide-mounted 20µm coronal brain sections were washed three times with PBS (5 minutes each), incubated with 3% (v/v in methanol) hydrogen peroxide (H_2O_2, Sigma) in order to quench endogenous peroxidase activity and blocked with 1% (w/v) bovine serum albumin (BSA, Sigma, UK) and 0.2% (w/v) sodium azide (Sigma, UK) in 0.1% Triton X-100 (BDH, UK) in PBS and incubated overnight with either primary antibodies: rabbit anti-glial fibrillary acidic protein (GFAP, 1:1000, Dako) or rabbit anti-ionized calcium binding adaptor molecule 1 (IBA1, 1:1000, Wako). The following day sections were washed three times (5 minutes each) with PBS and incubated for 1 hour with the secondary antibody: biotinylated donkey anti-rabbit (1:400; Jackson ImmunoResearch). In order to remove excess secondary antibody, sections were washed three times (5 minutes each) with PBS prior to incubation with avidin-biotinylated horseradish peroxidase complex (Vectastatin® ABC Kit, Vector) in PBS for 30 minutes. Sections were subsequently washed three times (5 minutes each) with PBS and peroxidase labelling was visualised with incubation (10 minutes) with 3, 3'-diaminobenzidine (DAB) Peroxidase (HRP) Substrate Kit (Vector). Sections were then washed for 5 minutes with dH_2O to terminate the DAB reaction and then 5 minutes in tap water. The sections were subsequently dehydrated in 60°C oven for 1 hour and immersed in xylene to clear for 20 minutes before being coverslipped with DPX mounting medium. All steps were conducted at room temperature and all antibody solutions were prepared in PBS with 1% BSA, 0.1% Triton X-100 and 0.2% sodium azide. The specificity of immunoreactivity was confirmed by omitting the primary antibody; immunostaining was visualised using Zeiss Axiovision light microscope and images were captured using Zeiss AxioCam MRc and the software Axiovision Release 4.6. (Zeiss, UK).

3.2.5.5 **Thioflavin-S Staining**

Staining for amyloid plaques in mice brain was performed on frozen slide-mounted 20µm coronal brain sections. Sections were washed three times with PBS and incubated with Thioflavin-S (1% w/v aqueous solution, Sigma) for 8 minutes. Sections were washed twice (3 minutes each) in 80% ethanol followed by a 3 minutes wash in 95% ethanol. Finally, sections were rinsed 3 times in PBS; coverslipped with Vectashield Mounting Medium containing nuclear marker 4',6-diamidino-2-phenylindole•2HCl (DAPI; Vector Laboratories, UK); and fluorescent

staining was visualized using Zeiss microscope (Imager.Z1) and images were captured using Zeiss AxioCam MRm and the software Axiovision Release 4.8.2. (Zeiss, UK).

3.2.5.6 **Immunofluorescence**

3.2.5.6.1 GFAP Staining

Frozen slide-mounted sections were washed three times (5 minutes each) with PBS, blocked with 1% (w/v) bovine serum albumin (BSA. Sigma, UK) and 0.2% (w/v) sodium azide (Sigma, UK) in 0.1% Triton X-100 (BDH, UK) in PBS for 1 hour, and incubated overnight for single staining with rabbit anti-GFAP (1:1000). The following day sections were three times (5 minutes each) with PBS and were subsequently incubated for two hours with the goat anti-rabbit Alexa Fluor 546-conjugated antibody (1:500, Molecular Probes). Sections were then washed three times with PBS (5 minutes each) and coverslipped with Vectashield Mounting Medium containing DAPI. All steps were conducted at room temperature and all antibody solutions were prepared in PBS with 1% BSA, 0.1% Triton X-100 and 0.2% sodium azide. The specificity of immunoreactivity was confirmed by omitting the primary antibody; and the immunofluorescent staining was visualized using Zeiss microscope (Imager.Z1) and images were captured using Zeiss AxioCam MRm and the software Axiovision Release 4.8.2. (Zeiss, UK).

3.2.5.6.2 IBA1 and Phospho-p38 Double Immunofluorescence

Frozen slide-mounted 20µm transverse spinal cord sections were washed three times with PBS (5 minutes each) and incubated overnight with the primary antibody rabbit anti-Phospho-p38 (P-p38, 1:100, Cell Signaling). The following day, sections were washed three times with PBS (5 minutes each) and incubated for 1½ hour with the secondary antibody: biotinylated donkey anti-rabbit (1:400). In order to remove excess secondary antibody, sections were washed three times (5 minutes each) with PBS prior to incubation with ABC Kit in PBS for 30 minutes. Subsequently sections were washed three times (5 minutes each) with PBS, incubated for 10 minutes with biotinyl tyramide (1:75) in amplification diluent (NEN, Life Science Products), which was followed by three times (5 minutes each) washes with PBS prior to two hours incubation with Extra-Avidin conjugated FITC (1:500, Sigma). Section were then washed three times (5 minutes each) with PBS and incubated overnight with the second primary antibody: rabbit anti-IBA1 (1:1000). The subsequent day, sections were washed three times (5 minutes each) with

PBS and incubated for two hours with the secondary antibody: donkey anti-rabbit antibody conjugated to Alexa Fluor 546 (Molecular Probes, 1:1000). Sections were finally washed three times with PBS (5 minutes each) and coverslipped with Vectashield Mounting Medium containing DAPI. All steps were conducted at room temperature and all antibody solutions were prepared in PBS with 1% BSA, 0.1% Triton X-100 and 0.2% sodium azide. The specificity of immunoreactivity was confirmed by omitting the primary antibody; and the immunofluorescent staining was visualized using Zeiss microscope (Imager.Z1) and images were captured using Zeiss AxioCam MRm and the software Axiovision Release 4.8.2. (Zeiss, UK).

3.2.6 Quantification of Histological and Immunohistological Staining

3.2.6.1 **Quantification of GFAP, IBA1 and Thioflavin-S Staining in the Brain**

Tissue sections stained with GFAP, IBA1, and Thioflavin-S were quantified by the percentage area occupied (immunoreactivity burden) using the ImageJ software (NIH). Three defined regions of 8×10^4 μm^2 were placed onto the cortex, hippocampus, and the thalamus. Images were converted to 8-bit greyscale, thresholded within a linear range (constant per stain), and the percentage of area covered by GFAP, IBA1, and Thioflavin-S immunoreactivity was calculated in each of the three regions of interest. Three sections were randomly selected from each animal at least 200 μm^2 apart from at least four animals per experimental group.

3.2.6.2 **Quantitative Assessment of Spinal Cord GFAP Immunoreactivity**

Quantitative assessment of GFAP immunoreactivity was calculated by determining immunofluorescensce intensity within 1×10^4 μm^2 boxes placed onto areas of the lateral, central and medial dorsal horn laminae I-III using Axiovision LE 4.8 software (Zeiss, UK). Background fluorescence intensity of each tissue section was also determined and subtracted from the values obtained. Obtained intensity values were normalised to the non-transgenic wild-type (WT) control contralateral dorsal horn mean. Three L3-L5 sections (at least 160 µm apart) from each animal were randomly selected from at least four animals per experimental group.

3.2.6.3 **Quantitative Assessment of Spinal Cord Activated Microglia**

Quantitative assessment of number of IBA1 immunopositive microglial cells that also expressed P-p38 immunoreactivity were calculated by counting the frequency of IBA1 immunopositive cells

in a defined region of 4×10^4 μm^2 placed onto the superficial laminae of the dorsal horn (laminae I-III) using Axiovision LE 4.8 software. Three L3-L5 sections from each animal were randomly selected from at least four animals per experimental group.

3.2.7 Western Blots

Lumbar spinal cord (L3–L5) tissue from WT and TASTPM mice 28 days post MIA injection were dissected into ipsilateral and contralateral dorsal horn prior to being homogenized on ice in lysis buffer (Tris-HCl, 20 mM pH 7.5, 10 mM NaF, 150 mM NaCl, 1% Nonidet P-40, 1 mM phenylmethylsulphonyl fluoride, 1 mM Na_3VO_4, 10 µg/ml leupeptin and trypsin inhibitor) with complete mini cocktail protease inhibitor. Tissue lysates were then centrifuged at 13,000 rpm for 20 min at 4°C. The protein concentration of the supernatant was determined using the NanoDrop spectrometer. Equal protein concentrations per sample (20µg - 60µg protein) were added to Laemmli's sample buffer, boiled for 5 min at 95°C, and subjected to 10% SDS-PAGE. Wet transfer was performed using the Bio-Rad Trans-Blot® Cell (Bio-Rad Laboratories, Hertfordshire, U.K.) for 1 hour at 4°C, and the membrane was then blocked with 5% non-fat dried milk in TBS-T (50 mM Tris-HCl, pH 7.6, 150 mM NaCl, 0.1% Tween 20) for 30 minutes at room temperature. The blot was probed with rabbit anti-mu opioid receptor (1:1000, µ-OR, Immunostar), and mouse anti-amyloid 1-16 (1:1000, 6E10, Cambridge Biosciences, UK) antibodies. Results were visualised with horseradish peroxidase-coupled anti-mouse or anti-rabbit immunoglobulin (Dako) using enhanced chemiluminescence detection reagents ECL (EMD Millipore, UK) Western blotting detection system according to the manufacturer's instructions, and the immune complex visualized by the BioSpectrum® Imaging System. The protein bands were densitometrically analyzed with Quantity One (Bio-Rad Laboratories, UK). Western blot for β-actin (1:1000, Cell Signaling, UK) were performed as loading controls. Data was expressed as protein expression relative to respective saline controls.

3.2.8 Real-time Reverse Transcription Polymerase Chain Reaction

Lumbar segments (L3-L5) of the spinal cord, thalamus and brainstem were dissected 28 days post MIA administration, and snap-frozen in liquid nitrogen. The thalamus and brainstem were bisected into left (ipsilateral) and right (contralateral) sides to site of MIA knee joint injection. Spinal cords were divided into dorsal and ventral horn. The dorsal horn was subsequently

bisected into left (ipsilateral to intra-articular MIA injection) and right (contralateral) dorsal horn. Total RNA was then isolated from minced tissue using the miRCURY RNA Isolation Kit (Exiqon) according to the manufacturer's protocol. The total RNA concentration was determined using the NanoDrop spectrometer. Total RNA (50-100ng) was used to synthesize first strand cDNA, using SuperScript VILO cDNA Synthesis Kit (Thermo Fisher Science) according to the manufacturer's protocol. Expression levels of the following genes were analysed: mu opioid receptor (μ-OR), delta opioid receptor (δ-OR), kappa opioid receptor (κ-OR) and 18S rRNA was used a reference transcript. Amplification was performed with a Light Cycler 480 (Roche) using Syber Green I Master (Roche) using the primers: μ-OR (ATACAGGCAGGGGTCCATAG and GTCCATAACACACAGTGATGATGA) (Lynch et al 2008), δ-OR (GCATCGTCCGGTACACCAA and AAAGCCAGATTGAAGATGTAGATGTTG), κ-OR (GCAGCCTGAATCCTGTTCTC and TCATCCCTCCCACATCTCTC) (Kurrikoff et al 2004), and 18S rRNA (GCTGGAATTACCGCGGCT and CGGCTACCACATCCAAGGAA) (Denning et al 2008). The instrument was programmed as follows: 95°C for 5 minutes and 45 cycles of three steps of 10 seconds each including denaturing at 95°C, annealing at 60°C and primer extending at 72°C. All samples were run as duplicates and the 18S rRNA was used as the housekeeping gene. The relative gene expression levels were calculated according to the $2^{-\Delta\Delta Ct}$ method, where Ct represents the threshold cycle.

3.2.9 Plasma β-Endorphin Enzyme Immuno-Assay (EIA)

3.2.9.1 **Blood Sample Collection and Processing**

WT and TASTPM mice were terminally anaesthetised with an overdose of sodium pentobarbital (Euthatal®, ~150mg/kg body weight) 28 days post MIA injection and using a 25G needle attached to 1ml syringe a cardiac puncture was performed and approximately 0.5ml of blood was drawn per mouse. The blood sample was then transferred into 1.5ml tube containing heparin-coated beads. Samples were placed on ice for half an hour prior centrifuging at 13,000rpm for 20 minutes at 4°C in order to separate the plasma from the cells. The supernatant (plasma) was collected, transferred into a new 1.5ml tube and stored at -20°C until use. The cardiac puncture was performed by Mr Thomas Pitcher.

3.2.9.2 **β-Endorphin EIA**

β-Endorphin levels in the plasma samples were assessed by EIA using the Endorphin, beta (Mouse, Bovine, Ovine, Camel) - EIA Kit (Phoenix Pharmaceuticals) according the manufacturer's protocol. Briefly, 50µl of plasma samples, assay buffer (total binding), peptide standards (0.01ng/ml - 100ng/ml), or positive control were added to the 96-well plate prior to addition and two hours incubation with 25µl of primary antibody and 25µl of biotinylated peptide. Subsequently, each well was washed four times with 350µl of the assay buffer provided before addition and one hour incubation with 100µl of streptavidin-horseradish peroxidase (SA-HRP) solution. Further four washes with 350µl of the assay buffer were performed and 100µl of substrate solution (TMB) was added to each well and the plate was incubated for one hour prior to the addition of 100µl of 2N HCl into each well in order to stop the reaction and the optical density was read using a plate reader at 450nm. A standard curve (four parameter logistic curve) was plotted using the known concentrations of standard peptide as described in the manufacturer's guide. The concentration of β-Endorphin in the plasma sample was determined in accordance to the standard curve (Figure 3.1).

All samples were run in duplicates thus the concentration of each plasma sample was obtained by calculating the mean of the duplicate values. Each plasma sample was diluted (1:2) in assay buffer therefore the measured concentration of β-Endorphin in each of the plasma sample was multiplied by the dilution factor in order obtain the actual concentration. All the incubations were conducted at room temperature, shaking at 300rpm.

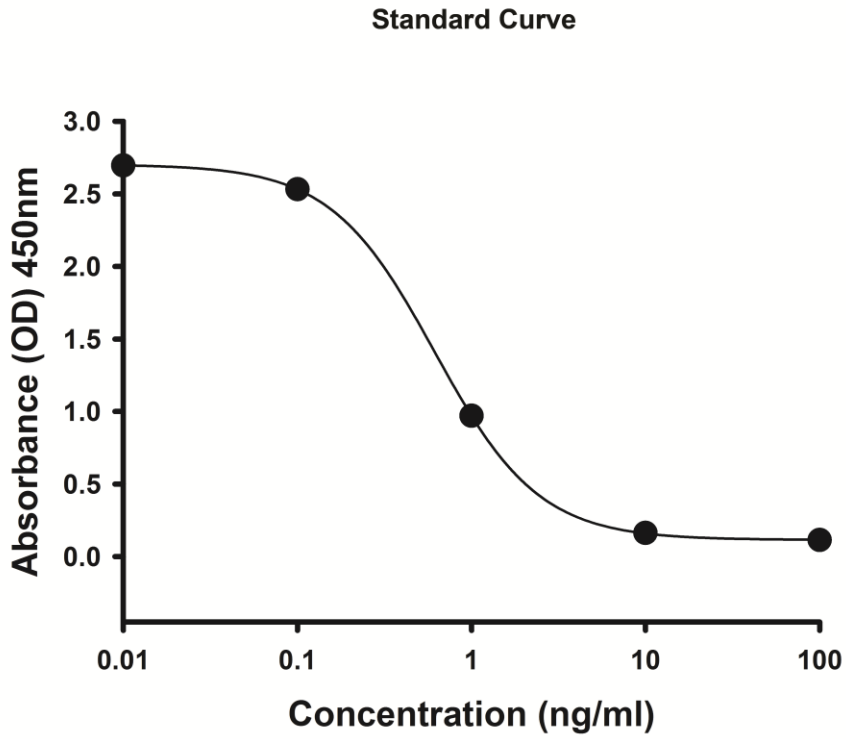

Figure 3.1: A Representation of Standard Curve for β-endorphin EIA

Representation of the standard curve with concentration of standard peptide on the log scale (x-axis) and its corresponding optical densisty (OD) reading on the linear scale (y-axis). Values are plotted as mean of duplicates.

3.2.10 Statistical Analysis

The data were analysed using SigmaPlot 12.5 (Systat Software, San Jose, CA). The statistical tests performed and the numbers of animals used are displayed in the results section and within the figure legends. Where data were not normally distributed, the appropriate non-parametric test was applied. Graphs were generated using GraphPad Prism 5 (Graphpad Software Inc., San Diego, USA). All data are presented as mean ± standard error mean (SEM) and a probability value less than 0.05 ($p < 0.05$) was considered statistically significant.

3.3 Results

In order to investigate the mechanisms of chronic pain in AD, in this chapter, we examined the development and maintenance of chronic pain using the chemical MIA for induction of OA pain in the transgenic TASTPM mouse model of AD. For this purpose, we assessed the behavioural response to MIA at regular intervals over a period of 28 days. The characteristic plastic changes in pain pathway 28 days post MIA were also examined. Finally, we evaluated the efficacy of analgesics during the early and late phase, in the development and maintenance of OA pain, respectively, were able to initially induce analgesia in MIA-injected WT; and then examined if these analgesics were also as potent in the transgenic TASTPM mouse model of AD following MIA administration.

3.3.1 MIA-induced Mechanical Hypersensitivity and Weight Bearing

Behaviour was assessed prior to (baseline observations, day 0) and at regular intervals: 3, 7, 10, 14, 17, 21, 24 and 28 days following MIA injection.

3.3.1.1 **Altered MIA-induced Mechanical Hypersensitivity in TASTPM Mice**

As expected, an intra-articular injection of MIA into the left knee of WT mice significantly reduced withdrawal thresholds in response to mechanical stimulation (hypersensitivity) in the ipsilateral hind paw (Figure 3.2A). Compared to saline injected WT mice, the average ipsilateral 50% PWT was significantly decreased in the WT group injected with MIA on day 3 (WT saline, 0.89g ± 0.02g; WT MIA, 0.42g ± 0.06g) which reduced further on day 7 (WT saline, 0.84g ± 0.04g; WT MIA, 0.08g ± 0.02g) and remained significantly different from saline group up to day 28. Whilst an intra-articular injection of saline did not result in any significant alteration in the ipsilateral hind paw mechanical thresholds throughout the course of the study (WT saline: baseline, 0.86g ± 0.04g; day 28, 0.86g ± 0.02g).

Similarly, the TASTPM mice injected with MIA also developed significant mechanical hypersensitivity in the ipsilateral hind paw 3 days post MIA injection (TASTPM saline, 0.91g ± 0.03g; TASTPM MIA, 0.49g ± 0.09g) which becomes increasingly severe by day 7 (TASTPM saline, 0.91g ± 0.06g; TASTPM MIA, 0.14g ± 0.03g) compared to their respective TASTPM saline controls. In addition, as observed in WT mice, an intra-articular injection of saline did not

cause any significant alteration in the ipsilateral hind paw mechanical thresholds throughout the course of the study (TASTPM saline: baseline, 0.88g ± 0.04g; day 28, 0.89g ± 0.04g). However, MIA injected TASTPM mice displayed a partial recovery of mechanical hypersensitivity in the ipsilateral hind paw initiating from day 14 (0.21g ± 0.05g) reaching significantly different from MIA injected WT mice on day 21 (WT MIA, 0.08g ± 0.02g; TASTPM MIA, 0.28g ± 0.07g) (Figure 3.2A). This observation was most evident when an area under the curve (AUC) analysis was completed, which demonstrated that over a period of 28 days post MIA injection, both WT and TASTPM mice displayed significantly reduced AUC compared to their respective saline groups; but WT MIA injected mice had significantly lower AUC compared to their respective TASTPM group. Further analysis revealed that in the early developmental phase (day 0 - day 7) the AUC was significantly reduced in both WT and TASTPM mice injected with MIA in comparison to their respective saline controls however no significant difference between the two MIA injected groups. Whereas, it was during the later phase of the MIA-induced OA pain (day 10 - day 28) in which the MIA injected TASTPM mice exhibited significantly greater AUC compared to MIA injected WT mice (Figure 3.2B). Therefore, indicating that it is the late maintenance of mechanical hypersensitivity phase which is affected in the transgenic TASTPM mouse model of AD.

Expectedly, when comparing the mechanical thresholds in the contralateral hind paws, we observed no significant alteration in both WT and TASTPM mice injected with MIA compared to their respective saline controls (Figure 3.3A). This observation was confirmed with the AUC analysis that also showed no significant difference in the contralateral hind paw mechanical thresholds when comparing the four experimental groups over the period of 28 days, early (day 0 - day 7) nor the late phase (day 10 - day 28) (Figure 3.3B). In addition, it was evident that the contralateral 50% PWT of MIA injected WT and TASTPM mice were comparable to those of the saline injected ipsilateral paw withdrawal thresholds. Therefore, this set of data confirms that there is no effect of MIA on the contralateral hind paw mechanical thresholds.

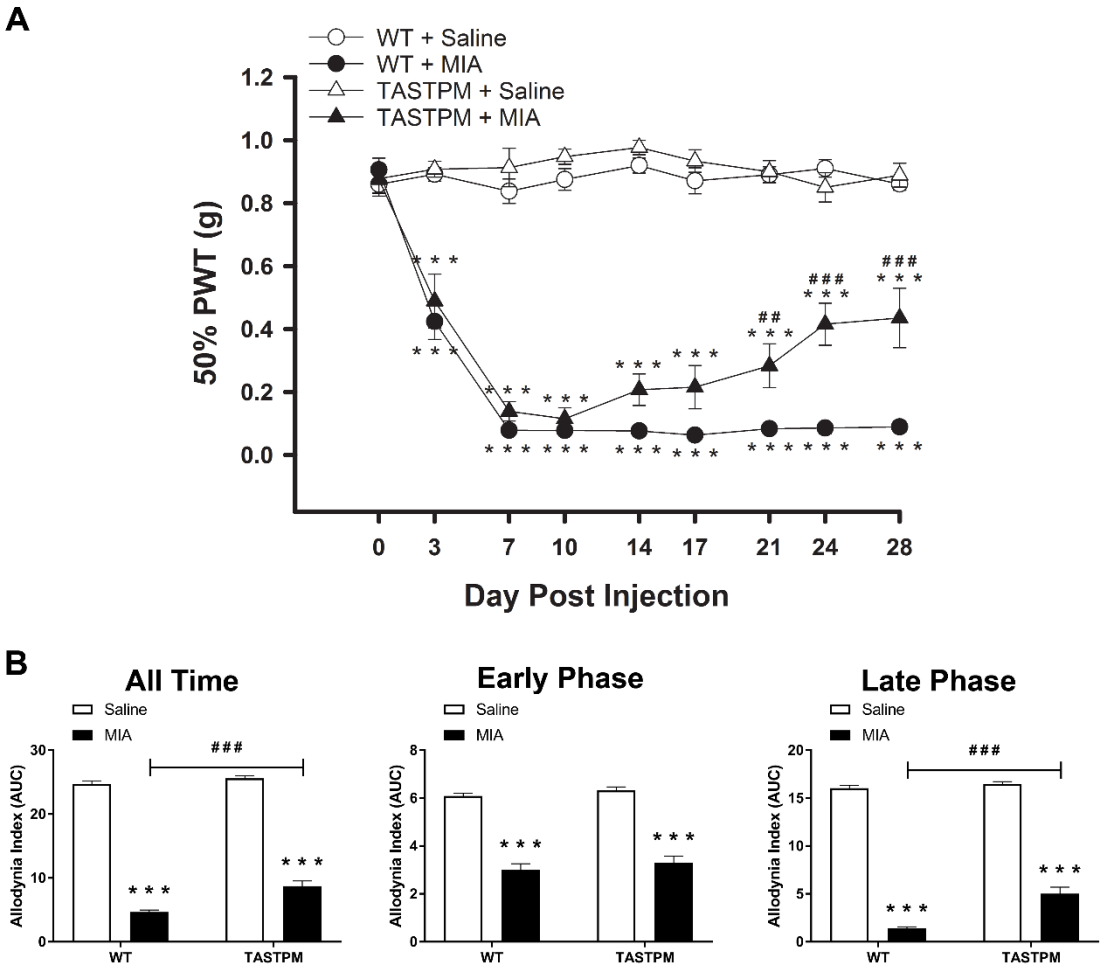

Figure 3.2: Partial Reversal of MIA-induced Mechanical Hypersensitivity in the Ipsilateral Hind Paw of TASTPM

A representation of mechanical withdrawal responses in the ipsilateral hind paw of 6 months old TASTPM and age and gender matched wild-type (WT) that were measured at regular intervals prior to (baseline, 0) and up to 28 days post intra-articular administration of MIA (1mg/10µl) or saline (control) into the left knee joint (A). Alteration in behaviour compared between experimental groups (MIA vs. Saline) within genotype (WT or TASTPM) (* * * $p < 0.001$) and between genotype (TASTPM vs. WT) within experimental group (Saline or MIA) ($^{\#\#}$ $p < 0.01$, $^{\#\#\#}$ $p < 0.001$) was detected using two-way repeated measures analysis of variance (ANOVA) followed by Tukey multiple comparison test. Data is expressed as mean 50% paw withdrawal threshold (PWT) ± SEM (n = 8-10 mice per experimental group). Area under the curve (AUC) for ipsilateral hind paw (B) was calculated and expressed as allodynia index where a lower value represents more severe mechanical hypersensitivity. All time is the analysis of AUC for baseline - day 28, early phase (baseline - day 7), and late phase (day 10 - day 28). Statistical comparisons between experimental groups within genotype (* * * $p < 0.001$) and between genotype within experimental group ($^{\#\#}$ $^{\#}$ $p < 0.001$) were observed using two-way ANOVA followed by Tukey multiple comparison test. All values are expressed as mean AUC ± SEM (n = 8-10 mice per experimental group).

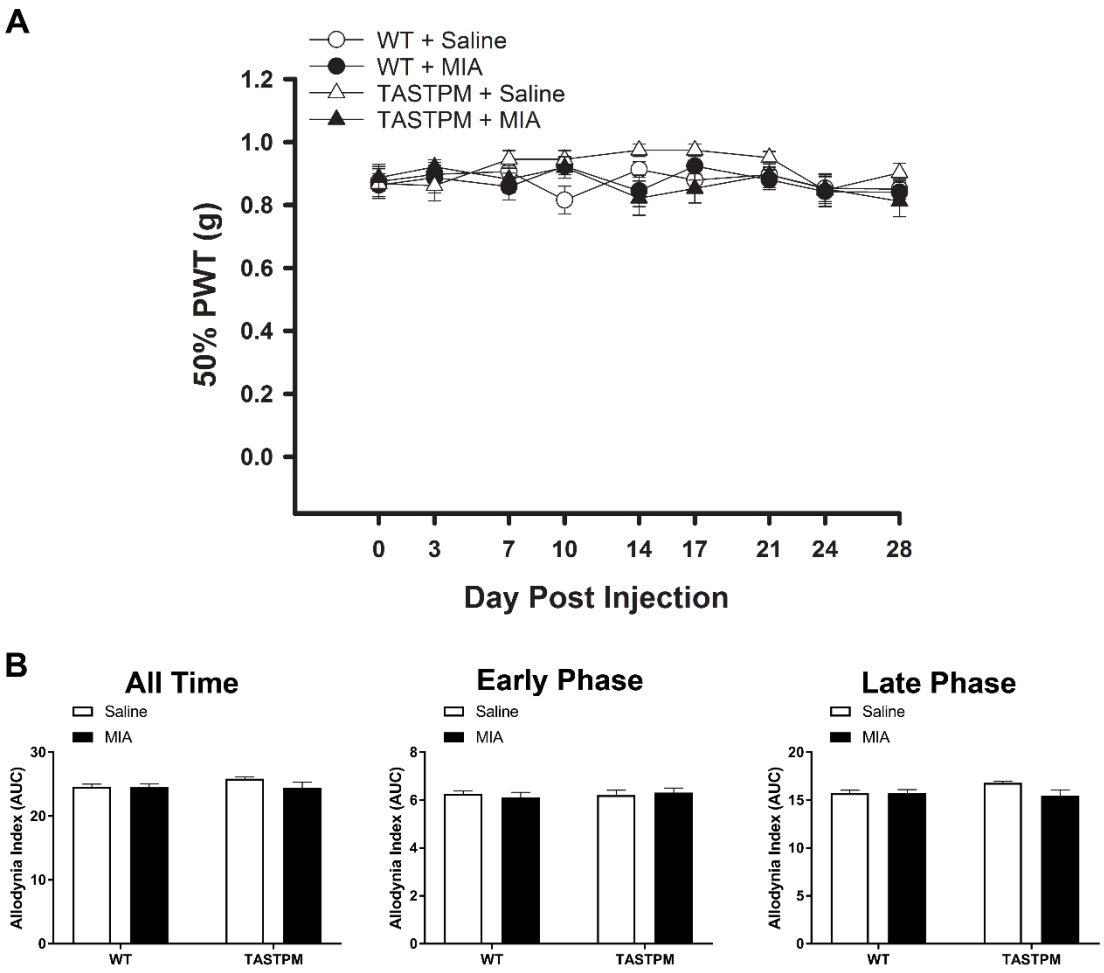

Figure 3.3: Unaltered Contralateral Hind Paw Mechanical Thresholds Post MIA Administration

A representation of mechanical withdrawal responses in the contralateral hind paw of 6 months old TASTPM and age and gender matched wild-type (WT) that were measured at regular intervals prior to (baseline, 0) and up to 28 days post intra-articular administration of MIA (1mg/10µl) or saline (control) into the left knee joint (A). No significant change in the contralateral 50% paw withdrawal threshold (PWT) of WT and TASTPM injected with MIA compared to saline controls was detected using two-way repeated measures ANOVA ($p > 0.05$). Data is expressed as mean 50% PWT ± SEM (n = 8-10 mice per experimental group). Area under the curve (AUC) for contralateral hind paw (B) was calculated and expressed as allodynia index. All time is the analysis of AUC for baseline - day 28, early phase (baseline - day 7), and late phase (day 10 - day 28). No alteration between experimental group (MIA vs. Saline) and genotype (WT vs. TASTPM) was detected at any time point using two-way ANOVA ($p > 0.05$). All values are expressed as mean AUC ± SEM (n = 8-10 mice per experimental group).

3.3.1.2 **Weight Asymmetry Absent in TASTPM**

As previously reported, WT mice injected with MIA displayed significant reduced percentage of weight borne on the ipsilateral hind limb compared to their respective saline control on day 3 which remains consistently different up till day 28. Whilst saline injected mice did not display any significant alteration in weight borne on their ipsilateral hind limb throughout the course of the study. In contrast, TASTPM mice injected with MIA did not exhibit any significant weight asymmetry compared to the saline injected TASTPM group throughout the course of the study (Figure 3.4A). These observations were also apparent from the AUC analysis that revealed significantly reduced weight borne on the ipsilateral hind limb by MIA injected WT mice compared to their respective saline group and also the TASTPM mice injected with MIA. In addition, TASTPM injected with MIA displayed similar AUC compared to the TASTPM mice injected with saline. Further analysis during the early (day 0 - day 7) and late (day 10 - day 28) phases confirmed the same trend (Figure 3.4B). Thus, weight asymmetry was observed to be absent in the TASTPM mouse model of AD following an intra-articular injection of MIA.

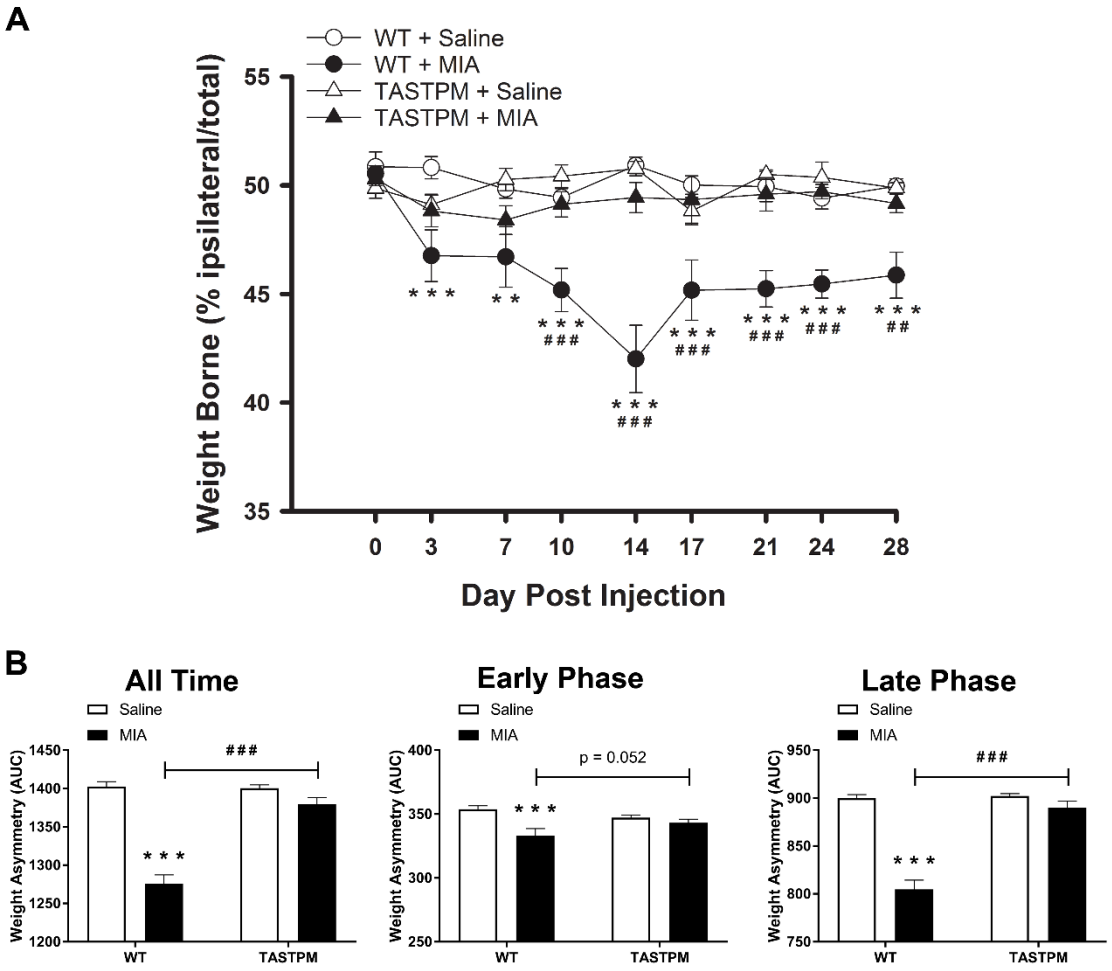

Figure 3.4: MIA-induced Weight Asymmetry Absent in TASTPM

Weight borne on ipsilateral hind limb, calculated as percentage of ipsilateral weight borne/total weight borne (ipsilateral + contralateral weight borne), by 6 months old TASTPM and age and gender-matched wild-type (WT), was monitored at regular intervals prior to (baseline, 0) and up to 28 days post intra-articular administration of MIA (1mg/10µl) or saline (control) into the left knee joint (A). Alteration in weight distribution were compared to between experimental groups within genotype (* * * $p < 0.001$) and between genotype within experimental group ($^{\#\#}$ $p < 0.01$, $^{\#\#\#}$ $p < 0.001$) was detected using two-way repeated measures ANOVA followed by Tukey multiple comparison test. Data is as mean weight borne ± SEM (n = 8-10 mice per experimental group). Area under the curve (AUC) analysis (B) were calculated and expressed as weight asymmetry where a lower value represents more severe weight asymmetry. All time is the analysis of AUC for baseline - day 28, early phase (baseline - day 7), and late phase (day 10 - day 28). Statistical comparisons between experimental groups within genotype (* * * $p < 0.001$) and between genotype within experimental group ($^{\#\#}$ $p < 0.01$, $^{\#\#\#}$ $p < 0.001$) were conducted using two-way ANOVA followed by Tukey multiple comparison test. All values are expressed as mean ± SEM (n = 8-10 mice per experimental group).

3.3.2 MIA Causes Histopathological Changes in the Knee Joint

3.3.2.1 **MIA-induced Cartilage Degradation**

Histological observation of the knee joint was carried out 28 days post intra-articular administration of MIA. In the WT mice, toluidine blue staining of knee joints from saline injected ipsilateral and MIA injected contralateral knee joints (control) displayed smooth and intact cartilage and proteoglycans (Figure 3.5A). However, at the same time point MIA injection resulted in loss of cartilage and proteoglycans in the ipsilateral knee joint of WT mice (Figure 3.5B and arrowheads in Figure 3.5b). A similar pattern of toulidine blue staining was evident in the saline injected ipsilateral and MIA injected contralateral TASTPM knee joints (control) (Figure 3.5C); and loss of cartilage and proteoglycans in the ipsilateral knee joint of TASTPM mice 28 days post MIA administration (Figure 3.5D and arrowheads in Figure 3.5d).

3.3.2.2 **MIA-induced Inflammation in the Synovial Membrane**

In addition, microscopic examination of the knee joint using H&E, 28 days post MIA injection into the knee joint, was conducted. Saline injected ipsilateral and MIA injected contralateral knee joints (control) of WT mice displayed minimal frequency of haematoxylin positive nuclei within the synovial membrane (Figure 3.6A). However, at the same time point MIA injection resulted synovial lining thickening and increase in haematoxylin positive cell nuclei within the synovial membrane in the ipsilateral WT knee joint (Figure 3.6B and arrowheads in Figure 3.6b). A similar pattern of H&E staining was also evident in the knee joints of the transgenic TASTPM model of AD whereby the control knee joints displayed minimal nuclei staining (Figure 3.6C) whilst synovial hyperplasia was evident 28 days post MIA injection in the ipsilateral knee joint (Figure 3.6D and arrowheads in Figure 3.6d).

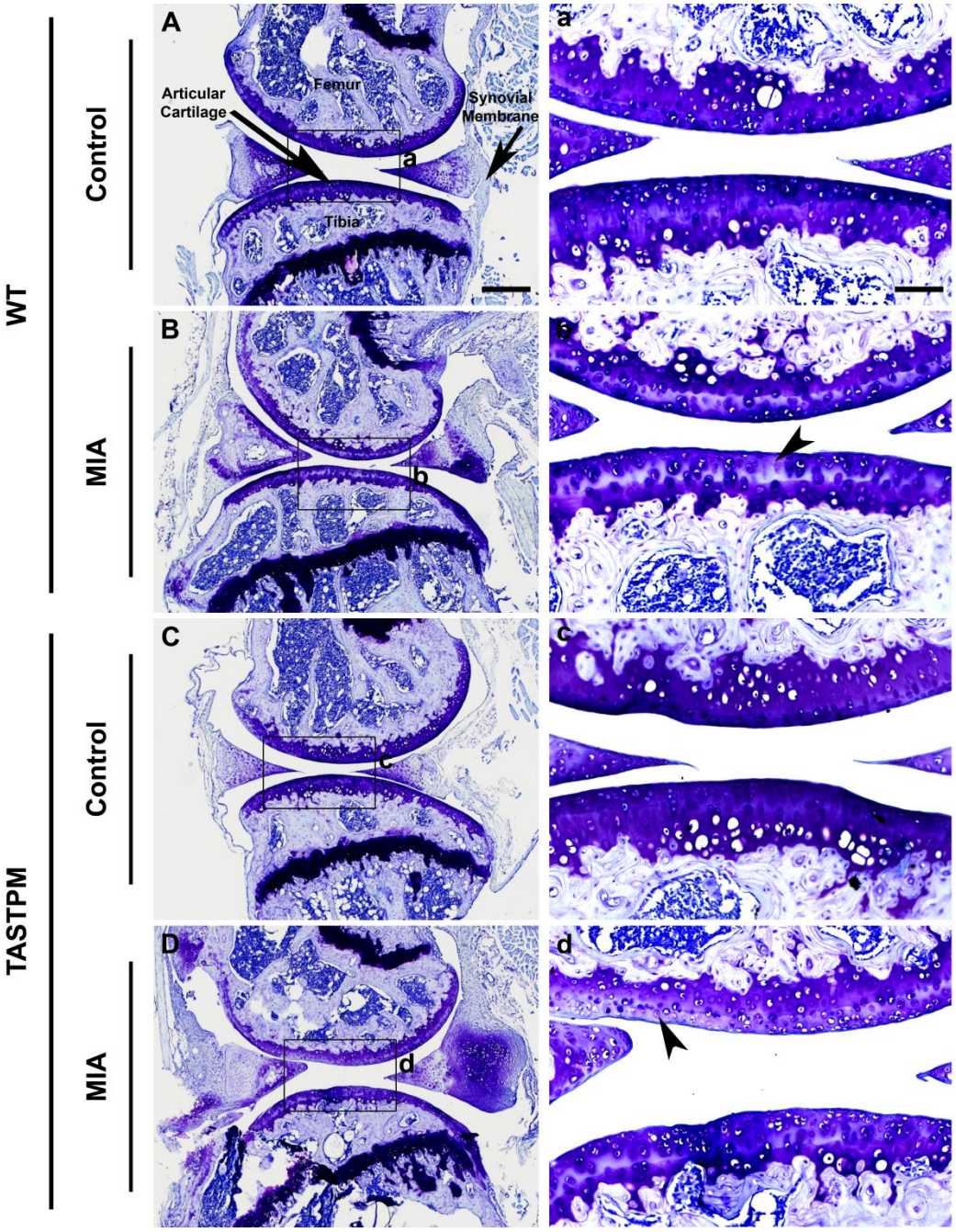

Figure 3.5: MIA-induced Knee Cartilage Degradation

Representation of toluidine blue staining of articular cartilage from control and MIA injected (ipsilateral) knee joints of wild-type (WT, A-B) and TASTPM (C-D) mice 28 days post MIA. High magnification images for each experimental group representing the outlined box (a-d). Intact articular cartilage with regular and intense staining for proteoglycans were observed in the control WT and TASTPM mice. Whereas, 28 days post MIA injection, degradation and loss of ipsilateral articular cartilage (arrowheads) was induced in both WT and TASTPM knee joints. The scale bar represents 200µm (A-D) and 100µm (a-d).

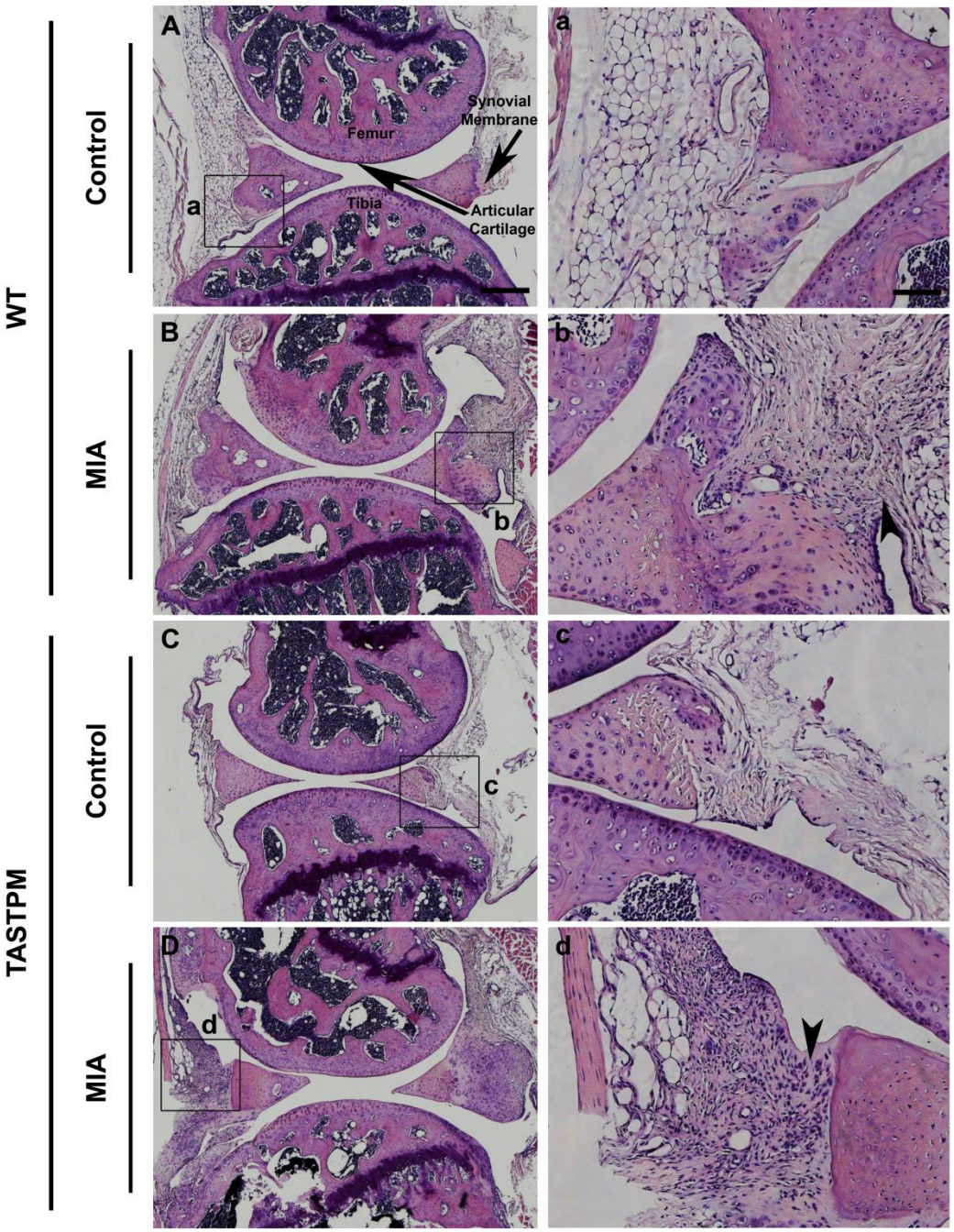

Figure 3.6: MIA-induced Inflammation in the Synovial Membrane

Representation of haematoxylin and eosin staining (H&E) of articular cartilage from control and MIA injected (ipsilateral) knee joints of wild-type (WT, A-B) and TASTPM (C-D) mice 28 days post MIA. High magnification images for each experimental group representing the outlined box (a-d). H&E staining displayed minimal nuclei within the synovial membrane of WT and TASTPM controls. However, 28 days post MIA resulted in thickening of the synovial membrane lining and infiltration cells in the ipsilateral synovial membrane of MIA injected animals only (arrowheads). The scale bar represents 200µm (A-D) and 100µm (a-d).

3.3.3 MIA-induced Changes in the Spinal Cord

In order to examine whether MIA injection in the knee joint results in changes in the dorsal horn of the spinal cord, tissue was obtained 28 days post injection and immunohistochemically analysed.

3.3.3.1 **Lack of Spinal Microgliosis in TASTPM Spinal Cord**

Intra-articular administration of MIA induced spinal changes such as an increase in the microglial response have been reported in both rat and mice MIA models of OA. Therefore, in order to evaluate whether MIA injection in the knee induces a microglial response in spinal cord dorsal horn, we utilised immunohistochemical methods using IBA1 as a marker. In WT mice, the number of IBA1 expressing microglial cells was significantly increased in the ipsilateral dorsal horn of the MIA injected mice compared to their respective contralateral dorsal horn and of the WT control mice. In contrast, TASTPM mice injected with MIA did not display any change in the number of IBA1 labelled cells in the ipsilateral dorsal horn compared to their respective contralateral dorsal horn and of the TASTPM control mice (Figure 3.7). Thus, these set of data highlights the partial recovery of mechanical hypersensitivity and absence of weight asymmetry in MIA injected TASTPM mice is accompanied by lack of microgliosis in the ipsilateral dorsal horn.

It was also noteworthy that the TASTPM control mice exhibited higher number of IBA1 positive cells compared to that observed in the dorsal horn of WT controls. Therefore, indicating that there is an elevated basal frequency of IBA1 positive microglial cells in the dorsal horn of the transgenic TASTPM model of AD.

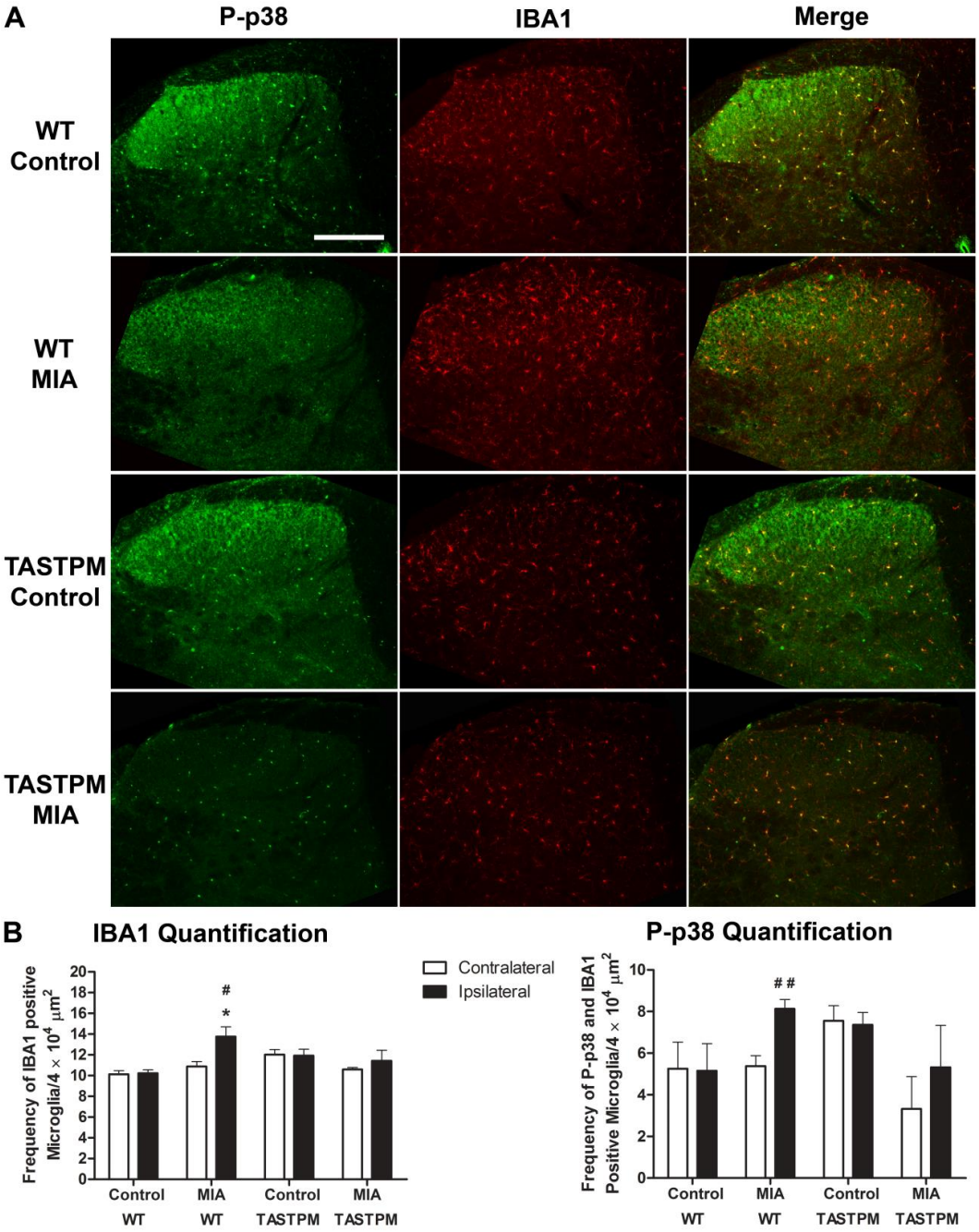

Figure 3.7: Lack of MIA-induced Spinal Microgliosis Exhibited by TASTPM Mice

Representative images showing phospho-p38 (P-p38) expressing microglia (IBA1) in the dorsal horn of the spinal cord (L4-L5) 28 days after intra-articular injection of saline (control) or MIA of TASTPM and age and gender-matched wild-type (WT) mice (A). The scale bar represents 200µm. (B) Quantification of IBA1 immunopositive and P-p38 expressing IBA1 cell frequency was conducted in pooled L4 and L5 dorsal horn of MIA and control mice. WT mice exhibited significantly greater frequency of IBA1 immunopositive microglia in the ipsilateral dorsal horn compared to WT control ipsilateral (* $p < 0.05$, Student's *t*-test) and WT MIA contralateral, where increase in activated microglia was also evident ($^{\#}$ $p < 0.05$, $^{\#\#}$ $p < 0.01$, Student's *t*-test). Contrastingly no apparent changes in microglial or activated microglia were observable in the ipsilateral MIA injected TASTPM mice compared to neither TASTPM control ipsilateral nor TASTPM MIA contralateral ($p > 0.05$, Student's *t*-test). Data is shown as mean ± SEM (n = 4 per experimental group).

3.3.3.2 **MIA Failed to Induce Microglial Activation in TASTPM**

As lack of spinal microgliosis was observed in the TASTPM ipsilateral dorsal horn post MIA administration, we examined if there was any change in the activation of microglia using phospho-p38 (P-p38) as a marker for microglial activation. As observed with IBA1 staining, WT mice injected with MIA displayed significantly greater number of IBA1 positive cells that also expressed P-p38 in the ipsilateral dorsal horn of the spinal cord compared to their respective contralateral dorsal horn, a change which failed to reach significance when compared to WT control ipsilateral dorsal horn (Student's *t*-test, $p = 0.07$). In contrast, administration of MIA did not induce any significant alteration in the frequency of P-p38 expressing IBA1 positive microglial cells in the ipsilateral dorsal horn compared to its respective contralateral and the to that of TASTPM control (Figure 3.7). Therefore, suggesting that increase in spinal microglial response to MIA which is evident in the WT mice is likely to be absent in the transgenic TASTPM model of AD.

3.3.3.3 **No Astrocytosis in MIA Model of Osteoarthritis**

Having established lack of spinal microgliosis in TASTPM mice 28 days after unilateral administration of MIA, we went onto evaluate the expression of astrocytes using GFAP as a marker. The WT mice displayed no change in ipsilateral GFAP immunoreactivity intensity in the dorsal horn 28 days following MIA injection as compared to ipsilateral dorsal horn of WT controls or its contralateral dorsal horn (Figure 3.8). Similarly, the TASTPM mice also exhibited unaltered astroglial expression in the dorsal horn four weeks post MIA administration compared to TASTPM controls.

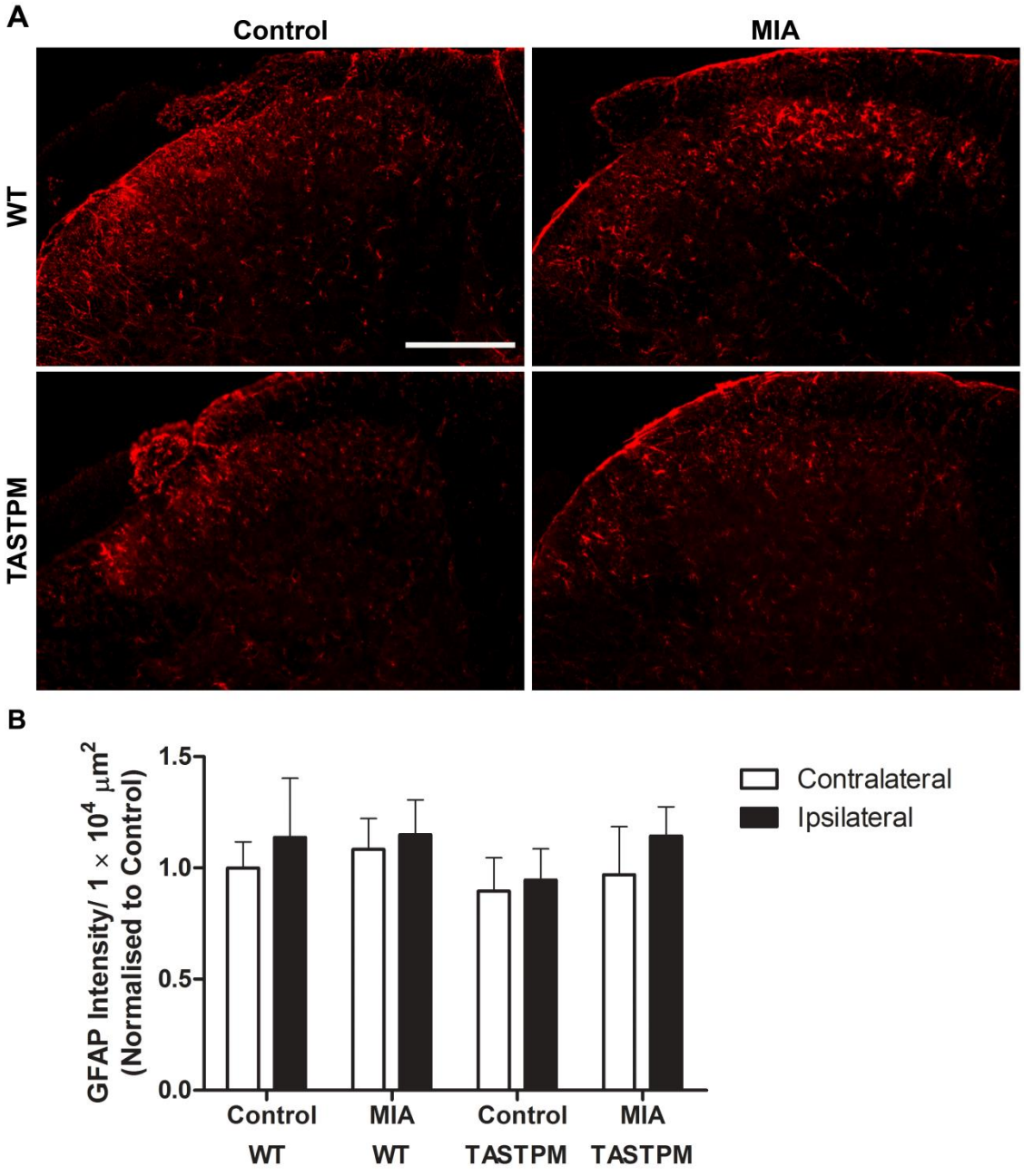

Figure 3.8: No Astrocytosis Post MIA Administration

Representative images showing glial fibrillary acidic protein (GFAP) immunoreactivity in the ipsilateral dorsal horn of the spinal cord (L4-L5) 28 days after intra-articular injection of saline (control) or MIA of TASTPM and age and gender-matched wild-type (WT) mice (A). The scale bar represents 200μm. (B) Quantification of GFAP immunoreactivity fluorescence intensity (normalised to WT control contralateral dorsal horn) revealed no significant alteration in astrocytes post 28 days post MIA administration in the WT nor in the TASTPM mice ($p > 0.05$, two-way ANOVA). Data values are expressed as normalised mean ± SEM ($n = 4$ per experimental group).

3.3.3.4 **MIA and APP/Aβ**

As reported in the previous chapter, intraneuronal accumulation of APP/Aβ was present in the spinal cord grey matter of transgenic TASTPM mice. Therefore, we examined if a chronic pain condition had any impact on the expression of APP/Aβ in the dorsal horn. Here we report a reduction in dorsal horn (ipsilateral and contralateral) expression of APP/Aβ in TASTPM mice 28 days post MIA compared to TASTPM control, which failed to reach statistical significance ($p > 0.05$, two way ANOVA) (Figure 3.9).

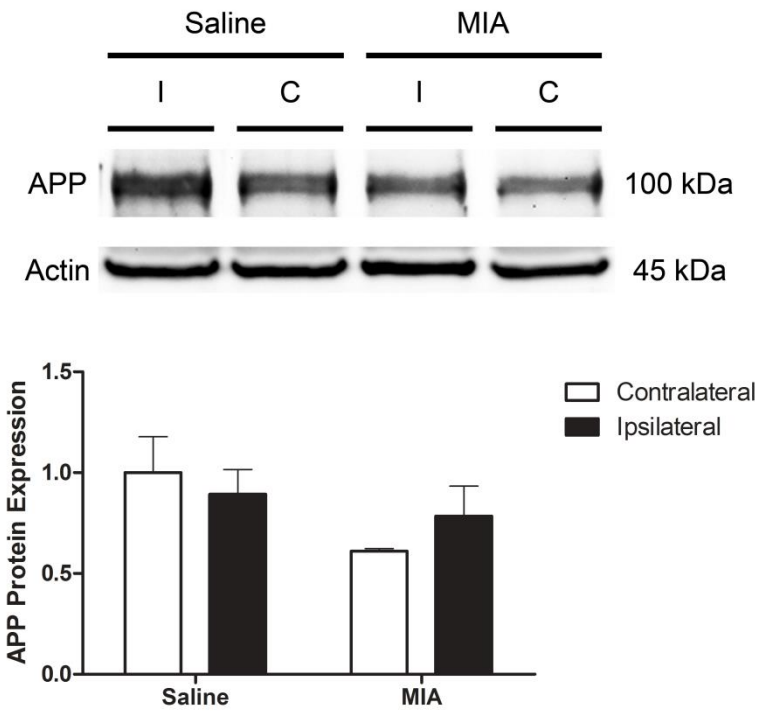

Figure 3.9: No Change in APP/Aβ Expression in the Dorsal Horn of TASTPM Spinal Cord 28 Days Post MIA

Representative blot showing APP/Aβ expression in the dorsal horn of TASTPM 28 days post intra-articular injection of MIA (1 mg) or saline control. Quantitative analysis of APP/Aβ revealed unaltered expression of APP/Aβ in the lumbar (L3-L5) dorsal horn of TASTPM mice injected with MIA compared to their respective saline controls and when comparing within each experimental group between ipsilateral and contralateral dorsal horns ($p > 0.05$, two way ANOVA) relative to β-actin (loading control). Data values are expressed as mean ± SEM (n = 4 per experimental group).

3.3.4 MIA-induced Changes in the Brain

Following examination of spinal cord changes 28 days post an intra-articular injection of MIA in the left knee joint, we assessed whether MIA induced changes along the pain pathway in the supraspinal structures, namely the thalamus.

3.3.4.1 **MIA-induced Increased Thalamic Microgliosis in TASTPM**

MIA injected WT mice did not present with any significant alteration in IBA1 burden (percentage of area occupied by IBA1 immunoreactivity) in the thalamus 28 days post intra-articular injection compared to their respective WT controls. In contrast, TASTPM mice injected with MIA displayed significantly increased IBA1 burden in the thalamus compared to TASTPM controls (Figure 3.10). It was noteworthy that TASTPM mice exhibited significantly greater percentage of area occupied by IBA1 immunoreactivity in the thalamus compared to WT controls. Therefore, suggesting that MIA injection in the periphery is coincided with exacerbation of neuroinflammation in the TASTPM brain.

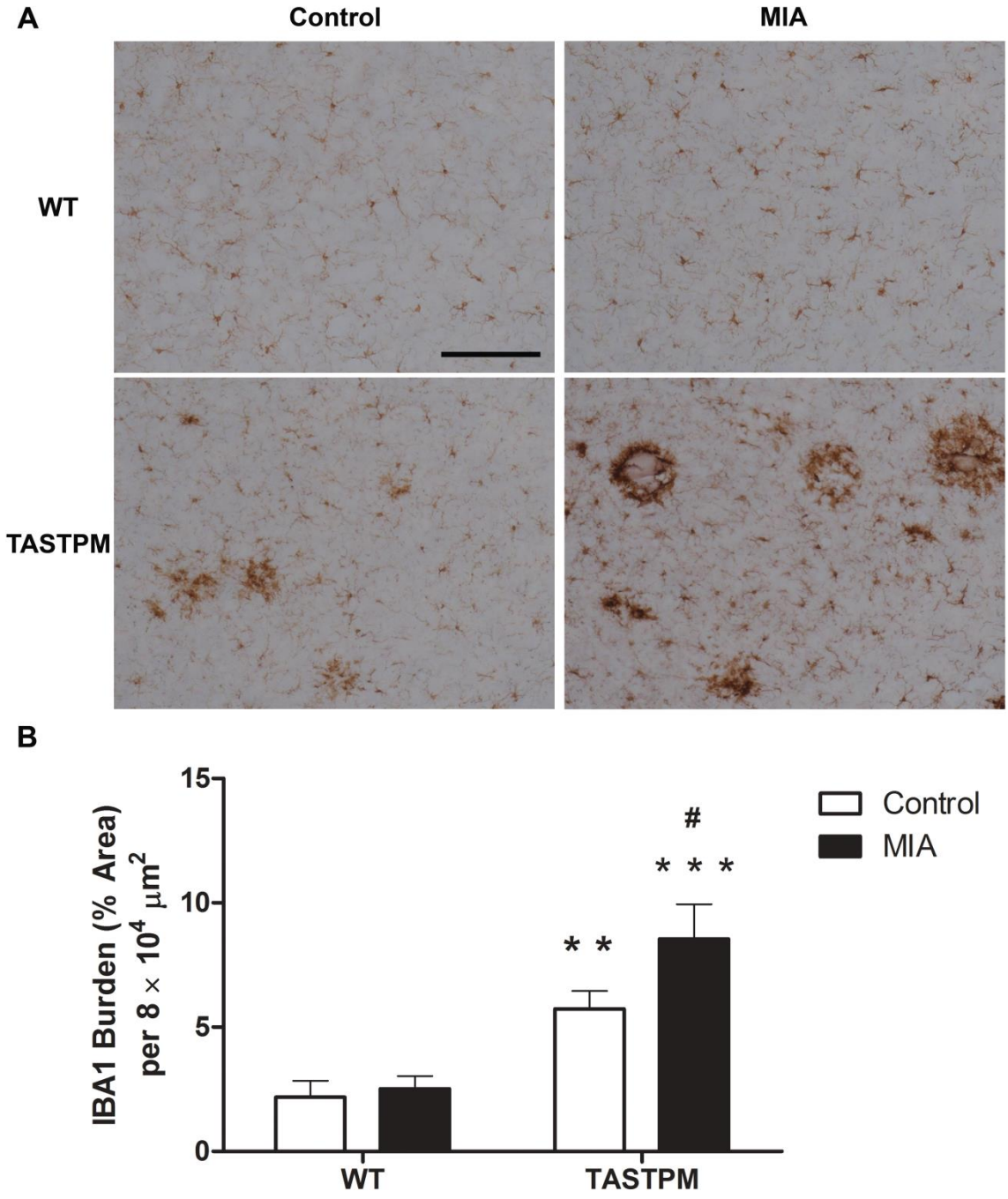

Figure 3.10: MIA-induced Increase in Thalamic Microgliosis in TASTPM

Representation of IBA1 immunoreactive microglial cells 28 days after intra-articular injection of saline (control) or MIA, in the thalamus of 6 months old TASTPM and age-and gender matched wild-type (WT) mice (A). The scale bar represents 200µm. Alteration of percentage of area occupied by IBA1 immunoreactivity (IBA1 burden) compared between genotype (TASTPM vs. WT) within experimental group (Control or MIA) (* * $p < 0.01$, * * * $p < 0.001$); and between experimental groups (MIA vs. Control) within genotype (WT or TASTPM) ($^{\#}$ $p < 0.05$) were detected using two-way ANOVA followed by Tukey multiple comparison test (B). Data is shown as mean ± SEM (n = 6 - 8 per experimental group).

3.3.4.2 **MIA-induced Increased Trend of Thalamic Astrocytosis in TASTPM**

Subsequently we also assessed whether there was any alteration in the astrocytes response in the thalamus post MIA injection. WT mice did not show any significant change in the percentage of area occupied by GFAP immunoreactivity 28 days post MIA administration compared to WT controls. However, the TASTPM mice displayed a trend of increased GFAP burden (not statistically significant, $p = 0.113$, two-way ANOVA, Tukey post-hoc test) post MIA administration compared to TASTPM controls. It was clearly evident as with IBA1 immunoreactivity, that the transgenic TASTPM mice exhibited significantly greater GFAP burden compared to the WT group (Figure 3.11). Thus, reinforcing the neuroinflammatory characteristic recapitulated in TASTPM model of AD. Collectively, these data show that MIA administration in the periphery is associated with increase in astrocytosis in the thalamus which however is not significant.

3.3.4.3 **No Effect of MIA on Supraspinal Amyloid Plaques in TASTPM Mice**

Due to an increase in gliosis observed in the thalamus of TASTPM mice injected with MIA, we went onto explore further if AD-associated amyloid pathology is also affected. Quantitative analysis of Thioflavin-S staining in the thalamus revealed no significant difference in the percentage of area occupied by amyloid plaques in the MIA injected TASTPM compared their respective controls. In addition to the thalamus, we also examined the plaque load in the cortex and hippocampus of MIA injected TASTPM compared to TASTPM controls in order to examine whether those areas which are reported to be affected in AD show any alteration in amyloid pathology. Similar to the thalamus, there were no significant changes observed in the cortex nor the hippocampus of the TASTPM mice administrated with MIA compared to TASTPM controls (Figure 3.12). These data indicate that the AD-associated neuroinflammation in the thalamus is exacerbated in the MIA injected TATSPM mice whilst no effect on the amyloid plaque burden. Thus, suggesting the increase in gliosis in the thalamus correlating to the chronic pain state rather than AD-associated amyloid plaques.

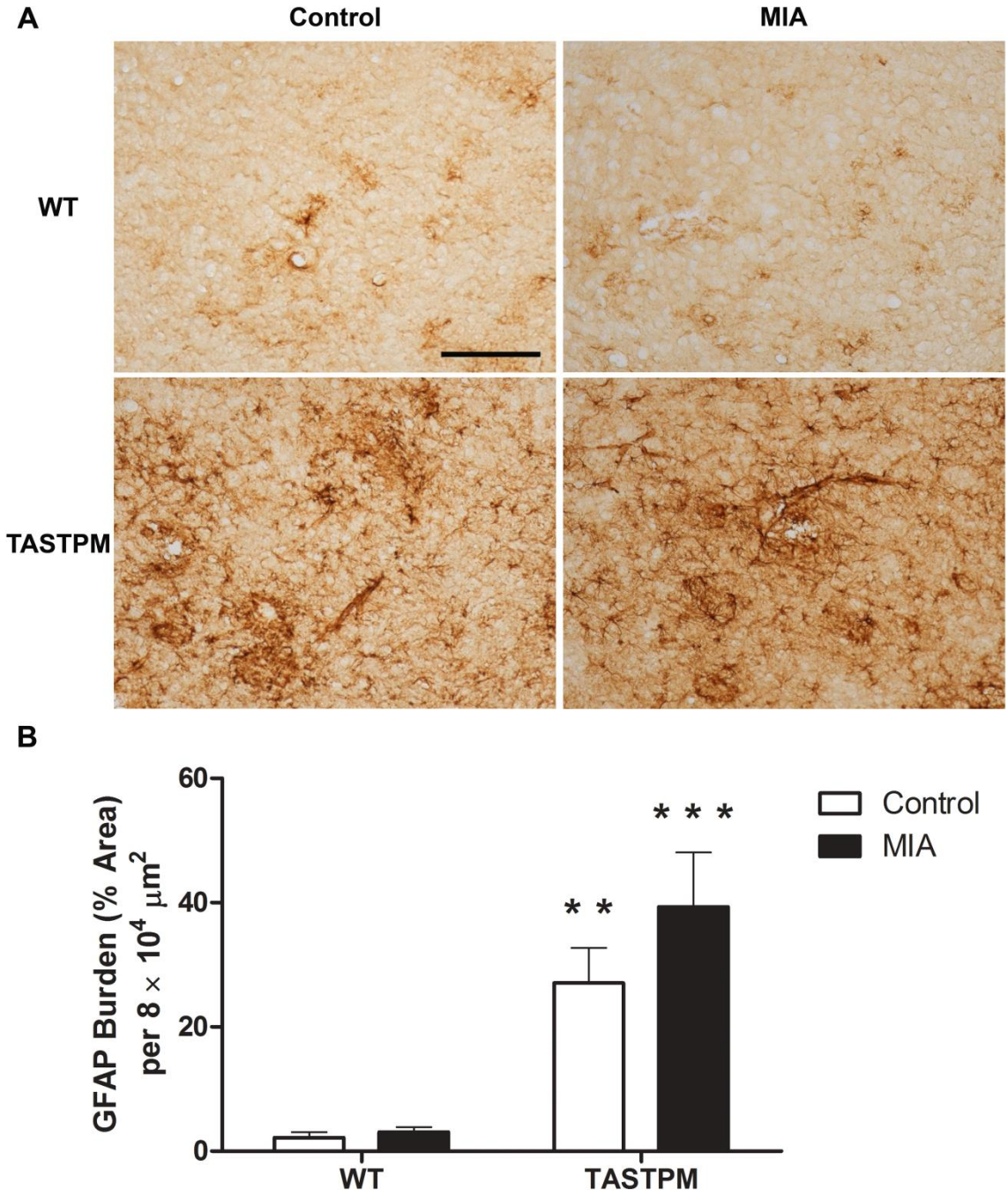

Figure 3.11: MIA-induced Increased Trend of Astrocytosis in TASTPM Thalamus

Representation of glial fibrillary acidic protein (GFAP) immunoreactive astrocytes 28 days post intra-articular administration of saline (control) or MIA, in the thalamus of 6 months old TASTPM and age-and gender matched wild-type (WT) mice (A). The scale bar represents 200µm. Alteration of percentage of area occupied by GFAP immunoreactivity (GFAP burden) compared between genotype (TASTPM vs. WT) within experimental group (Control or MIA) (* * $p < 0.01$, * * * $p < 0.001$); and between experimental groups (MIA vs. Control) within genotype (WT or TASTPM) ($p > 0.05$) were detected using two-way ANOVA followed by Tukey multiple comparison test (B). Data is shown as mean ± SEM (n = 4 per experimental group).

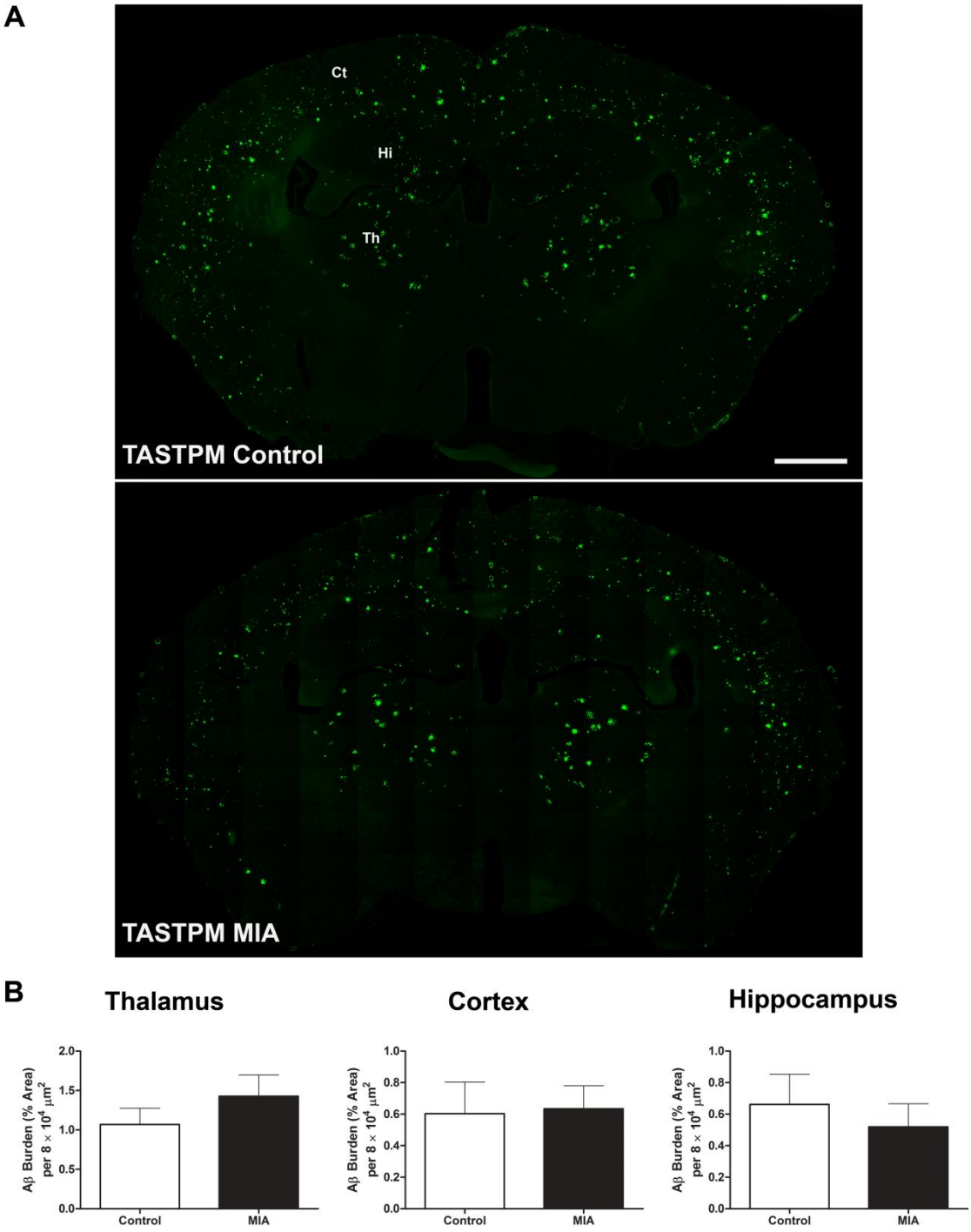

Figure 3.12: No Effect of MIA on AD-associated Amyloid Plaques in the Brain of TASTPM

Representation of β-amyloid 1-16 (6E10) immunoreactivity 28 days post intra-articular administration of saline (control) or MIA, in the brain of 6 months old TASTPM mice (A). The scale bar represents 1mm. No significant effect of MIA administration on percentage of area occupied by 6E10 immunoreactivity (Aβ burden) was detected in the thalamus, cortex and hippocampus of TASTPM mice compared to TASTPM controls ($p > 0.05$, Student's *t*-test) (B). Data is shown as mean ± SEM (n = 6 - 8 per experimental group).

3.3.5 Analgesic Interventions

In addition to the examination of the MIA-induced characteristic plastic changes in the knee joint and regions involved in the pain pathway, namely the spinal cord and thalamus, we went onto evaluate the effectiveness of analgesics at different intervals post OA induction. As weight bearing asymmetry was absent in the MIA injected transgenic TASTPM mice; we considered robust, and therefore only examined, reversal of mechanical hypersensitivity as a measure of analgesia. Reversal of mechanical hypersensitivity induced up to day 7 and from day 10 to day 28 were taken as representation of early/inflammatory and late/established stage of the OA chronic pain, respectively. The analgesics selected for this study (early: celecoxib and diclofenac; late: paracetamol, morphine and gabapentin) are commonly used for treatment of chronic pain conditions in individuals including patients with OA and also have been shown to be effective in rodent models of chronic pain.

3.3.5.1 **Early Intervention**

The analgesics selected to evaluate the analgesic effect around 7 days post MIA administration were celecoxib and diclofenac.

3.3.5.1.1 Celecoxib

MIA injected WT and TASTPM mice were administrated with celecoxib (30 mg/kg) or vehicle control. Oral administration of celecoxib in WT mice 6-7 days post unilateral MIA intra-articular injection resulted significant reversal of ipsilateral mechanical hypersensitivity 1 hour post administration compared to the ipsilateral PWT of vehicle WT controls and to their respective pre-injection values. The effect of celecoxib diminished and ipsilateral PWT returned to back to pre-injection values 6 hours post drug administration in the WT mice (Figure 3.13A). Similarly, TASTPM mice injected with MIA displayed significant increase in ipsilateral 50% PWT 1 hour post administration of celecoxib compared to TASTPM vehicle control and their respective pre-injection values. In contrast, the effect of celecoxib was somewhat prolonged in TASTPM mice, as they displayed significantly greater ipsilateral mechanical thresholds 3 hours post celecoxib compared to their respective pre-injection mean; before returning back to the pre-injection values at 6 hours post drug administration (Figure 3.13B). Collectively, celecoxib displayed to

potentially have an analgesic effect in both WT and TASTPM mice injected with MIA during the early/inflammatory phase of OA.

3.3.5.1.2 Diclofenac

In contrast, subcutaneous administration of diclofenac (30 mg/kg) shows a trend but not a significant effect in the WT mice 7-9 days post unilateral MIA administration compared to their respective vehicle controls; although a significant increase in ipsilateral mechanical threshold 3 hours post diclofenac was observed compared to their respective pre-injection (Figure 3.14A). A similar trend was observed for the effect of diclofenac in MIA injected TASTPM mice, but the significant reversal was observed at an earlier time-point of 1 hour compared to their respective pre-injection; that diminished at the remaining time points (Figure 3.14B). Thus, demonstrating that diclofenac administration between day 7 and day 9 after MIA injection may not be as effective analgesic in both WT and TASTPM mice during the early inflammatory phase of the disease.

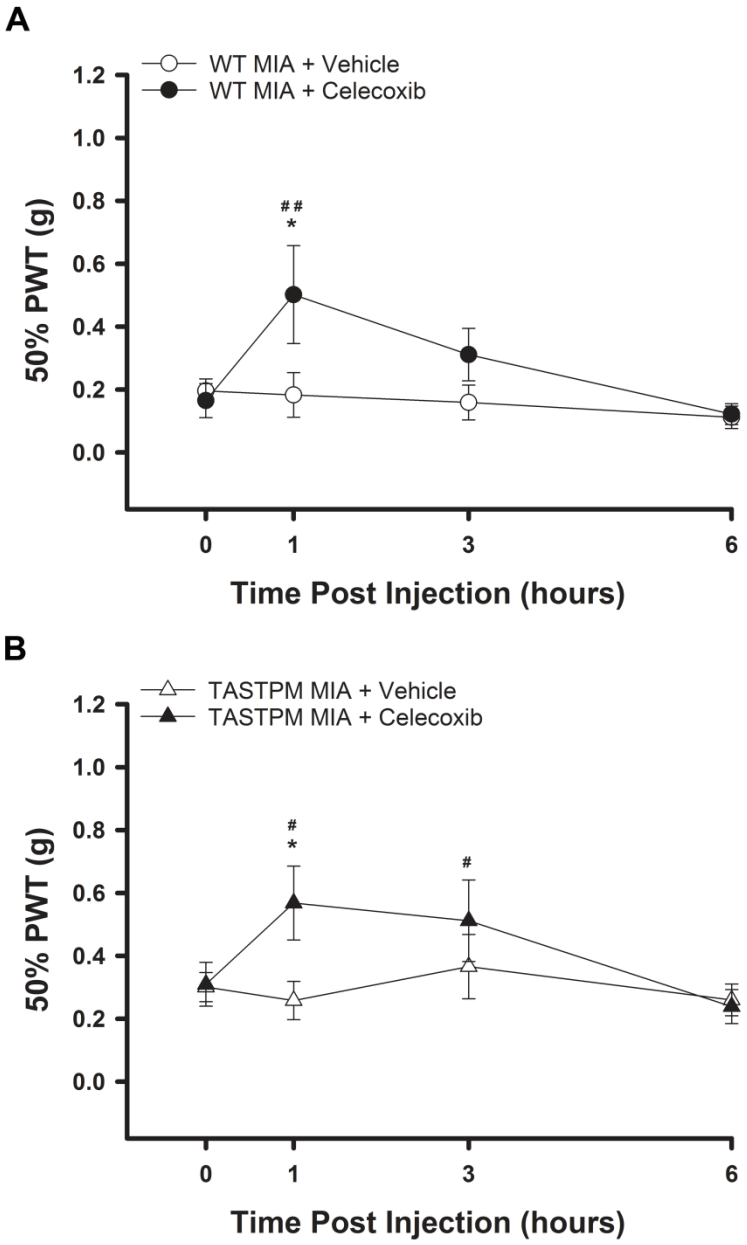

Figure 3.13: Celecoxib Induced Reversal of MIA-induced Mechanical Hypersensitivity in the Ipsilateral Hind Paw

The effect of celecoxib on the ipsilateral hind paw 50% paw withdrawal threshold (PWT) of MIA injected wild-type (WT, A) and TASTPM (B) mice at regular intervals prior to (0, pre-injection) and up to 6 hours following oral administration of celecoxib (30 mg/kg) or vehicle control (methyl cellulose) on day 6 and 7 post MIA injection (crossover). Both WT and TASTPM mice displayed partial reversal of mechanical hypersensitivity 1 hour post oral administration of celecoxib which significant compared to their respective vehicle controls (* $p < 0.05$) and to respective pre-injection values ($^{\#}$ $p < 0.05$; $^{\#\#}$ $p < 0.01$) using two-way repeated measures ANOVA followed by Tukey multiple comparison test, which returned back to pre-injection thresholds after 6 hours. Data is shown as mean ± SEM (n = 6 - 8 mice per group).

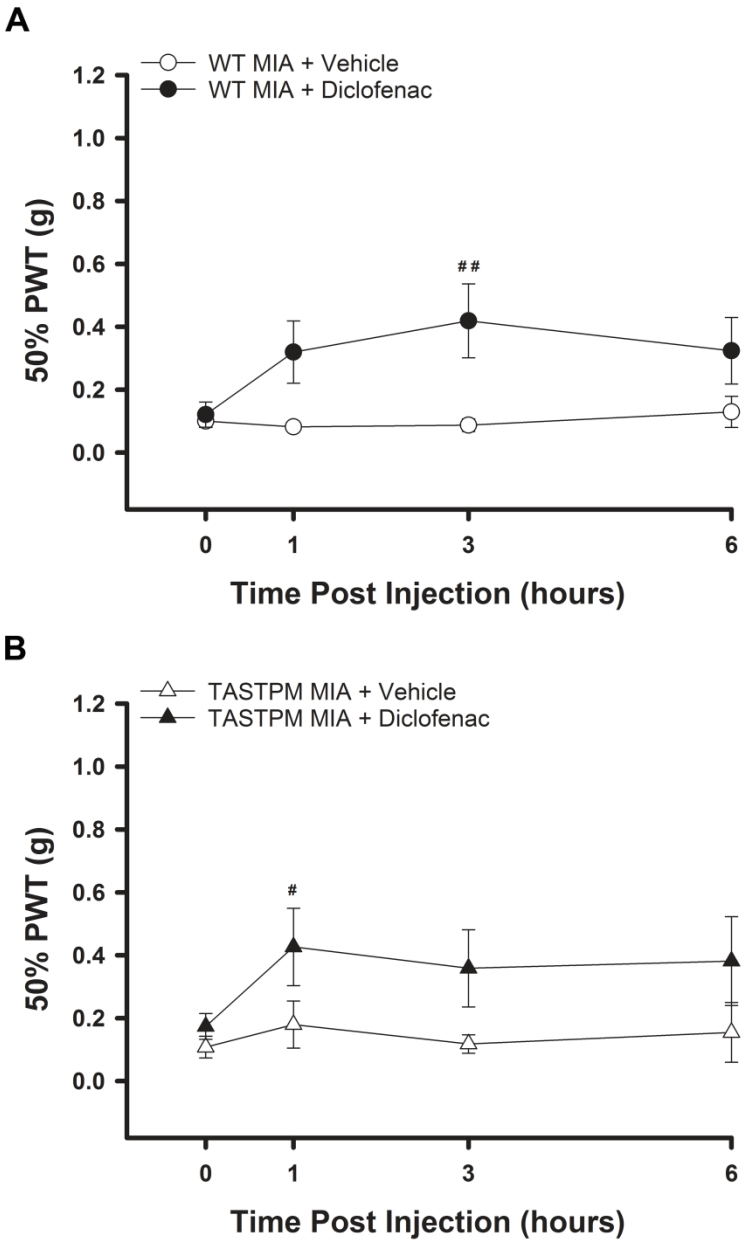

Figure 3.14: Trend of Diclofenac Induced Increase in Mechanical Thresholds in the Ipsilateral Hind Paw in the MIA Model of OA

Ipsilateral mechanical withdrawal responses of MIA injected wild-type (WT, A) and TASTPM (B) mice were assessed at regular intervals prior to (0, pre-injection) and up to 6 hours following subcutaneous administration of diclofenac (30mg/kg) or saline (vehicle control) on day 7 and day 9 post MIA injection. There was no significant difference, at any time point, in the 50% paw-withdrawal threshold (PWT) within genotype (WT or TASTPM) and between treatment groups (diclofenac vs. vehicle). However, diclofenac injected WT and TASTPM mice displayed significantly greater mechanical withdrawal thresholds compared to their respective pre-injection mean at 3 hours and 1 hour interval, respectively ($^{\#}$ $p < 0.05$; $^{\#\#}$ $p < 0.01$). Statistical analyses were conducted using two way repeated measures ANOVA followed by Tukey multiple comparison test. The 50% PWT values a presented as mean ± SEM (n = 7 - 8 mice per experimental group).

3.3.5.2 **Late Intervention**

The analgesics selected to evaluate the analgesic effect from days 10 to 28 post MIA administration, representing the late phase of OA, were paracetamol, gabapentin and morphine.

3.3.5.2.1 Paracetamol

MIA and saline injected WT and TASTPM mice were administrated with paracetamol (300 mg/kg) 28 days post MIA. Oral administration of paracetamol in MIA injected WT mice did not induce any significant reversal of ipsilateral mechanical hypersensitivity at any time-point compared to their respective pre-injection mean (Figure 3.15A). Similarly, paracetamol failed to induce analgesia in the ipsilateral hind paw at any time-point in MIA injected TASTPM mice compared to their respective pre-injection values (Figure 3.15B). Therefore, indicating that the dose tested at the time-point post MIA injection is ineffective in both WT and TASTPM.

3.3.5.2.2 Morphine

However, analgesic effects were evident MIA and saline injected WT and TASTPM mice that received an injection of morphine (6 mg/kg) 28 days post intra-articular injection. Subcutaneous administration of morphine in MIA injected WT mice resulted in significant reversal of ipsilateral mechanical hypersensitivity that becomes apparent at 30 minutes and peaking at 60 minutes compared to its respective pre-injection values; before return to pre-injection mean at 3 hours. Whilst, there was no effect of morphine observed at any time point in the saline injected WT mice (Figure 3.16A). Similarly, MIA injected TASTPM mice exhibited significant increase in the ipsilateral 50% PWT at 30 minutes, which peaks at 1 hour post morphine administration compared to its respective pre-injection values; prior to restoring back to pre-injection mean 3 hours post drug administration (Figure 3.16B). Thus, indicating an evident analgesic effect of morphine in both WT and TASTPM mice 28 days post injection with MIA.

3.3.5.2.3 Gabapentin

Interestingly, gabapentin, an anti-epileptic drug that has been shown to induce analgesia in chronic pain models of neuropathy as well as MIA induced OA; displayed significant reversal of MIA-induced ipsilateral mechanical hypersensitivity in WT mice compared to WT vehicle control three hours post administration. In addition, the analgesic effect started to appear 1 hour and

peaking at 3 hours post oral administration of gabapentin (60 mg/kg) in MIA injected WT mice that showed significant increased PWT compared to their respective pre-injection values (Figure 3.17A). However, gabapentin failed to have any effect on the ipsilateral mechanical thresholds of MIA-injected TASTPM mice at any time-point compared to their respective vehicle controls and to their respective pre-injection mean (Figure 3.17B). Therefore, suggesting a possible alteration in processing of chronic pain state the transgenic model of AD which resulted in lack of gabapentin analgesic effect.

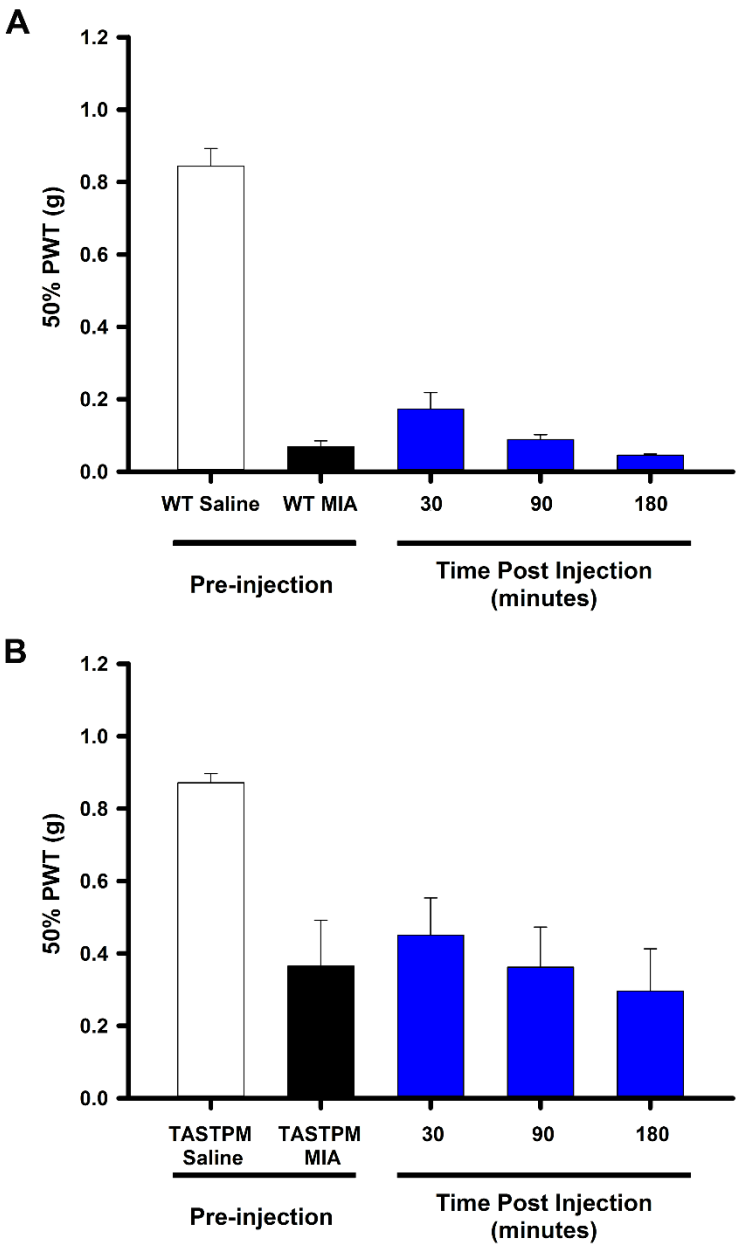

Figure 3.15: No effect of Paracetamol on MIA-induced Mechanical Hypersensitivity in the Ipsilateral Hind Paw

Ipsilateral mechanical withdrawal responses of MIA or saline injected wild-type (WT, A) and TASTPM (B) mice were assessed at regular intervals prior to (pre-injection) and up to 180 minutes following oral administration of paracetamol (300mg/kg) on day 28 post MIA injection. Both WT and TASTPM mice displayed mechanical hypersensitivity in comparison to their respective saline groups prior to and at each time interval. There was no significant difference, at any time point, in the ipsilateral 50% paw withdrawal threshold (PWT) in both MIA injected WT or TASTPM mice when compared to their respective pre-injection values. Statistical analysis was conducted using two way repeated measures ANOVA. The 50% PWT values are presented as mean ± SEM (n = 5 - 9 mice per experimental group).

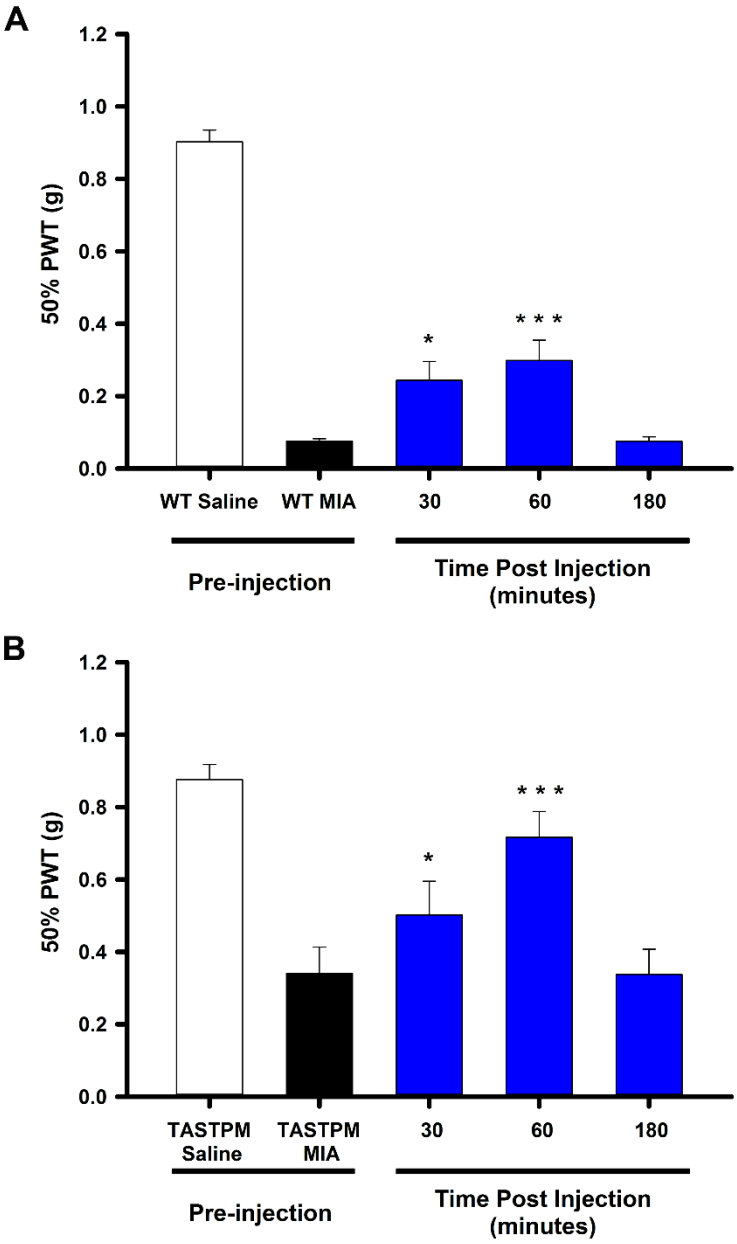

Figure 3.16: Morphine Resulted in Reversal of MIA-induced Ipsilateral Mechanical Hypersensitivity in WT and TASTPM

The effect of morphine on the ipsilateral hind paw 50% PWT of MIA or saline injected wild-type (WT, A) and TASTPM (B) mice at regular intervals prior to (pre-injection) and up to 3 hours following s.c. administration of morphine sulfate (6 mg/kg) on day 28 post MIA injection. Both WT and TASTPM mice displayed mechanical hypersensitivity in comparison to their respective saline groups prior to and at each time interval. Morphine induced significant reversal of MIA-induced mechanical hypersensitivity as early as 30 minutes post administration reaching its peak effect at 1 hour in both WT and TASTPM mice compared to their respective baseline (* $p < 0.05$; * * * $p < 0.001$) using two-way repeated measures ANOVA followed by Tukey multiple comparison test. Data is shown as mean ± SEM (n = 8 - 10 mice/group).

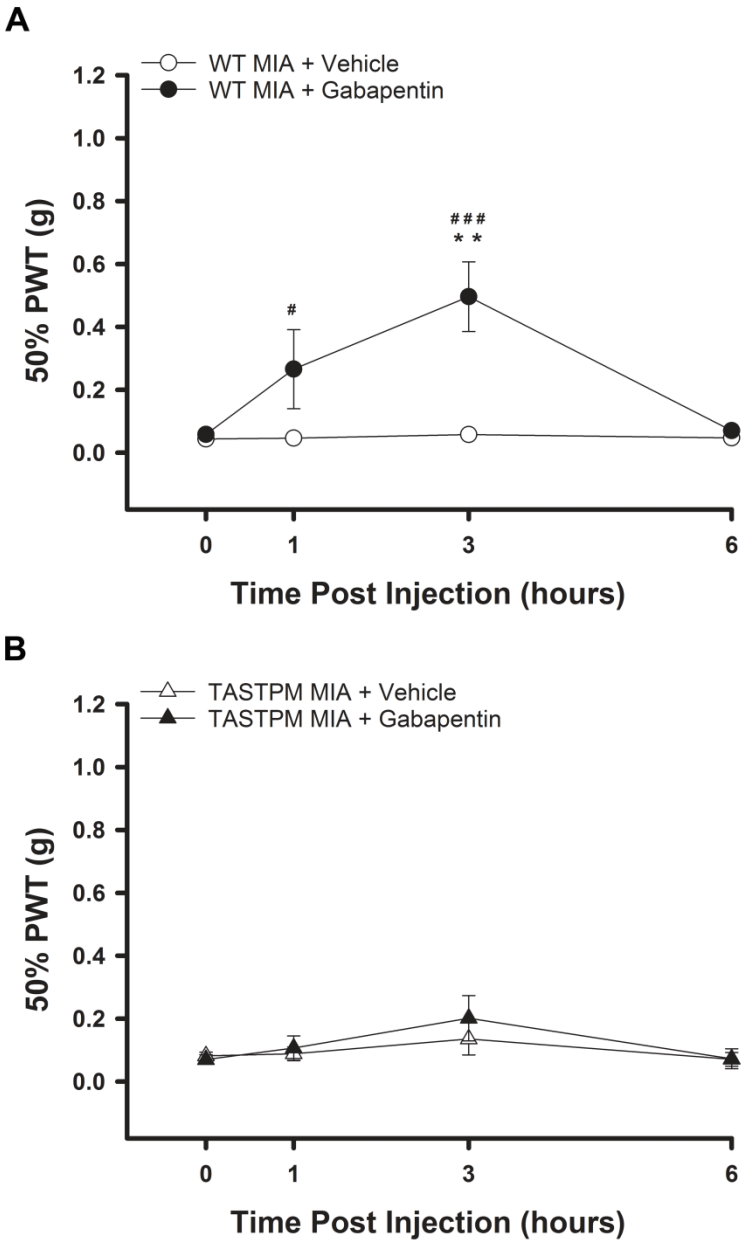

Figure 3.17: Gabapentin Fails to Reverse MIA-induced Mechanical Hypersensitivity in TASTPM

Ipsilateral mechanical withdrawal responses of MIA injected wild-type (WT, A) and TASTPM (B) mice were assessed at regular intervals prior to (0, pre-injection) and up to 6 hours following oral administration of gabapentin (60mg/kg) or distilled water (vehicle control) on day 22 and day 24 post MIA injection (crossover). Administration of gabapentin resulted in partial reversal of MIA-induced mechanical hypersensitivity only in the WT mice compared to their respective vehicle controls (* * $p < 0.01$) which became apparent at the 3 hours interval. In addition, significant increase in the 50% paw withdrawal threshold (PWT) were observed at 1 and 3 hours post gabapentin administration when compared to pre-injection values ($^{\#}$ $p < 0.05$ and $^{\#\#}$ $p < 0.01$). Statistical analysis was conducted using two way repeated measures ANOVA followed by Tukey multiple comparison test. The 50% PWT values a presented as mean ± SEM (n = 8 - 9 mice per experimental group).

3.3.5.3 **Overview of Analgesic Interventions**

Following the evaluation of analgesic effect over a time-course we examined the peak percentage of reversal of mechanical hypersensitivity in order to compare the extent of analgesia induced in MIA injected WT and TASTPM mice (Table 3.2). Our results demonstrate comparable reversal of mechanical hypersensitivity induced by celecoxib (WT: 37.4% ± 18.6%; TASTPM: 43.9% ± 13.2%), diclofenac (WT: 32.7% ± 15.3%; TASTPM: 23.5% ± 13.6%) and paracetamol (WT: 10.9% ± 5.7%; TASTPM: 21.9% ± 10.4%) in MIA injected WT and TASTPM mice. In contrast administration of morphine induced significantly greater level of reversal of mechanical hypersensitivity in the ipsilateral hind paw of TASTPM mice (58.7% ± 8.9%) compared to WT OA mice (24.3% ± 5.8%). Whilst, interestingly gabapentin which induced analgesia in WT mice injected with MIA (40.0% ± 10.0%) failed to have any effect on TASTPM mice (7.8% ± 7.1%).

Collectively these data highlight that drugs that induce analgesia in MIA-injected non-transgenic WT mice does not necessarily have the same impact in the transgenic mouse model of AD. Therefore, indicating towards a possible alteration in nociceptive processing in chronic OA pain in this model of AD as a result differing analgesic responses were observed.

Table 3.2: Summary of Analgesic Interventions

Intervention	Analgesic	WT	TASTPM	*t*-test (p-value)
Early **(Day 0 – Day 7)**	Diclofenac	**32.7% ± 15.3%**	23.5% ± 13.6%	> 0.05
	Celecoxib	**37.4% ± 18.6%**	**43.9% ± 13.2%**	> 0.05
Late **(> Day 10)**	Paracetamol	10.9% ± 5.7%	21.9% ± 10.4%	> 0.05
	Morphine	**24.3% ± 5.8%**	**58.7% ± 8.9%**	**< 0.01**
	Gabapentin	**40.0% ± 10.0%**	7.8% ± 7.1%	**< 0.05**

Values represent the percentage reversal of MIA-induced ipsilateral mechanical hypersensitivity in the WT and TASTPM ipsilateral hind paw by early and late analgesic intervention. Percentage values in bold represent significant reversal of MIA-induced ipsilateral mechanical hypersensitivity in comparison to respective pre-injection values. Alterations in the percentage reversal of MIA-induced mechanical hypersensitivity by analgesics between the two experimental groups were assessed using the Student's *t*-test. Data are expressed as mean ± SEM (n = 5 - 10 per experimental group).

3.3.6 Opioidergic System Responsible for the Altered Chronic Pain Behaviour

As reported in the previous chapter, elevated opioidergic tone was observed to be responsible for altered nociceptive thresholds in response to acute noxious thermal stimulation. Therefore, in order to test the hypothesis whether the increased opioidergic tone in TASTPM mice may underlie the altered behavioural responses to MIA observed we administrated the opioid antagonist, naloxone 24 days post MIA and assessed mechanical thresholds. Furthermore, we examined the expression of opioid receptors in spinal and supraspinal structures involved in pain processing.

3.3.6.1 **Naloxone Causes Increased MIA-induced Mechanical Hypersensitivity in TASTPM**

So firstly, we injected naloxone and assessed whether it contributed to the partial recovery of MIA-induced mechanical hypersensitivity exhibited by the transgenic mouse model of AD. Our results demonstrate that administration of naloxone methiodide, which is unable to penetrate through the blood-brain barrier (Inglis et al 2008); fails to have any effect in both MIA injected WT and TASTPM mice (Figure 3.18A). No effect of naloxone methiodide was evident in the WT and TASTPM contralateral hind paw at any time point.

In contrast, naloxone hydrochloride, which can readily cross the blood-brain-barrier induced decrease in mechanical thresholds in TASTPM, however not significant compared to their respective pre-injection value ($p = 0.09$) at 30 minutes post drug administration, whilst no change in WT mice injected with MIA was observed at any time-point. It was noteworthy, that naloxone hydrochloride reduced mechanical thresholds of MIA injected TASTPM mice to comparable levels of that exhibited by MIA injected WT mice at 30 minutes post administration, which diminished and recovered to pre-injection value for the remaining time-points up to 3 hours (Figure 3.18B). No effect of naloxone hydrochloride was evident in the WT and TASTPM contralateral hind paw at any time point. Collectively, these observations indicate that increased opioidergic tone, in particular in the CNS, may contribute towards the altered chronic pain behaviour exhibited by TASTPM mice in a model of OA chronic pain.

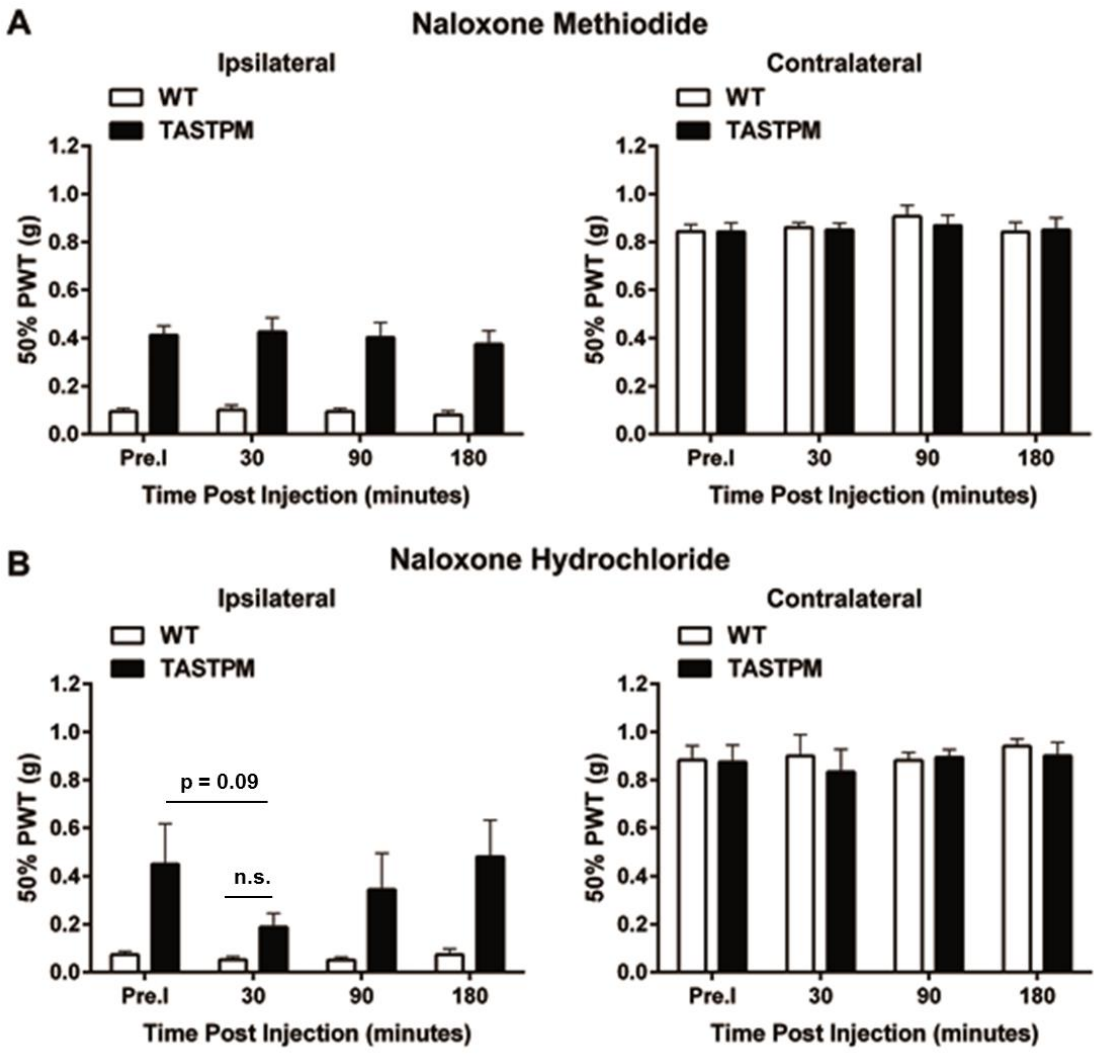

Figure 3.18: Trend of Naloxone Mediated Increase in Ipsilateral MIA-induced Mechanical Hypersensitivity only in TATSPM Mice

Mechanical withdrawal responses of MIA injected mice were assessed in both hind paws at regular intervals prior to (pre-injection, Pre.I) and up to 180 minutes following i.p. administration of naloxone methiodide (1mg/kg, A) and naloxone hydrochloride (1mg/kg, B) three weeks post MIA injection. Prior to administration of naloxone methiodide or naloxone hydrochloride, WT mice exhibited significantly lower ipsilateral mechanical thresholds compared to TASTPM ipsilateral hind paw. No significant alteration in 50% paw withdrawal threshold (PWT) was induced by naloxone methiodide in WT and TASTPM ipsilateral and contralateral hind paws at any time point. Whilst, naloxone hydrochloride induced a trend of reduced ipsilateral mechanical thresholds only in the TASTPM ipsilateral hind paw 30 minutes post administration, though insignificant compared to its respective pre-injection values ($p = 0.09$) and not significantly different (n.s.) from the WT ipsilateral hind paw. This effect in the TASTPM ipsilateral hind paw recovered to pre-injection values at 90 minutes post naloxone hydrochloride administration. No effect of naloxone hydrochloride was observed in the ipsilateral hind paw of WT mice and the contralateral hind paws of both genotypes at any time interval. Alteration in behaviour compared between experimental groups was detected using two-way repeated measures ANOVA followed by Student-Newman-Keuls post-hoc test. The 50% PWT values a presented as mean ± SEM (n = 5-9 mice per group).

3.3.6.2 **Increased Plasma β-endorphin in MIA-injected TASTPM**

In addition to the pharmacological evidence of enhanced opioidergic tone exhibited by the TASTPM mice that led to the partial recovery of mechanical hypersensitivity observed; we went on to examine opioidergic peptide, β-endorphin, expression in plasma of MIA-injected TASTPM mice compared to WT group injected with MIA using EIA. We observed significantly higher levels of plasma β-endorphin in the MIA-injected TASTPM in comparison to WT controls that received MIA (Figure 3.19A). Moreover, we were able to demonstrate a significant positive relationship between the ipsilateral mechanical paw withdrawal thresholds on day 28 with the plasma concentrations of β-endorphin (R^2 = 0.589, $p < 0.05$) (Figure 3.19B). Hence these data reinforce the notion that the transgenic TASTPM exhibit an increased endogenous opioidergic tone that may underlie the altered behaviour response to chronic OA pain in a transgenic mouse model of AD.

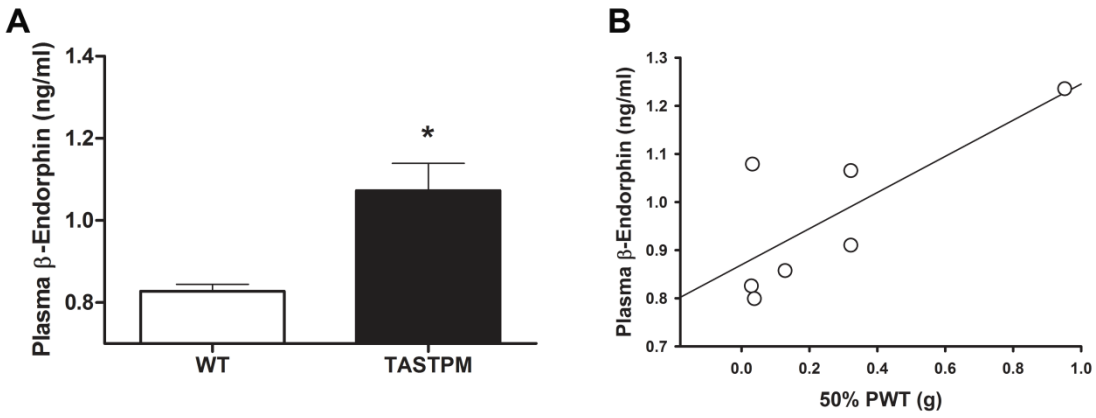

Figure 3.19: Increased Plasma β-endorphin Exhibited in TASTPM Mice

Plasma concentration of β-endorphin was determined by EIA 28 days post administration of MIA in the left knee joint of wild-type (WT) and TASTPM (A). MIA-injected TASTPM displayed significantly greater levels of plasma β-endorphin compared to WT (* $p < 0.05$, Student's *t*-test). Data is presented as mean ± SEM (n = 3 - 4 per experimental group). A positive relationship between the level of plasma concentration of β-endorphin and ipsilateral 50% paw withdrawal threshold (PWT) 28 days post MIA injection was detected using linear regression (R^2 = 0.589, $p < 0.05$). Data plotted as individual animal plasma β-endorphin and 50% PWT observed on day 28.

3.3.6.3 **Reduced Dorsal Horn mRNA Expression of Mu-OR in MIA-injected TASTPM**

Furthermore, we examined the relative expression of the opioid receptors (μ-OR, δ-OR, and κ-OR) in the ipsilateral and contralateral dorsal horns of MIA-injected TASTPM mice compared to WT controls. The saline injected WT and TASTPM mice displayed comparable level of mRNA expression of μ-OR, δ-OR, and κ-OR in the ipsilateral and contralateral dorsal horns (data not shown). Therefore, data from MIA injected WT and TASTPM mice were normalised to their respective saline group. It became evident that there was a significant reduction in the ipsilateral and contralateral μ-OR relative expression in the dorsal horn of TASTPM mice 28 days post MIA injection compared to their WT counterparts (Figure 3.20A). Whilst, the relative expression of δ-OR (Figure 3.20B) and κ-OR (Figure 3.20C) were comparable in the TASTPM and WT dorsal horns 28 days post MIA. Thus, indicating that there is only an alteration, a significant reduction, of μ-OR mRNA expression in the dorsal horn of TASTPM mice compared to WT controls 28 days post MIA administration.

3.3.6.4 **Mu-OR Receptor Protein Expression in MIA-injected TASTPM Dorsal Horn Unchanged**

Intriguingly, despite the reduced μ-OR mRNA expression in the dorsal horn of TASTPM mice, we were not able to detect any alteration in the dorsal horn μ-OR protein expression in the TASTPM mice compared to WT injected with MIA, in neither the ipsilateral nor the contralateral (Figure 3.21). The underlying reason for this observation is somewhat unclear but it may be due to the inability of the antibody to differentiate between the inactive membrane-bound and the activated internalised phosphorylated μ-OR. As a result, the total pool of μ-OR in the dorsal horn may remain equivalent in the TASTPM and WT mice, but the proportion of the activated phosphorylated μ-OR may be greater in representation in the TASTPM dorsal horn; a hypothesis that is required to be tested in future studies.

3.3.6.5 **Unaltered Supraspinal Expression of Mu-OR in MIA-injected TASTPM**

As expression of μ-OR mRNA in the spinal cord dorsal horn of TASTPM mice was significantly reduced 28 days post MIA, we subsequently assessed if there are any alterations in the supraspinal structures involved in nociceptive processing, namely the thalamus and brainstem.

The saline injected WT and TASTPM mice displayed comparable mRNA expression of μ-OR in the ipsilateral and contralateral brainstem and thalamus (data not shown). Hence data from MIA injected WT and TASTPM mice were normalised to their respective saline group. No alteration in μ-OR mRNA relative expression (ipsilateral and contralateral) was detected in both the brainstem (Figure 3.22A) and thalamus (Figure 3.22B) of the TASTPM compared to WT injected with MIA. Therefore, suggesting that changes in the supraspinal opioidergic system may not be directly contributing to the partial recovery of MIA-induced mechanical hypersensitivity in the transgenic TASTPM mouse model of AD.

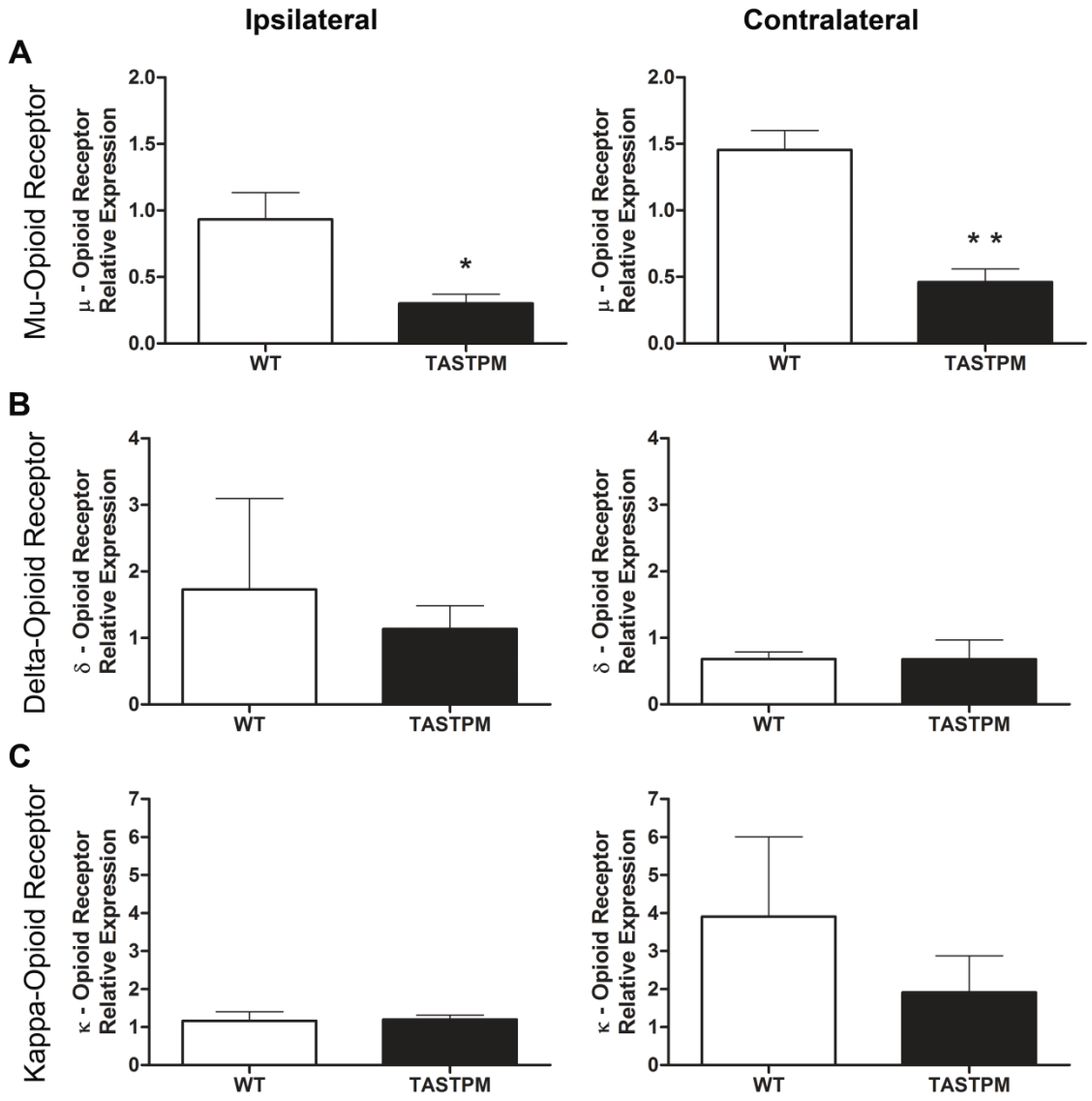

Figure 3.20: Reduced Mu-Opioid Receptor mRNA Expression in the TASTPM Dorsal Horn

RT-PCR analyses of opioid receptors (mu, delta, and kappa) mRNA expression in the dorsal horn of wild-type (WT) and TASTPM mice spinal cord 28 days post an intra-articular injection of MIA. TASTPM mice displayed significantly lower expression of mu opioid receptors in both ipsilateral and contralateral dorsal horn in comparison to WT mice post MIA (A) (* $p < 0.05$, * * $p < 0.01$, Student's *t*-test). No alterations in delta (B) or kappa (C) opioid receptors were evident ($p > 0.05$, Student's *t*-test). Data values are expressed as normalised values to genotype respective saline controls (n = 4 per experimental group).

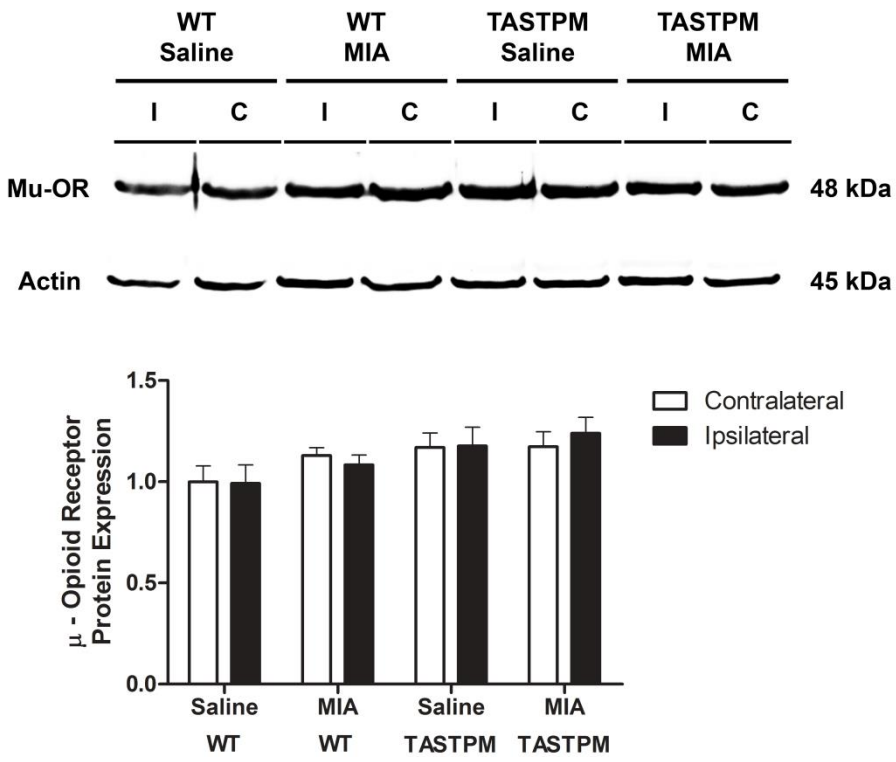

Figure 3.21 Unaltered Mu-Opioid Receptor Protein Expression in the TASTPM Dorsal Horn

Representative blot showing mu-opioid receptor (Mu-OR) expression in the dorsal horn of WT and TASTPM mice 28 days post an intra-articular injection of MIA (1 mg) or saline. Quantitative analysis of mu-opioid receptor western blot revealed unaltered expression of mu-opioid receptor in the lumbar (L3-L5) dorsal horn of TASTPM and WT mice injected with MIA compared to their respective saline controls and when comparing within each experimental group between ipsilateral and contralateral dorsal horns ($p > 0.05$, two way ANOVA) relative to β-actin (loading control). Data values are expressed as mean ± SEM ($n = 4$ per experimental group).

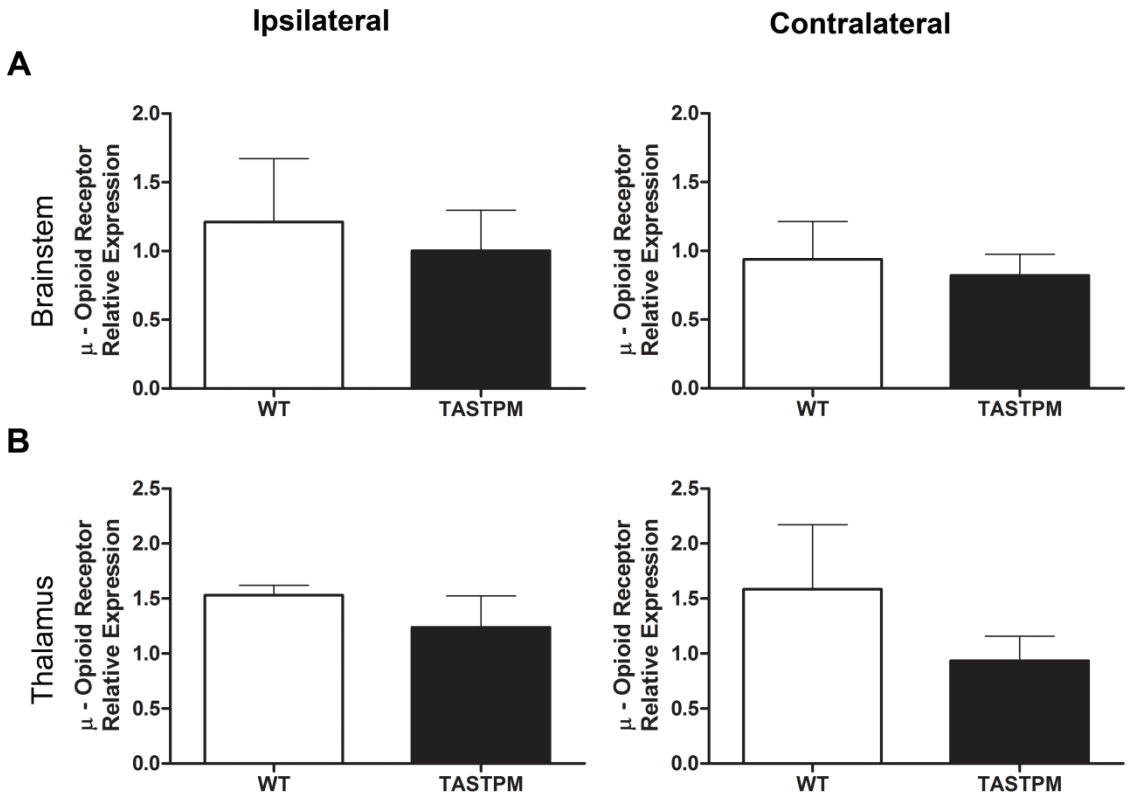

Figure 3.22: Unaltered Supraspinal mRNA Expression of Mu-Opioid Receptor in TASTPM Mice

RT-PCR analysis of mu opioid receptor expression in the brainstem (A) and thalamus (B) of wild-type (WT) and TASTPM mice spinal cord 28 days post an intra-articular injection of MIA. No significant alteration in the neither ipsilateral nor contralateral supraspinal structures was evident ($p > 0.05$, Student's *t*-test). Data values are expressed as normalised values to genotype respective saline controls (n = 4 per experimental group).

3.4 Discussion

The aim of the present chapter was to test the hypothesis that AD-related pathology and neuroinflammation in key regions of the pain pathway, namely the spinal cord and thalamus, may alter the sensitivity to chronic pain in AD. For this purpose, we examined the development of OA pain, via an intra-articular injection of MIA, and the characteristic plastic changes in the pain pathway in the transgenic TASTPM model of AD compared to age-and gender-matched WT controls.

The principle finding of the present study is the absence of weight bearing asymmetry and partial recovery of mechanical hypersensitivity exhibited by MIA-injected TASTPM mice. Biochemical and pharmacological assessment indicated that the endogenous opioid may underlie the partial recovery of mechanical hypersensitivity in TASTPM following MIA administration, as illustrated by an increase in plasma β-endorphin concentration and the ability of systemic administration of opioid receptor antagonist naloxone to unmask MIA-induced mechanical hypersensitivity. Therefore, indicating the reduced susceptibility of chronic pain maintenance in the TASTPM model of AD, which may be dependent on the elevated endogenous opioidergic tone.

Furthermore, immunohistochemical analysis revealed lack of spinal microglial response exhibited by MIA injected TASTPM mice in comparison to WT. Increase in spinal microglia is known to play an important role in central sensitisation, as attenuation of microglial activation, via administration of glial inhibitors, have been shown to correlate with reduced pain-like behaviours in the neuropathic (partial nerve ligation) and inflammatory (zymosan) models of chronic pain (Clark et al 2007, Staniland et al 2010). Therefore, lack of microglial response in TASTPM following administration of MIA demonstrates attenuation in the central spinal mechanisms involved in the maintenance of chronic pain in the model of AD. These observations were made despite no gross differences when comparing knee joint pathology, which highlight a level of discrepancy between joint pathology and presentation of pain as clinical symptoms in OA (Hannan et al 2000).

Multiple components of human OA disease progression, symptoms, and associated pathology with the use of intra-articular injection of MIA as an animal model of OA have been reported (Gregory et al 2013). Our data has confirmed findings of previous research in which intra-articular administration of MIA induces an immediate development of mechanical allodynia and leads to a decrease in the percentage of weight borne on the ipsilateral hind limb on day 3 which persisted for up to 28 days in the non-transgenic WT mice (Combe et al 2004, Ogbonna et al 2013). These behavioural outcome measures are representation of referred allodynia and ongoing pain, respectively. Mechanical allodynia was assessed by the application of von Frey monofilaments to the plantar surface of the hind paw, and not the knee, thereby it is a measure of referred pain. Patients with OA display hyperalgesic responses upon application of noxious stimuli in the area around the OA knee and commonly report referred pain in adjacent joints or nearby limbs to that of the affected joint, which confers translational value of hind paw allodynia (Bajaj et al 2001, Farrell et al 2000). In addition, evidence from preclinical studies propose that the underlying mechanism involved in generating referred pain is characterised by an increase in afferent activity, lowered nociceptive threshold of spinal nerves to innocuous stimulation and an expansion of receptive field of spinal neurons to include adjacent anatomical regions to that which is affected (Schaible et al 2002). Moreover, it has been shown that the cell bodies for the nerves from the knee co-localise in the DRG containing cell bodies from nerves that supply the hind paw. Therefore implicating that referred pain can be as a result of the cross-communication between sensory neurons at DRG level (Fernihough et al 2004).

In contrast, TASTPM mice did not display any sign of weight bearing asymmetry at any time point and also exhibited a partial recovery of ipsilateral mechanical hypersensitivity initiating from day 14 post MIA administration. Despite these behavioural observations, comparable histopathological changes in the knee joint in the form of degradation of articular cartilage accompanied by inflammation in the synovial membrane were exhibited by the TASTPM and WT mice 28 days post MIA administration. An observation which shares similarity with evidence provided by Nwosu and colleagues (2016) who demonstrated that a lower dose of MIA (0.1mg) in rats displayed comparable mechanical hypersensitivity as at a higher dose (1mg) but failed to exhibit changes in weight bearing, that were evident at a higher dose. Furthermore, knee joint

pathology in terms of knee joint diameter and inflammation was shown to be similar between the two different doses of MIA. Likewise, evidence arising from mouse MIA-induced OA also displayed MIA-concentration dependant behavioural changes. Specifically, no weight asymmetry and delay in the onset of mechanical hypersensitivity was observed at lower doses (0.5mg and 0.75mg) in comparison to 1mg intra-articular MIA administration (Ogbonna et al 2013). In addition, intra-articular administration of MIA (0.1mg) in κ-OR knockout mice resulted in increased mechanical hypersensitivity despite no change in peripheral knee joint pathology relative to WT controls. These behavioural changes were demonstrated to coincide with greater microglial activation in the lumbar spinal cord compared to control littermates (Negrete et al 2017). Therefore, mechanical hypersensitivity and absence of ongoing pain exhibited by the transgenic model of AD may suggest that MIA induced milder OA. This could be a result of diminished spinal microglial response to peripheral inflammation in TASTPM mice compared to WT controls, which may possibly suggest blunted central sensitisation in this model of AD.

The underlying reason for the discrepancies between the two behavioural measures could possibly be due to different mechanisms involved in the functional presentation of pain-like behaviour. It was suggested that weight bearing asymmetry is likely to be driven by peripheral and central sensitisation, as a quantitative sensory testing study demonstrated lower pain pressure thresholds exhibited by individuals with OA in comparison to healthy controls in the affected joint as well as remote sites not affected by OA, indicative of spreading of OA-associated sensitisation (Suokas et al 2012). Therefore, it was postulated that whilst low pain pressure thresholds in the affected joint may reflect nociception (owing to local inflammation and/or tissue damage), the reduced pain pressure thresholds at remote sites from the affected joint supports the hypothesis of that central sensitisation and/or reduced descending inhibitory control may underlie the chronic musculoskeletal pain. Whereas, the reduced PWTs are spinal reflexes that are associated to central sensitisation in this model of OA and may reflect the convergence of nociceptive inputs from both the knee and the hind paw onto neurons in the spinal cord (Fernihough et al 2004, Schaible et al 2002).

The perception of pain in OA is established due to activation and/or sensitisation of primary afferent nerve terminals within the knee joint which propagates nociceptive information to the

spinal cord where input for the periphery is integrated and processed prior to projection to specific brain regions via various ascending pain pathways (Schaible 2012). Examination along the pain pathway, namely the spinal cord, using immunohistochemistry revealed significantly increased ipsilateral microglia whilst unaltered astrocytes in the dorsal horn of WT mice 28 days post MIA compared to WT control and to its respective contralateral dorsal horn. In contrast, no change in neither microglial nor astrocyte frequency was observed in the ipsilateral dorsal horn of MIA injected TASTPM mice compared to their respective controls. Increase in microglia has consistently been reported in rodent model of MIA, however, astroglial responses have been somewhat variable with some studies showing an increase (Sagar et al 2011, Yu et al 2013) and others reporting no change (Lee et al 2011a, Ogbonna et al 2013, Thakur et al 2012) post MIA administration. Spinal glial activation post MIA was shown to correlate with OA-associated pain behaviour, as illustrated by administration of COX-inhibitor (nimesulide) and glial inhibitor (minocycline), which resulted in reduction of spinal microglial and astroglial response in the ipsilateral dorsal horn and attenuation of MIA-induced referred allodynia (Sagar et al 2011). Furthermore, it has been suggested that the underlying reason for this increase in microglia, in MIA model of rodents, may not be directly linked to peripheral inflammation; but may contribute to spinal mechanisms of central sensitisation as peripheral inflammation has been shown to be resolved by day 7 (Bove et al 2003, Lee et al 2011a, Ogbonna et al 2013, Thakur et al 2012). Therefore, lack of microglial response in the TASTPM dorsal horn 28 days post MIA may suggest alteration in the spinal mechanisms that contribute to OA associated central sensitisation, which in turn is reflected in their behavioural outcome as absence of MIA- induced ongoing pain and reduced severity of mechanical hypersensitivity.

Owing to the lack of microglial response observed four weeks post MIA in the TASTPM ipsilateral dorsal horn, we were keen to evaluate whether there is any alteration in its activated state of microglia, using P-p38 as a marker (Clark et al 2012, Lee et al 2011a). Our data revealed similar trends of changes only evident in the ipsilateral dorsal horn of MIA injected WT mice but not the transgenic TASTPM animals following MIA administration. Microglia activation in the spinal cord is known to play a critical component of chronic pain development. In rat model of MIA-induced OA and rheumatoid arthritis induced by collagen spinal microgliosis

(IBA1 immunopositive cells that also express P-p38) was evident in the spinal dorsal horn, which correlate with decrease in grip force strength and increase in mechanical hypersensitivity, respectively (Clark et al 2012, Lee et al 2011a, Nieto et al 2016). Moreover it was noteworthy that Lee and colleagues (2011a) demonstrated increased P-p38 expressing microglial cells in the ipsilateral dorsal horn during the first week post administration of MIA, which subsides but remains significantly elevated till the week 3 in comparison to naive control group (end-point of study). This may reinforce the notion that MIA-induced inflammation and cartilage degradation in the knee joint may induce sensitisation of primary afferent nerve free endings via release of cytokines and chemokines from peripheral tissue and immune cells accompanied by release of neuronal pro-inflammatory mediators. Such sensitisation of sensory neurons in the periphery leads to release of pro-nociceptive neurotransmitter from its central terminals in the superficial dorsal horn of the spinal cord, which in turn induce activation of microglia that results in release pro-inflammatory mediators to further promote neuronal hyper-excitability in the spinal cord resulting in persistent pain (Schaible 2012). Altogether, MIA injection into the knee joint induces peripheral sensitisation (activation sensory afferents) leading to development of central sensitisation which collectively contribute to the associated persistent pain (Nieto et al 2016).

Thus, failure to detect spinal microgliosis in TASTPM mice at the same time point reinforces the notion that the TASTPM mice may exhibit an alteration in the central spinal mechanisms involved in the maintenance of chronic pain in the transgenic mouse model of AD that may underlie the altered behavioural presentation. The possible explanation for these observations in the TASTPM mice remains elusive and therefore further studies are warranted in order to establish the underlying mechanisms. For this purpose, it would be of great relevance to characterise the temporal profile of MIA-induced behavioural and histopathological changes at the early developmental phase (up to day 7), during which behavioural changes, in terms of mechanical hypersensitivity, are comparable to WT controls, to establish if spinal microgliosis is also induced in the transgenic model of AD. In addition, having established in the previous chapter that the transgenic TASTPM mice exhibit reduced excitatory VGLUT2 (presumable interneurons) expression in the spinal cord, it would be of great interest to examine if these MIA-induced behavioural alteration and lack of spinal microgliosis is a result of reduced hyper-

excitability in the TASTPM dorsal horn post MIA administration due to the diminished excitatory neurotransmission. Finally, in order to improve our understanding on whether these behavioural changes in TASTPM mice are due AD-associated cognitive deficits and amyloid plaques in the brain, at the age of 6 months old, further studies are required to characterise the MIA-model in 3 months old TASTPM mice, which do not exhibit any cognitive deficits and no amyloid plaques are developed at this point.

Moving further along the pain pathway, in the process of investigating the underlying reason for altered MIA-induced behaviour in TASTPM model of AD, we went onto examine the thalamus, a relay station for nociceptive input propagation, for gliosis and AD associated amyloid pathology, which is evident in the transgenic mice (reported in previous chapter). The present study illustrates significantly increase in microgliosis and trends of increased astrocytosis in the thalamus of TASTPM mice four weeks post MIA administration compared to TASTPM controls; whilst no alteration were observed in WT. The increase in gliosis is a representation of neuroinflammation in AD. These observations are in agreement with preclinical studies that have also demonstrated increased gliosis in the brain of APP/PS1 mice in models of collagen induced rheumatoid arthritis and Col-IL1β^{xat} transgenic mouse model of OA (Kyrkanides et al 2011, Park et al 2011). The reason for exacerbation of thalamic neuroinflammation can possibly be explained by the MIA-induced inflammation in the periphery, the knee joint, which may induce an increase in circulating pro-inflammatory cytokines as observed in the serum patients suffering from arthritis (Hussein et al 2008). Synovial membrane inflammation is highly correlated and also plays an important role in pain in individuals with OA (Hill et al 2007, Scanzello & Goldring 2012). In addition, an intra-articular injection of MIA has been shown to results in elevation of TNF-α and IL-6 in the knee synovium and capsule. The level of TNF-α and IL-6 in the knee joint increased gradually, peaking at day four post MIA and remained elevated up to day 28 (Orita et al 2011). Systemic inflammation can reach the CNS and there are several routes by which pro-inflammatory cytokines in the periphery can influence neuroinflammation in the CNS which include: (1) direct diffusion of inflammatory cytokine through the incomplete BBB in the circumventricular organs; (2) signalling through the BBB to perivascular macrophages and cells of the brain parenchyma via activation of brain endothelial

cells; (3) vagal sensory afferent signal from the thoracic abdominal cavity to the brain; and (4) active transport of cytokines across the BBB via cytokine transporters (Perry 2004, Perry et al 2007). It has been shown that microglia from a diseased brain are more susceptible to systemic challenges in comparison to healthy brain as systemic inflammation in a diseased brain has been shown to exacerbate the progression of disease (Perry et al 2010). Thus, further strengthening the notion that neuroinflammation in a model of AD may be elevated following inflammation in the periphery due to administration of MIA.

However, an opposing effect of peripheral inflammation on amyloid deposition in the brain of AD mice has been shown with Park et al (2011) demonstrating a reduction in amyloid burden whilst Kyrkanides et al (2011) reported exacerbated amyloid pathology in the mouse models of AD. The underlying reason may be owing to the dual role of glial cells in AD, which can either, be pro-inflammatory that contribute towards pathogenesis of AD yielding greater amyloid deposits; or have a protective component whereby the amyloid deposits are actively phagocytised and degraded (Cai et al 2014, Wyss-Coray 2006). In fact, the study conducted by Kyrkanides et al (2011) suggests that the mechanism that may underlie the peripherally induced neuroinflammation to AD pathology could be the neuroinflammatory signals hindering the capacity of glial cells to clear Aβ plaques; or it might be due to a shift of equilibrium whereby the rate of Aβ production overwhelms its degrading. On the contrary evidence from Park et al (2011) argues that activated microglia contributes directly in clearance of Aβ. In contrast to these observations, our results displayed no detectable alteration in the cortical, hippocampal, and thalamic amyloid pathology burden in the TASTPM mice that received an intra-articular injection of MIA. Altogether these observations may suggest that the increase in thalamic gliosis is in response of MIA injection in the periphery may be independent of AD-associated amyloid plaques in TASTPM. Another possibility for this observation may be the extent of inflammation in the periphery induced by MIA and subsequently the level of influence on the CNS. Evidence provided by Kyrkanides et al (2011) and Park et al (2011) demonstrated increase in gliosis which is more than doubled in the brains of APP/PS1 mice in both models of arthritis in comparison to APP/PS1 controls; whilst in the MIA-induced model of OA pain in the TASTPM resulted in approximately 49% increase and around 45% elevation in thalamic microglial and

astroglial burden, respectively, in comparison to TASTPM control group. Thus, indicating a possible milder inflammation induced in MIA in comparison to collagen induced rheumatoid arthritis and Col-IL1β^{xat} transgenic mouse model of OA, as a result reduced level of increase in neuroinflammation in the CNS of the transgenic mouse model of AD, which in turn fails to have any significant impact on AD-associated plaque pathology. Nevertheless, these findings do not undermine the notion that amyloid deposits are still present in thalamus of TASTPM mice brains and therefore may influence and/or compromise neuronal activity in the thalamic nuclei responsible for nociceptive processing.

Furthermore, having established, in the previous chapter, increased opioidergic tone in AD, which resulted in reduced thermal sensitivity in the transgenic mouse model, we tested the hypothesis whether it is the endogenous opioids that result in the MIA-induced behavioural alterations displayed by the TASTPM mice. Endogenous opioids may block pain via multiple mechanisms including actions on the mu opioid receptors located in the periphery, spinal cord, and the brain (cortical and sub-cortical regions) (Stein et al 2003). Here we report increase in plasma concentration of opioid peptide β-endorphin was evident in MIA-injected TASTPM mice in comparison to WT mice 28 days post MIA. Synthesis of β-endorphin is carried out primarily in the anterior pituitary gland from its precursor protein proopiomelanocortin (POMC), with further evidence also indicating the potential of immune cells in its production under inflammatory conditions. This synthesis in the anterior pituitary gland can be regulated by the hypothalamic–pituitary–adrenal axis through the corticotropin-releasing hormone (CRH) release from the hypothalamus, which serves as a signal (normally in response to stress and/or pain) for cleavage of POMC to generate β-endorphin opioid peptides (Sprouse-Blum et al 2010, Stein et al 2003). In individuals with AD, increase in CRH mRNA per neurons in the parventricular hypothalamic nucleus has been reported, which in turn induces hyperactivity of the hypothalamic–pituitary–adrenal axis that may underlie the elevation of opioidergic peptides as observed in the transgenic TASTPM mice (Raadsheer et al 1995, Scherder et al 2003).

Moreover, a positive relationship between the level of plasma β-endorphin and mechanical withdrawal thresholds on four weeks post MIA suggests that elevated opioidergic tone in TASTPM mice may be responsible for the lack of ongoing pain and partial reversal of

mechanical hypersensitivity (anti-nociceptive) displayed post MIA. Indeed previous research has demonstrated that elevation of β-endorphin, via cold water swim stress and/or injection of the opioid peptide into the inflamed paw, was able to increase paw pressure thresholds (anti-nociceptive) in the inflamed paw but not the unaffected paw in a naloxone-reversible manner in rats with adjuvant induced mono-arthritis (Stein et al 1990). In addition, increased MIA-induced mechanical allodynia was demonstrated upon blockade of κ-OR/dynorphin in κ-OR knockout mice compared to WT littermates. This pain-like behaviour coincided with attenuated anxiety-like responses and cognitive impairment accompanied by enhanced depression-like behaviour, which coincided with reduced basal levels of CRH in the amygdala and hippocampus of κ-OR knockout mice relative WT littermates (Negrete et al 2017). Thus, indicating lack of opioid peptides and function results in increased presentation of nociceptive sensitivity in MIA-model of OA.

In order to test this possibility in our model we examined the effect of the opioid antagonist naloxone on mechanical hypersensitivity on day 24 post MIA administration. Here we show that the partial recovery of mechanical hypersensitivity in TASTPM may depend on the elevated endogenous opioids, as illustrated by the ability of systemic administration of naloxone hydrochloride, but not naloxone methiodide, to unmask mechanical hypersensitivity. As aforementioned, naloxone methiodide is incapable of penetrating the BBB which restricts its mechanism of action to the periphery; whilst naloxone hydrochloride has been reported to readily cross the BBB which allows it to act on both the periphery and the CNS (Inglis et al 2008). These findings would implicate that the increased opioidergic tone within the CNS may be the chief contributor to the altered pain-like behaviour displayed by TASTPM post MIA administration.

Recent evidence has demonstrated that treadmill exercise over a period of four weeks resulted in restoration of weight bearing and alleviation of hind paw tactile hypersensitivity in a rat MIA model of advanced OA pain (Allen et al 2017). The underlying reason for the exercise-induced pain relief was indicated to be dependent upon on the endogenous opioid system as naloxone administration was shown to unmask the weight asymmetry and produced conditioned place aversion in exercised rats that had OA. Further evidence provided in a model of neuropathic

pain (L5-L6 spinal nerve ligation model) showed exercise over a period of two weeks prior to surgery resulted in significant reversal of mechanical and thermal hypersensitivity (Stagg et al 2011). Moreover, it was suggested that this exercise induced recovery is associated with increase in the opioidergic tone within the CNS, as illustrated by systemic administration of naloxone hydrochloride and intracerebroventricular administration of naloxone methiodide which resulted in increase in mechanical hypersensitivity. In addition, increased immunoreactivity of opioid peptides (enkephalins and β-endorphins) were detected in the PAG and RVM of exercised rats compared to sedentary, which collectively postulate elevated opioid peptide expression in the brainstem may induce reversal of neuropathic pain via increase in descending inhibitory control (Stagg et al 2011). Therefore, in our model of AD it could be postulated that the increased opioidergic function in the CNS that may contribute to the altered pain behaviour displayed by TASTPM that had OA pain, which requires extensive future studies in order to be determined. For this purpose, one possible future direction may be pharmacological experiments evaluating the effect of naloxone methiodide injected either intrathecally or into the intracerebroventricular, during the reversal of MIA-induced mechanical hypersensitivity phase in the TASTPM mice, are required in order to establish the contribution of spinal and supraspinal regions that may underlie the altered behavioural phenotype.

As in the CNS endogenous opioids can block transmission of nociceptive input via: (1) inhibiting release excitatory neurotransmitter in the dorsal horn; and (2) enhancing descending inhibition via the brainstem (PAG and RVM), we assessed the relative expression of μ-OR in the spinal cord and supraspinal structures including: brainstem and the thalamus 28 days post MIA injection (Vonsy et al 2009). The opioid receptors are G- inhibitory protein coupled receptors (Go/Gi), which upon activation inhibits voltage-gated calcium channels or activate the inwardly rectifying potassium channels which results in decrease in neuronal excitability. It can also inhibit cyclic adenosine monophosphate (cAMP) and activate mitogen-activated protein kinase (MAPK) cascades which affect cellular cytoplasmic as well as transcriptional activities. The mechanism of action can also be G-protein independent whereby the agonist-receptor complex induces receptor phosphorylation which allows recruitment and binding of β-arrestin resulting a cascade of phosphorylation, which modify gene transcription (Dickenson & Kieffer 2013).

Recent evidence suggests that agonist binding to μ-OR results in receptor phosphorylation at either serine or threonine residue (mainly at S375 by exogenous and at S363 by endogenous agonist) that may allow β-arrestin which promotes desensitisation of G-protein signalling and induce receptor internalisation. The internalised μ-OR reduces the pool of available membrane-bound binding sites for opioid agonist and it is only following dephosphorylation that it is recycled and restored on the plasma membrane (Mann et al 2015). Autoradiographic analysis of opioid receptors in human post-mortem tissue revealed a reduction of μ-OR ligand binding in the hippocampus (42% - 48%) and subiculum (46%); whilst δ-OR binding was observed to be lower in the amygdala (51%) and ventral putamen (30%) of AD subjects compared to healthy controls (Jansen et al 1990, Mathieu-Kia et al 2001). In contrast κ-OR binding was shown to be elevated in the putamen (dorsal: 57%; ventral: 93%) and the cerebellar cortex (155%); with reduction only observed in the hippocampus (39%) (Mathieu-Kia et al 2001). These findings highlight the involvement of the endogenous opioidergic system in the pathogenesis and/or clinical presentation of AD as regions involved in learning, memory, emotion and motor function are affected.

Our data demonstrated significantly reduced expression of μ-OR mRNA in the spinal cord; whereas no alteration in its protein expression was evident in MIA-injected TASTPM mice in comparison to WT mice 28 days post MIA. The underlying reason for our observation of reduced μ-OR mRNA whilst unchanged protein expression remains to be determined; but it may possibly be due to the inability of the antibody to differentiate between the inactive membrane-bound and the activated internalised phosphorylated μ-OR. As a result, the total pool of μ-OR in the dorsal horn may remain comparable in the TASTPM and WT mice, but the proportion of the activated phosphorylated μ-OR may be altered in representation of the TASTPM dorsal horn; a hypothesis that is required to be tested in future studies in terms of the functional ligand binding and/or activity of the receptor. Thus, suggesting that the spinal cord may be the site of action of endogenous opioid peptides in the transgenic TASTPM model of AD that may underlie the alteration in maintenance of mechanical allodynia in OA. Furthermore RT-PCR analysis of the brainstem and thalamus revealed no significant alteration in the expression of μ-OR of MIA-injected TASTPM and WT mice. However, whether the protein expression remains unaltered is

to be examined in future studies. Another possible future direction may be analysing the expression of opioid peptide (enkephalin and β-endorphin) along with the μ-OR in the PAG and RVM in particular (immunohistochemically or in-situ hybridisation) in order to elucidate the role they may play in descending modulation.

In addition to the characterising the MIA-induced behavioural and histological changes in the periphery and the CNS in AD mice, the present study also evaluated the efficacy of pharmacological intervention during different phases of OA. The use of NSAIDs, paracetamol and opiates are amongst the drugs that are often prescribed for symptomatic pain relief in patients with OA. Furthermore, rodent MIA model of OA have been demonstrated to display pain-related behaviour in a biphasic temporal profile, whereby the early phase is described as the NSAID-sensitive inflammatory lasting up to approximately 7 days; whilst the following late phase is characterised by persistent pain behaviour which is NSAID-resistant but responsive to gabapentin and morphine (Bove et al 2003, Fernihough et al 2004, Ogbonna et al 2013). Therefore, in the present study we attempted to administrate NSAID drugs (diclofenac and celecoxib) during the early inflammatory phase (up to day 7 post MIA) and non-NSAIDs during the later phase (paracetamol, morphine, and gabapentin).

The use of NSAIDs (i.e. diclofenac, celecoxib, and naproxen) is a common therapeutic intervention for management of mild-moderate OA pain. NSAIDs possess anti-inflammatory, anti-pyretic and analgesic properties via inhibition of COX enzymes and subsequent synthesis pro-nociceptive prostaglandins (PG). Of the two COX enzymes (COX-1 and COX-2), COX-1, is considered to be the 'house-keeping' isoforms, that is constitutively expressed in most tissue types; whereas COX-2 is induced in response inflammatory conditions where it acts as a major source for PG synthesis (Vane & Botting 1996). As aforementioned, administration of MIA into the knee joint results in local inflammation which leads to release of substance P, bradykinin and PG in the close vicinity that sensitise peripheral free nerve endings which in turn lead to decrease in the nociceptive thresholds and increase in spinal nociceptive input (Bove et al 2003, Combe et al 2004). Biochemical analysis of inflammatory mediators such as PGs in the knee joint synovial fluid revealed a four-fold increase in PGE_2 on day three post MIA compared to control naive, whilst PGE_2 levels on day 24 following MIA injection were restored and similar

in comparison to the control rats (Rashid et al 2013). Altogether evidence from these studies reinforce the notion that the MIA-induced inflammatory response in the knee joint is an early phenomenon in this model of OA which may induce pain via sensitisation of primary afferent free endings in the periphery via inflammatory mediators (i.e. PGs).

The ability of the NSAID celecoxib (COX-2 selective inhibitor) to reverse MIA-induced mechanical hypersensitivity in WT mice within seven days post OA induction is consistent with the early inflammatory component of MIA-associated pain. It is consistent with previous findings that have illustrated reversal of mechanical hypersensitivity and partial recovery from weight bearing deficits within first week post MIA administration in rats (Fernihough et al 2004, Rashid et al 2013). The data presented in this chapter provides evidence for similar anti-nociceptive effect of celecoxib induced in MIA-injected TASTPM mice at the same time point. Thus, implicating that the early peripheral mechanisms, in particular the inflammatory aspect of MIA administration in the knee joint driving increased spinal nociceptive input resulting in pain, may be shared in the WT and this model of AD. Therefore, similar pain management strategies of early OA pain can be employed in patients with AD as it is applied to the cognitively-intact individuals.

However, administration of diclofenac, a COX-1 and COX-2 inhibitor, showed only a trend, which was not significant, of mechanical hypersensitivity reversal in WT mice within the first 10 days of OA-induction. A finding which has also been reproduced as tactile allodynia was shown to be was unaltered following administration of diclofenac in MIA-injected rats around this time point post OA induction. Whereas, diclofenac has been shown to have the potential to reverse MIA induced mechanical hyperalgesia (paw pressure) and decrease nociception induced by movement of the affected joint in a rat model of OA (Beyreuther et al 2007, Fernihough et al 2004, Ferreira-Gomes et al 2012a). As a result indicating that there may be a limitation in either: (1) the behavioural test we employed in the current study which may have not permitted the detection of the analgesic properties of diclofenac in our model of OA; and/or (2) the choice of day post MIA administration (day 7 and 9) which may have surpassed the inflammatory phase which has been outlined to last for up to day 7 (Bove et al 2003). Similar to celecoxib observation, comparable effects of diclofenac were detected in the MIA injected TASTPM mice

at the same time point. Altogether our data on the effect of NSAIDs on MIA-induced mechanical hypersensitivity demonstrate comparable level of pain relief in the transgenic TASTPM model of AD in comparison to WT controls, which indicates that the inflammatory drive induced by MIA in the periphery, the knee joint, may be unaltered.

Paracetamol is often prescribed to patients for long term treatment (mild to moderate pain) where the adverse effects of NSAIDs raise concerns (Towheed et al 2006). Likewise to NSAIDs, paracetamol has anti-pyretic and analgesic properties but exhibits no anti-inflammatory characteristic; therefore it is no classed as an NSAID. The underlying mechanism of action in unclear, however it has been postulated that paracetamol acts via inhibition of PG synthesis via inhibition of COX-2 (Jozwiak-Bebenista & Nowak 2014). Paracetamol administration in MIA rat model of OA has demonstrated reversal of mechanical hyperalgesia during the early phase (day 3); whilst no effect on mechanical hyperalgesia and tactile allodynia was detected upon administration 14 days post MIA injection (Fernihough et al 2004).

Data presented in this study, in line with previous evidence, depict that administration of paracetamol, on day 28 post MIA, failed to reverse mechanical allodynia in WT mice (Fernihough et al 2004). Thus, indicating diminished analgesic potency of paracetamol in late and established phase of MIA induced OA. In the present study, we provide additional evidence in a model of AD, which also exhibited similar response to paracetamol as the non-transgenic WT mice. Therefore, suggesting that paracetamol on its own may not be an effective pain management option in both individuals with AD and cognitively intact patients at advanced stages of OA. This raises further concerns as relatively greater prescription and/or use of paracetamol have recently been reported in individuals with cognitive impairment for analgesia in comparison to cognitively intact individuals, which may reflect clinical difficulties in assessment of pain in such population (Achterberg et al 2013, Haasum et al 2011).

Opioids (i.e. morphine) have the ability to be used as an alternative for pain-relief in OA patients who cannot use NSAIDs or paracetamol (Nuesch et al 2009). Morphine is an analgesic which induces its anti-nociceptive effect via activation of the inhibitory μ-OR located in the spinal cord and supraspinal sites, which in response leads to reduced neurotransmitter release form primary afferent nociceptive terminals and blockade of presumably descending nociceptive

facilitatory output from the brainstem, which in turn results in attenuation of spinal and brain processing of nociceptive input (Yaksh 1997). In the periphery, opioid receptors have been reported to be present on and may be able to modulate the excitability of small afferent terminals which results in reduction of nociceptive input to the CNS an therefore the anti-nociceptive effect (Przewlocki & Przewlocka 2001). In fact, CFA injection into the hindpaw of conditional μ-OR expressed Nav1.8 sensory neurons revealed that despite similar development of inflammatory pain, the opioid agonist (i.e. morphine, fentanyl, and loperamide) induced analgesia was diminished in comparison to control littermates, particularly at lower doses. Moreover, μ-OR expression, which was demonstrated to elevated after CFA administration in the DRG of controls littermates did not display any shift in the conditional knockout mice. This implicates a key contribution of peripheral μ-OR in systemic opiate-induced analgesia in a model of inflammatory pain (Weibel et al 2013).

Our results demonstrate that the effects of morphine on mechanical withdrawal thresholds in the non-transgenic WT mice are in agreement with previous reports where similar doses resulted in reversal of MIA-induced mechanical hyperalgesia and tactile allodynia (Combe et al 2004, Fernihough et al 2004). Moreover, morphine has also been shown to reverse weight bearing asymmetry, reduction of cooling hypersensitivity, and decrease the nociception induced by movement of the affected joint in rodent MIA model of OA (Combe et al 2004, Ferreira-Gomes et al 2012a, Vonsy et al 2009). Interestingly, here we show the transgenic TASTPM mice not only exhibit an anti-nociceptive effect of morphine but display a significantly heightened response in comparison to WT. Recent evidence has demonstrated greater prescription of transdermal opioids (i.e. buprenorphine and fentanyl) and long-term usage in individuals with AD, despite significantly lower use of opioid amongst these individuals compared to cognitively-intact controls. The underlying reason may be difficulty in ingestion of oral medicine in moderate to severe AD individuals, higher risk of mortality and/or the transdermal opioid scheme provide with greater ease as they need to be replaced after 3-7 days (Achterberg et al 2013, Hamina et al 2017). However, It is difficult to interpret the underlying reason for this observation owing to the increased opioidergic tone detected in the transgenic model of AD, which would suggest a reduced sensitivity to exogenous opioid agonist, morphine (Smith & Yancey 2003). Therefore

future direction in evaluating whether basal phosphorylation of the opioid receptors by endogenous agonist share common features including receptor internalisation and desensitisation as reported with the use of an exogenous agonist such as morphine (Mann et al 2015). In addition, it would be of great relevance to examine the functional activity of the μ-opioid receptor via examining the expression levels of downstream mediators (i.e. cAMP, MAPK, and β-arrestin) as well as possibly the rate at which the receptor is dephosphorylated, recycled and restored onto the plasma membrane (i.e. activity of protein phosphatase) in the transgenic model of AD.

Finally, use of anti-epileptic drugs such as gabapentin has been reported for treatment of neuropathic pain with little but evidence for its effectiveness in treatment of OA has also been provided (Epstein & Childers 1998, Rosner et al 1996). The development of persistent pain via elevated level of spinal nociceptive input has been associated with increased mRNA expression of α2δ1 in the DRGs and dorsal spinal cord of animal models of neuropathic pain (spinal nerve ligation) and osteoarthritis (MIA) (Rahman et al 2009, Zhou & Luo 2014). Gabapentin is likely to modulate activity of voltage-gated calcium channels, probably through its ability to bind to α2δ1 subunit. As a result, decrease in neurotransmitter release and propagation of action potential in nociceptive neurons which in turn dampens nociceptive neuronal hyper-excitability. Furthermore, evidence of a glutamate-dependant activation of the descending noradrenergic inhibitory pathway in the locus coeruleus (LC) has been proposed to also play a role in the anti-nociceptive properties mediated by gabapentin in model of peripheral nerve injury via release of noradrenaline in the spinal cord that in turn activates α-adrenoceptors located on spinal primary afferent terminals and GABAergic neurons, resulting in reduced neurotransmitter release and increase in spinal GABA release, respectively; thus dampening spinal hyper-excitability (Hayashida et al 2008, Kukkar et al 2013, Ossipov et al 2010).

Gabapentin administration on day 24 post MIA resulted in reversal of mechanical allodynia in WT mice, which is consistent with previous finding in which gabapentin at similar time points has been demonstrated to reverse MIA-induced tactile allodynia and weight bearing deficits (Fernihough et al 2004, Ivanavicius et al 2007). The effectiveness of gabapentin in relieving MIA-induced mechanical hypersensitivity can partially be explained by the overlapping

components of common central mechanisms associated with neuropathic pain, illustrated by increase in microglial response in the dorsal horn. In addition, an increase in expression of ATF-3, a marker of nerve damage, has been reported in the DRG of MIA-injected rat model of OA in a dose-dependent manner, as early as 3 days post MIA (Ferreira-Gomes et al 2012b, Ivanavicius et al 2007, Thakur et al 2012). In the rat MIA-induced OA there is no damage nerve as such, but it has been suggested that there may be injury to nerves endings located at the joint that may trigger ATF-3 expression but at a smaller scale (Ferreira-Gomes et al 2012b). However, evidence stemming from mouse MIA-induced OA reveals that the relative expression of ATF-3 in the DRG was significantly lower than the ATF-3 expression levels in the DRG from nerve injury model (Ogbonna et al 2013). Therefore, implicating that MIA (1mg)-induced mechanical hypersensitivity in the mouse hindpaw is not associated with a significant degree of nerve damage at the joint; and indicating the possibility of MIA-induced inflammation that drives peripheral sensitisation and increases afferent input in the dorsal horn of the spinal cord. Furthermore, it was suggested that the subtle and less severe histopathological changes in comparison to that observed in the rat knee at this dose (1mg) may account for the differences in ATF-3 expression in the two species. A higher dose of MIA may induced nerve damage in mouse, as observed in rats (abovementioned); a possibility that cannot be evaluated in mice as doses higher than 1mg can reach the general circulation resulting in lethal effects (Ogbonna et al 2013). Altogether, suggesting that there may be no detectable nerve damage in the mouse MIA (1mg)-induced OA model.

In contrast to our observations in the MIA-injected WT mice, gabapentin failed to have any impact on MIA-induced mechanical hypersensitivity exhibited by the TASTPM mice at any time point. The lack of analgesic effect of gabapentin coupled with diminished spinal microgliosis in response to inflammation in the periphery may suggest an attenuated central sensitisation in the TASTPM mice. It could be speculated that the attenuation of MIA-induced spinal microgliosis in TASTPM may be owed to the elevated opioidergic tone, which in turn, inhibit the release of microglial activating mediators (i.e. ATP and CSF1) from primary afferent terminals in the dorsal horn, a hypothesis that could be explored in the future.

Another possibility could be degeneration of noradrenergic neurons in LC of AD patients that may underlie the lack of gabapentin effect in the transgenic mice. Despite degeneration of noradrenergic neurons in the LC, elevated level of noradrenaline and its metabolite 3-methoxy-4-hydroxyphenylgycol (MHPG) in the CSF and plasma have been observed in AD individuals that increase with the progression of AD. Increase in CSF noradrenaline concentration has been suggested to reflect either: (1) increased synaptic noradrenaline level, possibly due to impaired clearance; and/or (2) increased noradrenergic activity, which may be associated with cognitive impairment and agitation in AD (Elrod et al 1997, Raskind et al 1984). Elevation of CSF noradrenaline may serve as an endogenous pain inhibitory system as evidence from a post-traumatic pain study revealed significantly lower concentration noradrenaline and MHPG in the CSF of patients experiencing pain, which may implicate the inhibition of descending noradrenergic inhibitory pathway (Cui et al 2012). Taking this into account it can be postulated that elevated CSF and plasma noradrenaline may exert an anti-nociceptive effect and therefore may also contribute to altered behavioural presentation by TASTPM mice post MIA administration, a hypothesis which demands further evaluation. One possibility to test this hypothesis may be to assess the concentration of plasma noradrenaline and/or level of dorsal horn α2-adrenoceptors in the transgenic TASTPM mice compared to WT controls. In addition, an investigation into the expression of gabapentin binding site, the α2δ1 subunit of the voltage-gated calcium channels, in the periphery, dorsal root ganglion, as well as α2δ1 subunit in the spinal cord along with evaluation of neurodegeneration in the LC of the transgenic TASTPM mice. It would be of great interest to examine alteration in the calcium channel α2δ1 subunit in response to MIA, firstly in non-transgenic WT mice and subsequently assess whether these alterations are also evident in the TASTPM mice post MIA. Altogether, these experiments will help in elucidating whether: (1) increased noradrenergic supply and binding in the spinal dorsal horn; and/or (2) alteration in the expression of α2δ1 calcium channel subunit (periphery and/or CNS) contribute to the altered behaviour phenotype and/or may underlie the lack of response to gabapentin exhibited by the transgenic TASTPM model of AD.

In summary, work presented in this chapter implicates that the transgenic TASTPM mice exhibit altered maintenance of mechanical allodynia and fail to display sign of ongoing pain at any time

point following an injection of MIA into the knee joint, possibly due to an increase in the inhibitory endogenous opioid system. These changes are in parallel with diminished spinal microgliosis, in response to inflammation in the periphery, coupled to lack of analgesic effect of gabapentin, which indicates blunted central sensitisation in TASTPM. Collectively, dampening the hyper-excitability within the CNS that is required for maintenance of persistent pain. Consequently, changes in the central mechanisms of pain processing may underlie the alteration in the effectiveness of pharmacological interventions in AD. Therefore, further studies are essential in order to elucidate the underlying mechanisms of chronic pain in AD which would provide better understanding and guidance on management of pain in this susceptible population.

3.4.1 Chapter Key Findings

In this chapter we provide preclinical evidence for altered development and treatment of persistent pain, in a clinical relevant model of OA pain, in 6 months old TASTPM AD mice. In particular report:

- An intra-articular administration of MIA failed to induce ongoing pain; and resulted in partial recovery of mechanical hypersensitivity, which was associated with increased endogenous inhibitory opioids.
- OA-like condition associated with supraspinal neuroinflammation in the thalamus without any impact on thalamic amyloid depositions.
- Comparable behavioural responses to NSAID administration were observed during the early phase of OA pain compared to WT controls.
- Altered responsiveness to analgesics during the late phase of OA pain compared to WT:
    - No difference in the effect of paracetamol, as it failed to induce analgesia in both genotypes.
    - Hypersensitivity to morphine, which may reflect alterations in the opioidergic system in this model of AD.

- Diminished response to gabapentin, which coupled with lack of spinal microgliosis, in response to inflammation in the periphery, suggests blunted central sensitisation in this transgenic mouse.

❖ Implications for possible alterations in the maintenance (late phase) of OA pain in the TASTPM mice.

The data presented here suggests that impaired opioidergic system coupled with decreased excitation in the spinal cord may underlie the reduced maintenance of OA-associated allodynia in the TASTPM model of AD.

3.4.2 Future Direction Leading to Chapter 4

So far the data presented in this thesis have demonstrated increased excitation and/or reduced inhibition in the spinal cord contribute to the impaired nociceptive sensitivity, in both acute and chronic pain models, associated with AD-related pathology in the TASTPM mouse model. In a clinically relevant model of OA, we show increase in ongoing neuroinflammation despite no change in AD pathology, amyloid plaques, in the brain of the preclinical AD mice. In order to evaluate the translational significance of these observations, in the next chapter (Chapter 4), we aim to assess AD-related pathological lesions and neuroinflammation in the post-mortem tissue (spinal cord and brain) obtained from individuals with AD. In particular, we would investigate whether presence of a chronic pain condition in this population has any impact on the AD-associated changes in comparison to AD individuals with no clinical record of pain. These experiments would in principle enable us to determine whether there are any common features that are shared amongst the preclinical mouse model and the human AD disease in chronic pain conditions.

Chapter 4 Neuropathology and Neuroinflammation in Alzheimer's disease Post-Mortem Tissue: A Case-Control Study

4.1 Introduction

Alzheimer's disease (AD) is the most prevalent neurodegenerative disease and is the leading cause of dementia in the elderly population. The current global prevalence of dementia has been estimated to be over 45 million people worldwide of which around 850,000 people are affected in the United Kingdom (UK) (Prince et al 2016, Prince et al 2014). Clinically AD is characterised by an insidious onset and a gradual and progressive deterioration of cognitive abilities ranging from loss of memory to impairment of judgement and reasoning (Tanzi & Bertram 2001). The neuropathological signatures of AD are the aggregation and extracellular deposition of β-amyloid (Aβ) plaques and accumulation of intracellular hyperphosphorylated tau in the form of neurofibrillary tangles (NFT). These hallmarks are accompanied by neuronal loss, synaptic dysfunction, brain atrophy, and inflammation (Serrano-Pozo et al 2011). The Aβ plaques are mainly present in the cortex that increases in density; whereas, NFT are initially observed in the locus coeruleus and transentorhinal region which spreads to the limbic and the associated cortical regions with the progression of AD (Figure 4.1). In addition, NFT have been shown to demonstrate a stereotypical spatiotemporal progression which correlates with the severity of cognitive decline. Therefore, the topographic staging of NFT is used for the pathological diagnosis of AD (Braak & Braak 1991b).

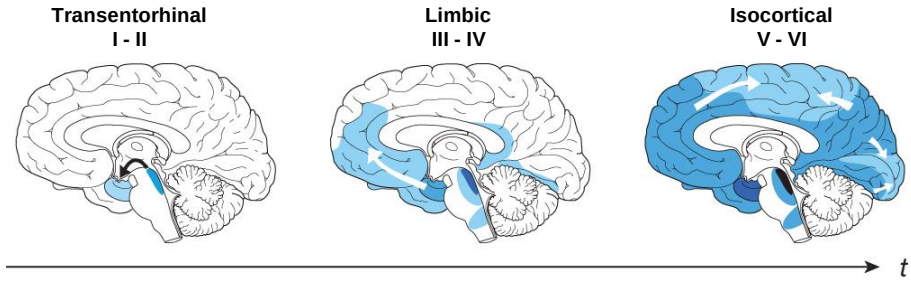

Figure 4.1: Neurofibrillary Changes in Alzheimer's disease - Braak's Staging

A representation of the distribution pattern of neurofibrillary changes (NF) (i.e. neurofibrillary tangles and neuropil threads) in the brain of a typical AD subject. Six stages (I-VI) can be distinguished. Stages I-II display NF alterations initially occur in the locus coeruleus and a single layer of the transentorhinal cortex (Transentorhinal I-II). The principle characteristics of stages II-IV is the severe involvement of the entorhinal and transentorhinal layer and spread to the amygdala (Limbic II-IV). Stages V and VI are marked by isocortical involvement, with NF changes appearing in the associated cortical regions (Isocortical V-VI). The increasing density of shading represents the increasing severity of NF changes (Braak & Braak 1991b). Image adapted from (Jucker & Walker 2013).

Pain is an important clinical issue in individuals with AD that is reported less often compared to age-matched cognitively-intact people. As a consequence, treatment of pain in patients with AD is frequently inappropriate. This has led to question whether patients with AD generally experience less pain compared to the cognitively-intact healthy controls; or is it possibly due the deteriorating ability of these individual to communicate pain sensations which in turn hinder their capacity to report pain (Scherder & Bouma 2000). The former possibility may be due to an alteration in the perception of pain in this susceptible patient group. In fact, it has been speculated that AD is associated with dysfunctional pain perception due to the presence of neuropathological hallmarks of AD affecting brain and spinal cord areas responsible for the experience and registration of pain (Scherder et al 2003). As a result, there may be a delay in diagnosis and potentially disease-modifying treatment of chronic pain conditions such as osteoarthritis (OA) for which pain is an early ongoing symptom.

So far we have demonstrated in previous chapters, impairment in nociceptive sensitivity, in both acute and chronic pain models, were associated with increased inhibition and reduced excitation in the spinal cord that correlated with AD pathology in the transgenic TASTPM model of AD. In addition, we have intriguingly discovered an increase in ongoing neuroinflammation in the thalamus of TASTPM mice in the clinically relevant model of OA pain, despite no change in deposition of amyloid plaques. Thus, these data suggest alterations in the key regions involved in nociceptive processing in this model of AD. Therefore, in order to evaluate the translational significance of preclinical observations in a model of chronic OA pain, in the present chapter we sought to examine whether such changes were common in human post-mortem tissue obtained from AD individuals with chronic pain. Similarities between results from animal models of AD and those from experiments using human post-mortem tissue samples are important as they suggest that such experimental models used are replicating some aspects of human disease with some degree of accuracy.

4.1.1 Alterations in the Pain Processing Systems in Alzheimer's disease

The multidimensional components of pain perception are processed via various ascending pathways that constitute of the medial and lateral pain systems (outlined in Figure 4.2). The lateral pain system involves ascending pathways that mediate the sensory-discriminative aspect

of pain; whilst the medial system mediates the emotional-affective and cognitive-evaluative components of pain (Achterberg et al 2013, Monroe et al 2012).

4.1.1.1 **Medial Pain System Affected in Alzheimer's disease**

Histological changes have been reported to affect largely the medial pain system in AD, which is involved in the emotional-affective and cognitive-evaluative aspect of pain (Scherder et al 2003). Nociceptive inputs from the spinal cord, in response to noxious stimuli in the periphery, propagate via the medial thalamic structures to the cortical regions through the spinothalamic tract (via intra-laminar nuclei), spinoreticular tract (via parabrachial nucleus, PbN, and locus coeruleus, LC), and spinomesencephalic tract (via periaqueductal grey, PAG) in the medial pain system. The midbrain and pontine reticular formations are interconnected, and so are the intra-laminar and medial thalamic nuclei (Willis & Westlund 1997). Collectively, the medial thalamic nuclei structures transmit nociceptive information to the anterior cingulate cortex and insula. The anterior cingulate cortex is involved in the affective processing of pain in relation to cognitive-evaluative component; whereas the insula contributes to the processing of affective component of pain integrating the sensory-discriminative aspect (Brooks & Tracey 2005, Starr et al 2009). In parallel, nociceptive inputs to the PbN and LC are integrated and propagated to the amygdala and hypothalamus, where the emotional-affective and autonomic responses to pain are characterised, respectively (Willis & Westlund 1997).

Braak and Braak (1991b) provide evidence for neurofibrillary changes in the thalamus and more recently, Rub and colleagues (2002) have shown cytoskeletal tau pathology preceding deposition of Aβ in the intra-laminar nuclei of the thalamus. In addition, a study conducted by Ogomori and co-workers (1989) which examined amyloid deposition in the central nervous system (CNS) showed amyloid deposits in the thalamus of all AD cases examined. A finding which is further reinforced by a recent positron emission tomography (PET) neuroimaging study that revealed greater retention of ^{11}C-Pittsburgh compound B (^{11}C-PiB), a marker for fibrillary Aβ deposition, and reduced glucose metabolism (^{18}F-fluorodeoxyglucose) in the thalamus of AD patients compared to cognitively intact healthy controls (Rodriguez-Vieitez et al 2016). The findings suggest that an increase in amyloid plaque pathology is accompanied by neuronal and synaptic dysfunction in the thalamus of AD individuals.

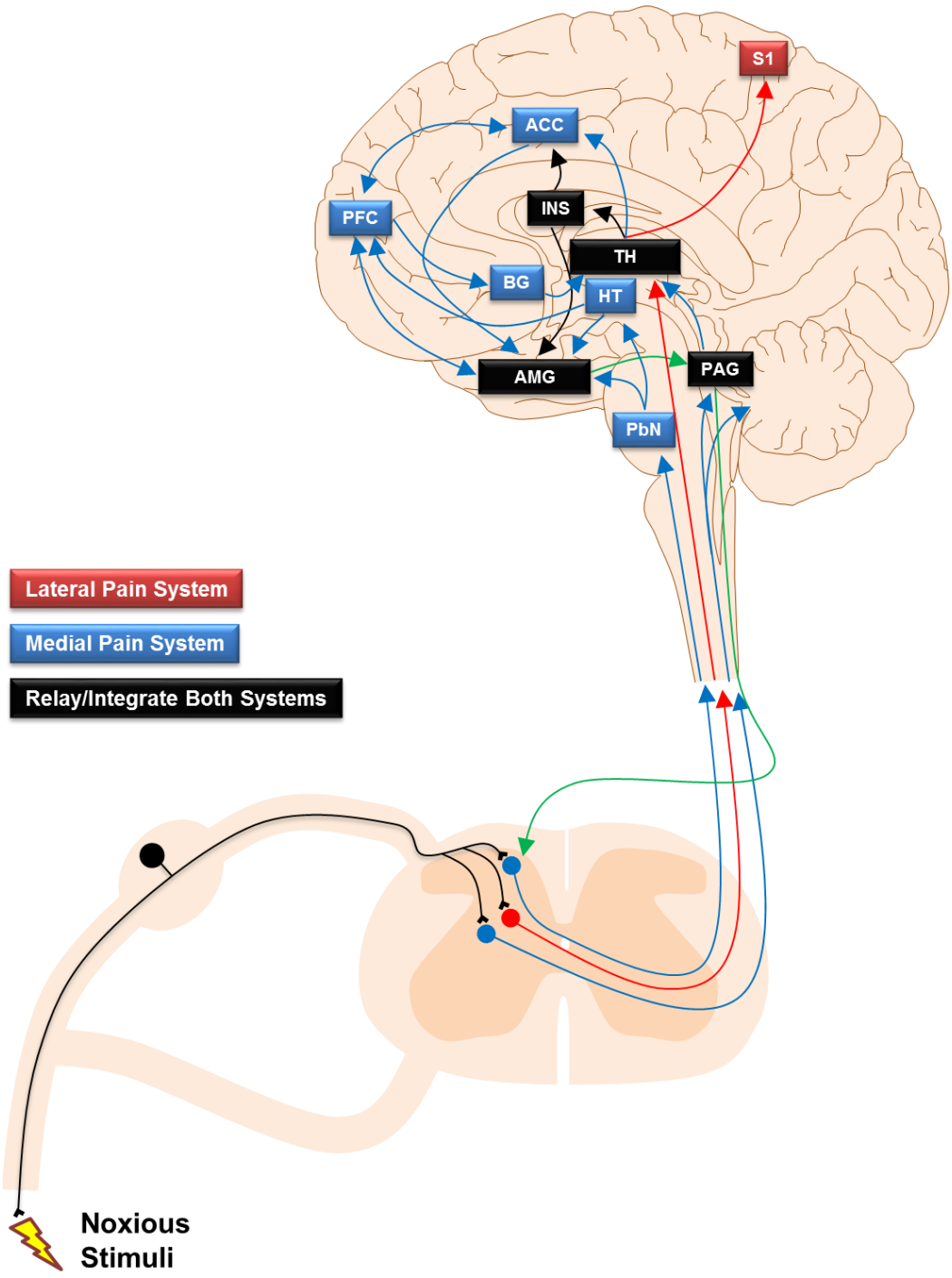

Figure 4.2: A Simplified Schematic of the Pain Systems

A representation of the subcortical and cortical areas and pathways of the medial (blue) and lateral pain systems (red), which correspond to emotional-affective/cognitive-evaluative and sensory-discriminative aspects of pain, respectively. There are a number of brain areas contribute to processing of both inputs from the medial and lateral pain systems (black). Both inputs from the medial and lateral pain systems converge onto the periaqueductal grey (PAG) which modulates spinal nociceptive transmission via descending pathways (green). Abbreviations: ACC, anterior cingulate cortex; AMG, amygdala; BG, basal ganglia; HT, hypothalamus; INS, insula; PbN, parabrachial nucleus; PFC, prefrontal cortex; and S1, primary somatosensory cortex; TH, thalamus. Figure modified from Scherder et al (2003) and Kuner and Flor (2017).

Further pathological changes are reported in the brainstem areas that include the PbN and PAG, that receive nociceptive inputs from the spinal cord via the spinoreticular and spinomesencephalic tracts, respectively (Rub et al 2001). The PbN projects to the amygdala and the hypothalamus, areas which are concerned with the emotional and autonomic responses to pain; whilst the PAG plays an important role in modulation of the dorsal horn circuits (anti-nociceptive) (Todd 2010, Willis & Westlund 1997). In the hypothalamus, histaminergic neurons of the tuberomammillary nucleus are affected in AD which may underlie the blunted autonomic responses to pain (Panula et al 1998, Rainero et al 2000).

Moreover, neurodegeneration in the LC which is involved in the cognitive-evaluative aspect of pain via meditating nociceptive information to the cerebral cortex (i.e. primary somatosensory cortex, prefrontal cortex, and anterior cingulate cortex) in order to allow attention to be given to pain (Llorca-Torralba et al 2016, Willis & Westlund 1997, Zarow et al 2003). In addition, to the presence of AD-associated neuropathological hallmarks, neuroimaging studies have reported severe atrophy in the thalamic medial and intra-laminar nuclei and its connections that are involved in pain processing namely, anterior cingulate cortex, insula, amygdala, prefrontal cortex and hippocampus (Callen et al 2002, Foundas et al 1997, Rombouts et al 2000). Collectively, it has been postulated that in AD the cognitive-evaluative and emotional-affective dimensions of pain, represented by the medial nociceptive pathway may be affected due to AD-associated lesions and neurodegeneration within the limbic structures, hippocampus and prefrontal cortex (Hyman et al 1984).

4.1.1.2 **Lateral Pain System Largely Spared in Alzheimer's disease**

Despite observation of AD-associated neuropathological changes in the medial pain system, the lateral pain system which represents the sensory-discriminative aspect of pain has reported to be largely spared (Farrell et al 1996). This system involves the transmission of nociceptive information from the spinal cord dorsal horn to the lateral thalamus via the spinothalamic tract, which in turn processes and propagates input to the somatosensory cortices (Willis & Westlund 1997). Braak and Braak (1991b) reported moderate neurofibrillary change in the reticular thalamic nucleus; whilst the primary sensory areas were generally less severely affected in comparison to the association areas. Furthermore, it was only at Braak's stage VI when severe

neuropil thread tau pathology was observed in the primary somatosensory cortex (Braak & Braak 1991b). Altogether, these observations suggest that the sensory-discriminative aspect of pain may be preserved due to the reduced extent and/or unaltered AD-associated neuropathological lesions affecting the regions involved (Farrell et al 1996).

4.1.2 Alzheimer's disease Pathology Affecting the Spinal Cord

Though extensive body of research is focussed on neuropathological changes in the brain of AD patients; a few studies have reported AD-related changes in the spinal cord, the "first sensory synapse". Hyperphosphorylated tau in the form of neuropil threads and NFT were observed in the spinal cord of AD individuals, mainly in the ventral horn and at late stages (Braak's stage V-VI) of AD (Guo et al 2016, Saito & Murayama 2000, Schmidt et al 2001). In addition, a recent study by Dugger and colleagues (2013) reported NFT, neuropil threads and pre-tangles in the spinal cord, mainly the ventral horn, of both AD and non-demented individuals, with the former exhibited tau neuropathology in greater proportion of cases compared to the latter. Moreover, amyloid deposits have also been reported in spinal cord of AD patients as Ogomori and co-workers (1989) observed diffuse deposits in a third of the AD patients examined. Collectively, these findings highlight the progression of AD-associated neuropathology to the spinal cord of these disease-affected individuals.

4.1.3 Overview of Pain Processing Affected by Alzheimer's disease Pathology

Altogether, AD-associated pathology and neurodegeneration have been identified in key regions of the pain pathway, which may potentially interfere with multidimensional processing of nociceptive inputs. In addition, clinical experimental studies have reported that there may be an alteration in the sensory perception of chronic pain in AD individuals. However, it still remains elusive whether AD individuals with a chronic pain condition display any alteration in AD-associated pathological changes compared to AD patients with no clinical history of pain. Therefore, it is of great relevance to investigate if the AD-associated neuropathology has an impact on the perception of pain in AD. A better understanding of neuropathological changes and any alterations is important to elucidate the underlying mechanisms in order to identify novel potentials for therapeutic interventions which are required for improvement in clinical management of pain in individuals with AD.

4.1.4 Chapter Aims

So for this purpose, we set out to examine AD-associated pathological lesions and neuroinflammation in spinal cord, the site of “first sensory synapse” along with six supraspinal regions that are involved in both the medial (i.e. anterior cingulate cortex, amygdala, prefrontal cortex, and insula) and lateral (including primary somatosensory cortex and VPL thalamic nuclei) pain systems involved in multidimensional processing of nociceptive inputs. As a result, the aims of the present chapter were:

1. To confirm AD associated pathology is present in key regions of the pain pathway.
2. To examine if AD cases with a clinical history of chronic pain show any alteration in severity of pathology in key regions of the pain pathway in the brain and spinal cord using AD post-mortem tissue with no clinical evidence of pain as a control cohort.
3. To examine if neuroinflammation is altered in the brain and spinal cord of AD individuals with chronic pain compared to their AD control group with no clinical history of pain.

4.2 Materials and Methods

4.2.1 Subjects

The brains from a total of 28 AD patients (14 with history of chronic pain; and 14 no chronic pain history, controls) and spinal cords from a total of eleven AD patients (6 with a history of chronic pain; and 5 with no chronic pain history) were obtained from the London Neurodegenerative Diseases Brain Bank, King's College London with neuropathological finding at autopsy confirming features of AD. The assessment of AD pathology was carried out by neuropathologists blind to the clinical diagnosis and in accordance to the Braak's staging for NFT (Braak & Braak 1991b). Brains and spinal cords of five healthy controls were selected as negative control for AD pathology (≤ Braak's NFT Stage II).

All brains and spinal cords were collected with informed consent from the next of kin. The study was conducted in accordance to the law and under the ethical approval of the Brains for Dementia Research (Ref: TRID_134).

4.2.2 Clinical Assessment

A retrospective review was carried out by Professor Clive Ballard (CB) and Yahyah Aman (YA) on all the notes available for each case, including in-patients notes and clinic letters. Features were recorded as present or absent. Criteria and definitions were as follows: (i) definite AD: histopathological proven according to Braak's staging of NFTs (Braak's stages II-V were considered for selection); (ii) record of chronic pain: persistent use (≥ 1 year) of analgesics (i.e. co-codamol and co-proxamol) and/or diagnosis of a chronic pain condition (i.e. osteoarthritis). Individuals with AD with no documented record of chronic pain were considered to be AD individuals without chronic pain based upon which age and Braak's stage matched patients were selected as controls.

4.2.3 Histology and Immunohistology

Histology and immunohistology was performed 7µm thick formalin-fixed, paraffin-embedded spinal cord and brain tissue sections from several brain structures involved in supraspinal processing of nociceptive inputs that include: thalamus, primary somatosensory cortex,

amygdala, anterior cingulate cortex, insula and prefrontal cortex. Slide-mounted sections were provided by King's College London Brain Bank.

4.2.3.1 **Luxol Fast Blue and Eosin Stain**

Luxol fast blue and eosin stain was conducted with slight modification (Kluver & Barrera 1953) in order to differentiate between the white matter (myelinated nerve fibres) and grey matter, respectively. Briefly, paraffin-embedded sections were de-waxed in xylene (2 × 10 minutes each), passed through absolute alcohol (100%) (4 × 5 minutes each), and incubated overnight at 60°C in 0.1% (w/v in 95% ethanol and 0.05% acetic acid) Luxol fast blue MBS (du Pont) (Fisher Scientific). The following day, sections were immersed in 95% ethanol (10 seconds) and washed in running distilled water (dH_2O) until clear in order to rinse off the excess stain. Subsequently the Luxol fast blue stain was differentiated in 0.05% (w/v) lithium carbonate (Sigma) for 30 seconds before immersion in 75% ethanol (30 seconds) and then into dH_2O until clear in order to visualise the sharp blue stained white matter compared to the colourless grey matter. Following, Luxol fast blue, sections were immersed in eosin (10 minutes) in order to stain the grey matter, and rinsed in dH_2O before dehydration at 60°C for one hour. Finally, sections were cleared in xylene (20 minutes) and coverslipped with dibutylphthalate in xylene (DPX, Sigma) mounting medium.

4.2.3.2 **Haematoxylin and Eosin (H&E) Stain**

In order to examine the cell population and distribution in each of the regions of interest, haematoxylin and eosin (H&E) was performed. Briefly, paraffin-embedded sections were de-waxed in xylene (2 × 10 minutes each) rehydrated by passing sections through absolute alcohol (4 × 5 minutes each); and then in dH_2O (5 minutes). Subsequently, sections were immersed in Gill's (2) haematoxylin solution (Sigma) for 5 minutes and rinsed under running tap water until clear. Sections were then differentiated in acid-alcohol solution (5 seconds) and rinsed under running tap water (5 minutes) to blue. Following, haematoxylin, sections were immersed in eosin solution (10 minutes), excess eosin rinsed with tap water before placing sections in dH_2O and dehydrating at 60°C for one hour. Finally, sections were cleared in xylene (20 minutes) and coverslipped with DPX mounting medium. The histological stain was visualised using Zeiss

Axiovision light microscope and images were captured using Zeiss AxioCam MRc and the software Axiovision Release 4.6. (Zeiss, UK).

4.2.3.3 **Immunohistochemistry**

Immunohistochemistry was performed on slide-mounted 7µm thick formalin-fixed, paraffin-embedded spinal cord and brain tissue sections. The following antibodies were used for immunohistochemistry: anti-phospho paired helical fragment (PHF) tau (AT8, Thermo Scientific), anti-β-amyloid 1-16 (6E10, Biolegend), and anti-ionized calcium binding adaptor molecule 1 (IBA1, Wako). As a secondary detection system, the Supersensitive™ Immunohistochemistry Polymer-HRP Detection System Kit (BioGenex) was used to visualise the antibody reactions with 3, 3'diaminobenzidine (DAB) as the chromogen.

Briefly, paraffin-embedded sections were de-waxed in xylene (2 × 10 minutes each) rehydrated by passing sections through absolute alcohol (4 × 5 minutes each); and then in dH_2O (5 minutes). Epitope retrieval method include: heat-induced epitope retrieval (HIER) for 15 minutes of tissue sections immersed in sodium citrate solution (10mM, pH 6) for IBA1 immunoreactivity; HIER was followed by immersion of sections in 70% formic acid (VWR) (20 minutes) for 6E10 immunoreactivity; whilst no pre-treatment was performed for AT8 staining. Following the necessary pre-treatments sections were washed (3 × 5 minutes each) with phosphate buffered saline (PBS, 10mM, pH 7.4) and incubated in 1% hydrogen peroxide (H_2O_2, Sigma) for 30 minutes in order to quench endogenous peroxidase activity and blocked. Subsequently, sections were washed with three times (5 minutes each) with PBS and incubated either: one hour at room temperature (6E10) or overnight at 4°C (IBA1, and AT8) with the appropriately diluted primary antibody in PBS. Details of the source and dilution of the primary antibodies are provided in Table 4.1. Subsequently, sections were washed two times (5 minutes each) with PBS and incubated at room temperature for 20 minutes with Super Enhancer™ Reagent (HK518, BioGenex). In order to remove the excess Super Enhancer™ Reagent, sections were washed two times with PBS (5 minutes each) prior to incubation with Poly-HRP Reagent (HK519, BioGenex) for 30 minutes at room temperature. Sections were washed three times with PBS (5 minutes each) and peroxidase labelling was visualised with incubation with the chromogen DAB (HK124 and HK520, BioGenex) for 10 minutes. Subsequently, sections were

washed with dH_2O (5 minutes) in order to terminate the DAB reaction and then 5 minutes in tap water. Sections were then lightly counterstained with Gill's (2) haematoxylin solution (30 seconds) and rinsed under running tap water until blue. Finally sections were, rinsed in dH_2O, dehydrated in 60°C oven for 1 hour and immersed in xylene to clear for 20 minutes before being coverslipped DPX mounting medium. The specificity of immunoreactivity was confirmed by omitting the primary antibody; immunostaining was visualised using Zeiss Axiovision brightfield microscope and images were captured using Zeiss AxioCam MRc and the software Axiovision Release 4.6. (Zeiss, UK).

Table 4.1: List of Primary Antibodies Used for Immunohistochemistry and Immunofluorescence

Antibody (Clone)	Species	Dilution	Source
Phospho-PHF Tau (AT8) [A]	Mouse	1:800	Thermo Scientific
β-amyloid 1-16 (6E10) [1; B]	Mouse	1:1000	Biolegend
IBA1 [2; A]	Rabbit	1:1000/1:500*	Wako
CD68 (PG-M1) [2; A]	Mouse	1:200*	Dako

[1], pre-treatment: heat-induced epitome retrieval in sodium citrate solution (10mM, pH 6) for 15 minutes and 70% formic acid for 20 minutes; [2], pre-treatment: only heat-induced epitope retrieval in sodium citrate solution (10mM, pH 6) for 15 minutes; [A], primary antibody incubation overnight at 4°C; [B], primary antibody incubation for 1 hour at room temperature; *, Antibody dilution for immunofluorescence.

4.2.3.4 **Immunofluorescence**

Immunofluorescence was performed on slide-mounted 7µm thick formalin-fixed, paraffin-embedded spinal cord and brain tissue sections. Double staining was performed using the following antibodies: mouse anti-CD68 and rabbit anti-IBA1 in order examine the frequency of activated and/or phagocytic microglia. Details of the source and dilution of the primary antibodies are provided in Table 4.1. Briefly, paraffin-embedded sections were de-waxed in xylene (2 × 10 minutes each) rehydrated by passing sections through absolute alcohol (4 × 5 minutes each); and then in dH_2O (5 minutes) prior to a HIER for 15 minutes of tissue sections in sodium citrate solution (10mM, pH 6). Subsequently, sections were blocked with 1% (w/v)

bovine serum albumin (BSA, Sigma, UK), 0.2% (w/v) sodium azide (Sigma, UK), and 0.1% (v/v) Triton X-100 (BDH, UK) in PBS for 30 minutes, and incubated overnight at 4°C with a combination of the primary antibodies: mouse anti-CD68 and rabbit anti-IBA. The following day sections were three times (5 minutes each) with PBS and were subsequently incubated for 1½ hours with the goat anti-mouse conjugated with Alexa Fluor 488 (1:400; Molecular Probes, USA) and Alexa Fluor 546-conjugated goat anti-rabbit antibody (1:400; Molecular Probes, USA). Sections were then washed three times with PBS (5 minutes each), immersed in 0.1% (w/v in 70% ethanol) Sudan Black B for 20 minutes, rinsed under running tap water until clear and coverslipped with Vectashield Mounting Medium containing nuclear marker 4',6-diamidino-2-phenylindole·2HCl (DAPI; Vector Laboratories, UK). All antibody solutions were prepared in PBS with 1% BSA, 0.1% Triton X-100 and 0.2% sodium azide. The specificity of immunoreactivity was confirmed by omitting the primary antibody; immunostaining using Zeiss microscope (Imager.Z1) and images were captured using Zeiss AxioCam MRm and the software Axiovision Release 4.8.2. (Zeiss, UK).

4.2.4 Quantification of Immunohistological Staining

4.2.4.1 **Semi-quantitative Scoring of Immunohistochemistry**

4.2.4.1.1 Aβ and Tau Pathology Grading

The presence and severity of Aβ and tau pathology in the brain regions including: thalamus, primary somatosensory cortex, amygdala, anterior cingulate cortex, insula and prefrontal cortex. Tau neuropathology was assessed semi-quantitatively based on a four-point grading scale ranging from 0 to 3 (0, absent; 1, mild; 2, moderate; 3, severe), as demonstrated in Figure 4.3A-C. This criterion for quantification has been previously described, which appear to improve inter-rater and intra-rater reliability (Alafuzoff et al 2008). The Aβ immunopositive deposits were assessed in accordance to a previously described criterion by Mirra and colleagues (1991), with some modifications. Briefly, a four-point grading system was employed: 0, absent; 1, mild (at least one diffuse or neuritic deposition up to 5 neuritic plaques); 2, moderate (≥ 6 but < 20 neuritic plaques); and severe (≥ 20 neuritic plaques) in a single viewing field under ×10 magnification (Figure 4.3D-F). For each region, all sections were sampled and the thresholds

were based upon the extent of Aβ or hyperphosphorylated tau neuropathological profiles, namely, plaques and tangles respectively.

Aβ (6E10) and tau (AT8) pathological staining was examined by YA, blind to case clinical features. Intra-rater reliability was examined by grading all the regions (blind to clinical features and previous grading values) for each case and for each staining twice a week apart. Mary Johnson (MJ, University of Newcastle) graded AT8 stained sections blind to clinical features and YA grading values; so that the inter-rater reliability could be tested. In the spinal cord, Aβ and tau pathology were recorded as either absent or present in the dorsal and ventral horns.

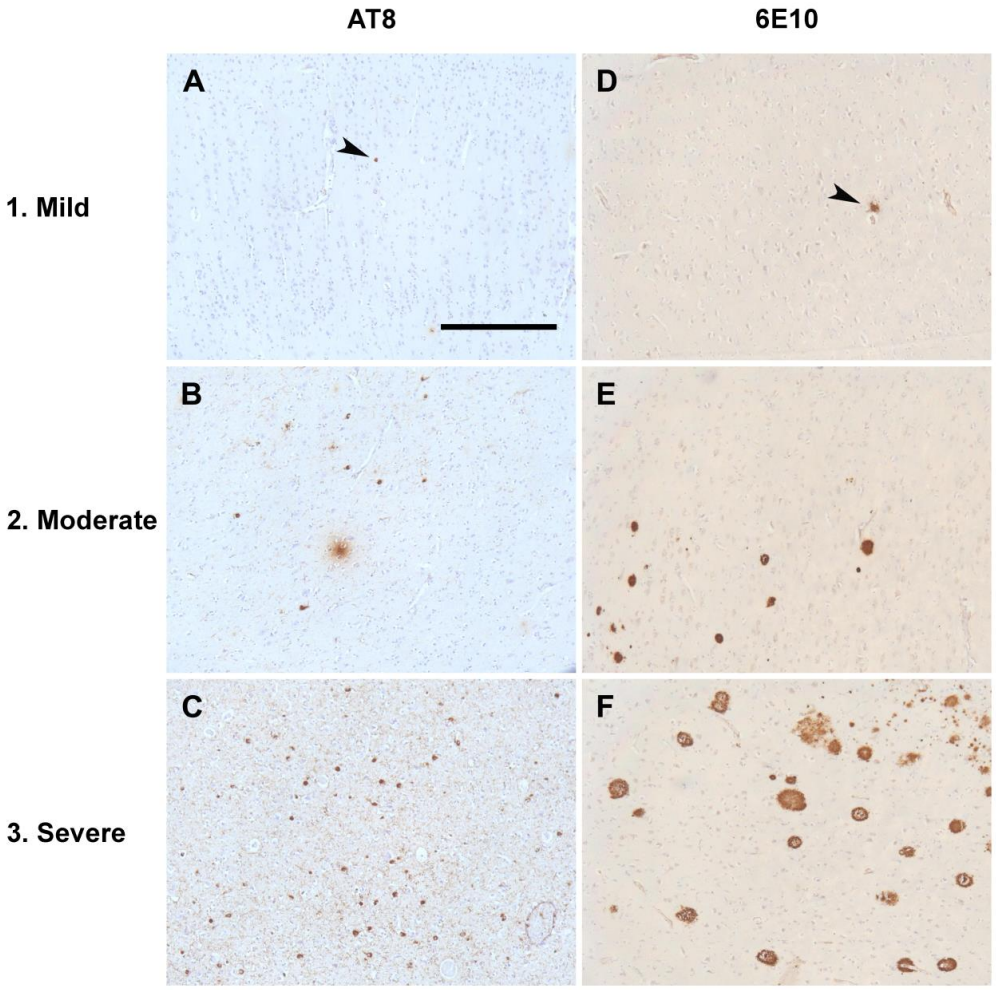

Figure 4.3: Representation of Tau and Amyloid Grading System

Tau (AT8, A-C) and amyloid (6E10, D-F) pathology was assessed using a four-point grading system: 0: absent (below mild threshold); 1, mild (A and D); 2, moderate (B and E); and 3, severe (C and F). The arrowheads highlight the neuropathological lesion identified as the minimum required in order to be classified as mild according to the semi-quantitative grading criteria. These thresholds were set for the prefrontal cortex. All images were taken at ×10 stage objective and the scale bar represents 500µm.

4.2.4.1.2 IBA1 Density Grading

The frequency of IBA1 immunopositive microglia in the brain regions including: thalamus, primary somatosensory cortex, amygdala, anterior cingulate cortex, insula and prefrontal cortex; were assessed semi-quantitatively based on a three-point grading scale ranging from 1 to 3 (1, sparse; 2, moderate; 3, frequent) as demonstrated in Figure 4.4, blind to case clinical features.

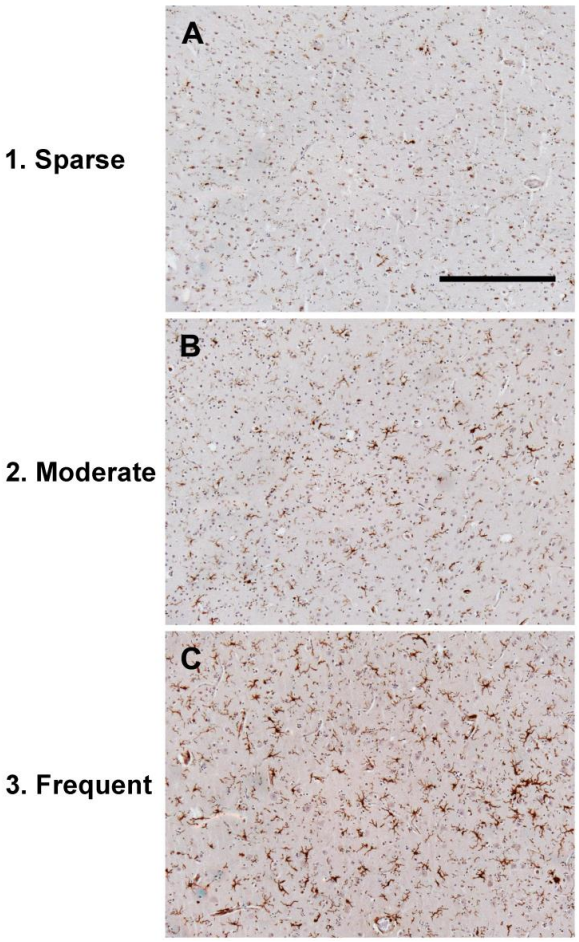

Figure 4.4: Representation of Microglial Density Grading System

IBA1 labelled microglial frequency was assessed using a three-point grading system: 1, sparse (A); 2, moderate (B); and 3, frequent (C). These thresholds were set for the prefrontal cortex. All images were taken at ×10 stage objective and the scale bar represents 500µm.

Intra-rater reliability was examined by grading all the regions (blind to clinical features and previous grading values) for each case and for each staining twice a week apart.

4.2.4.2 **Quantification of Immunofluorescence**

The frequency of IBA1 immunopositive microglia that express CD68 were quantified in the spinal cord and brain regions including: thalamus, primary somatosensory cortex, amygdala, anterior cingulate cortex, insula and prefrontal cortex. For each region of interest, 4-10 images of cortical, sub-cortical and spinal horn dorsal horn grey matter at ×20 magnification were taken per case. For cortical and sub-cortical regions images were obtained in a zig-zag sequence whilst for the spinal cord images were taken superficial and deep dorsal horn. All images were taken blind to the case clinical features and were taken randomly in order to ensure an unbiased representation of regions. Quantitative assessment of number of IBA1 immunopositive microglial cells that also expressed CD68 immunoreactivity were calculated by counting the frequency of IBA1 immunopositive cells in a defined region of 1.5×10^5 μm^2 using Axiovision LE 4.8 software.

4.2.5 Statistical Analysis

The data was analysed with SPSS for Windows version 23.0 (SPSS, Chicago, Illinois, USA). The statistical tests performed and the numbers of subjects are displayed in the results section within the figure legends. Comparison of categorical demographic data (i.e. gender and clinical diagnosis) was conducted between AD individuals with chronic pain compared to AD controls using chi-squared (χ^2) test. For each brain region, comparisons for average immunoreactivity were made between subjects with AD that displayed a clinical history of chronic pain and AD individuals with no clinical report of pain using the Mann-Whitney U Test. All data are presented as mean ± standard error mean (SEM) or standard deviation (SD). The probability value less than 0.05 ($p < 0.05$) was considered statistically significant. Graphs were generated using GraphPad Prism 5 (Graphpad Software Inc., San Diego, USA).

Spearman rank order correlation (ρ) and linear regression (R^2) were conducted in order to test the relationship between the severity of tau and Aβ pathology as well as microglial frequency in each brain region and the progression of AD, using increasing Braak's stage as a marker. The level of significance for this test was set at $p < 0.01$ because of multiple comparisons.

Cohen's kappa and Cronbach's alpha statistics were used to test for inter-rater and intra-rater reliability, respectively, for semi-quantitative assessment of tau, Aβ and IBA1 immunoreactivity.

Power calculations based on previous measurements of a synaptic protein by Western blotting on human post-mortem tissue proposed group sizes of 12 will give greater than 90% power to detect a difference of 0.4 units with an overall SD of 0.2 in a two sample test. These power calculations were conducted and provided by Professor Clive Ballard.

4.3 Results

In order to test the hypothesis that AD-associated pathology and neuroinflammation is present in key regions of the pain pathway we carried out an immunohistochemical study which assessed whether initially these regions are affected, and if so, if there is an alteration in the extent of pathology and/or neuroinflammation in AD individuals with a clinical history of a chronic pain condition compared to AD control cohort. For this purpose, key regions involved in nociceptive processing namely, the spinal cord and supraspinal structure that include thalamus, primary somatosensory cortex, amygdala, anterior cingulate cortex, insula and prefrontal cortex were examined for tau and Aβ pathology as well as for markers for neuroinflammation: microglial response and activation.

4.3.1 Clinical Data

For the purpose of this study AD cases were defined as patient group with neuropathologically confirmed AD who presented with a clinical history of a chronic pain condition diagnosis (i.e. OA) and/or persistent use (≥ 1 year) of analgesics. AD controls represent the group of AD patients without any clinical history of pain/persistent analgesic use reported.

4.3.1.1 **Patient Demography: Supraspinal Structures**

The demographic detail of all patients from whom supraspinal structures were available are summarised in Table 4.2. Twenty-eight patients (14 AD cases and 14 AD controls) with confirmed AD (Braak's stage II-V) at autopsy were examined in this study. The clinical diagnosis of dementia was present in seventeen of the 28 patients examined (7 AD cases and 10 AD controls; χ^2 test, $p = 0.246$). There was no significant difference between AD cases and AD controls in terms of Braak's staging of tau pathology in AD as both groups had similar proportion of cases distributed at each Braak's stage examined (χ^2 test, $p = 0.714$). AD cases exhibited comparable proportion of female (χ^2 test, $p = 1.000$), and the mean: age of death (Mann-Whitney U Test, $p = 0.963$) and post-mortem delay (PMD) (Mann-Whitney U Test, $p = 0.241$) to AD controls.

Table 4.2: Demographic Detail of Patient – Supraspinal Regions

	AD Controls	AD Cases
Number of Cases	14 [1]	14 [2]
Age at Death (years ± SD)	85.93 ± 5.57	83.93 ± 9.15
PMD (hours ± SD)	48.93 ± 21.72	41.29 ± 16.69
Gender		
Male	5	5
Female	9	9
Clinical Diagnosis		
Control	4	7
Dementia	10	7
Braak's Stage		
II	0	1
III	4	3
IV	3	5
V	7	5
Pain Condition		
Osteoarthritis	0	10
Other	0	3
Analgesics		
Paracetamol	0	1
Opioid	0	1
NSAID	0	1
Paracetamol + Opioid	0	6
Paracetamol + NSAID	0	1
Paracetamol + Opioid + NSAID	0	3

[1] The prefrontal cortex, insula, and primary somatosensory cortex were unavailable for two cases.

[2] The prefrontal cortex, insula, and primary somatosensory cortex were unavailable for one case.

Abbreviations: NSAID, non-steroidal anti-inflammatory drug; PMD, post-mortem delay; SD, standard deviation.

The AD cases were most commonly diagnosed with OA, which affected 71.4% (10 of 14 cases) of the patients examined, with other pain conditions (i.e. back pain and neck pain) reconstituting the remaining 21.4% (3 of 14 cases) along with one case that did not exhibit any clinical pain diagnosis but persistent use of analgesic was reported. Moreover, persistent use of analgesic was reported in thirteen of the 14 cases examined, in which the most frequently (6 cases of 14) used drug combination was paracetamol and opioid (i.e. co-codamol and co-proxamol).

4.3.1.2 **Patient Demography: Spinal Cord**

The demographic detail of all patients, from whom spinal cord sections were available, is displayed in Table 4.3. Eleven patients (6 AD cases and 5 AD controls) with confirmed AD-associated neuropathological tau pathology graded from Braak's stage II-V at autopsy were examined in this study. The clinical diagnosis of dementia was present in five of the 11 patients examined (3 AD cases and 2 AD controls χ^2 test, $p = 0.740$). There was no significant difference between AD cases and AD controls in terms of Braak's staging of tau pathology in AD as both groups had similar proportion of cases distributed at each Braak's stage examined (χ^2 test, $p = 0.402$). AD individuals with clinical history of a chronic pain condition group had comparable proportion of female (χ^2 test, $p = 0.376$), and the mean: age of death (Mann-Whitney U Test, $p = 0.537$) and PMD (Mann-Whitney U Test, $p = 0.429$) to that in the AD controls cohort.

In AD cases, OA was the mostly diagnosed pain condition, which affected two thirds (4 of 6 cases) of the patients examined; with other pain conditions such as peripheral neuropathy reconstituting the remaining 33.3% of the cases (2 of 6). Furthermore, persistent use of analgesic was reported in five of the 6 cases examined, in which the most frequently (2 cases of 6) used drug combination was paracetamol and opioid (i.e. co-codamol and co-proxamol).

Table 4.3 Demographic Detail of Patient – Spinal Cord

	AD Controls	AD Cases
Number of Cases	5	6
Age at Death (years ± SD)	87.40 ± 8.20	85.00 ± 4.47
PMD (hours ± SD)	45.60 ± 21.80	37.67 ± 12.16
Gender		
Male	2	4
Female	3	2
Clinical Diagnosis		
Control	3	3
Dementia	2	3
Braak's Stage		
II	0	1
III	3	1
IV	1	1
V	1	3
Pain Condition		
Osteoarthritis	0	4
Other	0	2
Analgesics		
Paracetamol	0	1
Opioid	0	1
NSAID	0	0
Paracetamol + Opioid	0	2
Paracetamol + NSAID	0	1
Paracetamol + Opioid + NSAID	0	0

Abbreviations: NSAID, non-steroidal anti-inflammatory drug; PMD, post-mortem delay; SD, standard deviation.

4.3.2 Regional Representation

Prior to staining with any markers for AD-associated neuropathology and neuroinflammation, we conducted histological examination of the supraspinal and spinal structures used for this study in order to identify the regions of interest for assessment.

4.3.2.1 **Cortex**

Firstly, cortical sections were stained with Luxol fast blue and eosin (LB&E) in order to identify the difference between the white matter and grey matter, respectively (Figure 4.5A). All assessments of neuropathology and neuroinflammation markers were conducted in the cortical grey matter. Subsequently sections were stained with a nuclear stain marker, haematoxylin and eosin (H&E) as marker for grey matter (Figure 4.5B), which allowed the identification of nuclear cell size and distribution in the cortical grey matter (Figure 4.5C).

4.3.2.2 **Thalamus**

Similar sequence of staining was conducted for each case on the thalamus sections (Figure 4.5D-F). The different nuclei of the thalamus were labelled according to the human brain atlas (DeArmond et al 1976). Of the identified thalamic nuclei, the region of interest was the ventral lateral/ventral posterior lateral nucleus (VL/VPL) of the thalamus as it is the site that receives (from the spinal cord) and relays nociceptive information to the supraspinal structures involved in pain processing via the spinothalamic tract (Treede et al 1999, Willis & Westlund 1997). Thus examination of AD associated pathology and neuroinflammation was conducted only in the VL/VPL nucleus of the thalamus.

4.3.2.3 **Amygdala**

In addition, sections from the amygdala were stained with LB&E and H&E (Figure 4.5G-I) and based upon the human brain atlas (DeArmond et al 1976), region of interest; amygdala, was identified medial in relation to the lateral ventricle. All assessments were conducted within the amygdala grey matter.

4.3.2.4 **Spinal Cord**

Finally, LB&E stain of the spinal cord differentiated between the grey matter and white matter (Figure 4.5J). The dorsal and ventral horns of the spinal cord grey matter were identified and H&E stain was conducted in order to examine nuclear cell population (Figure 4.5K-L). All assessments were conducted within the grey matter of the spinal cord.

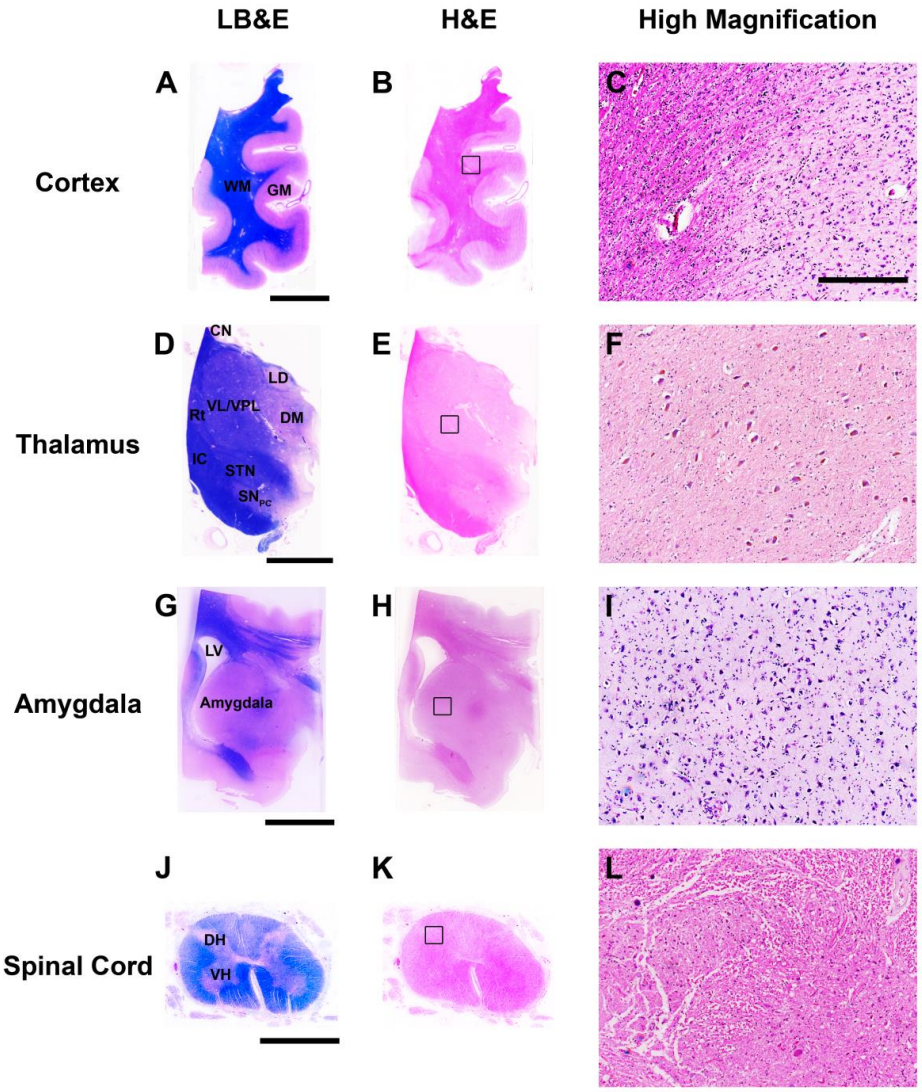

Figure 4.5: Representation of Regions of Interest

A representation of luxol fast blue and eosin (LB&E), haematoxylin and eosin (H&E), and a higher magnification of H&E depicting the neuronal population are outlined in the cerebral cortex (A-C), thalamus (D-F), amygdala (G-I) and the spinal cord (J-L), respectively. The scale bar represents 10mm (A-B, D-E, and G-H), 5mm for (J-K), and 200µm for all the high magnification images (C, F, I, and L). Abbreviations: WM, white matter; GM, grey matter; CN, body of the caudate nucleus; LD, lateral dorsal nucleus; DM, dorsal medial nucleus; VL/VPL, ventral lateral/ventral posterior lateral nucleus; Rt, reticular nucleus; IC, internal capsule; STN, subthalamic nucleus; SN_{PC}, substantia nigra pars compacta; LV, lateral ventricle; DH, dorsal horn of the spinal cord; and VH, ventral horn of the spinal cord.

4.3.3 Tau Pathology

Intracellular inclusions of hyperphosphorylated tau along with extracellular deposition of aggregated Aβ are considered to be the pathological hallmarks of AD. Therefore, in the present study we initially assessed whether AD-related tau pathological lesions, visualised using antibody against phosphorylated tau (AT8), are present in key regions of the pain pathway.

4.3.3.1 **Tau Pathology Present in Supraspinal Structures Involved in Pain Processing**

As expected, aggregated AT8 immunopositive profiles were evident in the form of NFT (Figure 4.6A), neuropil threads (Figure 4.6B), and/or dystrophic neurites (Figure 4.6C) in the cortical and sub-cortical supraspinal regions examined in this study.

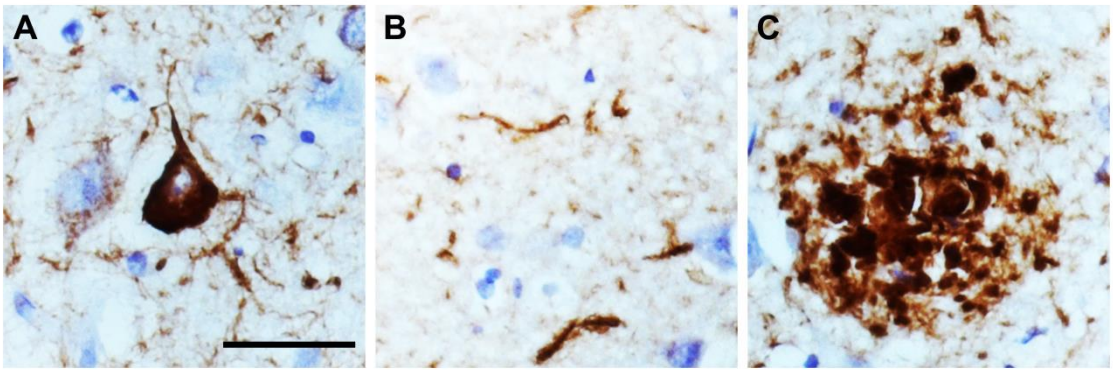

Figure 4.6: Representation of AD-associated Tau Pathology in the Brain

Tau AT8 immunopositive inclusions were present in the form of neurofibrillary tangle (A), neuropil threads (B) and dystrophic neurites (C). Images were taken from the anterior cingulate cortex of an AD patient. The scale bar represents 50µm.

4.3.3.2 **Increase in Tau Pathology as AD Progresses**

In order to determine whether AD progression results in exacerbation of hyperphosphorylated tau pathology in the supraspinal regions involved in pain processing, AT8-immunostained sections were graded from the prefrontal cortex, amygdala, anterior cingulate cortex, insula, primary somatosensory cortex, and thalamus. Figure 4.7 illustrates the extent of AT8-immunoreactivity graded in a range of thresholds from mild, moderate to severe in each individual supraspinal region.

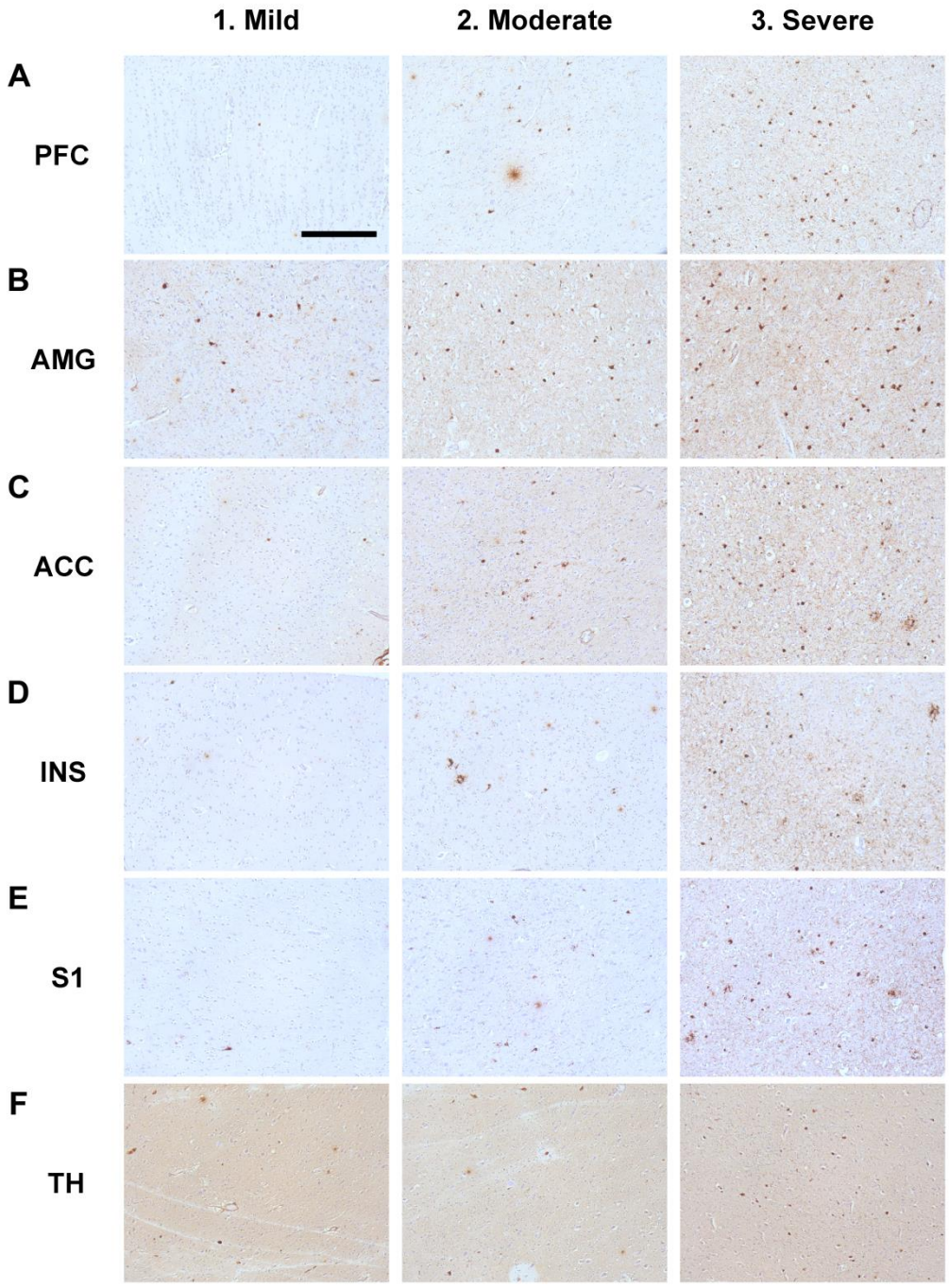

Figure 4.7 Supraspinal Regional Tau Pathology Grading Thresholds

A representation of mild (1), moderate (2), and severe (3) AT8 immunoreactivity thresholds in the prefrontal cortex (PFC, A); amygdala (AMG, B); anterior cingulate cortex (ACC, C); insula (INS, D); primary somatosensory cortex (S1, E), and the thalamus (TH, F). Images displaying AT8 immunoreactivity lower than the mild thresholds were considered as absent (0). All images were taken at ×10 stage objective and the scale bar represents 500µm.

A high degree of internal consistency was found using Cronbach's alpha statistics between the regional analysis of AT8 anti-tau immunoreactivity twice, a week apart, by the same observer

(Cronbach's alpha = 0.980). Cohen kappa statistics showed a strong inter-rater reliability between observations made by YA and MJ (Cohen's kappa = 0.864) with agreement on 90% of the cases examined.

The percentage of subjects in the supraspinal region displaying absent to severe tau pathology grade at each individual Braak's stage of AD are outlined in Table 4.4.

AT8 immunoreactivity was observed to be exclusively absent in all supraspinal regions at Braak's stage 0-II; whereas, individuals at Braak's stage III displayed occasional mild hyperphosphorylated aggregated tau in all supraspinal areas except the amygdala, in which variable tau pathology was observed. Furthermore, majority of AD patients at Braak's stage IV and V showed mild-moderate and moderate-severe AT8 immunoreactivity, respectively, in supraspinal areas involved in pain processing. A strong positive correlation and relationship between with the extent of AT8 immunoreactivity and Braak's staging of AD was detected in the prefrontal cortex ($\rho = 0.878$, $p < 0.001$; $R^2 = 0.755$, $p < 0.001$), amygdala ($\rho = 0.737$, $p < 0.001$; $R^2 = 0.593$, $p < 0.001$), anterior cingulate cortex ($\rho = 0.901$, $p < 0.001$; $R^2 = 0.805$, $p < 0.001$), insula ($\rho = 0.889$, $p < 0.001$; $R^2 = 0.765$, $p < 0.001$), primary somatosensory cortex ($\rho = 0.873$, $p < 0.001$; $R^2 = 0.765$, $p < 0.001$), and the thalamus ($\rho = 0.739$, $p < 0.001$; $R^2 = 0.534$, $p < 0.001$). Therefore, indicating that AD-associated tau neuropathology is present in key supraspinal regions involved in nociceptive progressing; and as AD progresses the pain processing supraspinal regions become increasingly affected by AD-associated tau pathology.

Table 4.4: Regional Extent of Tau Pathology - Percentage of Subjects

Region	Braak's (n)	Absent (n)	Mild (n)	Moderate (n)	Severe (n)
PFC	0-II (5)	100.0 (5)	0.0 (0)	0.0 (0)	0.0 (0)
	III (8)	75.0 (6)	25.0 (2)	0.0 (0)	0.0 (0)
	IV (7)	14.3 (1)	42.9 (3)	28.6 (2)	14.3 (1)
	V (10)	0.0 (0)	0.0 (0)	30.0 (3)	70.0 (7)
AMG	0-II (5)	100.0 (5)	0.0 (0)	0.0 (0)	0.0 (0)
	III (8)	25.0 (2)	50.0 (4)	12.5 (1)	12.5 (1)
	IV (7)	14.3 (1)	14.3 (1)	42.9 (3)	28.6 (2)
	V (13)	0.0 (0)	0.0 (0)	38.5 (5)	61.5 (8)
ACC	0-II (5)	100.0 (5)	0.0 (0)	0.0 (0)	0.0 (0)
	III (8)	50.0 (4)	50.0 (4)	0.0 (0)	0.0 (0)
	IV (7)	0.0 (0)	42.9 (3)	57.1 (4)	0.0 (0)
	V (13)	0.0 (0)	0.0 (0)	53.8 (7)	46.2 (6)
INS	0-II (5)	100.0 (5)	0.0 (0)	0.0 (0)	0.0 (0)
	III (8)	62.5 (5)	37.5 (3)	0.0 (0)	0.0 (0)
	IV (7)	14.3 (1)	57.1 (4)	28.6 (2)	0.0 (0)
	V (10)	0.0 (0)	0.0 (0)	40.0 (4)	60.0 (6)
S1	0-II (5)	100.0 (5)	0.0 (0)	0.0 (0)	0.0 (0)
	III (8)	87.5 (7)	12.5 (1)	0.0 (0)	0.0 (0)
	IV (7)	14.3 (1)	14.3 (1)	42.9 (3)	28.6 (2)
	V (10)	0.0 (0)	0.0 (0)	20.0 (2)	80.0 (8)
TH	0-II (5)	100.0 (5)	0.0 (0)	0.0 (0)	0.0 (0)
	III (8)	37.5 (3)	62.5 (5)	0.0 (0)	0.0 (0)
	IV (7)	0.0 (0)	57.1 (4)	42.9 (3)	0.0 (0)
	V (13)	0.0 (0)	46.2 (6)	30.8 (4)	23.1 (3)

A table representing the percentage of subjects that displayed absent, mild, moderate or severe tau pathology grade, at individual Braak's stage of AD, in the supraspinal regions.

Abbreviations: n, number of subjects; ACC, anterior cingulate cortex; AMG, amygdala; INS, insula; PFC, prefrontal cortex; S1, primary somatosensory cortex; TH, thalamus.

4.3.3.3 **Unaltered Tau Pathology in AD Cases Compared to AD Controls**

The mean tau pathology grades in each supraspinal region and at individual Braak's stage are presented in Table 4.5.

Having confirmed the presence of tau pathology in supraspinal regions, we went on to assess if there is any alteration in the extent of tau pathology severity in AD cases, AD patients who displayed a clinical history of a chronic pain condition/persistent analgesic use, compared to AD controls. Immunohistochemical grading analysis of AT8 immunoreactivity revealed moderate to severe tau pathology exhibited by majority of the individuals in the AD controls cohort in the prefrontal cortex (58.3%), amygdala (78.6%), anterior cingulate cortex (64.3%), insula (58.3%), and primary somatosensory cortex (66.7%); whilst mild to moderate tau pathology was observed in the thalamus of eleven of the 14 control patients (78.6%). Comparable proportion of AD cases patient group displayed moderate to severe AT8 immunoreactivity in the prefrontal cortex (46.2%), amygdala (64.3%), anterior cingulate cortex (57.1%), and primary somatosensory cortex (53.8%); whereas in the insula only five out of the 13 case individuals (38.5%) displayed moderate-severe tau pathology. In addition, similar proportion of individuals in AD cases cohort showed mild-moderate AT8 immunoreactivity in the thalamus (78.6%). Statistical analysis demonstrated that AD cases displayed no change in the extent of tau pathology in the prefrontal cortex (Mann-Whitney U Test, $p = 0.272$), amygdala (Mann-Whitney U Test, $p = 0.217$), anterior cingulate cortex (Mann-Whitney U Test, $p = 0.962$), insula (Mann-Whitney U Test, $p = 0.250$), primary somatosensory cortex (Mann-Whitney U Test, $p = 0.625$), and the thalamus (Mann-Whitney U Test, $p = 0.840$) when compared to the AD controls cohort.

Further analysis comparing the extent of tau pathology exhibited by AD cases relative to their respective AD controls cohort at each individual Braak's NFT stage also revealed no notable significant change (Mann-Whitney U Test, $p > 0.05$) in the prefrontal cortex, amygdala, anterior cingulate cortex, insula, primary somatosensory cortex and the thalamus. However, a trend of lower proportion of AD cases displayed moderate to severe AT8 immunoreactive profiles at Braak's stages IV-V compared to AD controls. Therefore, our data demonstrates that the presence of chronic pain and/or persistent use of analgesics do not have an impact on tau pathology exhibited by AD individuals in supraspinal areas involved in pain processing.

Table 4.5: Supraspinal Regional Tau Pathology Comparison Between AD Cases vs. AD Controls

Region	Braak's Stage	AD Controls (n)	AD Cases (n)	p-value *
PFC	II-V	1.83 ± 0.35 (7/12)	1.31 ± 0.35 (6/13)	0.272
	II	-	0.00 ± 0.00 (0/1)	-
	III	0.50 ± 0.23 (0/4)	0.00 ± 0.00 (0/3)	0.180
	IV	2.00 ± 0.58 (2/3)	1.00 ± 0.41 (1/4)	0.195
	V	2.80 ± 0.20 (5/5)	2.60 ± 0.25 (5/5)	0.513
AMG	II-V	2.21 ± 0.26 (11/14)	1.71 ± 0.30 (9/14)	0.217
	II	-	0.00 ± 0.00 (0/1)	-
	III	1.25 ± 0.63 (1/4)	1.00 ± 0.58 (1/3)	0.853
	IV	2.67 ± 0.33 (3/3)	1.25 ± 0.48 (2/4)	0.064
	V	2.57 ± 0.20 (7/7)	2.67 ± 0.21 (6/6)	0.735
ACC	II-V	1.64 ± 0.29 (9/14)	1.71 ± 0.24 (8/14)	0.962
	II	-	0.00 ± 0.00 (0/1)	-
	III	0.25 ± 0.25 (0/4)	1.00 ± 0.00 (0/3)	0.066
	IV	1.67 ± 0.33 (2/3)	1.50 ± 0.29 (2/4)	0.683
	V	2.43 ± 0.20 (7/7)	2.50 ± 0.22 (6/6)	0.805
INS	II-V	1.75 ± 0.33 (7/12)	1.23 ± 0.30 (5/13)	0.250
	II	-	0.00 ± 0.00 (0/1)	-
	III	0.50 ± 0.29 (0/4)	0.33 ± 0.33 (0/3)	0.683
	IV	1.67 ± 0.33 (2/3)	0.75 ± 0.25 (0/4)	0.076
	V	2.80 ± 0.20 (5/5)	2.40 ± 0.25 (5/5)	0.221
S1	II-V	1.83 ± 0.37 (8/12)	1.54 ± 0.39 (7/13)	0.625
	II	-	0.00 ± 0.00 (0/1)	-
	III	0.25 ± 0.25 (0/4)	0.00 ± 0.00 (0/3)	0.386
	IV	2.33 ± 0.33 (3/3)	1.50 ± 0.65 (2/4)	0.354
	V	2.80 ± 0.20 (5/5)	2.80 ± 0.20 (5/5)	1.000
TH	II-V	1.36 ± 0.23 (6/14)	1.36 ± 0.23 (4/14)	0.840
	II	-	0.00 ± 0.00 (0/1)	-
	III	0.50 ± 0.29 (0/4)	1.00 ± 0.00 (0/3)	0.180
	IV	1.67 ± 0.33 (2/3)	1.25 ± 0.25 (1/4)	0.307
	V	1.71 ± 0.29 (4/7)	1.83 ± 0.40 (3/6)	0.878

Data is presented as mean ± SEM (* Mann-Whitney U Test).

Abbreviations: n, number of moderate-severe patients/ total number of patients; ACC, anterior cingulate cortex; AMG, amygdala; INS, insula; PFC, prefrontal cortex; S1, primary somatosensory cortex; TH, thalamus.

4.3.3.4 **Tau Pathology Absent in the Spinal Cord**

A number of reports have provided evidence for deposition of hyperphosphorylated tau in the spinal cord of AD patients (Dugger et al 2013, Guo et al 2016, Saito & Murayama 2000). Therefore, we went on to examine AT8 immunoreactivity in the spinal cord. In contrast to previous findings, our results showed no evident tau neuropathological profiles in the spinal cord grey matter, in any of the spinal cord samples examined. Intriguingly, AT8 immunoreactivity marked blood vessel-like structures with no specific AD-related tau neuropathological characteristics examined as outlined in Figure 4.8. Therefore, indicating absence of AD-associated tau neuropathology in the sample of cases used for this study.

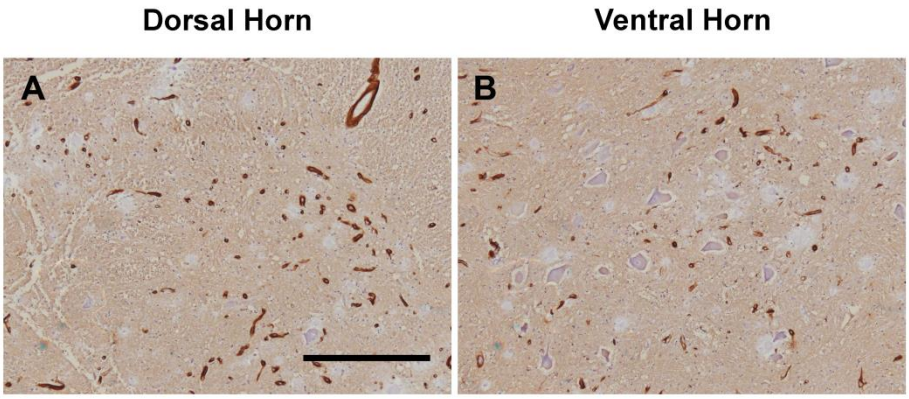

Figure 4.8: No Tau Pathology Detected in the AD Spinal Cord

Representation of AT8 immunoreactivity in the dorsal (A) and ventral (B) horns of the spinal cord. There were no neuropathological features of tau associated with AD present in the spinal cord grey matter as we detected non-specific labelling of blood-vessels. All images were taken at ×10 stage objective and the scale bar represents 500µm.

Collectively, these data confirm the presence of AD-associated tau pathology only in the supraspinal regions involved in the processing of nociceptive inputs. In addition, supraspinal tau pathology increases in severity as Braak's NFT stage increases, which indicate that the pain processing regions are: (1) affected by tau pathology in AD, and (2) become increasingly affected as the disease progresses. Comparison of AD cases versus AD controls revealed unaltered tau pathology in any of the individual supraspinal regions examined. Thus, indicating no significant alteration in AD-associated tau pathology in AD individuals with a history of chronic pain and/or persistent analgesic use compared to the AD controls.

4.3.4 Amyloid Pathology

As aforementioned amyloid plaques is also one of the key pathological signatures of AD. Thus, we went onto examine whether AD-associated amyloid pathology is present in key regions of the pain pathway.

4.3.4.1 **Amyloid Pathology Present in Supraspinal Structures Involved in Pain Processing**

Expectedly, we observed amyloid deposition. 6E10 immunoreactive profiles, in the supraspinal structures presented in the form of intraneuronal accumulations (Figure 4.9A), diffuse (Figure 4.9B) and neuritic plaques (Figure 4.9C).

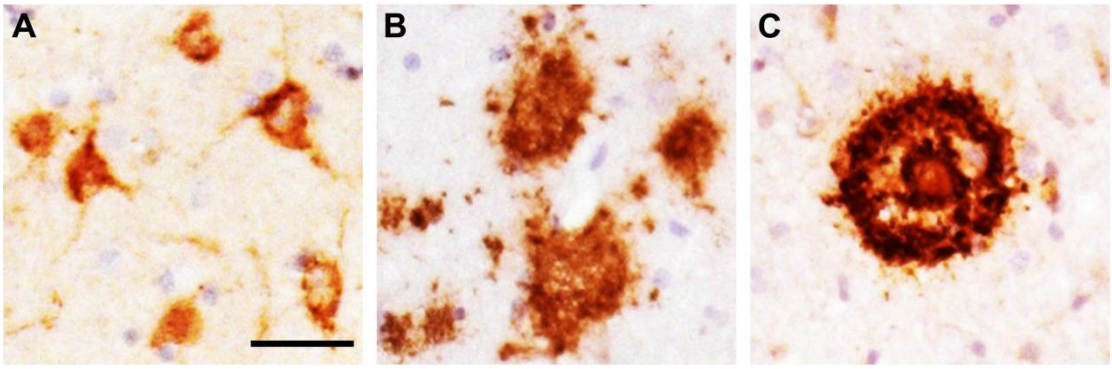

Figure 4.9: Representation of AD-associated Amyloid Pathology in the Brain

Amyloid 6E10 immunopositive inclusions were present in the form of intraneuronal accumulation (A), diffuse deposits (B) and neuritic amyloid plaques (C). All images were taken from patients with AD from the amygdala (A) and the anterior cingulate cortex (B-C). The scale bar represents 25µm.

4.3.4.2 **Increase in Amyloid Pathology as AD Progresses**

Having confirmed the presence of Aβ immunoreactivity in the supraspinal structures we went onto initially examine its progression as AD Braak's stage increases. For this purpose, 6E10 immunoreactivity was graded in the prefrontal cortex, amygdala, anterior cingulate cortex, insula, primary somatosensory cortex, and thalamus. Figure 4.10 outlines the extent of 6E10-immunoreactivity graded in a range of thresholds from mild, moderate to severe in each individual supraspinal region.

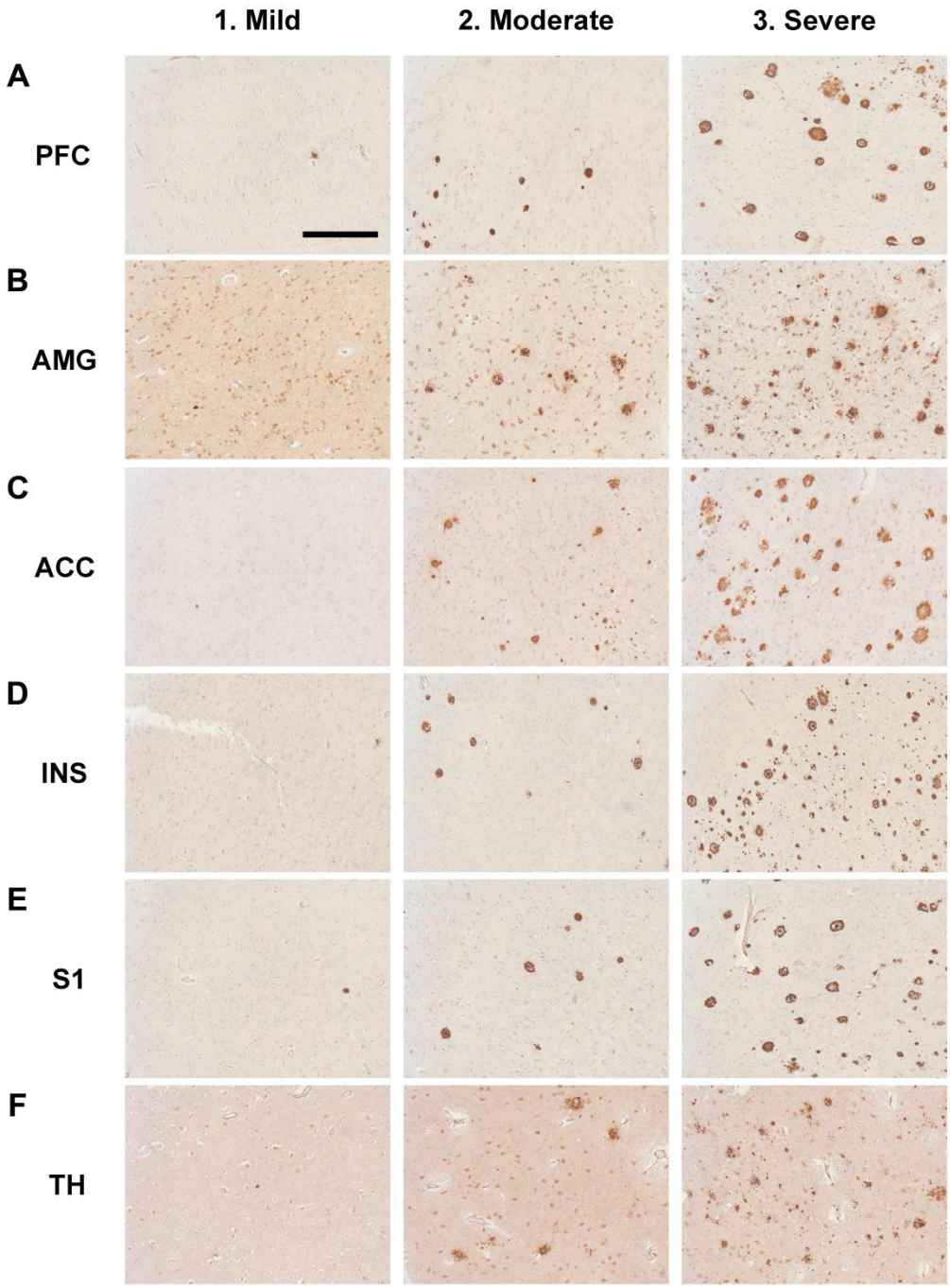

Figure 4.10: Supraspinal Regional Amyloid Pathology Grading Thresholds

A representation of mild (1), moderate (2), and severe (3) 6E10 immunoreactivity thresholds in the prefrontal cortex (PFC, A); amygdala (AMG, B); anterior cingulate cortex (ACC, C); insula (INS, D); primary somatosensory cortex (S1, E), and the thalamus (TH, F). Images displaying 6E10 immunoreactivity lower than the mild thresholds were considered as absent (0). All images were taken at ×10 stage objective and the scale bar represents 500µm.

A strong internal consistency in amyloid pathology grading was evident using Cronbach's alpha statistics between the regional analysis of 6E10 anti-Aβ1-16 immunoreactivity twice, a week apart, by the same observer (Cronbach's alpha = 0.949).

The proportion of subjects displaying a range (absent to severe) Aβ1-16 immunoreactivity in the supraspinal structures are shown in Table 4.6.

Amyloid pathology was present in the form of 6E10 immunoreactive diffuse and neuritic plaques in all supraspinal structures of AD patient at Braak's stage 0-II, which suggest the appearance of amyloid pathology in the cortical and sub-cortical brain regions may precede the deposition of aggregated tau lesions. However, unlike hyperphosphorylated tau depositions, amyloid pathology in all brain regions was observed to be quite variable, as the proportion of cases at Braak's stages 0-III exhibited 6E10 immunoreactivity grading across the full spectrum (absent to severe) of the amyloid grading system. It was only at Braak's stages IV and V where the 6E10 grading for most cases displayed moderate to severe amyloid pathology in the brain regions examined in this study. Analysis of the association of Aβ pathology with the progression of AD revealed a strong positive correlation and relationship between with the extent of 6E10 immunoreactivity and Braak's stage of AD in the prefrontal cortex ($\rho = 0.694$, $p < 0.001$; $R^2 = 0.428$, $p < 0.001$), amygdala ($\rho = 0.792$, $p < 0.001$; $R^2 = 0.619$, $p < 0.001$), anterior cingulate cortex ($\rho = 0.678$, $p < 0.001$; $R^2 = 0.464$, $p < 0.001$), insula ($\rho = 0.712$, $p < 0.001$; $R^2 = 0.455$, $p < 0.001$), primary somatosensory cortex ($\rho = 0.715$, $p < 0.001$; $R^2 = 0.496$, $p < 0.001$), and the thalamus ($\rho = 0.708$, $p < 0.001$; $R^2 = 0.527$, $p < 0.001$). Therefore, indicating that AD-associated Aβ pathology is not only present in key supraspinal regions involved in nociceptive progressing but is also increasingly affecting these regions with the progression of AD.

Table 4.6: Regional Extent of Amyloid Pathology - Percentage of Subjects

Region	Braak's (n)	Absent (n)	Mild (n)	Moderate (n)	Severe (n)
PFC	0-II (5)	40.0 (2)	20.0 (1)	20.0 (1)	20.0 (1)
	III (8)	37.5 (3)	37.5 (3)	12.5 (1)	12.5 (1)
	IV (7)	14.3 (1)	0.0 (0)	14.3 (1)	71.4 (5)
	V (10)	0.0 (0)	0.0 (0)	0.0 (0)	100.0 (10)
AMG	0-II (5)	80.0 (4)	0.0 (0)	20.0 (1)	0.0 (0)
	III (8)	50.0 (4)	12.5 (1)	25.0 (2)	12.5 (1)
	IV (7)	0.0 (0)	14.3 (1)	14.3 (1)	71.4 (5)
	V (13)	0.0 (0)	0.0 (0)	7.7 (1)	92.3 (12)
ACC	0-II (5)	40.0 (2)	20.0 (1)	20.0 (1)	20.0 (1)
	III (8)	12.5 (1)	62.5 (5)	12.5 (1)	12.5 (1)
	IV (7)	0.0 (0)	14.3 (1)	42.9 (3)	42.9 (3)
	V (13)	0.0 (0)	0.0 (0)	15.4 (2)	84.6 (11)
INS	0-II (5)	40.0 (2)	20.0 (1)	40.0 (2)	0.0 (0)
	III (8)	50.0 (4)	25.0 (1)	25.0 (1)	0.0 (0)
	IV (7)	14.3 (1)	0.0 (0)	57.1 (4)	28.6 (2)
	V (10)	0.0 (0)	0.0 (0)	30.0 (3)	70.0 (7)
S1	0-II (5)	60.0 (3)	0.0 (0)	40.0 (3)	0.0 (0)
	III (8)	50.0 (4)	25.0 (2)	25.0 (2)	0.0 (0)
	IV (7)	0.0 (0)	28.6 (2)	14.3 (1)	57.1 (4)
	V (10)	0.0 (0)	0.0 (0)	30.0 (3)	70.0 (7)
TH	0-II (5)	80.0 (4)	0.0 (0)	0.0 (0)	20.0 (1)
	III (8)	62.5 (5)	25.0 (2)	0.0 (0)	12.5 (1)
	IV (7)	14.3 (1)	14.3 (1)	28.6 (2)	42.9 (3)
	V (13)	0.0 (0)	0.0 (0)	15.4 (2)	84.6 (11)

A table representing the percentage of patients that displayed absent, mild, moderate or severe amyloid pathology grade, at individual Braak's stage of AD, in the supraspinal regions.

Abbreviations: n, number of subjects; ACC, anterior cingulate cortex; AMG, amygdala; INS, insula; PFC, prefrontal cortex; S1, primary somatosensory cortex; TH, thalamus.

4.3.4.3 **No Change in Amyloid Pathology in AD Cases Compared to AD Controls**

The mean 6E10 immunoreactivity grades in each brain area as well as at each individual Braak's stage are outlined in Table 4.7.

As AD-associated amyloid pathology was confirmed in the brain regions involved in the processing of pain, we assessed whether AD cases display any change in the extent of 6E10 immunoreactivity compared to the AD controls cohort. Over 80% of the individuals in AD controls group exhibited moderate to severe 6E10 immunoreactivity in each of the brain areas examined. In contrast, patients in the AD cases cohort displayed a lower percentage of cases (ranging from 53.8% to 71.4%) with moderate to severe graded amyloid pathology. However, analysis of 6E10 immunoreactive AD-associated profile grading showed no significant alteration in the prefrontal cortex (Mann-Whitney U Test, $p = 0.162$), amygdala (Mann-Whitney U Test, $p = 0.451$), anterior cingulate cortex (Mann-Whitney U Test, $p = 0.181$), insula (Mann-Whitney U Test, $p = 0.586$), primary somatosensory cortex (Mann-Whitney U Test, $p = 0.546$), and the thalamus (Mann-Whitney U Test, $p = 0.227$) of AD cases compared to AD controls.

Furthermore, analysis at each individual Braak's stage of AD also revealed unaltered (Mann-Whitney U Test, $p > 0.05$) severity of 6E10 immunopositive amyloid plaques in the prefrontal cortex, amygdala, anterior cingulate cortex, insula, primary somatosensory cortex and the thalamus of AD cases compered to AD controls cohort. However, a trend of lower proportion of AD cases displayed moderate to severe amyloid pathology at Braak's stages IV-V compared to AD controls. Collectively these data confirm the presence of amyloid pathology in the brain regions involved in pain processing but presence of chronic pain does not induce any alterations in AD individuals examined in the present study.

Table 4.7: Supraspinal Regional Amyloid Pathology Comparison Between AD Cases vs. AD Controls

Region	Braak's Stage	AD Controls (n)	AD Cases (n)	p-value *
	II-V	2.58 ± 0.23 (10/12)	1.85 ± 0.39 (8/13)	0.162
	II	-	0.00 ± 0.00 (0/1)	-
PFC	III	1.75 ± 0.48 (2/4)	0.33 ± 0.33 (0/3)	0.064
	IV	3.00 ± 0.00 (3/3)	2.00 ± 0.71 (3/4)	0.186
	V	3.00 ± 0.00 (5/5)	3.00 ± 0.00 (5/5)	1.000
	II-V	2.43 ± 0.29 (12/14)	2.14 ± 0.31 (10/14)	0.451
	II	-	0.00 ± 0.00 (0/1)	-
AMG	III	1.25 ± 0.75 (2/4)	1.00 ± 0.58 (1/3)	0.853
	IV	2.67 ± 0.33 (3/3)	2.50 ± 0.50 (3/4)	1.000
	V	3.00 ± 0.00 (7/7)	2.83 ± 0.17 (6/6)	0.280
	II-V	2.50 ± 0.20 (12/14)	2.00 ± 0.28 (9/14)	0.181
	II	-	0.00 ± 0.00 (0/1)	-
ACC	III	1.75 ± 0.48 (2/4)	1.00 ± 0.00 (0/3)	0.186
	IV	2.67 ± 0.33 (3/3)	2.00 ± 0.41 (3/4)	0.252
	V	2.86 ± 0.14 (7/7)	2.83 ± 0.17 (6/6)	0.909
	II-V	2.08 ± 0.26 (10/12)	1.69 ± 0.37 (8/13)	0.586
	II	-	0.00 ± 0.00 (0/1)	-
INS	III	1.25 ± 0.48 (2/4)	0.33 ± 0.33 (0/3)	0.190
	IV	2.33 ± 0.33 (3/3)	1.75 ± 0.63 (3/4)	0.554
	V	2.60 ± 0.25 (5/5)	2.80 ± 0.20 (5/5)	0.513
	II-V	2.17 ± 0.27 (10/12)	1.77 ± 0.36 (7/13)	0.546
	II	-	0.00 ± 0.00 (0/1)	-
S1	III	1.25 ± 0.48 (2/4)	0.33 ± 0.33 (0/3)	0.190
	IV	2.67 ± 0.33 (3/3)	2.00 ± 0.58 (2/4)	0.430
	V	2.60 ± 0.25 (5/5)	2.80 ± 0.20 (5/5)	0.513
	II-V	2.29 ± 0.30 (11/14)	1.71 ± 0.35 (8/14)	0.227
	II	-	0.00 ± 0.00 (0/1)	-
TH	III	1.00 ± 0.71 (1/4)	0.33 ± 0.33 (0/3)	0.554
	IV	2.67 ± 0.33 (3/3)	1.50 ± 0.65 (2/4)	0.195
	V	2.86 ± 0.14 (7/7)	2.83 ± 0.17 (6/6)	0.909

Data is presented as mean ± SEM (* Mann-Whitney U Test).

Abbreviations: n, number of moderate-severe patients/ total number of patients; ACC, anterior cingulate cortex; AMG, amygdala; INS, insula; PFC, prefrontal cortex; S1, primary somatosensory cortex; TH, thalamus.

4.3.4.4 **Amyloid Pathology Present in Spinal Cord**

Amyloid deposits have been reported to be present in the spinal cord individuals with AD (Ogomori et al 1989). Here, we confirm the presence of amyloid deposits in the spinal cord grey matter, both the dorsal (Figure 4.11A and C) and ventral (Figure 4.11B and D) horns. In order to assess whether presence of chronic pain has any impact of amyloid pathology in the spinal cord we recorded presence or absence of amyloid deposits in both the dorsal and ventral horns. A comparison between AD cases with AD controls revealed no significant difference AD-associated amyloid pathology in both the dorsal (AD control, 40.0% of patients; AD case, 50.0% of individuals; χ^2 Test, $p = 0.740$) and ventral (AD control, 40.0% of patients; AD case, 83.3% of individual; χ^2 Test, $p = 0.137$) horns of the spinal cord (Figure 4.11E-F). Thus, suggesting that chronic pain and/or persistent use of analgesics does not have any impact on the presence of amyloid pathology in the spinal cord of AD cases compared to their respective controls.

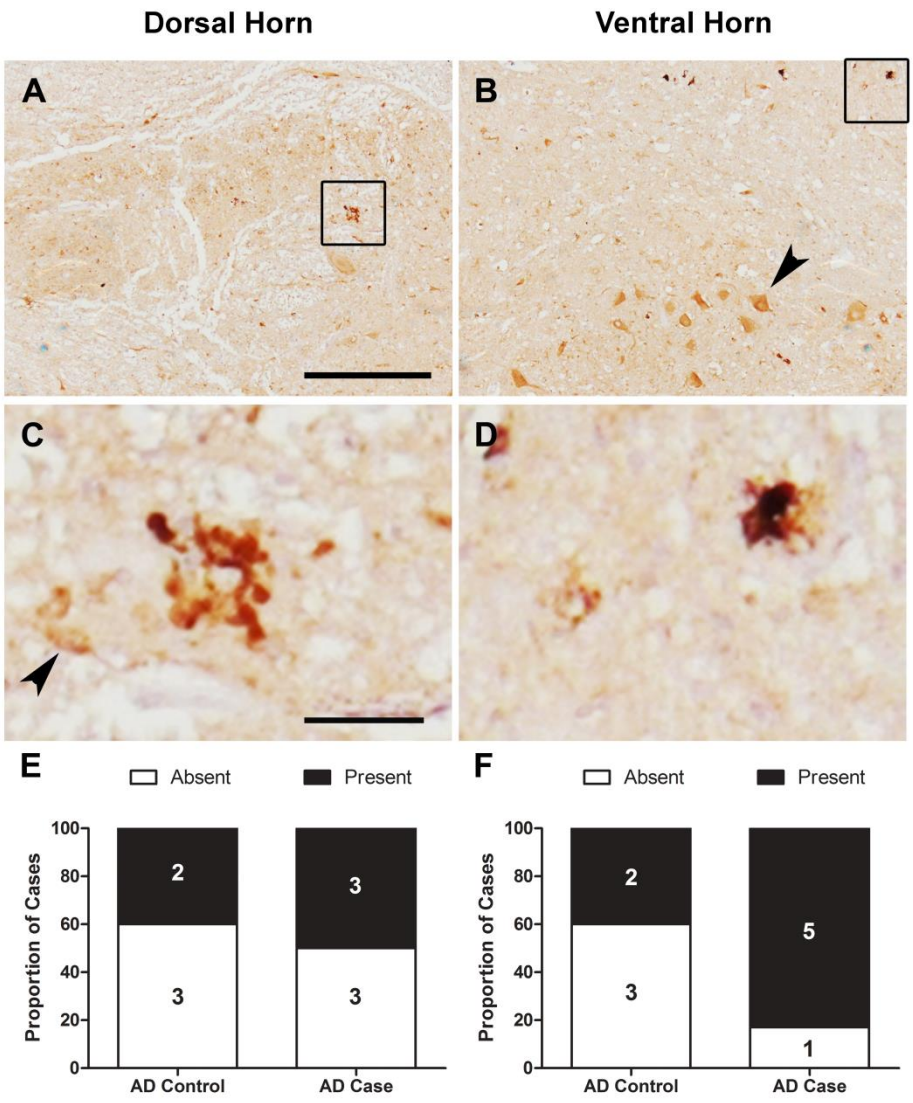

Figure 4.11: Aβ Deposition Present in the AD Spinal Cord

Representation of amyloid deposits in the dorsal (A) and ventral (B) horns of the spinal cord. A higher magnification image as indicated by the boxed-outline in A and B reveals Aβ deposition in the dorsal (C) and ventral (D) horns of the spinal cord, respectively. The arrowheads mark the intraneuronal accumulation of Aβ in the spinal cord. Examination of proportion of cases that displayed AD-related amyloid pathology revealed AD cases had comparable number of cases that displayed amyloid deposits in the dorsal (E) and ventral (F) horns compared to AD controls (χ^2 Test, $p > 0.05$). Data are presented as proportion of cases (n = 5-6). The scale bar represents: 500µm (A-B) and 60µm (C-D).

4.3.5 Microglial Response

In addition to the AD-associated pathological hallmarks, we assessed whether AD-related neuroinflammation is altered in AD individuals with chronic pain compared to their AD control group in the supraspinal structures. For this purpose, IBA1 was used as a pan-marker for microglia which is constrictively expressed by microglia and is upregulated in neuroinflammation. Microglial cells undergo morphological changes that reflect their motility, migration and activation properties (Minett et al 2016). The microglial morphologies were observed in six different forms that included: ramified (Figure 4.12A-C), hypertrophic (Figure 4.12D-E), dystrophic (Figure 4.12G-I), amoeboid (Figure 4.12J), rod-shaped (Figure 4.12K), and plaque associated (Figure 4.12L-N). Ramified microglia represent the 'surveying' non-reactive microglial morphology appearance which is characterised by thin and highly branched processes. Hypertrophic microglia is often called activated microglia that display an enlarged cell body accompanied by either hyper-ramified or short thick processes (Bachstetter et al 2015). Whilst, dystrophic microglia has been recognised to be an indication of microglial senescence in the aging human brain, which presents with processes that are shortened, gnarled, beaded, or fragmented cytoplasmic processes, as well as loss of fine ramifications and formation of spheroidal swelling (Streit et al 2014). Rod-shaped microglia are characterised by a narrow cell body with a few planer processes, although the physiological and/or pathological functions of this subset of microglia is still elusive (Bachstetter et al 2017). Amoeboid microglia are another form of an activated microglia phenotype that is characterised by an enlarged cell body and few to no processes (Bachstetter et al 2015, Ransohoff & Perry 2009).

A semi-quantitative grading analysis of IBA1 immunoreactive microglial frequency was carried out in only in the supraspinal regions that included: prefrontal cortex, amygdala, anterior cingulate cortex, insula, primary somatosensory cortex, and the thalamus. Figure 4.13 outlines the extent of IBA1-immunoreactivity graded in a range of thresholds from sparse, moderate to frequent in each individual supraspinal region. A strong internal consistency in microglial grading was evident using Cronbach's alpha statistics between the regional analysis of IBA1 immunoreactivity twice, a week apart, by the same observer (Cronbach's alpha = 0.920).

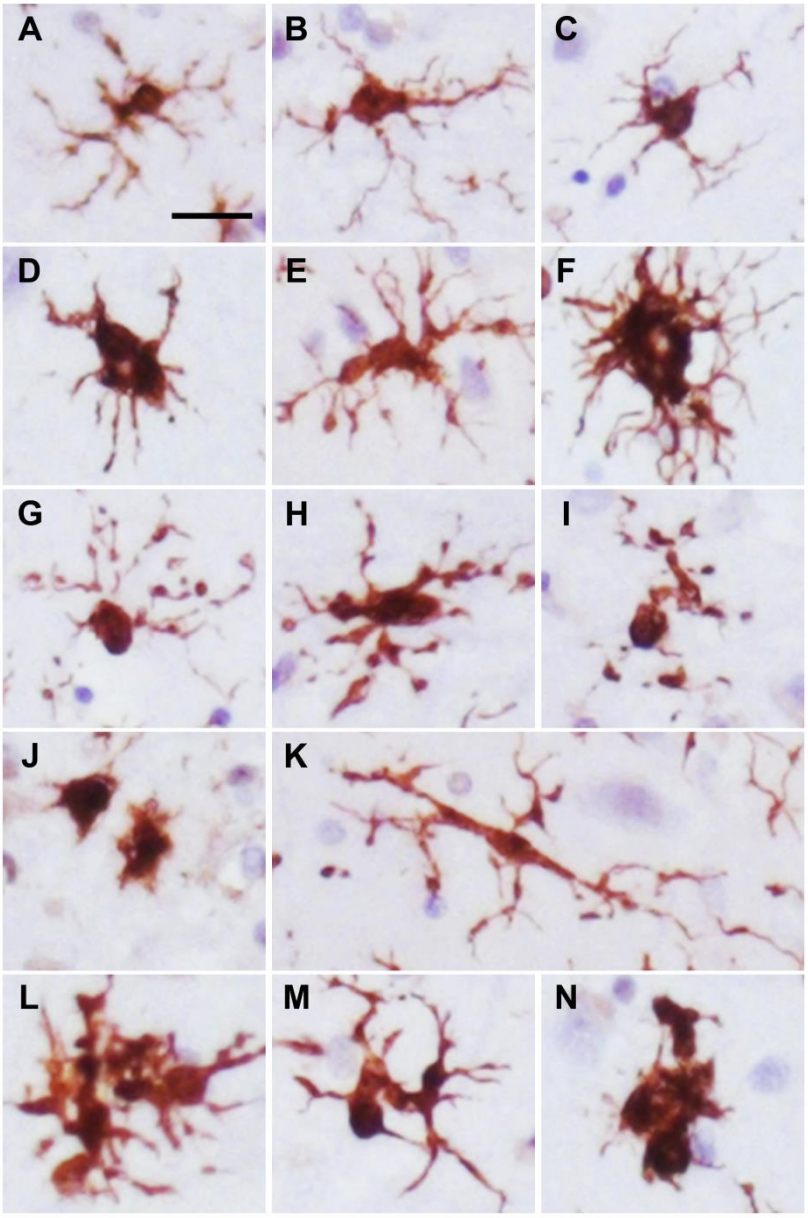

Figure 4.12: Representation of Microglial Morphology in the Brain

IBA1 labelled microglia representing six different morphologies: 1) ramified and surveying (A-C); 2) activated hypertrophic (D-F); 3) senescent dystrophic (G-I); 4) activated amoeboid (J); 5) rod-shaped (K); and 6) plaque associated microglia (L-N). Images were taken from the anterior cingulate cortex of control and AD individuals. The scale bar represents 25µm.

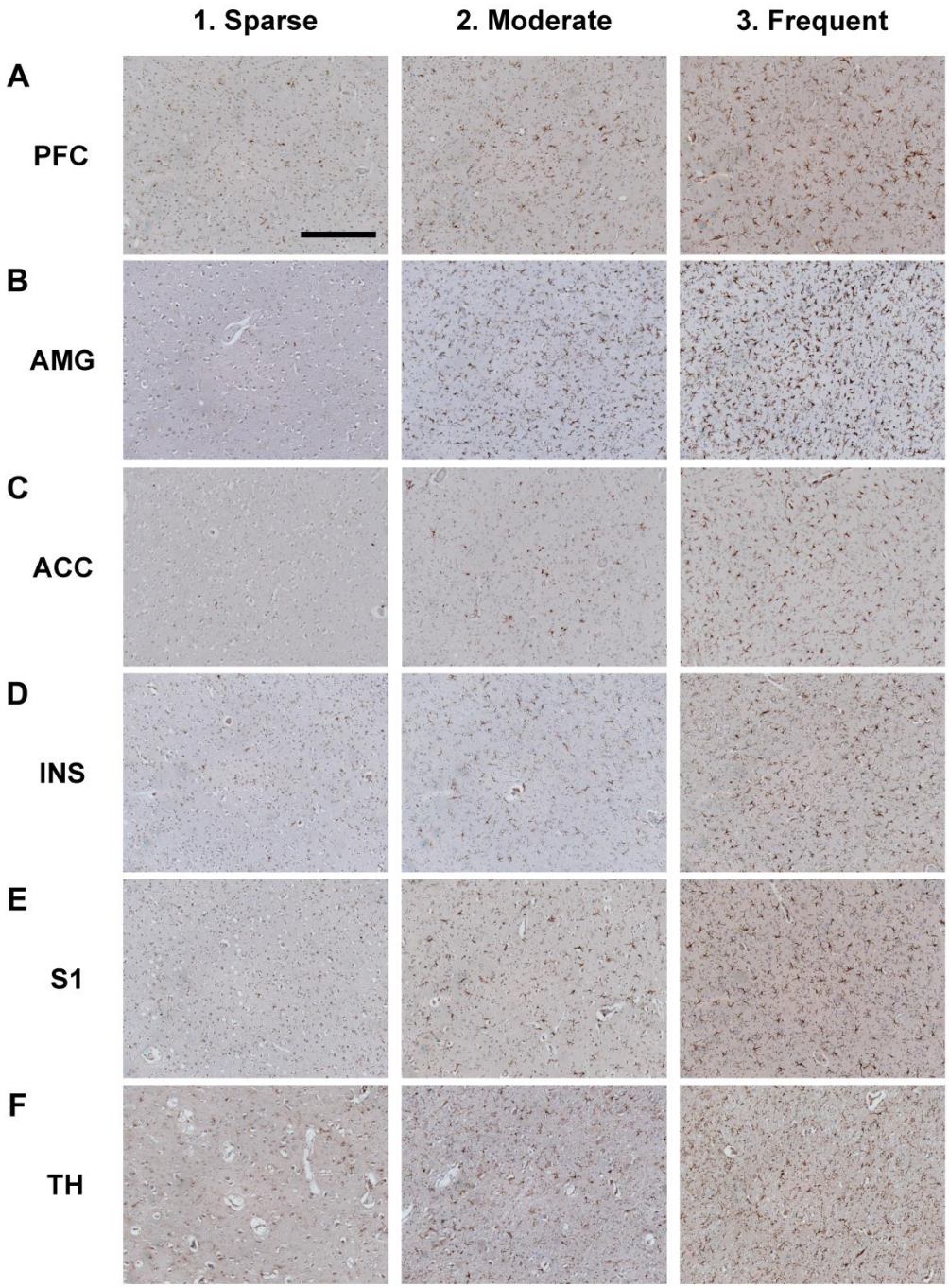

Figure 4.13: Supraspinal Regional Microglial Frequency Thresholds

A representation of sparse (1), moderate (2), and frequent (3) IBA1 immunoreactivity thresholds in the prefrontal cortex (PFC, A); amygdala (AMG, B); anterior cingulate cortex (ACC, C); insula (INS, D); primary somatosensory cortex (S1, E), and the thalamus (TH, F). All images were taken at ×10 stage objective and the scale bar represents 500µm.

4.3.5.1 **Microglial Frequency Not Associated with Progression of AD**

The percentage of subjects displaying a range of sparse to frequent IBA1 immunoreactive microglial frequency in the brain areas are outlined in Table 4.8.

Our data generally demonstrated greater frequency of IBA1 immunoreactive microglial cells in the cortical regions and amygdala at Braak's stage 0-II, which gradually declined with the progression AD progresses; however, this failed to reach any statistical significance. In the thalamus, there was also no alteration in microglial frequency grades observed with increasing Braak's stage. Statistical analysis of microglial frequency in relation to AD progression depicted no significant association between IBA1 immunoreactivity grading and Braak's stage of AD in the prefrontal cortex (ρ = -0.311, $p > 0.01$; R^2 = 0.111, $p > 0.01$), amygdala (ρ = -0.242, $p > 0.01$; R^2 = 0.060, $p > 0.01$), anterior cingulate cortex (ρ = -0.225, $p > 0.01$; R^2 = 0.044, $p > 0.01$), insula (ρ = -0.175, $p > 0.01$; R^2 = 0.037, $p > 0.01$), primary somatosensory cortex (ρ = -0.392, $p > 0.01$; R^2 = 0.149, $p > 0.01$), and the thalamus (ρ = 0.108, $p > 0.01$; R^2 = 0.009, $p > 0.01$). Thus, indicating that microglial frequency remains unaltered with the progression of AD. Although, a general trend of decline may represent the gradual deterioration and subsequent loss of microglial cells that may occur at a greater rate in neurodegeneration compared to healthy aging (Streit et al 2014).

Table 4.8: Regional Microglial Frequency - Percentage of Subjects

Region	Braak's (n)	Sparse (n)	Moderate (n)	Frequent (n)
PFC	0-II (5)	0.0 (0)	40.0 (2)	60.0 (3)
	III (8)	0.0 (0)	75.0 (6)	25.0 (2)
	IV (7)	0.0 (0)	42.9 (3)	57.1 (4)
	V (10)	30.0 (3)	50.0 (5)	20.0 (2)
AMG	0-II (5)	0.0 (0)	60.0 (3)	40.0 (2)
	III (8)	12.5 (1)	50.0 (4)	37.5 (3)
	IV (7)	14.3 (1)	42.9 (3)	42.9 (3)
	V (13)	30.8 (4)	46.2 (6)	23.1 (3)
ACC	0-II (5)	20.0 (1)	40.0 (2)	40.0 (2)
	III (8)	25.0 (2)	50.0 (4)	25.0 (2)
	IV (7)	0.0 (0)	71.4 (5)	28.6 (2)
	V (13)	30.8 (4)	61.5 (8)	7.7 (1)
INS	0-II (5)	0.0 (0)	60.0 (3)	40.0 (2)
	III (8)	25.0 (2)	12.5 (1)	62.5 (5)
	IV (7)	0.0 (0)	57.1 (4)	42.9 (3)
	V (10)	40.0 (4)	20.0 (2)	40.0 (4)
S1	0-II (5)	20.0 (1)	20.0 (1)	60.0 (3)
	III (8)	12.5 (1)	75.0 (6)	12.5 (1)
	IV (7)	0.0 (0)	71.4 (5)	28.6 (2)
	V (10)	40.0 (4)	60.0 (6)	0.0 (0)
TH	0-II (5)	20.0 (1)	20.0 (1)	60.0 (3)
	III (8)	25.0 (2)	37.5 (3)	37.5 (3)
	IV (7)	14.3 (1)	42.9 (3)	42.9 (3)
	V (13)	15.4 (2)	23.1 (3)	61.5 (8)

A table representing the percentage of subjects that displayed sparse, moderate or frequent microglial frequency grade, at individual Braak's stage of AD, in the supraspinal regions.

Abbreviations: n, number of subjects; ACC, anterior cingulate cortex; AMG, amygdala; INS, insula; PFC, prefrontal cortex; S1, primary somatosensory cortex; TH, thalamus.

4.3.5.2 **No Change in Microglial Frequency in AD Cases Compared to AD Controls**

The mean semi-quantitative grading of IBA1 immunopositive cell frequency in each brain area as well as at each individual Braak's stage is shown in Table 4.9.

In the quest to explore any alteration in AD-associated neuroinflammation in chronic pain conditions, we examined if there is any alteration in microglial frequency in AD cases compared to the AD controls group in the supraspinal structures. Patients in the AD cases group displayed relatively greater proportion of individuals with moderate to frequent microglial frequency grade in the prefrontal cortex (AD controls, 83.3% vs. AD cases, 92.3%), insula (AD controls, 58.3% vs. AD cases, 92.3%), primary somatosensory cortex (AD controls, 66.7% vs. AD cases, 92.3%), and the thalamus (AD controls, 71.4% vs. AD cases, 92.6%); whereas, comparable moderate-frequent IBA1 frequency grade were observed in the amygdala (AD controls, 78.6% vs. AD cases, 78.6%) and anterior cingulate cortex (AD controls, 78.6% vs. AD cases, 78.6%). However, statistical analysis failed to show any significant differences in microglial frequency in the prefrontal cortex (Mann-Whitney U Test, $p = 0.629$), amygdala (Mann-Whitney U Test, $p = 0.785$), anterior cingulate cortex (Mann-Whitney U Test, $p = 0.752$), insula (Mann-Whitney U Test, $p = 0.115$), primary somatosensory cortex (Mann-Whitney U Test, $p = 0.097$), and the thalamus (Mann-Whitney U Test, $p = 0.269$) of AD cases compared to AD controls.

Further analysis at each individual Braak's stage of AD also revealed unaltered (Mann-Whitney U Test, $p > 0.05$) frequency of IBA1 immunoreactive cells in the prefrontal cortex, amygdala, anterior cingulate cortex, insula, primary somatosensory cortex and the thalamus of AD cases compared to AD controls. Altogether these data indicate comparable microglial frequency in the supraspinal areas involved in pain processing of AD individuals with a clinical history of chronic pain and/or persistent use of analgesics compared to AD controls.

Table 4.9: Supraspinal Regional Microglial Frequency Comparison Between AD Case vs. AD Control

Region	Braak's Stage	AD Controls (n)	AD Cases (n)	p-value *
PFC	II-V	2.17 ± 0.21 (10/12)	2.31 ± 0.18 (12/13)	0.629
	II	-	3.00 ± - (1/1)	-
	III	2.50 ± 0.29 (4/4)	2.00 ± 0.00 (3/3)	0.180
	IV	2.33 ± 0.33 (3/3)	2.75 ± 0.25 (4/4)	0.307
	V	1.80 ± 0.37 (3/5)	2.00 ± 0.32 (4/5)	0.650
AMG	II-V	2.07 ± 0.20 (11/14)	2.14 ± 0.21 (11/14)	0.785
	II	-	3.00 ± - (1/1)	-
	III	2.25 ± 0.25 (4/4)	2.00 ± 0.58 (2/3)	0.693
	IV	2.00 ± 0.58 (2/3)	2.50 ± 0.29 (4/4)	0.445
	V	2.00 ± 0.31 (5/7)	1.83 ± 0.31 (4/6)	0.701
ACC	II-V	2.00 ± 0.15 (11/14)	2.07 ± 0.20 (11/14)	0.752
	II	-	3.00 ± - (1/1)	-
	III	2.00 ± 0.41 (3/4)	2.33 ± 0.33 (3/3)	0.554
	IV	2.00 ± 0.00 (3/3)	2.50 ± 0.29 (4/4)	0.180
	V	2.00 ± 0.22 (5/7)	1.50 ± 0.22 (3/6)	0.135
INS	II-V	1.92 ± 0.26 (7/12)	2.46 ± 0.18 (12/13)	0.115
	II	-	2.00 ± - (1/1)	-
	III	2.00 ± 0.58 (2/4)	2.67 ± 0.33 (3/3)	0.430
	IV	2.00 ± 0.00 (3/3)	2.75 ± 0.25 (4/4)	0.066
	V	1.80 ± 0.49 (2/5)	2.20 ± 0.37 (4/5)	0.502
S1	II-V	1.75 ± 0.18 (8/12)	2.15 ± 0.15 (12/13)	0.097
	II	-	3.00 ± - (1/1)	-
	III	2.00 ± 0.41 (3/4)	2.00 ± 0.00 (3/3)	1.000
	IV	2.00 ± 0.00 (3/3)	2.50 ± 0.29 (4/4)	0.180
	V	1.40 ± 0.25 (2/5)	1.80 ± 0.20 (4/5)	0.221
TH	II-V	2.14 ± 0.23 (10/14)	2.50 ± 0.17 (13/14)	0.269
	II	-	3.00 ± - (1/1)	-
	III	2.00 ± 0.58 (2/4)	2.00 ± 0.00 (3/3)	1.000
	IV	1.67 ± 0.33 (2/3)	2.75 ± 0.25 (4/4)	0.056
	V	2.43 ± 0.30 (6/7)	2.50 ± 0.34 (5/6)	0.805

Data is presented as mean ± SEM (* Mann-Whitney U Test).

Abbreviations: n, number of moderate-frequent patients/ total number of patients; ACC, anterior cingulate cortex; AMG, amygdala; INS, insula; PFC, prefrontal cortex; S1, primary somatosensory cortex; TH, thalamus.

4.3.6 Activated/Phagocytic Microglia

Having observed no significant alteration in the frequency of IBA1 immunoreactive cells in patients in the AD cases cohort, it was important to examine whether there was any evidence of a microglial phenotypic shift from 'surveying' ramified to activated and/or phagocytic morphology. For this purpose, CD68 a marker for lysosomal and endosomal transmembrane glycoprotein of microglia that indicates of phagocytic activity was utilised (Minett et al 2016). The CD68 immunoreactivity was observed in all IBA1 immunopositive morphologies reported in section 4.3.5 above, namely: ramified (Figure 4.14A), hypertrophic (Figure 4.14B), dystrophic (Figure 4.14C), rod-like (Figure 4.14D), and plaque associated (Figure 4.14E). Of particular note was that the plaque associated microglia exhibited the greatest intensity and area occupied by CD68 immunoreactivity, which may be indicative of the activated nature of this phenotype.

4.3.6.1 **Elevated Microglial Activation Exhibited by AD Cases in Supraspinal Structures**

In order to investigate whether individuals in the AD cases group exhibit any alteration in microglial activation, the percentage of IBA1 positive cells that were also immunoreactive for CD68 was recorded as displayed in Table 4.10 and Figure 4.15.

Our findings demonstrate, in the current sample of subjects, over 70% of IBA1 immunoreactive cells also expressed CD68, an implication for microglial activation. Individuals in the AD cases group exhibited significantly greater percentage of CD68 immunopositive microglia in the amygdala (AD controls, 72.5% ± 4.8% vs. AD cases, 85.9% ± 2.9%; Mann-Whitney U Test, $p = 0.027$), anterior cingulate cortex (AD controls, 94.5% ± 1.1% vs. AD cases, 97.5% ± 0.8%; Mann-Whitney U Test, $p = 0.021$), and primary somatosensory cortex (AD controls, 86.4% ± 2.4% vs. AD cases, 93.5% ± 1.7%; Mann-Whitney U Test, $p = 0.013$). Whereas, comparable proportions of IBA1 positive microglia were observed to co-express CD68 in the prefrontal cortex (AD controls, 80.6% ± 4.1% vs. AD cases, 83.6% ± 4.0%; Mann-Whitney U Test, $p = 0.463$), insula (AD controls, 82.0% ± 4.6% vs. AD cases, 81.5% ± 5.2%; Mann-Whitney U Test, $p = 0.849$), and the thalamus (AD controls, 95.2% ± 1.1% vs. AD cases, 97.1% ± 0.7%; Mann-Whitney U Test, $p = 0.257$) of AD cases when compared to AD controls. Therefore, suggesting that there may be an exacerbation of neuroinflammation in some if not all supraspinal regions of

the pain pathway of AD individuals with a history of chronic pain and/or persistent use of analgesics compared to their respective AD controls cohort.

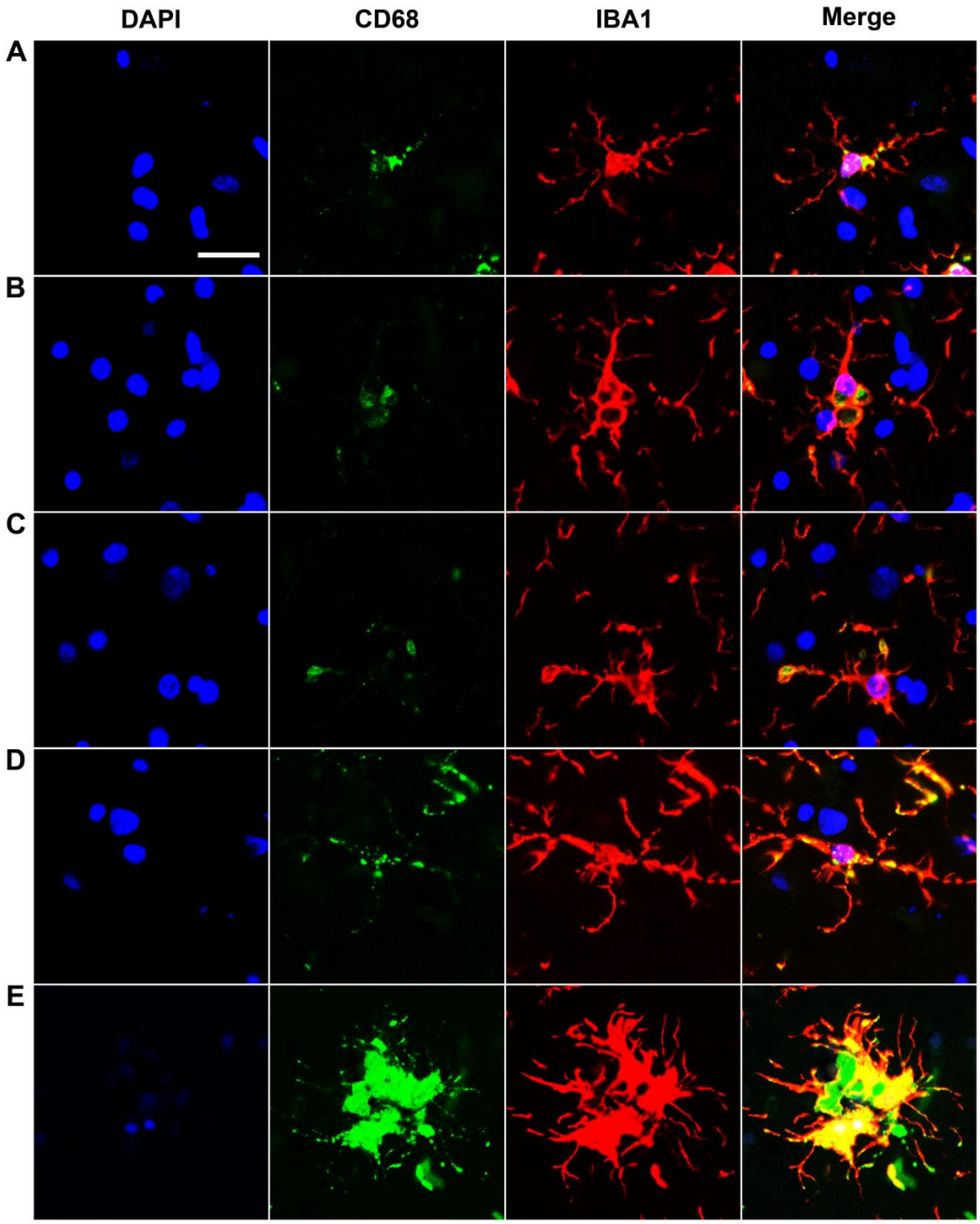

Figure 4.14: Representation of Activated/Phagocytic Microglia Morphology in the Brain

Representation of IBA1 labelled microglia that also expresses CD68, a marker for activation, in a diverse set of morphologies: 1) ramified and surveying (A); 2) activated hypertrophic (B); 3) senescent dystrophic (C); 4) rod-shaped (D); and 5) plaque associated microglia (E). All images were taken from the anterior cingulate cortex of AD individuals. The scale bar represents 25µm.

In order to investigate the stage of AD in which microglial activation is altered in the supraspinal structures of AD cases, an in-depth analysis at each individual Braak's stage for each supraspinal structure: prefrontal cortex (Figure 4.16A), amygdala (Figure 4.16B), anterior cingulate cortex (Figure 4.16C), insula (Figure 4.16D), primary somatosensory cortex (Figure 4.16E), and the thalamus (Figure 4.16F) were conducted. Quantitative assessment of individual supraspinal regions revealed significantly greater percentage of activated CD68 expressing IBA1 cells in the primary somatosensory cortex at Braaks' stage IV (Mann Whitney U Test, $p = 0.034$) and in the prefrontal cortex, amygdala, and anterior cingulate cortex of AD cases cohort especially at Braak's stage V (Mann-Whitney U Test $p < 0.05$). Trends of increased microglial activation were observed in AD cases at Braak's stage IV and V in all supraspinal regions apart from the thalamus. These findings suggest an exacerbation of neuroinflammation in the CNS in AD individuals with chronic pain and/or persistent use of analgesics. A finding which is further strengthened by our preclinical data which illustrate an increased microglial response in the thalamus of monosodium-iodoacetate (MIA) induced OA in the TASTPM model of AD (reported in Chapter 3).

Collectively, these data demonstrate that AD cases exhibit elevated microglial activation in the spinal cord and supraspinal regions, namely, amygdala, anterior cingulate cortex, and primary somatosensory cortex, which are involved in processing nociceptive information. Thus, implicating chronic pain and/or persistent analgesic use exacerbates neuroinflammation in key regions of the pain pathway.

Table 4.10: Supraspinal Regional Percentage of Activated/Phagocytic Microglia - A Comparison Between AD Case vs. AD Control

Region	Braak's Stage	AD Controls	AD Cases	p-value *
	II-V	80.6 ± 4.1	83.6 ± 4.0	0.463
	II	-	97.37 ± -	-
PFC	III	83.7 ± 11.3	67.6 ± 9.2	0.157
	IV	82.7 ± 5.8	87.1 ± 6.1	0.480
	V	**76.8 ± 4.5**	**87.8 ± 4.8**	**0.047**
	II-V	**72.5 ± 4.8**	**85.9 ± 2.9**	**0.027**
	II	-	100.0 ± -	-
AMG	III	**87.2 ± 1.0**	**78.2 ± 3.6**	**0.032**
	IV	76.5 ± 8.2	93.4 ± 2.3	0.077
	V	**62.3 ± 7.2**	**82.5 ± 4.9**	**0.022**
	II-V	**94.5 ± 1.1**	**97.53 ± 0.76**	**0.021**
	II	-	97.16 ± -	-
ACC	III	97.1 ± 1.4	96.1 ± 2.1	0.480
	IV	96.0 ± 1.2	98.4 ± 0.5	0.157
	V	**92.44 ± 1.8**	**97.7 ± 1.5**	**0.015**
	II-V	82.0 ± 4.6	81.5 ± 5.2	0.849
	II	-	100.0 ± -	-
INS	III	86.7 ± 10.0	64.7 ± 14.3	0.157
	IV	78.5 ± 7.7	85.4 ± 7.7	0.289
	V	80.4 ± 7.3	84.8 ± 6.8	0.602
	II-V	**86.4 ± 2.4**	**93.5 ± 1.7**	**0.013**
	II	-	100.0 ± -	-
S1	III	86.7 ± 6.6	88.8 ± 4.2	1.000
	IV	**88.7 ± 2.4**	**97.0 ± 1.2**	**0.034**
	V	84.9 ± 2.8	92.2 ± 2.7	0.094
	II-V	95.2 ± 1.1	97.1 ± 0.71	0.257
	II	-	98.1 ± -	-
TH	III	96.6 ± 2.0	97.9 ± 1.2	0.858
	IV	96.5 ± 1.8	97.7 ± 1.3	0.593
	V	93.8 ± 1.8	96.1 ± 1.4	0.389

Data is presented as mean percentage of IBA1 immunopositive cells expressing CD68 ± SEM (* Mann-Whitney U Test).

Abbreviations: ACC, anterior cingulate cortex; AMG, amygdala; INS, insula; PFC, prefrontal cortex; S1, primary somatosensory cortex; TH, thalamus.

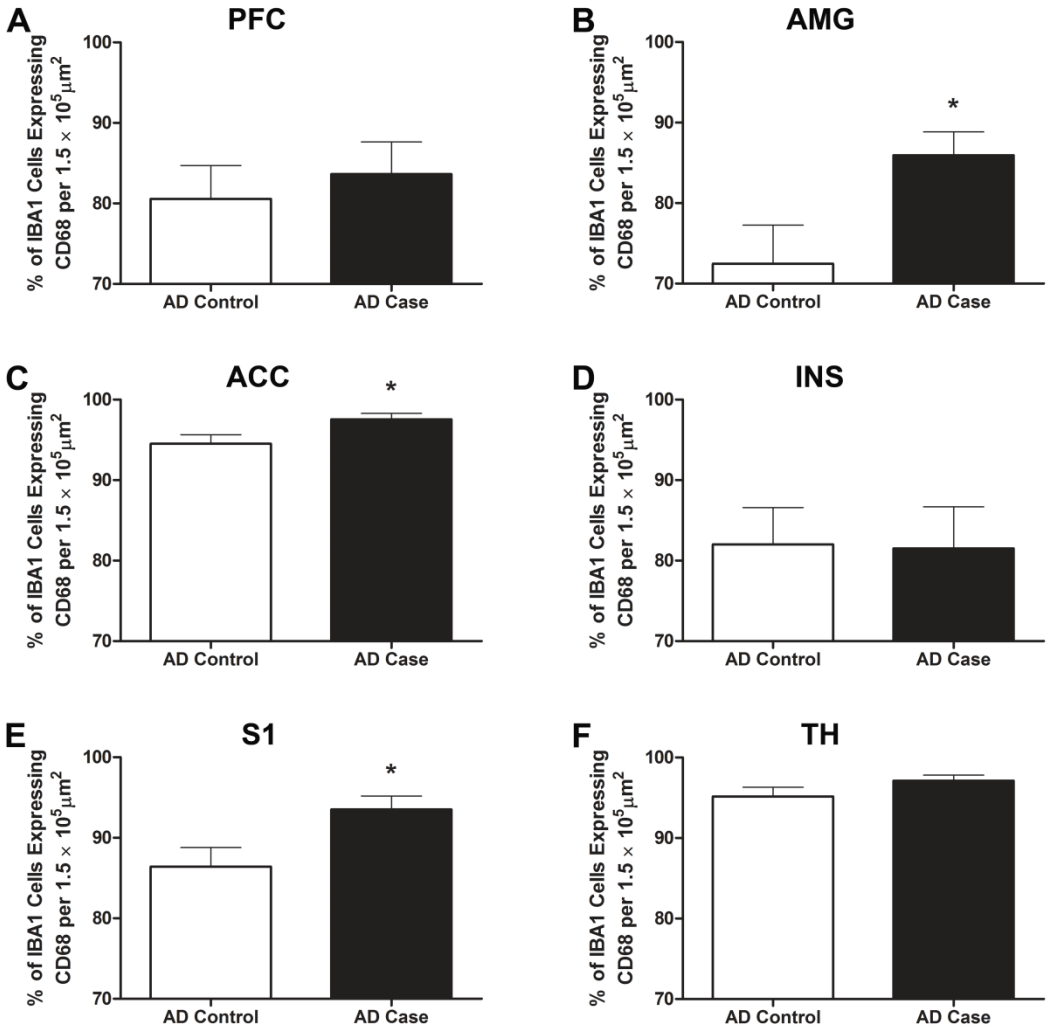

Figure 4.15: Increased Supraspinal Activated/Phagocytic Microglia in AD Individuals with Chronic Pain/Persistent Analgesic Use

Representation of AD case-control comparison in individual supraspinal regions involved in the pain pathway namely, the prefrontal cortex (PFC, A), amygdala (AMG, B); anterior cingulate cortex (ACC, C); insula (INS, D); primary somatosensory cortex (S1, E), and the thalamus (TH, F). AD cases displayed a general trend of increased microglial activation in each of the region examined with significant differences only detected in the amygdala (B), ACC (D) and the S1 (E) compared to the AD controls cohort (Mann-Whitney U Test, * $p < 0.05$). Data are presented as mean ± SEM (n = 12-14).

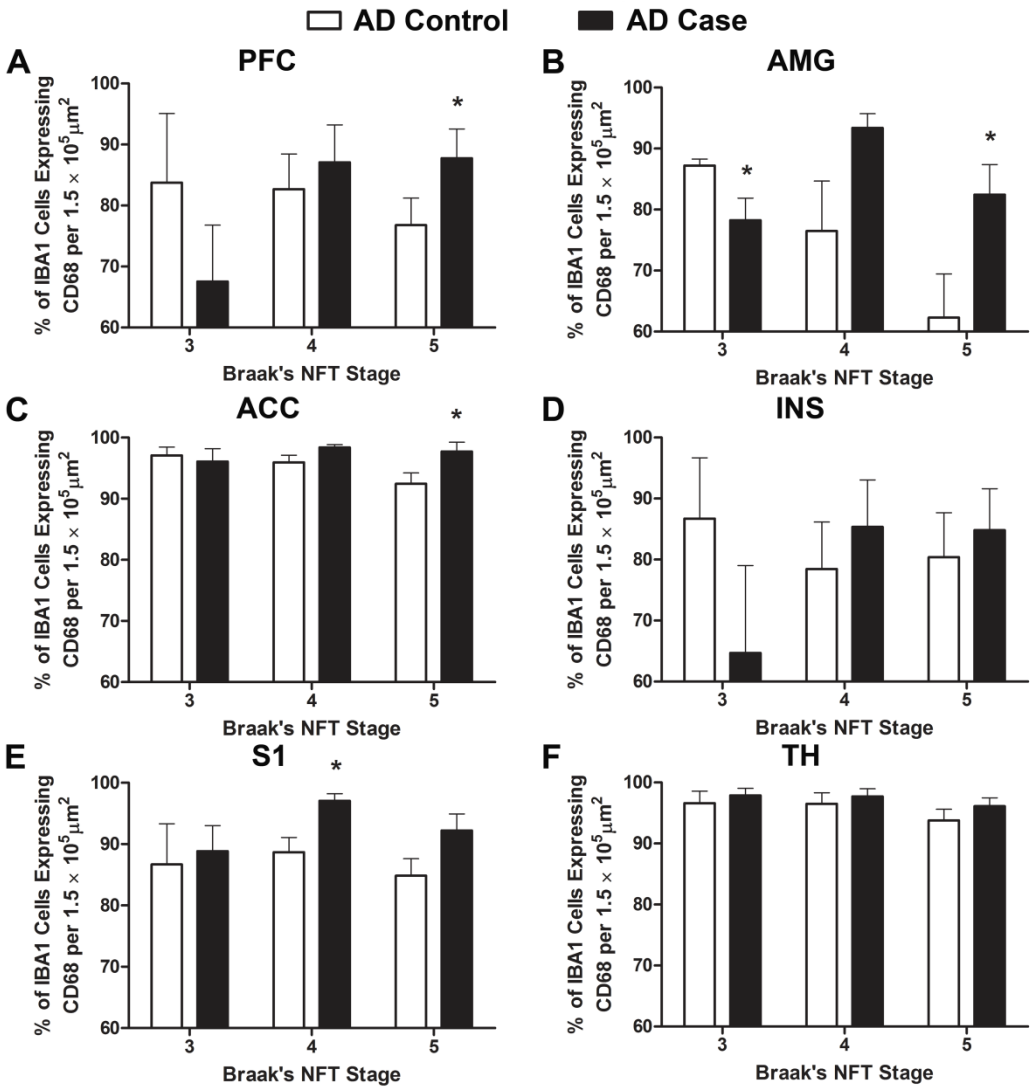

Figure 4.16: Increased Supraspinal Activated/Phagocytic Microglia in AD Individuals with Chronic Pain/Persistent Analgesic Use Predominantly at Braak's Stage V

Representation of AD case-control comparison at each individual Braak's stage in individual supraspinal regions involved in the pain pathway namely, the prefrontal cortex (PFC, A), amygdala (AMG, B); anterior cingulate cortex (ACC, C); insula (INS, D); primary somatosensory cortex (S1, E), and the thalamus (TH, F). AD cases displayed a trend of increased percentage of activated microglial cells generally at Braak's stage IV and V, which only reached significance in the S1 at Braak's stage IV and in PFC, amygdala and ACC at Braak's stage V (Mann-Whitney U Test, * $p < 0.05$). Data are presented as mean ± SEM (n = 3-7).

4.3.6.2 **Increase in Activated/Phagocytic Microglia Exhibited by AD Cases in the Spinal Cord**

Likewise to supraspinal structures, quantification of the percentage of IBA1 immunopositive cells that also expressed CD68 in the dorsal horn of the AD cases spinal cord revealed significantly greater percentage of co-localised cells compared to the AD controls group (Figure 4.17). As a result, indicating that there may be an increase in the spinal cord microglial activation of AD individuals that experience a chronic pain condition and/or persistent use of analgesics.

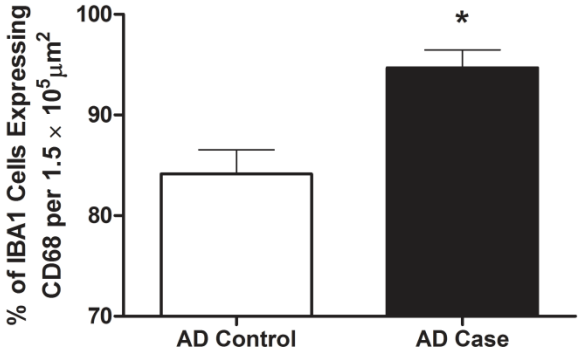

Figure 4.17: Greater Level of Activated/Phagocytic Microglia in the Spinal Cord of AD Individuals with Chronic Pain/Persistent Analgesic Use

AD cases displayed significantly higher percentage of IBA1 immunopositive microglial cells expressing CD68 compared to AD controls cohort (* $p < 0.05$, Mann-Whitney Rank Sum Test). Data values are presented as percentage mean ± SEM (n = 5-6)

4.4 Discussion

The aim of the present chapter was to investigate whether AD-associated neuropathological hallmarks and neuroinflammation in key regions of the pain pathway are altered in the presence of a chronic pain condition in individuals with AD. Here, we report and confirm the presence of AD-associated hyperphosphorylated tau inclusions and deposition of amyloid plaques in supraspinal areas involved in processing of nociceptive inputs; however only the amyloid plaques were apparent in the spinal cord grey matter. The principle findings of this work is that chronic pain in AD subjects may exacerbate neuroinflammation in regions involved in multidimensional processing of pain as these individual exhibited greater level of microglial activation in the amygdala, anterior cingulate cortex, primary somatosensory cortex and the spinal cord dorsal horn. Whereas AD-associated pathological hallmarks, NFT and amyloid plaques, remain relatively unaffected in AD cases when compared to AD controls. Therefore, implicating the presence of a chronic pain condition may underlie the increased microglial activity depicted by AD patients.

Intracellular inclusion of hyperphosphorylated tau in the form of NFT and extracellular amyloid plaques composed of aggregated Aβ represent the pathological hallmark of AD accompanied by cortical atrophy, neuroinflammation and synaptic dysfunction (Serrano-Pozo et al 2011). Severe, atrophy has been reported in the thalamic nuclei, anterior cingulate cortex, insula, amygdala and the hippocampus (Cho et al 2014, de Jong et al 2008, Scherder et al 2003). As expected, Aβ and NFT lesions were evident in these regions undergoing atrophy, which initially appear as occasional deposits in the cortical regions (prefrontal cortex, anterior cingulate cortex, and insula), amygdala, and the thalamus of AD subjects at Braak's stage II and Braak's stage III, respectively. Both, tau and amyloid lesions increase in severity with progression of AD. These findings are in line with evidence for the appearance of amyloid pathology preceding the deposition of aggregated tau in AD (Hardy & Higgins 1992). Therefore, this supports the hypothesis that appearance Aβ pathology is an earlier event in AD which leads to development of NFT and subsequent neurodegeneration.

Clinical experimental studies in the past have demonstrated alteration in the emotional aspect of pain with elevated pain tolerance and blunted autonomic responses to noxious stimuli in AD patients; whilst the sensory-discriminative component of pain is preserved (Benedetti et al 2004, Benedetti et al 1999, Rainero et al 2000). As aforementioned, the medial pain system is responsible for mediating the emotional-affective and cognitive-evaluative processing of nociceptive input, which is composed of the medial thalamic nuclei, amygdala, prefrontal cortex, anterior cingulate cortex, hypothalamus and the insula. Thus, presence of AD-associated lesions accompanied by neuronal cell death in these regions incline towards postulating the proposition that neuropathology in supraspinal areas that are involved in pain processing may induce an alteration in the non-discriminative aspect of pain in AD. As a result, individuals with AD may be more susceptible for alterations in pain perception owing to the dysfunction in regions that are involved in processing nociceptive inputs.

Although changes in the medial pain system, responsible for the emotional aspect of pain, were proposed in the past to underlie alteration in the perception of pain in AD, work carried out more recently demonstrates that there may also be an alteration in the sensory component of pain. Evidence provided by Cole et al. (2006) and Monroe et al. (Monroe et al 2016) showed that AD individuals compared to healthy controls exhibited higher pain thresholds to just noticeable pain and reduced sensitivity to noxious heat, respectively. As a result, implicating that there may be changes that also occur in the lateral pain system of individuals with AD that could possibly underlie the reduced sensitivity to noxious stimuli. These data highlight the importance of assessing regions involved in the lateral pain system and examining any AD-related dysfunction.

Thus, examination of regions involved in the lateral pain system, namely the primary somatosensory cortex and VL/VPL nucleus revealed AD-associated neuropathological changes in the form of intracellular NFT and extracellular amyloid plaques. In addition, we report, differently to previous findings, moderate to severe NFT and Aβ pathologies in primary somatosensory cortex of over 70% of the AD individuals at Braak's stage IV and exclusively in patients examined at Braak's stage V; which in the past has been reported to be generally less severely affected (Arnold 2000, Braak & Braak 1991b). Based upon evidence in the literature

there is a consensus that although modest degree of cortical atrophy is a macroscopic hallmark of AD, the primary motor, sensory and visual cortices have a greater tendency to be unaffected (Perl 2010). Therefore, our observation of moderate to severe AD-associated neuropathology in the primary somatosensory cortex appearing at Braak's stage IV should be taken with caution and further studies are warranted to re-evaluate the level of neuropathology and neurodegeneration affecting the primary sensory areas in individuals with AD.

Furthermore, neuropathology in the lateral thalamic nuclei in AD has rarely been examined in the past (Scherder et al 2003), but in the present study we provide evidence for NFT and amyloid plaques in the VL/VPL nuclei of the thalamus. In particular, we report mild-moderate tau and moderate to severe amyloid pathology in the VL/VPL nuclei at the late stages of AD (Braak's stage V). Previous studies have shown amyloid deposition and neurofibrillary changes in the anterior thalamic nuclei complex, reticular and the intra-laminar thalamic nuclei mainly in relation to the limbic system and a possible involvement in the alteration of non-discriminative processing of pain, i.e. autonomic, emotional and nocifensive reactions to painful stimuli, via the medial pain system in AD (Braak & Braak 1991a, Ogomori et al 1989, Rub et al 2002). Whereas, findings from the present study highlight the importance lateral thalamic nuclei, which also exhibits alterations in tau pathology accompanied by amyloid plaques in AD that could possibly underlie the altered sensory-discriminative dimension of pain perception described in individuals with AD.

Moreover in the present study we confirm findings by Ogomori and colleagues (1989) of amyloid deposits in the spinal cord of AD subjects. However, here we report amyloid deposits in ventral horn of 64% and dorsal horn of 45% of subjects examined, which is somewhat greater than the 33% of AD individuals reported by Ogomori and co-workers. Thus, it can implicate deposition of aggregated Aβ in the spinal cord and within the dorsal horn of the spinal cord may contribute to alteration in nociceptive input processing and projection in patients AD. However, in contrast to studies reporting neurofibrillary changes, we failed to detect any neuropathological hyperphosphorylated tau lesions in the spinal cord grey matter (Dugger et al 2013, Guo et al 2016, Saito & Murayama 2000, Schmidt et al 2001). The underlying reason for this is unclear, but one plausible explanation could be the choice of antibody AT8, which has shown to be

possess a reduced ability to detect neurofibrillary changes in the spinal cord in comparison to other antibodies, in particular against paired-helical filament 1 (Schmidt et al 2001).

Altogether, in the present study we show only amyloid changes in spinal cord in parallel with neurofibrillary and amyloid changes in supraspinal regions involved in both the medial and lateral pain systems involved in nociceptive processing of AD individuals. In addition, these regions become increasingly affected with the progression of AD, which may result in alteration of pain processing and consequently lead to the altered perception of pain sensation in these individuals.

The novelty of the present study was the examination of AD-associated pathological changes in AD individuals with a history of chronic pain condition. Despite, AD-associated neuropathological changes reported often in the supraspinal areas involved in processing of nociceptive inputs, no study till date, in our knowledge, has attempted to examine whether there are any pathological alterations in the same areas of AD individuals experiencing a chronic pain condition compared to AD controls cohort. Here we provide evidence for unaltered NFT and amyloid plaque severity in the prefrontal cortex, amygdala, anterior cingulate cortex, insula, primary somatosensory cortex, and the thalamus of AD individuals with a clinical history of chronic pain and/or persistent use of analgesics compared to AD controls. In addition, we failed to detect any difference in proportion of AD cases displaying any alteration in amyloid deposition compared to AD controls in spinal cord grey matter, neither dorsal nor ventral horns. Therefore, these data implicate that despite the presence of amyloid plaques deposition in the spinal cord as well as tau and amyloid lesions in supraspinal regions involved in the medial and lateral pain systems, a chronic pain condition and/or persistent use of analgesics in itself do not potentially have an impact on AD-associated neuropathological hallmarks. Therefore, suggesting that the level of AD-associated neuropathology induced dysfunction in these regions is maintained in a chronic pain condition in comparison to AD individuals with no pain report.

Epidemiological evidence reviewed by McGeer and co-worker (2016) suggest AD individuals are relatively spared if they have been using anti-inflammatory analgesics (i.e. NSAID) or have suffered with conditions, such as rheumatoid arthritis, where such drugs are routinely used. Although we observed no alteration in tau and amyloid pathology exhibited by AD patients with

a clinical history of chronic and/or persistent use of analgesics in the present study, our data does show a trend of a delay, although insignificant, in the development of moderate to severe pathology in these individuals as it becomes apparent at a later Braak's NFT stage compared to the AD controls cohort. Hence this may implicate a delay in the progression of AD pathological hallmarks in patients with chronic pain as up to approximately 36% of these individuals routinely use anti-inflammatory analgesics.

In AD neuroinflammation is defined by reactive glial cell (astrocytes and microglia) morphologies and is shown to actively play an important role in the pathogenesis of the disease (Heneka et al 2015). Our data demonstrated gradual but an insignificant decline in microglial response in relation to the progression of Braak's stage of AD in all supraspinal structures, except the thalamus where no alteration was observed. The underlying reason for this observation is unclear, but a plausible explanation could be that neuroinflammation is an early phenomenon of AD and/or that it may not just be the frequency but the phenotype which may be of greater importance in determining the different functions carried out by microglia in the disease (Heneka et al 2015, Minett et al 2016). In addition, it has been postulated that microglia in the early phase may play a role in clearance of Aβ via phagocytosis and is considered beneficial. However, over a period of time this microglial response fails to keep up with rate of Aβ production, which in turn leads to release of a plethora of cytotoxic cytokines and chemokines that induce neurodegeneration. Thus, chronic inflammation induced by Aβ turnover in AD results in inefficient clearance of amyloid depositions owing to the compromised microglial function characterised by the insufficient microglial capacity to carry out phagocytosis (Heneka et al 2015). As a result, gradual deterioration (i.e. dystrophy) and subsequent loss of microglial cells may occur at a greater rate in AD neurodegeneration compared to healthy aging (Streit et al 2014).

We show that AD cases with a clinical history of pain and/or persistent use of analgesics did not exhibit any alteration in the number of microglia in any of the supraspinal regions examined compared to their AD controls counterpart. However, using marker for microglial activation/phagocytosis (CD68) demonstrated AD patients with a history of chronic pain and/or persistent use of analgesics displayed significantly greater level of microglial activation in the

amygdala, anterior cingulate cortex, primary somatosensory cortex, and the spinal cord when compared to the AD controls cohort, despite no actual change in the frequency of IBA1 immunopositive microglial cells. Hence, indicating that it may not be only the frequency but also the functional state of the microglial cells that could help in understanding the contribution in inducing neuroinflammation (Minett et al 2016).

As aforementioned, the spinal cord dorsal horn receives peripheral nociceptive input which is processed and propagated via projection neurons to the thalamus through the spinothalamic tract. The thalamus, a relay for the sensory information, transmit the nociceptive information to sub-cortical and cortical regions including the primary somatosensory cortex where the intensity and location of pain is processed; as well as the amygdala and anterior cingulate cortex which are involved in the emotional-affective and the cognitive-evaluative aspect of pain perception (Willis & Westlund 1997). Thus, increase in microglial activation may represent exacerbated neuroinflammation along the pain pathway of AD individuals with a clinical history of chronic pain and/or persistent use of analgesics compared to AD controls. Based upon these observations, one could propose that the chronic pain condition may be the contributing factor in the elevated level of microglial activation. Indeed, evidence in the literature has suggested peripheral immune response can induce and/or aggravate, via blood-borne pro-inflammatory cytokines, neuroinflammation in the CNS, which could possibly explain increased microglial activation in AD cases with chronic pain (Heneka et al 2015, Perry & Teeling 2013). Therefore, our results implicate exacerbated microglial activation independent of AD-associated neuropathological amyloid and tau lesions which may exist due to the chronic pain condition exhibited by AD individuals.

In principle, the findings of this study highlight the changes in AD-associated pathology and neuroinflammation in key regions of the pain pathway that may be affected, which could potentially underlie the altered perception of pain in AD individuals. Given the advancements in the field of neuroimaging for PET-tracers for tau (e.g. ^{18}F-AV1451), Aβ (e.g. ^{11}C-PiB), and microglial activation (e.g. ^{11}C-(R)PK11195) it would be of great interest to evaluate longitudinal changes in these PET-tracers amongst AD individuals diagnosed with chronic pain compared to AD individuals with no pain condition (Cagnin et al 2001a, Villemagne et al 2017). Evidence

from such studies could potentially allow identification of supraspinal regions that display alterations in AD-related pathology and microglial activation which could in turn possibly aid in understanding the possible mechanisms of pain in AD. A better understanding of the underlying mechanisms of pain in AD would pave paths towards developing novel therapeutic interventions and essentially improved management of pain in these individuals.

In conclusion, despite the limitations inherent to any human post-mortem study, the major value of studying the human tissue in this way is that it allows identification of AD-associated pathological lesions as well as inflammatory changes that may coincide in AD cases with a clinical history of chronic pain compared to neuropathologically confirmed AD but no clinical record of chronic pain. The AD-related pathological hallmarks (amyloid deposits and NFT) were evident in all supraspinal regions involved in multidimensional processing of pain whilst only amyloid deposits evident in the spinal cord. Presence of a chronic pain condition did not alter AD-associated pathology however aggravated spinal and supraspinal microglial activation. Therefore, the present study indicates that there may be an exacerbation of neuroinflammatory response exhibited by AD patients experiencing chronic pain.

Collectively, in this chapter we highlight the neuropathological and inflammatory changes that take place in the key spinal and supraspinal regions involved in multidimensional processing of pain of AD individuals. We have demonstrated that human post mortem tissue displays exacerbated microglial activation independent of changes in AD-associated tau and amyloid pathologies in individuals with a history of chronic pain when compared to AD controls. Based on the sample size in the present study, it was difficult to assess the impact of different analgesics or pain conditions on the progression and/or extent of AD-related pathologies and inflammation. Therefore, a larger cohorts of AD patients that are diagnosed with different chronic pain conditions (i.e. OA and rheumatoid arthritis) and/or routinely taking different analgesics (i.e. opioid, NSAIDs or paracetamol) would be required in order to evaluate whether it is the pain condition on its own, or the combination with the analgesics used for pain management responsible for the alterations in the pain pathway. An ideal future study would be to carry out neuroimaging PET study as discussed above for further investigate the changes in the supraspinal structures of AD individuals with chronic pain condition compared to AD

controls. Altogether it would aid in revealing the alterations in pain mechanisms in AD which will in turn allow the development of new therapeutic targets for improving the clinical management of pain these individuals.

4.4.1 Chapter Key Findings

In the present chapter, we provide pathological evidence for AD-associated changes affecting key regions involved in the pain pathway in human AD. In particular, we have shown:

- AD-associated amyloid plaques and NFT were present in the supraspinal areas involved in pain processing, with the amyloid plaques also evident in the spinal cord, in human AD post-mortem tissue.
- Experience of a chronic pain condition/ persistent analgesic use in AD subjects did not alter the severity of AD-associated pathological hallmarks; however, it did correlate with exacerbated ongoing neuroinflammation in the spinal cord and supraspinal regions.

These data suggest an exacerbation of ongoing neuroinflammation in AD patients with a history of chronic pain/persistent analgesic use.

Chapter 5 General Discussion

5.1 Summary of Findings

The aim of the studies presented in this thesis was to explore and elucidate the underlying mechanisms of pain in Alzheimer's disease (AD). For this purpose, we utilised the double-mutant TASTPM mouse model of AD and human post-mortem tissue obtained from AD individuals with a clinical record of chronic pain, using AD without any reported pain as controls. In the preclinical TASTPM model we assessed nocifensive behavioural changes and associated plasticity in both, the periphery and central nervous system (CNS), following acute noxious stimulation as well as in a model of osteoarthritis (OA) chronic pain induced by an intra-articular administration of monosodium Iodoacetate (MIA) in the knee joint. In addition, we analysed AD-associated neuropathological hallmarks (i.e. extracellular β-amyloid (Aβ) plaques and intracellular neurofibrillary tangles (NFT)) and neuroinflammation (i.e. microgliosis) in both, the preclinical TASTPM mouse model as well as AD human post-mortem tissue, in key regions involved in pain transmission and processing, namely the spinal cord and thalamus, in order to evaluate the contribution of AD-associated pathology on the perception of physiological nociception and in pathological pain conditions. The principle findings of this thesis are:

1. Age-dependent reduced sensitivity to acute thermal stimulation in TASTPM model of AD, which coincided with impairment of cognition and AD-related pathology in the form of deposition of amyloid plaques in the brain and intraneuronal accumulation of APP/Aβ in the spinal cord at the age of 6 months old.
2. Impairment in mechanical thresholds, mechanical hyposensitivity, was associated with the formation of amyloid plaques in the spinal cord of 12 months old TASTPM mice.
3. Inability to develop ongoing pain and reduced susceptibility in maintenance of chronic OA pain following an intra-articular administration of MIA in 6 months old TASTPM mice was associated with diminished MIA-induced spinal microgliosis.
4. Pathological OA condition exacerbated supraspinal neuroinflammation in the thalamus of the transgenic TASTPM mice without any impact on thalamic amyloid depositions.
5. A common mechanism underlying the reduced sensitivity to acute nociception and impaired persistence of OA-associated allodynia was disruption in the endogenous opioidergic system exhibited by the transgenic TASTPM model of AD.

6. AD-associated amyloid plaques and NFT were present in the supraspinal areas involved in pain processing, with the former pathological profiles also evident in the spinal cord, in human AD post-mortem tissue.
7. Experience of a chronic pain condition in AD subjects did not alter the severity of AD-associated pathological hallmarks; however, it did correlate with exacerbation of ongoing neuroinflammation in the spinal cord and supraspinal regions.

Altogether, evidence presented in this thesis depicts impaired sensitivity exhibited by TASTPM mice to both acute nociception and chronic pain-like behaviour due to the disruption of the endogenous inhibitory opioidergic system, which coincides with AD-associated Aβ pathology and cognitive impairment. Support for the translational aspect of preclinical persistent pain results is provided by data obtained from human AD post-mortem tissue which has revealed amyloid plaque deposition in the spinal cords and brain regions involved in pain processing, namely the thalamus; as well as exacerbation of ongoing CNS neuroinflammation in AD individuals with a history of chronic pain. Further preclinical and clinical studies are warranted in order to elucidate spatiotemporal progression of AD pathology in chronic pain conditions; and the level of impact on pain processing in both acute and chronic pain conditions, which may provide a greater insight into the underlying pain mechanisms and provide basis for new therapeutic targets for management of pain in AD.

5.2 Reduced Sensitivity of Pain in Alzheimer's disease

Pain is a subjective and multidimensional sensory and emotion experience, which serves as a critical biological warning system for self-protection in order to promote survival in a hostile and dangerous environment; and therefore it is important for the survival and wellbeing of the individual (Woolf 2010). An alteration in this sensory system in the form of decrease in nociceptive threshold would result in maladaptive increase in pain sensitivity (i.e. chronic pain); whilst an increase of nociceptive threshold would constitute a loss of functional reserve. Individuals with AD are in susceptible patient group in which pain is an important clinical issue that is often under-reported and inadequately managed (Corbett et al 2012). Under-treatment and inappropriate prescribing in this patient group results in reduced mobility, muscle weakness

and falls, which consequently has a major detrimental impact on quality of life. Moreover, pain has been recognised as a key contributor to the development of behavioural and psychological symptoms of dementia (BPSD) such as agitation and mood disorders, which are a major treatment challenge and can result in overprescribing of harmful anti-psychotic medications (Ballard et al 2014, Rajkumar et al 2017). However, it remains elusive whether the decrease in pain complaints and inadequate in its management are related to altered pain processing or the deteriorating ability of these patients to communicate which hinders their capacity to report pain sensations (Scherder & Bouma 2000).

Evidence stemming from clinical experimental pain studies have provided conflicting data on noxious pain thresholds and tolerance in individuals with AD. Such reports have suggested that pain responsiveness and tolerance are commonly, though variably, altered in AD; but with similar engagement of regional pain processing activity exhibited in comparison to those displayed by age-matched healthy controls (Benedetti et al 1999, Cole et al 2006, Jensen-Dahm et al 2014, Monroe et al 2016). As a result, making it difficult to understand the meaning of the sensory experience and the associated emotional context in this patient group; which may underlie the atypical behavioural responses (i.e. agitation and mood disorders) in this population (Scherder et al 2005). Therefore, warranting an investigation in order to evaluate if there was any alteration in the perception of physiological acute pain as well as in development and persistence of chronic pathological pain in AD.

For this purpose, we utilised the transgenic TASTPM mouse model, which recapitulates some of the behavioural and pathological characteristics of AD in human (Howlett et al 2008, Howlett et al 2004); and therefore, offered to be a powerful tool in order to assess the impact of AD on nocifensive behaviour and associated plasticity within the CNS in response to acute noxious stimulation and in chronic pain model of OA. Here we have shown, in Chapter 2, an age-dependent increase in nociceptive thresholds in the TASTPM mice implicating reduced sensory perception of pain in AD, which has been demonstrated in prior studies in amyloidogenic and tau models of AD (Mellone et al 2013, Shukla et al 2013). Thus our data adds further body of evidence to clinical studies demonstrating age-related loss of sensory perception of pain as illustrated by increased pain thresholds in the elderly (Lautenbacher 2012, Lautenbacher et al

2017); and increased pain thresholds in individuals with AD compared to cognitively intact control subjects, implicating possible alterations in the sensory-discriminative processing of pain (Cole et al 2006, Monroe et al 2016). In particular, thermal hyposensitivity preceded increases in mechanical nociceptive thresholds, as previously observed by Shukla et al (2013) in CRND8 model of AD, which in our model corresponded to development of AD-associated amyloid plaques accompanied by gliosis in the brain (6 months old) and spinal cord (12 months old), respectively. The assessment of thermal thresholds using the hot plate test involved integration of both the spinal and supraspinal-mediated components; whereas noxious mechanical thresholds evoked a spinal-mediated withdrawal reflex (Gregory et al 2013). This would suggest that amyloid plaques in regions involved in the processing and responding to an evoked-stimulus in the periphery may alter the nociceptive system such that there is a reduced nocifensive response to acute noxious stimulation.

The novelty of our work was the identification of intraneuronal accumulation of amyloid precursor protein/β-amyloid (APP/Aβ) in both the dorsal (lamina III and deeper) and ventral horns of the lumbar spinal cords of six months old TASTPM mice that develop into amyloid plaques in twelve months old transgenic AD mice. Intraneuronal Aβ has been shown to be associated with synaptic dysfunction and early cognitive impairments prior to the development of the AD pathological hallmark in the form of extracellular plaques in the brain (Iulita et al 2014, Leon et al 2010). Here we provide evidence for possible synaptic dysfunction in the spinal cord as intraneuronal APP/Aβ in the dorsal horn of 6 months old TASTPM spinal cord was concomitant with decreased dorsal horn vesicular glutamate transporter 2 (VGLUT2) expression, a marker for spinal cord intrinsic presumable glutamatergic interneuron population, indicating an alteration of glutamatergic function. The glutamatergic system has been identified to contribute to the synaptic dysfunction in AD (Parameshwaran et al 2008, Paula-Lima et al 2013, Ting et al 2007); and glutamate is present in primary afferent terminals, projection neurons as well as excitatory interneurons in the spinal cord where it plays pro-nociceptive roles (Todd et al 2003). Thus, the increased thermal nociceptive thresholds exhibited by the 6 months old TASTPM mice could be attributed to a reduced glutamatergic excitation and/or increased inhibition in the spinal cord.

Indeed, our results portray an increased synthesis and release of enkephalins in the spinal cord of 6 months old TASTPM mice which could contribute towards the elevated inhibitory tone. This likely possibility was further strengthened by our finding of the recovery of normal thermal sensitivity following administration of the opioid antagonist naloxone in TASTPM mice. Elevation of endogenous opioids may block pain via multiple mechanisms including actions on the mu (μ) opioid receptors (OR) located in the periphery, spinal cord, and the brain (cortical and sub-cortical regions) (Stein et al 2003). Increased endogenous opioidergic levels in AD has been reported in individuals with AD as well as in preclinical models of AD, as demonstrated by elevated CSF levels of opioid peptides and a reduction in opioid binding receptors in the dentate gyrus of human AD subjects (Jansen et al 1990, Muhlbauer et al 1986, Risser et al 1996); and increased levels of enkephalins have been found in the hippocampus and entorhinal cortex of a transgenic mouse model that over expresses the human APP (hAPP), which is associated with neuronal and cognitive impairments (Meilandt et al 2008). Knockdown or antagonism of the delta (δ)-OR in APP/PS1DE9 model of AD has revealed reductions in Aβ accumulation, plaque formation and associated gliosis and behavioural deficits, which supports the role of opioid peptides in Aβ generation and contribution in pathogenesis of AD (Teng et al 2010).

In fact, the elevated opioidergic tone was shown, in Chapter 3, to contribute to the altered chronic pain-like behaviour in the TASTPM model of AD. Here we demonstrated that despite the development of MIA-induced mechanical allodynia these transgenic mice failed to maintain the behavioural hypersensitivity and ongoing pain was undetectable in comparison to WT. These behavioural alterations were reinforced pharmacologically as illustrated by comparable effect of non-steroidal anti-inflammatory drugs (NSAID) during the early developmental phase of OA pain; whereas altered responsiveness to gabapentin and morphine administration during the late maintenance phase. Specifically, gabapentin, which resulted in reversal of mechanical hypersensitivity in MIA-injected WT mice, failed to alter mechanical thresholds in the TASTPM mice administrated with MIA. Whereas, administration of morphine resulted in heightened level of analgesia four weeks post MIA administration in the TASTPM mice compared to WT controls. These findings indicating altered mechanisms in the maintenance of chronic pain state in AD mice (Bove et al 2003, Combe et al 2004, Fernihough et al 2004).

Biochemical and pharmacological assessment demonstrated that increase of the endogenous opioid peptides may underlie the partial recovery of mechanical allodynia in TASTPM following MIA administration. This is illustrated by an increase in plasma β-endorphin concentration and the ability of systemic administration of opioid receptor antagonist naloxone to unmask MIA-induced mechanical hypersensitivity. A positive relationship between the level of plasma β-endorphin and mechanical withdrawal thresholds in parallel with reduced μ-OR expression in the TASTPM dorsal horn further strengthens the contribution of elevated opioidergic tone in partial reversal of MIA-induced mechanical allodynia in the TASTPM model of AD. Indeed, previous studies have demonstrated that increased levels of endogenous opioids, via either exercise, cold water swim stress and/or injection of the opioid peptide into the inflamed paw, were able to exert anti-nociceptive effect in rodent models of chronic pain (Allen et al 2017, Stagg et al 2011, Stein et al 1990). The synthesis of β-endorphin is regulated by the hypothalamic–pituitary–adrenal axis via the release of corticotroponin-releasing hormone (CRH) from the hypothalamus (Sprouse-Blum et al 2010, Stein et al 2003). In individuals with AD increased levels of CRH are reported, which induce hyperactivity of the hypothalamic–pituitary–adrenal axis which may contribute to the elevated opioidergic peptides observed in the transgenic TASTPM mice (Raadsheer et al 1995, Scherder et al 2003).

In addition, immunohistochemical evaluation of the dorsal horn revealed lack of spinal microglial response, to peripheral inflammation in the joint exhibited, by TASTPM mice in comparison to WT, which may suggest that alteration in spinal plasticity may contribute to altered behavioural response displayed by the TASTPM mice in the form of partial recovery of MIA-induced allodynia and inability to develop ongoing pain. Spinal microgliosis in rodent models of chronic pain is known to play an important role in central sensitisation, as attenuation of microglial activation, via administration of glial inhibitors, have been shown to correlate with reduced pain behaviours (Clark et al 2007, Clark et al 2012, Lee et al 2011a, Nieto et al 2016, Sagar et al 2011, Staniland et al 2010). Therefore, dampened microglial response in TASTPM dorsal horn following administration of MIA demonstrates attenuation in the central spinal mechanisms involved in the maintenance of chronic pain in the model of AD. These findings coupled with the lack of analgesic effect of gabapentin in the transgenic TASTPM mice following MIA injection

indicate towards a possibility blunted spinal central sensitisation in response to inflammation in the periphery, which may underlie the impaired persistent-pain like behaviour exhibited by the TASTPM model of AD.

It is plausible that intraneuronal APP/Aβ in the spinal cord may alter the nociceptive system via either reduced excitation and/or increased inhibition, which results in reduced nocifensive response to acute noxious stimulation. Furthermore, the reduced susceptibility of persistent pain maintenance in the TASTPM mice may be due also to the elevated endogenous opioidergic tone. Hence further strengthening the postulation that an alteration in the opioidergic system in AD may contribute to the reduced sensory perception of pain in the disease. As a result it could be indicated that AD may have an impact on the sensory-discriminative component of pain, such that nociceptive transmission is impaired in both acute and chronic pain conditions.

5.3 Alzheimer's disease Pathology Affecting the Lateral Pain System

The lateral pain system is responsible for encoding the sensory-discriminative aspect of pain via the spinothalamic tract, which originates from deep dorsal horn laminae (III-VI) distributing nociceptive information to areas of the cortex, mainly the primary somatosensory cortex, via the lateral, predominantly the ventral posteriolateral (VPL), nuclei of the thalamus (Hunt & Mantyh 2001, Treede et al 1999, Willis & Westlund 1997). In AD, the lateral pain system is thought to be largely spared as illustrated by less severe NFT pathology and diminished cortical atrophy affecting primary somatosensory cortex even at the terminal stages of AD (Braak's stage VI); and largely the medial group of thalamic nuclei are reported to be affected in AD, which are associated with the non-discriminative processing of pain (Arnold 2000, Braak & Braak 1991b, Perl 2010, Scherder et al 2003).

However, data from our AD autopsy analysis differs as illustrated by increase in neuropathological NFT in both the primary somatosensory cortex and ventral lateral/VPL (VL/VPL) nuclei of the thalamus, with the progression of AD, using Braak's NFT stage as a surrogate marker. In particular, we show moderate-severe NFT pathology exhibited by the primary somatosensory cortex in all AD individuals at Braak's stage V, an observation which is comparable to other cortical regions that have extensively been reported to be severely affected

in AD, namely the prefrontal cortex. Whereas, the VL/VPL at the same Braak's stage (V) largely exhibits mild-moderate NFT pathology, indicating a milder impact of AD-associated tangles in the thalamic nuclei involved in sensory processing of pain. Nevertheless, moderate-severe extracellular amyloid plaque deposition was evident in both, primary somatosensory cortex and VL/VPL, in AD subjects, an observation similar to the results obtained from the TASTPM mice, which also displayed Aβ plaques in the thalamus.

The presence of NFT and amyloid plaques in regions involved in nociceptive processing is an implication for neurodegeneration. In fact, neuronal loss has been shown to follow the spatiotemporal pattern of NFT distribution, with greater neuronal cell loss reported in comparison to NFT-containing neurons owed to other additional factors that may also contribute in neuronal dysfunction and eventual death (GomezIsla 1997, GomezIsla et al 1996). It has been suggested that there may be two dissociate pathways that may underlie the greater neuronal loss in comparison to NFT-containing cells within the same region: one affecting NFT-containing neurons that will eventually become dysfunctional and degenerate to appear as extracellular ghost tangles; and another affecting NFT-free neurons, possibly owed to their presence in close vicinity of tangle containing neurons and thus exposure to the neurotoxic molecules secreted by glial cells in the inflammatory process (Bussiere et al 2003, Hof et al 2003, Serrano-Pozo et al 2011). This may consequently result in regional dysfunction and/or induce compensatory mechanisms owed to neurodegeneration, which may underlie the altered processing of nociceptive inputs in AD. Therefore, the temporal progression of AD associated pathology in the spinal cord and the supraspinal regions involved in encoding sensory-discriminative aspect of pain may contribute to the altered processing of nociceptive information in AD.

5.4 Translation: Preclinical Models to Human Post-Mortem Tissue

Many mouse models, for example the TASTPM model used in this thesis, recapitulate some of AD-associated pathology observed in human; the TASTPM, like other amyloidogenic transgenic lines, model the development of amyloid plaques but no tau pathology (Elder et al 2010, Howlett et al 2008, Howlett et al 2004, Kitazawa et al 2012). Therefore, it is of great importance to

validate results obtained from these models of AD with human post-mortem tissue in order establish translational value of the model. As NFT formation is not exhibited by the TASTPM mice, here we only compared amyloid plaques and microglial responses exhibited by AD individuals with chronic pain and MIA-induced chronic OA pain in the TASTPM model of AD, in relation to their respective controls.

Firstly, the concept of peripheral inflammation exacerbating ongoing neuroinflammation in the CNS as an underlying mechanism contributing to the increased microglial activation in human post-mortem tissue of AD individuals with chronic pain. This notion gains a body of support from the preclinical TASTPM model of AD, as an intra-articular administration of MIA induced, as expected, inflammation in the synovial membrane, which coincided with increased microgliosis in the TASTPM thalamus, which was affected with amyloid plaques accompanied by microgliosis at the age of 6 months old; whilst no change was observed in the thalamus of MIA-injected WT mice. Further preclinical evidence obtained from modelling chronic pain conditions such as OA and rheumatoid arthritis revealed increase in microgliosis in the brains of APP/PS1 transgenic mouse models of AD (Kyrkanides et al 2011, Park et al 2011). In fact, intra-articular administration of MIA has been shown to results in elevation of tumour necrosis factor α (TNF-α) and interlukin-6 (IL-6) in the knee synovium and capsule as evident in human chronic pain conditions (i.e. arthritis and OA) (Hussein et al 2008, Orita et al 2011). This may suggest inflammation in the periphery may fuel ongoing neuroinflammation in the CNS via systemic circulation of pro-inflammatory mediators.

Secondly, we observed no change in amyloid plaque deposition in the brains AD individuals with chronic pain compared to AD controls without any clinical pain reports, which is a feature also reflected in the transgenic TASTPM mice after MIA-induced OA. In the preclinical mouse model of AD, we showed comparable levels of amyloid pathology burden within the cortex, hippocampus, and the thalamus following MIA administration compared to TASTPM controls. Although these observations are reflecting the results we obtained from AD human post-mortem tissue, evidence in the literature clinical as well as preclinical using APP/PS1 model of AD, pathological assessment in a model of chronic pain (i.e. OA and rheumatoid arthritis), provide contrasting views on amyloid deposition. Epidemiological evidence reviewed by McGeer and

co-worker (2016) suggests that AD individuals are relatively spared if they have been using anti-inflammatory analgesics, such as NSAID, or have suffered with conditions, such as rheumatoid arthritis, where such drugs are routinely used; which would suggest reduced amyloid deposition in AD subjects with chronic pain. In support of this notion Park et al (2011) suggest the underlying mechanism of decrease in amyloid plaque deposition may be due to increase in microglial activation which can contribute directly in degradation and clearance of Aβ. On the contrary, Kyrkanides et al (2011) reported increased amyloid deposition in the brains of APP/PS1 mice with OA and suggests that the mechanism that may underlie the peripherally induced neuroinflammation to AD pathology could be the neuroinflammatory signals hindering the capacity of glial cells to clear Aβ plaques; or it might be due to a shift of equilibrium whereby the rate of Aβ production overwhelms its degrading. Thus, these preclinical AD studies assessing AD-pathology in models of chronic pain highlight the dual role of microglia in promoting Aβ pathogenesis as well as degrading and clearing amyloid deposits. Therefore, further studies are required in order to evaluate and clarify mechanisms underlying CNS neuroinflammation following inflammation in the periphery and how they can modulate microglial activity in relation to pathogenesis of Aβ.

Similarities between results from models of AD and those from experiments using human post-mortem tissue samples are important as they suggest that such experimental models used are replicating some aspects of the human disease with some degree of accuracy. The data presented in this thesis is reassuring as experiments using TASTPM transgenic mouse model of AD with MIA-induced OA and human post-mortem tissue from AD individuals with a history of chronic pain and/or persistent use of analgesics display broadly similar results in terms of AD-associated amyloid pathology and neuroinflammation in the brain. Therefore, suggesting that in AD similar mechanisms may underlie the alterations in pathology and neuroinflammation observed in preclinical transgenic AD mice and human with chronic pain conditions. These findings highlight the translational value and further strengthen the utilisation of animal models in understanding human disease pathology and delineating the underlying mechanisms.

5.5 Limitations of Work

There are a number of limitations of the work presented in this thesis worth noting that need to be discussed. Firstly, the preclinical studies presented in this thesis were conducted on the transgenic TASTPM model of AD, which exhibits age-dependent impairment of cognition and development of amyloid plaques that become apparent at the age of 6 months old. However, additional cardinal features of AD, such as NFT and neuronal loss is largely absent, as illustrated by hyperphosphorylated tau only detected as dystrophic neurites, no NFT, surrounding amyloid plaques and minimal neuronal loss reported in plaque occupied area in the cortex and hippocampus of this model of AD (Howlett et al 2008, Howlett et al 2004). Thus, the TASTPM model of AD is representative of only some of the wide-spectrum of AD-associated behavioural and pathological changes as in human AD. This remains to be an issue with all current transgenic mouse models used for research in the field of AD as they model certain components of AD pathology and/or behaviour seen in human individual with the disease (Kitazawa et al 2012). Therefore, regardless of the incomplete recapitulation of human AD, the TASTPM model has offered to be a powerful tool in order to investigate the impact of AD-associated cognitive impairment and amyloid plaques on acute nociception and chronic pain-like behaviour.

Secondly, we used the MIA-model of OA in the studies presented in Chapter 3, which results in a dose-dependent robust and rapid onset of pain-like phenotype. Here we assessed OA-associated ongoing pain and referred mechanical allodynia using weight bearing and application of von Frey monofilament to the plantar surface of the hind paw, respectively. Patients with OA display hyperalgesic responses upon application of noxious stimuli in the area around the OA knee and commonly report referred pain in adjacent joints or nearby limbs to that of the affected joint, which confers translational value of hind paw allodynia (Bajaj et al 2001, Farrell et al 2000). Thus, such behavioural assessment in mouse model of OA recapitulate clinical presentations in human OA. However, studies have revealed that increasing the force applied, by the von Frey monofilament, to rodent hind paw which may potentially lift the hind paw can result in interference of primary hyperalgesia due to movement of the knee joint that can lead to additional potential source of pain-like behaviour (Teeple et al 2013). In order to

minimise such effect, studies presented in this thesis used a cut-off of 1.00 g von Frey filament in order to prevent lifting of the hind paw or to cause any potential tissue damage. In order to further refine and add to our results, assessment of primary hyperalgesia in the knee joint using pressure application measurement would enable to characterise pain-like behaviour at site of injury in OA providing a better translation to the assessment in clinical OA. Moreover, ongoing pain was not evident in the TASTPM mice following MIA, which could be further characterised pharmacologically using the conditioned place preference test, as previously reported (Allen et al 2017). Collectively, these future studies will substantially add body of evidence to current results of pain-like behaviour in a model of AD with OA chronic pain.

Thirdly, despite being one of the possible ways to view disease-related changes in a human brain, post-mortem tissue provides with prolonged post-mortem delay (PMD) ranging from several hours to several days, which can result in post-translational modification of proteins (i.e. phosphorylation) thereby affecting enzyme activity, nucleic acid integrity, oxidative modification, and protein integrity (Blair et al 2016, Samarasekera et al 2013). Moreover, formalin-fixed and paraffin-embedded tissue may be advantageous in enhancing the visualisation of abnormal protein; however prolonged fixation can be deleterious to protein detection owed to protein cross-linking making it difficult to visualise protein of interest (Samarasekera et al 2013). In order to minimise these limitations, we selected the AD with chronic pain and without chronic pain cohorts that exhibited closely-matched length of PMD; however, with the length of time in fixation solution could not have been controlled as the cases examined in Chapter 3 were from post-mortem brains collected between the years 2003-2014. Therefore, regions of interest that were obtained from wet-fixed tissue, the prefrontal cortex, primary somatosensory cortex and insula, it was impossible to control the length of time in fixation, which could have varied from one year to twelve years in fixation prior to embedding in paraffin; thus, may have an impact on immunohistochemical staining. However, as our experiments were designed to assess AD-associated pathological hallmarks, namely the amyloid plaques and NFT, such degradation was limited owed to the insoluble nature of aggregated deposits which are resistant and therefore less prone to fixation induced degradation (Samarasekera et al 2013). Furthermore, glial markers such as glial fibrillary acidic protein (GFAP) for astrocytes have been reported to be

unaffected due to PMD (Blair et al 2016). Thus, data presented here is likely to be sparred by fixative degradation owed to PMD due to the choice of markers used for immunohistochemical analysis. In order to minimise the likelihood of such limitations it is important to carry out multiple experiments in order to assess protein and associated RNA alterations using Western blot and micro-array analysis, respectively, which would potentially enable validation of immunohistochemical findings.

In addition, human post-mortem study was conducted on neuropathologically confirmed AD autopsy, where clinical report of symptomatic AD presentation was absent in some cases. Although clinicopathological studies have suggested that despite the incomplete clinical record, higher levels of AD-associated neuropathological changes typically correlate with greater likelihood of cognitive impairments (Hyman et al 2012). Furthermore, we had limited access to detailed neuropathological analysis and therefore cannot completely rule out the presence of mixed pathologies in the samples examined. Therefore, future studies should be conducted in order to tackle such issues where we assess clinically and pathologically confirmed AD autopsy with detailed pathological reports in order to minimise interference of any additional pathology (i.e. α-synuclein) and their potential impact of AD-associated neuropathological lesions, neurodegeneration, and neuroinflammation.

Finally, we conducted semi-quantitative grading of AD-related pathology and neuroinflammation on results obtained from AD autopsy, presented in Chapter 4, which may inform us of the gross regional changes but not the intricacies of such alterations in AD individuals with chronic pain compared those without any clinical pain reports. Quantitative assessment of frequency/density of amyloid plaques, NFT profiles and microglial cells, therefore may not reflect the functional or dysfunctional activity in the regions of interest. Consequently, future studies could be directed towards characterising the phenotype of AD-lesions and microglial cells, in order to quantify the proportion of such phenotypes which will aid in elucidating the possible functional activity (Gomez-Nicola & Boche 2015, Minett et al 2016). As a result, these data will provide us a better understanding of the impact of AD-associated pathology on regions involved in pain processing; thus, help in identifying mechanisms underlying altered sensory perception of pain in AD.

5.6 Future Directions

Data presented in this thesis demonstrates an increase in the endogenous inhibitory opioidergic tone contributes to the elevated acute nociceptive thresholds and impaired maintenance of OA-associated mechanical hypersensitivity in the transgenic TASTPM model of AD; thereby implicating a reduced sensory perception of pain in AD. In addition, results from human post-mortem tissue from AD individuals with a clinical record of chronic pain display comparable changes (i.e. increased CNS neuroinflammation) as to those exhibited by TASTPM mice with OA, which reassures the translational value of the preclinical model of AD. There is much scope for further investigations and with more time, future experiments could investigate and delineate more precise mechanism underlying pain in AD. The following are some suggestions for possible future research avenues:

1. **Examine alterations in regions involved descending pathways modulating pain transmission in TASTPM model of AD.** The work presented here mainly focusses on the spinal cord and the thalamus along with the associated cortex in association with nociceptive processing in AD. We aim to expand our field of view in order to explore whether AD-associated amyloid plaques and associated neurodegeneration and neuroinflammation affects the brainstem, mainly in the periaqueductal grey (PAG), rostral ventromedial medulla (RVM), parabrachial nucleus (PbN) and locus coeruleus (LC) using immunohistochemical techniques. Furthermore, as increase in the expression of opioid peptides has been postulated to underlie altered sensory perception of pain in AD, it is warranted to assess the expression of opioid peptides (i.e. β-endorphins and enkephalins) and their receptors (i.e. μ-OR and δ-OR) in the TASTPM brainstem (i.e. PAG). In parallel with the preclinical work, we have recently obtained Brains for Dementia Research ethics approval (TRID_221) to explore changes in the opioid system in the post-mortem brainstem tissue (PAG, RVM and PbN) obtained from same set of patients' cohort examined in Chapter 4. Together, these experiments would potentially enhance our understanding on whether the descending modulation of pain transmission contributes to the reduced sensitivity to pain in preclinical AD mouse model and its translational significance.

2. **Assessment of neurodegeneration in key regions of the pain pathway of TASTPM model of AD.** As Howlett et al (2008) have provided evidence for minimal neurodegeneration in plaque occupied areas in the cortex and the hippocampus, it is required to characterise whether such neurodegeneration takes place within the key regions of the pain pathway, namely the spinal cord and the thalamus. Therefore, it is important to evaluate, using immunohistochemistry, whether regions involved in nociceptive processing are undergoing neurodegeneration that may underlie altered nociceptive sensitivity.
3. **Investigating the role of glutamatergic, monoaminergic, and cholinergic system in inducing alteration of nocifensive behaviour in the transgenic mouse model of AD.** Here we have shown alteration in one, the opioidergic system, of the many neurotransmission system that are affected in AD, which possess the capacity to either directly and/or indirectly modulate nociceptive transmission (Ferreira-Vieira et al 2016, Simic et al 2017). Therefore, pharmacological evaluation of their inhibitors in models of chronic pain conditions (i.e. inflammatory and/or neuropathic pain) as well as biochemical and immunohistochemical analysis of neurotransmitters and receptors, respectively, would aid in understanding the relative contribution of these neurotransmission systems in altered nociception in AD.
4. **Examining MIA-associated temporal changes in the transgenic TASTPM model of AD.** Studies conducted in Chapter 3 delineate changes in the TASTPM mice 28 days post administration of MIA; therefore it is difficult to fully understand the underlying mechanisms associated with OA progression. As similar behavioural hypersensitivity were evident during the early developmental phase it would be of great interest to examine changes in the spinal cord (i.e. neuronal activation and microgliosis), quantification of knee joint pathology, as well as plasma concentration of opioid peptides (i.e. β-endorphins) and cytokines (i.e. TNFα) at different intervals (i.e. day 7, 14, and 28) post MIA administration in order to elucidate the pathological and biochemical changes contributing to the partial recovery of mechanical hypersensitivity displayed by the TASTPM mice. In addition to nociceptive behaviour, emotional (i.e. depression and anxiety) and cognitive components of OA pain can be characterised

and evaluation of analgesics impact on such behaviour as these aspects have been demonstrated to be altered due to changes in opioid levels in MIA-model of OA (Negrete et al 2017). In fact symptoms of depression have been illustrated to be alleviated following analgesic treatment of pain in people with dementia (Erdal et al 2017). Thus these data would also provide further detail on the nociceptive and emotional components of pain in the MIA-model as well enable evaluation of the translational component of mouse model to observations in patients with dementia experiencing pain.

5. **Investigating the impact of AD pathology on the development of chronic pain in the clinic.** Given the advancements in the field of neuroimaging for positron emission tomography (PET)-tracers for tau (e.g. ^{18}F-AV1451), Aβ (e.g. ^{11}C-PiB), and microglial activation (e.g. ^{11}C-(R)PK11195) it would be of great interest to evaluate longitudinal changes in these PET-tracers amongst AD individuals diagnosed with chronic pain compared to AD individuals with no pain condition (Cagnin et al 2001a, Villemagne et al 2017). Evidence from such studies could potentially allow identification of supraspinal regions that display alterations in AD-related pathology and microglial activation which could in turn possibly aid in understanding the possible mechanisms of pain in AD. A better understanding of the underlying mechanisms of pain in AD would pave paths towards developing novel therapeutic interventions and essentially improved management of pain in these individuals.

5.7 Conclusions

In conclusion, the preclinical studies presented in this thesis have demonstrated reduced sensory perception of pain, in both acute nociceptive thresholds and persistence of a chronic pain state, in the transgenic TASTPM model of AD, which coincides with the disease-associated cognitive impairment and Aβ pathology in the CNS. Elevation of the endogenous inhibitory opioid peptides was identified as the common underlying mechanism that may be responsible for the reduced sensitivity to acute noxious stimulation as well as the inability to develop ongoing pain and partial recovery of mechanical allodynia in model of OA exhibited by the TASTPM mice. In clinical cases with reduced sensory perception of pain would constitute a loss

of functional reserve which can consequently lead to increased incidence of BPSD and harmful behaviour (i.e. unable to detect if a hot bath as too hot) owed to the impairment of the protective mechanism of pain sensation in individuals with AD. In addition, here we provide support for the translational aspect of TASTPM model of AD, as illustrated by preclinical chronic pain results overlapping with data obtained from human AD post-mortem tissue, which revealed amyloid plaque deposition in the spinal cords and brain regions involved in pain processing, namely the thalamus; as well as exacerbation of ongoing CNS neuroinflammation in AD individuals with a history of chronic pain. Further studies are warranted in order to elucidate spatiotemporal progression of AD pathology in chronic pain conditions; and the level of impact on pain processing in both acute and chronic pain conditions, which may provide a greater insight into the underlying pain mechanisms and provide basis for new therapeutic targets for management of pain in AD.

Taken together, the findings of this thesis have important clinical implications for the care of patients with AD who have deteriorating cognitive function along with reduced sensitivity to pain. Altered pain sensitivity could be considered in assessing clinical risk as it may be associated with neuropsychiatric symptoms as well as an increased risk of injury during daily routine activities. Finally, these data highlight the need to re-evaluate current treatments, such as opioids, or develop novel therapeutic strategies for management of pain in individuals with AD.

References

Abaei M, Sagar DR, Stockley EG, Spicer CH, Prior M, et al. 2016. Neural correlates of hyperalgesia in the monosodium iodoacetate model of osteoarthritis pain. *Mol Pain* 12

Abou-Raya S, Abou-Raya A, Helmii M. 2012. Duloxetine for the management of pain in older adults with knee osteoarthritis: randomised placebo-controlled trial. *Age Ageing* 41: 646-52

Abraira VE, Ginty DD. 2013. The sensory neurons of touch. *Neuron* 79: 618-39

Achterberg WP, Pieper MJ, van Dalen-Kok AH, de Waal MW, Husebo BS, et al. 2013. Pain management in patients with dementia. *Clin Interv Aging* 8: 1471-82

Alafuzoff I, Arzberger T, Al-Sarraj S, Bodi I, Bogdanovic N, et al. 2008. Staging of neurofibrillary pathology in Alzheimer's disease: a study of the BrainNet Europe Consortium. *Brain Pathol* 18: 484-96

Alafuzoff I, Thal DR, Arzberger T, Bogdanovic N, Al-Sarraj S, et al. 2009. Assessment of beta-amyloid deposits in human brain: a study of the BrainNet Europe Consortium. *Acta Neuropathol* 117: 309-20

Albrecht D, Loggia M, Borra R, Hooker J, Opalacz A, et al. 2015. Activation of spinal glia in sciatica; a pilot [C-11]PBR28 study. *J Nucl Med* 56

Allaman I, Gavillet M, Belanger M, Laroche T, Viertl D, et al. 2010. Amyloid-beta aggregates cause alterations of astrocytic metabolic phenotype: impact on neuronal viability. *J Neurosci* 30: 3326-38

Allen B, Ingram E, Takao M, Smith MJ, Jakes R, et al. 2002. Abundant tau filaments and nonapoptotic neurodegeneration in transgenic mice expressing human P301S tau protein. *J Neurosci* 22: 9340-51

Allen J, Imbert I, Havelin J, Henderson T, Stevenson G, et al. 2017. Effects of Treadmill Exercise on Advanced Osteoarthritis Pain in Rats. *Arthritis Rheumatol*

Alzheimer A. 1911. Concerning unsual medical cases in old age. *Z Gesamte Neurol Psy* 4: 356-85

Alzheimer A, Forstl H, Levy R. 1991. On certain peculiar diseases of old age. *Hist Psychiatry* 2: 71-101

Aman Y, Pitcher T, Simeoli R, Ballard C, Malcangio M. 2016. Reduced thermal sensitivity and increased opioidergic tone in the TASTPM mouse model of Alzheimer's disease. *Pain* 157: 2285-96

Anthony IC, Norrby KE, Dingwall T, Carnie FW, Millar T, et al. 2010. Predisposition to accelerated Alzheimer-related changes in the brains of human immunodeficiency virus negative opiate abusers. *Brain* 133: 3685-98

Arcuri C, Mecca C, Bianchi R, Giambanco I, Donato R. 2017. The Pathophysiological Role of Microglia in Dynamic Surveillance, Phagocytosis and Structural Remodeling of the Developing CNS. *Front Mol Neurosci* 10: 191

Arnold SE. 2000. Part III. Neuropathology of Alzheimer's disease. *Dis Mon* 46: 687-705

Attems J, Thomas A, Jellinger K. 2012. Correlations between cortical and subcortical tau pathology. *Neuropathology and applied neurobiology* 38: 582-90

Bachstetter AD, Ighodaro ET, Hassoun Y, Aldeiri D, Neltner JH, et al. 2017. Rod-shaped microglia morphology is associated with aging in 2 human autopsy series. *Neurobiol Aging* 52: 98-105

Bachstetter AD, Van Eldik LJ, Schmitt FA, Neltner JH, Ighodaro ET, et al. 2015. Disease-related microglia heterogeneity in the hippocampus of Alzheimer's disease, dementia with Lewy bodies, and hippocampal sclerosis of aging. *Acta Neuropathol Commun* 3: 32

Baeta-Corral R, Defrin R, Pick CG, Gimenez-Llort L. 2015. Tail-flick test response in 3xTg-AD mice at early and advanced stages of disease. *Neurosci Lett* 600: 158-63

Bagyinszky E, Giau VV, Shim K, Suk K, An SSA, Kim S. 2017. Role of inflammatory molecules in the Alzheimer's disease progression and diagnosis. *J Neurol Sci* 376: 242-54

Bajaj P, Graven-Nielsen T, Arendt-Nielsen L. 2001. Osteoarthritis and its association with muscle hyperalgesia: an experimental controlled study. *Pain* 93: 107-14

Bales KR, Verina T, Dodel RC, Du Y, Altstiel L, et al. 1997. Lack of apolipoprotein E dramatically reduces amyloid beta-peptide deposition. *Nat Genet* 17: 263-4

Ballard C, Corbett A, Howard R. 2014. Prescription of antipsychotics in people with dementia. *Br J Psychiatry* 205: 4-5

Ballard CG, Gauthier S, Cummings JL, Brodaty H, Grossberg GT, et al. 2009. Management of agitation and aggression associated with Alzheimer disease. *Nature reviews. Neurology* 5: 245-55

Ballatore C, Lee VM, Trojanowski JQ. 2007. Tau-mediated neurodegeneration in Alzheimer's disease and related disorders. *Nat Rev Neurosci* 8: 663-72

Baron R, Binder A, Wasner G. 2010. Neuropathic pain: diagnosis, pathophysiological mechanisms, and treatment. *Lancet Neurol* 9: 807-19

Barres BA. 2008. The Mystery and Magic of Glia: A Perspective on Their Roles in Health and Disease. *Neuron* 60: 430-40

Basbaum AI, Bautista DM, Scherrer G, Julius D. 2009. Cellular and molecular mechanisms of pain. *Cell* 139: 267-84

Baseer N, Al-Baloushi AS, Watanabe M, Shehab SA, Todd AJ. 2014. Selective innervation of NK1 receptor-lacking lamina I spinoparabrachial neurons by presumed nonpeptidergic Adelta nociceptors in the rat. *Pain* 155: 2291-300

Bauer U, Pitzer S, Schreier MM, Osterbrink J, Alzner R, Iglseder B. 2016. Pain treatment for nursing home residents differs according to cognitive state - a cross-sectional study. *BMC Geriatr* 16: 124

Beaudry H, Daou I, Ase AR, Ribeiro-da-Silva A, Seguela P. 2017. Distinct behavioral responses evoked by selective optogenetic stimulation of the major TRPV1+ and MrgD+ subsets of C-fibers. *Pain*

Bekar LK, Wei HS, Nedergaard M. 2012. The locus coeruleus-norepinephrine network optimizes coupling of cerebral blood volume with oxygen demand. *J Cereb Blood Flow Metab* 32: 2135-45

Benedetti F, Arduino C, Vighetti S, Asteggiano G, Tarenzi L, Rainero I. 2004. Pain reactivity in Alzheimer patients with different degrees of cognitive impairment and brain electrical activity deterioration. *Pain* 111: 22-9

Benedetti F, Vighetti S, Ricco C, Lagna E, Bergamasco B, et al. 1999. Pain threshold and tolerance in Alzheimer's disease. *Pain* 80: 377-82

Bennett GJ, Xie YK. 1988. A Peripheral Mononeuropathy in Rat That Produces Disorders of Pain Sensation Like Those Seen in Man. *Pain* 33: 87-107

Beyreuther B, Callizot N, Stohr T. 2007. Antinociceptive efficacy of lacosamide in the monosodium iodoacetate rat model for osteoarthritis pain. *Arthritis Res Ther* 9: R14

Bijlsma JW, Berenbaum F, Lafeber FP. 2011. Osteoarthritis: an update with relevance for clinical practice. *Lancet* 377: 2115-26

Blair JA, Wang C, Hernandez D, Siedlak SL, Rodgers MS, et al. 2016. Individual Case Analysis of Postmortem Interval Time on Brain Tissue Preservation. *PLoS One* 11: e0151615

Bleakman D, Alt A, Nisenbaum ES. 2006. Glutamate receptors and pain. *Semin Cell Dev Biol* 17: 592-604

Bondareff W, Mountjoy CQ, Roth M. 1982. Loss of neurons of origin of the adrenergic projection to cerebral cortex (nucleus locus ceruleus) in senile dementia. *Neurology* 32: 164-8

Bove SE, Calcaterra SL, Brooker RM, Huber CM, Guzman RE, et al. 2003. Weight bearing as a measure of disease progression and efficacy of anti-inflammatory compounds in a model of monosodium iodoacetate-induced osteoarthritis. *Osteoarthr Cartilage* 11: 821-30

Bowen DM, Smith CB, White P, Davison AN. 1976. Neurotransmitter-related enzymes and indices of hypoxia in senile dementia and other abiotrophies. *Brain* 99: 459-96

Braak H, Braak E. 1991a. Alzheimer's disease affects limbic nuclei of the thalamus. *Acta Neuropathol* 81: 261-8

Braak H, Braak E. 1991b. Neuropathological stageing of Alzheimer-related changes. *Acta Neuropathol* 82: 239-59

Braak H, Braak E, Bohl J. 1993. Staging of Alzheimer-related cortical destruction. *Eur Neurol* 33: 403-8

Braz JM, Nassar MA, Wood JN, Basbaum AI. 2005. Parallel "pain" pathways arise from subpopulations of primary afferent nociceptor. *Neuron* 47: 787-93

Brookmeyer R, Johnson E, Ziegler-Graham K, Arrighi HM. 2007. Forecasting the global burden of Alzheimer's disease. *Alzheimers Dement* 3: 186-91

Brooks J, Tracey I. 2005. From nociception to pain perception: imaging the spinal and supraspinal pathways. *J Anat* 207: 19-33

Brooks SP, Dunnett SB. 2009. Tests to assess motor phenotype in mice: a user's guide. *Nat Rev Neurosci* 10: 519-29

Brumovsky P, Watanabe M, Hokfelt T. 2007. Expression of the vesicular glutamate transporters-1 and -2 in adult mouse dorsal root ganglia and spinal cord and their regulation by nerve injury. *Neuroscience* 147: 469-90

Buffo A, Rolando C, Ceruti S. 2010. Astrocytes in the damaged brain: Molecular and cellular insights into their reactive response and healing potential. *Biochem Pharmacol* 79: 77-89

Burns A, Iliffe S. 2009. Alzheimer's disease. *BMJ* 338: b158

Bussiere T, Gold G, Kovari E, Giannakopoulos P, Bouras C, et al. 2003. Stereologic analysis of neurofibrillary tangle formation in prefrontal cortex area 9 in aging and Alzheimer's disease. *Neuroscience* 117: 577-92

Cagnin A, Brooks DJ, Kennedy AM, Gunn RN, Myers R, et al. 2001a. In-vivo measurement of activated microglia in dementia. *Lancet* 358: 461-7

Cagnin A, Kassiou M, Meikle SR, Banati RB. 2007. Positron emission tomography imaging of neuroinflammation. *Neurotherapeutics : the journal of the American Society for Experimental NeuroTherapeutics* 4: 443-52

Cagnin A, Myers R, Gunn RN, Lawrence AD, Stevens T, et al. 2001b. In vivo visualization of activated glia by [11C] (R)-PK11195-PET following herpes encephalitis reveals projected neuronal damage beyond the primary focal lesion. *Brain* 124: 2014-27

Cagnin A, Rossor M, Sampson EL, Mackinnon T, Banati RB. 2004. In vivo detection of microglial activation in frontotemporal dementia. *Ann Neurol* 56: 894-7

Cai Z, Hussain MD, Yan LJ. 2014. Microglia, neuroinflammation, and beta-amyloid protein in Alzheimer's disease. *Int J Neurosci* 124: 307-21

Cai Z, Ratka A. 2012. Opioid system and Alzheimer's disease. *Neuromolecular Med* 14: 91-111

Callen DJ, Black SE, Caldwell CB. 2002. Limbic system perfusion in Alzheimer's disease measured by MRI-coregistered HMPAO SPET. *Eur J Nucl Med Mol Imaging* 29: 899-906

Cameron D, Polgar E, Gutierrez-Mecinas M, Gomez-Lima M, Watanabe M, Todd AJ. 2015. The organisation of spinoparabrachial neurons in the mouse. *Pain* 156: 2061-71

Cavanaugh DJ, Lee H, Lo L, Shields SD, Zylka MJ, et al. 2009. Distinct subsets of unmyelinated primary sensory fibers mediate behavioral responses to noxious thermal and mechanical stimuli. *Proc Natl Acad Sci U S A* 106: 9075-80

Chaplan SR, Bach FW, Pogrel JW, Chung JM, Yaksh TL. 1994. Quantitative assessment of tactile allodynia in the rat paw. *J Neurosci Methods* 53: 55-63

Chappell AS, Ossanna MJ, Liu-Seifert H, Iyengar S, Skljarevski V, et al. 2009. Duloxetine, a centrally acting analgesic, in the treatment of patients with osteoarthritis knee pain: a 13-week, randomized, placebo-controlled trial. *Pain* 146: 253-60

Chen G, Luo X, Qadri MY, Berta T, Ji RR. 2017. Sex-Dependent Glial Signaling in Pathological Pain: Distinct Roles of Spinal Microglia and Astrocytes. *Neurosci Bull*

Chishti MA, Yang DS, Janus C, Phinney AL, Horne P, et al. 2001. Early-onset amyloid deposition and cognitive deficits in transgenic mice expressing a double mutant form of amyloid precursor protein 695. *J Biol Chem* 276: 21562-70

Cho H, Kim JH, Kim C, Ye BS, Kim HJ, et al. 2014. Shape changes of the basal ganglia and thalamus in Alzheimer's disease: a three-year longitudinal study. *J Alzheimers Dis* 40: 285-95

Citron M, Westaway D, Xia WM, Carlson G, Diehl T, et al. 1997. Mutant presenilins of Alzheimer's disease increase production of 42-residue amyloid beta-protein in both transfected cells and transgenic mice. *Nature Medicine* 3: 67-72

Clark AK, Gentry C, Bradbury EJ, McMahon SB, Malcangio M. 2007. Role of spinal microglia in rat models of peripheral nerve injury and inflammation. *Eur J Pain* 11: 223-30

Clark AK, Grist J, Al-Kashi A, Perretti M, Malcangio M. 2012. Spinal cathepsin S and fractalkine contribute to chronic pain in the collagen-induced arthritis model. *Arthritis Rheum* 64: 2038-47

Clark AK, Yip PK, Malcangio M. 2009. The liberation of fractalkine in the dorsal horn requires microglial cathepsin S. *J Neurosci* 29: 6945-54

Cohen-Mansfield J. 2008. The relationship between different pain assessments in dementia. *Alzheimer Dis Assoc Disord* 22: 86-93

Cole LJ, Farrell MJ, Duff EP, Barber JB, Egan GF, Gibson SJ. 2006. Pain sensitivity and fMRI pain-related brain activity in Alzheimer's disease. *Brain* 129: 2957-65

Colloca L, Ludman T, Bouhassira D, Baron R, Dickenson AH, et al. 2017. Neuropathic pain. *Nat Rev Dis Primers* 3: 17002

Combe R, Bramwell S, Field MJ. 2004. The monosodium iodoacetate model of osteoarthritis: a model of chronic nociceptive pain in rats? *Neurosci Lett* 370: 236-40

Corbett A, Husebo B, Malcangio M, Staniland A, Cohen-Mansfield J, et al. 2012. Assessment and treatment of pain in people with dementia. *Nature reviews. Neurology* 8: 264-74

Corbett A, Husebo BS, Achterberg WP, Aarsland D, Erdal A, Flo E. 2014. The importance of pain management in older people with dementia. *Br Med Bull* 111: 139-48

Corder G, Tawfik VL, Wang D, Sypek EI, Low SA, et al. 2017. Loss of mu opioid receptor signaling in nociceptors, but not microglia, abrogates morphine tolerance without disrupting analgesia. *Nat Med* 23: 164-73

Cordero-Erausquin M, Inquimbert P, Schlichter R, Hugel S. 2016. Neuronal networks and nociceptive processing in the dorsal horn of the spinal cord. *Neuroscience* 338: 230-47

Cornali C, Franzoni S, Gatti S, Trabucchi M. 2006. Diagnosis of chronic pain caused by osteoarthritis and prescription of analgesics in patients with cognitive impairment. *J Am Med Dir Assoc* 7: 1-5

Costigan M, Scholz J, Woolf CJ. 2009. Neuropathic pain: a maladaptive response of the nervous system to damage. *Annu Rev Neurosci* 32: 1-32

Couchie D, Charriere-Bertrand C, Nunez J. 1988. Expression of the mRNA for tau proteins during brain development and in cultured neurons and astroglial cells. *J Neurochem* 50: 1894-9

Coull JA, Beggs S, Boudreau D, Boivin D, Tsuda M, et al. 2005. BDNF from microglia causes the shift in neuronal anion gradient underlying neuropathic pain. *Nature* 438: 1017-21

Coull JA, Boudreau D, Bachand K, Prescott SA, Nault F, et al. 2003. Trans-synaptic shift in anion gradient in spinal lamina I neurons as a mechanism of neuropathic pain. *Nature* 424: 938-42

Coyle DE. 1998. Partial peripheral nerve injury leads to activation of astroglia and microglia which parallels the development of allodynic behavior. *Glia* 23: 75-83

Craig-Schapiro R, Fagan AM, Holtzman DM. 2009. Biomarkers of Alzheimer's disease. *Neurobiol Dis* 35: 128-40

Cui J, He W, Yi B, Zhao H, Lu K, et al. 2014. mTOR PATHWAY IS INVOLVED IN ADP-EVOKED ASTROCYTE ACTIVATION AND ATP RELEASE IN THE SPINAL DORSAL HORN IN A RAT NEUROPATHIC PAIN MODEL. *Neuroscience* 275: 395-403

Cui YL, Xu JM, Dai RP, He L. 2012. The interface between inhibition of descending noradrenergic pain control pathways and negative affects in post-traumatic pain patients. *Upsala J Med Sci* 117: 293-99

D'Mello R, Dickenson AH. 2008. Spinal cord mechanisms of pain. *Br J Anaesth* 101: 8-16

de Jong LW, van der Hiele K, Veer IM, Houwing JJ, Westendorp RG, et al. 2008. Strongly reduced volumes of putamen and thalamus in Alzheimer's disease: an MRI study. *Brain* 131: 3277-85

de Silva R, Lashley T, Gibb G, Hanger D, Hope A, et al. 2003. Pathological inclusion bodies in tauopathies contain distinct complements of tau with three or four microtubule-binding repeat domains as demonstrated by new specific monoclonal antibodies. *Neuropathology and applied neurobiology* 29: 288-302

De Strooper B, Karran E. 2016. The Cellular Phase of Alzheimer's Disease. *Cell* 164: 603-15

DeArmond SJ, Fusco MM, Dewey MM. 1976. *Structure of the Human Brain: A Photographic Atlas*. New York: Oxford University Press. 186 pp.

Decosterd I, Woolf CJ. 2000. Spared nerve injury: an animal model of persistent peripheral neuropathic pain. *Pain* 87: 149-58

DeKosky ST, Scheff SW. 1990. Synapse loss in frontal cortex biopsies in Alzheimer's disease: correlation with cognitive severity. *Ann Neurol* 27: 457-64

Denning GM, Ackermann LW, Barna TJ, Armstrong JG, Stoll LL, et al. 2008. Proenkephalin expression and enkephalin release are widely observed in non-neuronal tissues. *Peptides* 29: 83-92

Dickenson AH, Kieffer B. 2006. Opiates: basic mechanisms In *Wall and Melzack's Textbook of Pain*, ed. SB McMahon, M Koltzenburg, pp. 427-42: Elsevier

Dickenson AH, Kieffer BL. 2013. Opiods: Basic Mechanisms In *Wall & Melzack's Textbook of Pain*, ed. SB McMahon, M Koltzenburg, I Tracey, DC Turk, pp. 413-28: Elsevier/Saunders

Dieppe PA, Lohmander LS. 2005. Pathogenesis and management of pain in osteoarthritis. *Lancet* 365: 965-73

Dixon WJ. 1980. Efficient analysis of experimental observations. *Annu Rev Pharmacol Toxicol* 20: 441-62

Dubin AE, Patapoutian A. 2010. Nociceptors: the sensors of the pain pathway. *J Clin Invest* 120: 3760-72

Dubois B, Feldman HH, Jacova C, Cummings JL, Dekosky ST, et al. 2010. Revising the definition of Alzheimer's disease: a new lexicon. *Lancet Neurol* 9: 1118-27

Dubois B, Feldman HH, Jacova C, Dekosky ST, Barberger-Gateau P, et al. 2007. Research criteria for the diagnosis of Alzheimer's disease: revising the NINCDS-ADRDA criteria. *Lancet Neurol* 6: 734-46

Dubuisson D, Dennis SG. 1977. The formalin test: a quantitative study of the analgesic effects of morphine, meperidine, and brain stem stimulation in rats and cats. *Pain* 4: 161-74

Duff K, Eckman C, Zehr C, Yu X, Prada CM, et al. 1996. Increased amyloid-beta 42(43) in brains of mice expressing mutant presenilin 1. *Nature* 383: 710-13

Dugger BN, Hidalgo JA, Chiarolanza G, Mariner M, Henry-Watson J, et al. 2013. The distribution of phosphorylated tau in spinal cords of Alzheimer's disease and non-demented individuals. *J Alzheimers Dis* 34: 529-36

Echeverry S, Shi XQ, Zhang J. 2008. Characterization of cell proliferation in rat spinal cord following peripheral nerve injury and the relationship with neuropathic pain. *Pain* 135: 37-47

Elder GA, Gama Sosa MA, De Gasperi R. 2010. Transgenic mouse models of Alzheimer's disease. *Mt Sinai J Med* 77: 69-81

Elrod R, Peskind ER, DiGiacomo L, Brodkin KI, Veith RC, Raskind MA. 1997. Effects of Alzheimer's disease severity on cerebrospinal fluid norepinephrine concentration. *Am J Psychiatry* 154: 25-30

Epstein B, Childers MK. 1998. The use of gabapentin for neuropathic and musculoskeletal pain: A case series. *J Neurol Rehabil* 12: 81-85

Erdal A, Flo E, Selbaek G, Aarsland D, Bergh S, et al. 2017. Associations between pain and depression in nursing home patients at different stages of dementia. *J Affect Disord* 218: 8-14

Fagan AM, Holtzman DM. 2000. Astrocyte lipoproteins, effects of apoE on neuronal function, and role of apoE in amyloid-beta deposition in vivo. *Microscopy research and technique* 50: 297-304

Falsig J, Porzgen P, Lotharius J, Leist M. 2004. Specific modulation of astrocyte inflammation by inhibition of mixed lineage kinases with CEP-1347. *J Immunol* 173: 2762-70

Farfara D, Lifshitz V, Frenkel D. 2008. Neuroprotective and neurotoxic properties of glial cells in the pathogenesis of Alzheimer's disease. *Journal of cellular and molecular medicine* 12: 762-80

Farina C, Aloisi F, Meinl E. 2007. Astrocytes are active players in cerebral innate immunity. *Trends in immunology* 28: 138-45

Farrell M, Gibson S, McMeeken J, Helme R. 2000. Pain and hyperalgesia in osteoarthritis of the hands. *J Rheumatol* 27: 441-7

Farrell MJ, Katz B, Helme RD. 1996. The impact of dementia on the pain experience. *Pain* 67: 7-15

Fayaz A, Croft P, Langford RM, Donaldson LJ, Jones GT. 2016. Prevalence of chronic pain in the UK: a systematic review and meta-analysis of population studies. *BMJ Open* 6: e010364

Feldt KS, Ryden MB, Miles S. 1998. Treatment of pain in cognitively impaired compared with cognitively intact older patients with hip-fracture. *J Am Geriatr Soc* 46: 1079-85

Fernihough J, Gentry C, Malcangio M, Fox A, Rediske J, et al. 2004. Pain related behaviour in two models of osteoarthritis in the rat knee. *Pain* 112: 83-93

Ferreira-Gomes J, Adaes S, Mendonca M, Castro-Lopes JM. 2012a. Analgesic effects of lidocaine, morphine and diclofenac on movement-induced nociception, as assessed by the Knee-Bend and CatWalk tests in a rat model of osteoarthritis. *Pharmacol Biochem Behav* 101: 617-24

Ferreira-Gomes J, Adaes S, Sarkander J, Castro-Lopes JM. 2010. Phenotypic alterations of neurons that innervate osteoarthritic joints in rats. *Arthritis Rheum* 62: 3677-85

Ferreira-Gomes J, Adaes S, Sousa RM, Mendonca M, Castro-Lopes JM. 2012b. Dose-dependent expression of neuronal injury markers during experimental osteoarthritis induced by monoiodoacetate in the rat. *Mol Pain* 8: 50

Ferreira-Vieira TH, Guimaraes IM, Silva FR, Ribeiro FM. 2016. Alzheimer's disease: Targeting the Cholinergic System. *Curr Neuropharmacol* 14: 101-15

Ferrell BA, Ferrell BR, Rivera L. 1995. Pain in cognitively impaired nursing home patients. *J Pain Symptom Manage* 10: 591-8

Filali M, Lalonde R, Theriault P, Julien C, Calon F, Planel E. 2012. Cognitive and non-cognitive behaviors in the triple transgenic mouse model of Alzheimer's disease expressing mutated APP, PS1, and Mapt (3xTg-AD). *Behav Brain Res* 234: 334-42

Floden AM, Combs CK. 2011. Microglia demonstrate age-dependent interaction with amyloid-beta fibrils. *J Alzheimers Dis* 25: 279-93

Foundas AL, Leonard CM, Mahoney SM, Agee OF, Heilman KM. 1997. Atrophy of the hippocampus, parietal cortex, and insula in Alzheimer's disease: a volumetric magnetic resonance imaging study. *Neuropsychiatry Neuropsychol Behav Neurol* 10: 81-9

Freund J. 1947. Some Aspects of Active Immunization. *Annu Rev Microbiol* 1: 291-308

Fuller S, Munch G, Steele M. 2009. Activated astrocytes: a therapeutic target in Alzheimer's disease? *Expert review of neurotherapeutics* 9: 1585-94

Gadd CA, Murtra P, De Felipe C, Hunt SP. 2003. Neurokinin-1 receptor-expressing neurons in the amygdala modulate morphine reward and anxiety behaviors in the mouse. *J Neurosci* 23: 8271-80

Games D, Adams D, Alessandrini R, Barbour R, Berthelette P, et al. 1995. Alzheimer-type neuropathology in transgenic mice overexpressing V717F beta-amyloid precursor protein. *Nature* 373: 523-7

Gao HM, Hong JS. 2008. Why neurodegenerative diseases are progressive: uncontrolled inflammation drives disease progression. *Trends in immunology* 29: 357-65

Garcia-Marin V, Garcia-Lopez P, Freire M. 2007. Cajal's contributions to glia research. *Trends Neurosci* 30: 479-87

Gehrmann J, Matsumoto Y, Kreutzberg GW. 1995. Microglia: intrinsic immuneffector cell of the brain. *Brain research. Brain research reviews* 20: 269-87

George DR, Whitehouse PJ, D'Alton S, Ballenger J. 2012. Through the amyloid gateway. *Lancet* 380: 1986-7

Go VL, Yaksh TL. 1987. Release of substance P from the cat spinal cord. *J Physiol* 391: 141-67

Goedert M, Ghetti B, Spillantini MG. 2012. Frontotemporal dementia: implications for understanding Alzheimer disease. *Cold Spring Harb Perspect Med* 2: a006254

Gold MS, Gebhart GF. 2010. Nociceptor sensitization in pain pathogenesis. *Nat Med* 16: 1248-57

Gomez-Nicola D, Boche D. 2015. Post-mortem analysis of neuroinflammatory changes in human Alzheimer's disease. *Alzheimers Res Ther* 7: 42

GomezIsla T. 1997. Profound loss of layer II entorhinal cortex neurons occurs in very mild Alzheimer's Disease (vol 16, pg 4491, 1996). *Journal of Neuroscience* 17: Cp3-Cp3

GomezIsla T, Price JL, McKeel DW, Morris JC, Growdon JH, Hyman BT. 1996. Profound loss of layer II entorhinal cortex neurons occurs in very mild Alzheimer's disease. *Journal of Neuroscience* 16: 4491-500

Gosselin RD, Suter MR, Ji RR, Decosterd I. 2010. Glial Cells and Chronic Pain. *Neuroscientist* 16: 519-31

Gregory NS, Harris AL, Robinson CR, Dougherty PM, Fuchs PN, Sluka KA. 2013. An overview of animal models of pain: disease models and outcome measures. *J Pain* 14: 1255-69

Grothe M, Heinsen H, Teipel SJ. 2012. Atrophy of the cholinergic Basal forebrain over the adult age range and in early stages of Alzheimer's disease. *Biol Psychiatry* 71: 805-13

Grothe M, Zaborszky L, Atienza M, Gil-Neciga E, Rodriguez-Romero R, et al. 2010. Reduction of basal forebrain cholinergic system parallels cognitive impairment in patients at high risk of developing Alzheimer's disease. *Cereb Cortex* 20: 1685-95

Gu Y, Oyama F, Ihara Y. 1996. Tau is widely expressed in rat tissues. *J Neurochem* 67: 1235-44

Guan Z, Kuhn JA, Wang X, Colquitt B, Solorzano C, et al. 2016. Injured sensory neuron-derived CSF1 induces microglial proliferation and DAP12-dependent pain. *Nat Neurosci* 19: 94-101

Guenette SY. 2003. Astrocytes: a cellular player in Abeta clearance and degradation. *Trends in molecular medicine* 9: 279-80

Guo Y, Wang L, Zhu M, Zhang H, Hu Y, et al. 2016. Detection of hyperphosphorylated tau protein and alpha-synuclein in spinal cord of patients with Alzheimer's disease. *Neuropsychiatr Dis Treat* 12: 445-52

Guzman RE, Evans MG, Bove S, Morenko B, Kilgore K. 2003. Mono-iodoacetate-induced histologic changes in subchondral bone and articular cartilage of rat femorotibial joints: an animal model of osteoarthritis. *Toxicologic pathology* 31: 619-24

Haasum Y, Fastbom J, Fratiglioni L, Kareholt I, Johnell K. 2011. Pain treatment in elderly persons with and without dementia: a population-based study of institutionalized and home-dwelling elderly. *Drugs Aging* 28: 283-93

Hamina A, Taipale H, Tanskanen A, Tolppanen AM, Karttunen N, et al. 2017. Long-term use of opioids for nonmalignant pain among community-dwelling persons with and without Alzheimer disease in Finland: a nationwide register-based study. *Pain* 158: 252-60

Hanesch U, Heppelmann B, Schmidt RF. 1991. Substance P- and calcitonin gene-related peptide immunoreactivity in primary afferent neurons of the cat's knee joint. *Neuroscience* 45: 185-93

Hannan MT, Felson DT, Pincus T. 2000. Analysis of the discordance between radiographic changes and knee pain in osteoarthritis of the knee. *J Rheumatol* 27: 1513-7

Hardy J, Allsop D. 1991. Amyloid Deposition as the Central Event in the Etiology of Alzheimers-Disease. *Trends Pharmacol Sci* 12: 383-88

Hardy J, Selkoe DJ. 2002. The amyloid hypothesis of Alzheimer's disease: progress and problems on the road to therapeutics. *Science* 297: 353-6

Hardy JA, Higgins GA. 1992. Alzheimer's disease: the amyloid cascade hypothesis. *Science* 256: 184-5

Harvey VL, Dickenson AH. 2009. Behavioural and electrophysiological characterisation of experimentally induced osteoarthritis and neuropathy in C57Bl/6 mice. *Mol Pain* 5: 18

Hayashida K, Obata H, Nakajima K, Eisenach JC. 2008. Gabapentin acts within the locus coeruleus to alleviate neuropathic pain. *Anesthesiology* 109: 1077-84

Hendriks SA, Smalbrugge M, Galindo-Garre F, Hertogh CM, van der Steen JT. 2015. From admission to death: prevalence and course of pain, agitation, and shortness of breath,

and treatment of these symptoms in nursing home residents with dementia. *J Am Med Dir Assoc* 16: 475-81

Heneka MT, Carson MJ, El Khoury J, Landreth GE, Brosseron F, et al. 2015. Neuroinflammation in Alzheimer's disease. *Lancet Neurol* 14: 388-405

Heneka MT, Rodriguez JJ, Verkhratsky A. 2010. Neuroglia in neurodegeneration. *Brain Res Rev* 63: 189-211

Henneberger C, Papouin T, Oliet SH, Rusakov DA. 2010. Long-term potentiation depends on release of D-serine from astrocytes. *Nature* 463: 232-6

Heppelmann B. 1997. Anatomy and histology of joint innervation. *J Peripher Nerv Syst* 2: 5-16

Heyman A, Wilkinson WE, Stafford JA, Helms MJ, Sigmon AH, Weinberg T. 1984. Alzheimer's disease: a study of epidemiological aspects. *Ann Neurol* 15: 335-41

Hickey L, Li Y, Fyson SJ, Watson TC, Perrins R, et al. 2014. Optoactivation of locus ceruleus neurons evokes bidirectional changes in thermal nociception in rats. *J Neurosci* 34: 4148-60

Hickman SE, Allison EK, El Khoury J. 2008. Microglial dysfunction and defective beta-amyloid clearance pathways in aging Alzheimer's disease mice. *Journal of Neuroscience* 28: 8354-60

Hill CL, Hunter DJ, Niu J, Clancy M, Guermazi A, et al. 2007. Synovitis detected on magnetic resonance imaging and its relation to pain and cartilage loss in knee osteoarthritis. *Ann Rheum Dis* 66: 1599-603

Hiller JM, Itzhak Y, Simon EJ. 1987. Selective changes in mu, delta and kappa opioid receptor binding in certain limbic regions of the brain in Alzheimer's disease patients. *Brain Res* 406: 17-23

Hirokawa N. 1994. Microtubule organization and dynamics dependent on microtubule-associated proteins. *Current opinion in cell biology* 6: 74-81

Hoe HS, Fu Z, Makarova A, Lee JY, Lu C, et al. 2009. The effects of amyloid precursor protein on postsynaptic composition and activity. *J Biol Chem* 284: 8495-506

Hof PR, Bussiere T, Gold G, Kovari E, Giannakopoulos P, et al. 2003. Stereologic evidence for persistence of viable neurons in layer II of the entorhinal cortex and the CA1 field in Alzheimer disease. *J Neuropathol Exp Neurol* 62: 55-67

Horgas AL, Tsai PF. 1998. Analgesic drug prescription and use in cognitively impaired nursing home residents. *Nurs Res* 47: 235-42

Howlett DR, Bowler K, Soden PE, Riddell D, Davis JB, et al. 2008. Abeta deposition and related pathology in an APP x PS1 transgenic mouse model of Alzheimer's disease. *Histol Histopathol* 23: 67-76

Howlett DR, Richardson JC, Austin A, Parsons AA, Bate ST, et al. 2004. Cognitive correlates of Abeta deposition in male and female mice bearing amyloid precursor protein and presenilin-1 mutant transgenes. *Brain Res* 1017: 130-6

Howorth PW, Teschemacher AG, Pickering AE. 2009. Retrograde adenoviral vector targeting of nociresponsive pontospinal noradrenergic neurons in the rat in vivo. *J Comp Neurol* 512: 141-57

Huang SW, Wang WT, Chou LC, Liao CD, Liou TH, Lin HW. 2015. Osteoarthritis increases the risk of dementia: a nationwide cohort study in Taiwan. *Sci Rep* 5: 10145

Hui J, Zhang ZJ, Zhang X, Shen Y, Gao YJ. 2013. Repetitive hyperbaric oxygen treatment attenuates complete Freund's adjuvant-induced pain and reduces glia-mediated neuroinflammation in the spinal cord. *J Pain* 14: 747-58

Hunt SP, Mantyh PW. 2001. The molecular dynamics of pain control. *Nat Rev Neurosci* 2: 83-91

Hunter DJ, Felson DT. 2006. Osteoarthritis. *BMJ* 332: 639-42

Hunter DJ, McDougall JJ, Keefe FJ. 2008. The symptoms of osteoarthritis and the genesis of pain. *Rheum Dis Clin North Am* 34: 623-43

Husebo BS, Achterberg W, Flo E. 2016. Identifying and Managing Pain in People with Alzheimer's Disease and Other Types of Dementia: A Systematic Review. *CNS Drugs* 30: 481-97

Husebo BS, Ballard C, Sandvik R, Nilsen OB, Aarsland D. 2011. Efficacy of treating pain to reduce behavioural disturbances in residents of nursing homes with dementia: cluster randomised clinical trial. *BMJ* 343: d4065

Hussein MR, Fathi NA, El-Din AM, Hassan HI, Abdullah F, et al. 2008. Alterations of the CD4(+), CD8 (+) T cell subsets, interleukins-1beta, IL-10, IL-17, tumor necrosis factor-alpha and soluble intercellular adhesion molecule-1 in rheumatoid arthritis and osteoarthritis: preliminary observations. *Pathol Oncol Res* 14: 321-8

Hyman BT, Phelps CH, Beach TG, Bigio EH, Cairns NJ, et al. 2012. National Institute on Aging-Alzheimer's Association guidelines for the neuropathologic assessment of Alzheimer's disease. *Alzheimers Dement* 8: 1-13

Hyman BT, Van Hoesen GW, Damasio AR, Barnes CL. 1984. Alzheimer's disease: cell-specific pathology isolates the hippocampal formation. *Science* 225: 1168-70

Inglis JJ, McNamee KE, Chia SL, Essex D, Feldmann M, et al. 2008. Regulation of pain sensitivity in experimental osteoarthritis by the endogenous peripheral opioid system. *Arthritis Rheum* 58: 3110-9

Isami K, Haraguchi K, So K, Asakura K, Shirakawa H, et al. 2013. Involvement of TRPM2 in peripheral nerve injury-induced infiltration of peripheral immune cells into the spinal cord in mouse neuropathic pain model. *PLoS One* 8: e66410

Iulita MF, Allard S, Richter L, Munter LM, Ducatenzeiler A, et al. 2014. Intracellular Abeta pathology and early cognitive impairments in a transgenic rat overexpressing human amyloid precursor protein: a multidimensional study. *Acta Neuropathol Commun* 2: 61

Ivanavicius SP, Ball AD, Heapy CG, Westwood FR, Murray F, Read SJ. 2007. Structural pathology in a rodent model of osteoarthritis is associated with neuropathic pain: increased expression of ATF-3 and pharmacological characterisation. *Pain* 128: 272-82

Jack CR, Jr., Albert MS, Knopman DS, McKhann GM, Sperling RA, et al. 2011. Introduction to the recommendations from the National Institute on Aging-Alzheimer's Association workgroups on diagnostic guidelines for Alzheimer's disease. *Alzheimers Dement* 7: 257-62

Jankowsky JL, Fadale DJ, Anderson J, Xu GM, Gonzales V, et al. 2004. Mutant presenilins specifically elevate the levels of the 42 residue beta-amyloid peptide in vivo: evidence for augmentation of a 42-specific gamma secretase. *Hum Mol Genet* 13: 159-70

Jansen KL, Faull RL, Dragunow M, Synek BL. 1990. Alzheimer's disease: changes in hippocampal N-methyl-D-aspartate, quisqualate, neurotensin, adenosine, benzodiazepine, serotonin and opioid receptors--an autoradiographic study. *Neuroscience* 39: 613-27

Janss AJ, Gebhart GF. 1988. Brainstem and spinal pathways mediating descending inhibition from the medullary lateral reticular nucleus in the rat. *Brain Res* 440: 109-22

Jawhar S, Trawicka A, Jenneckens C, Bayer TA, Wirths O. 2012. Motor deficits, neuron loss, and reduced anxiety coinciding with axonal degeneration and intraneuronal Abeta aggregation in the 5XFAD mouse model of Alzheimer's disease. *Neurobiology of Aging* 33: 196 e29-40

Jensen-Dahm C, Gasse C, Astrup A, Mortensen PB, Waldemar G. 2015. Frequent use of opioids in patients with dementia and nursing home residents: A study of the entire elderly population of Denmark. *Alzheimers & Dementia* 11: 691-99

Jensen-Dahm C, Werner MU, Dahl JB, Jensen TS, Ballegaard M, et al. 2014. Quantitative sensory testing and pain tolerance in patients with mild to moderate Alzheimer disease compared to healthy control subjects. *Pain* 155: 1439-45

Ji RR, Berta T, Nedergaard M. 2013. Glia and pain: Is chronic pain a gliopathy? *Pain* 154: S10-S28

Ji RR, Chamessian A, Zhang YQ. 2016. Pain regulation by non-neuronal cells and inflammation. *Science* 354: 572-77

Ji RR, Suter MR. 2007. p38 MAPK, microglial signaling, and neuropathic pain. *Mol Pain* 3: 33

Ji RR, Xu ZZ, Gao YJ. 2014. Emerging targets in neuroinflammation-driven chronic pain. *Nat Rev Drug Discov* 13: 533-48

Jonsson T, Stefansson H, Steinberg S, Jonsdottir I, Jonsson PV, et al. 2013. Variant of TREM2 associated with the risk of Alzheimer's disease. *N Engl J Med* 368: 107-16

Jozwiak-Bebenista M, Nowak JZ. 2014. Paracetamol: mechanism of action, applications and safety concern. *Acta Pol Pharm* 71: 11-23

Jucker M, Walker LC. 2013. Self-propagation of pathogenic protein aggregates in neurodegenerative diseases. *Nature* 501: 45-51

Kamer AR, Craig RG, Dasanayake AP, Brys M, Glodzik-Sobanska L, de Leon MJ. 2008. Inflammation and Alzheimer's disease: possible role of periodontal diseases. *Alzheimers Dement* 4: 242-50

Kapoor M, Martel-Pelletier J, Lajeunesse D, Pelletier JP, Fahmi H. 2011. Role of proinflammatory cytokines in the pathophysiology of osteoarthritis. *Nat Rev Rheumatol* 7: 33-42

Kidd BL, Urban LA. 2001. Mechanisms of inflammatory pain. *Br J Anaesth* 87: 3-11

Kim DS, Figueroa KW, Li KW, Boroujerdi A, Yolo T, Luo ZD. 2009. Profiling of dynamically changed gene expression in dorsal root ganglia post peripheral nerve injury and a critical role of injury-induced glial fibrillary acidic protein in maintenance of pain behaviors [corrected]. *Pain* 143: 114-22

Kim SH, Chung JM. 1992. An experimental model for peripheral neuropathy produced by segmental spinal nerve ligation in the rat. *Pain* 50: 355-63

King T, Vera-Portocarrero L, Gutierrez T, Vanderah TW, Dussor G, et al. 2009. Unmasking the tonic-aversive state in neuropathic pain. *Nat Neurosci* 12: 1364-6

Kitazawa M, Medeiros R, Laferla FM. 2012. Transgenic mouse models of Alzheimer disease: developing a better model as a tool for therapeutic interventions. *Curr Pharm Des* 18: 1131-47

Kluver H, Barrera E. 1953. A method for the combined staining of cells and fibers in the nervous system. *J Neuropathol Exp Neurol* 12: 400-3

Knapp M, Prince M. 2007. Dementia UK: THE FULL REPORT, London

Knowlton WM, Palkar R, Lippoldt EK, McCoy DD, Baluch F, et al. 2013. A sensory-labeled line for cold: TRPM8-expressing sensory neurons define the cellular basis for cold, cold pain, and cooling-mediated analgesia. *J Neurosci* 33: 2837-48

Koffie RM, Hyman BT, Spires-Jones TL. 2011. Alzheimer's disease: synapses gone cold. *Mol Neurodegener* 6: 63

Koistinaho M, Lin S, Wu X, Esterman M, Koger D, et al. 2004. Apolipoprotein E promotes astrocyte colocalization and degradation of deposited amyloid-beta peptides. *Nat Med* 10: 719-26

Kotulska K, Larysz-Brysz M, LePecheur M, Marcol W, Lewin-Kowalik J, et al. 2010. APP overexpression prevents neuropathic pain and motoneuron death after peripheral nerve injury in mice. *Brain Res Bull* 81: 378-84

Krabbe G, Halle A, Matyash V, Rinnenthal JL, Eom GD, et al. 2013. Functional impairment of microglia coincides with Beta-amyloid deposition in mice with Alzheimer-like pathology. *PLoS One* 8: e60921

Kuhl DE, Koeppe RA, Minoshima S, Snyder SE, Ficaro EP, et al. 1999. In vivo mapping of cerebral acetylcholinesterase activity in aging and Alzheimer's disease. *Neurology* 52: 691-9

Kukkar A, Bali A, Singh N, Jaggi AS. 2013. Implications and mechanism of action of gabapentin in neuropathic pain. *Arch Pharm Res* 36: 237-51

Kulkarni B, Bentley DE, Elliott R, Julyan PJ, Boger E, et al. 2007. Arthritic pain is processed in brain areas concerned with emotions and fear. *Arthritis and Rheumatism* 56: 1345-54

Kulmala HK. 1985. Some enkephalin- or VIP-immunoreactive hippocampal pyramidal cells contain neurofibrillary tangles in the brains of aged humans and persons with Alzheimer's disease. *Neurochem Pathol* 3: 41-51

Kummer C, Wehner S, Quast T, Werner S, Herzog V. 2002. Expression and potential function of beta-amyloid precursor proteins during cutaneous wound repair. *Exp Cell Res* 280: 222-32

Kuner R, Flor H. 2017. Structural plasticity and reorganisation in chronic pain. *Nat Rev Neurosci* 18: 113

Kurrikoff K, Koks S, Matsui T, Bourin M, Arend A, et al. 2004. Deletion of the CCK2 receptor gene reduces mechanical sensitivity and abolishes the development of hyperalgesia in mononeuropathic mice. *Eur J Neurosci* 20: 1577-86

Kurt MA, Davies DC, Kidd M. 1999. beta-Amyloid immunoreactivity in astrocytes in Alzheimer's disease brain biopsies: an electron microscope study. *Exp Neurol* 158: 221-8

Kwon M, Altin M, Duenas H, Alev L. 2014. The Role of Descending Inhibitory Pathways on Chronic Pain Modulation and Clinical Implications. *Pain Pract* 14: 656-67

Kyrkanides S, Tallents RH, Miller JN, Olschowka ME, Johnson R, et al. 2011. Osteoarthritis accelerates and exacerbates Alzheimer's disease pathology in mice. *J Neuroinflammation* 8: 112

LaFerla FM, Green KN, Oddo S. 2007. Intracellular amyloid-beta in Alzheimer's disease. *Nat Rev Neurosci* 8: 499-509

Laird FM, Cai H, Savonenko AV, Farah MH, He K, et al. 2005. BACE1, a major determinant of selective vulnerability of the brain to amyloid-beta amyloidogenesis, is essential for cognitive, emotional, and synaptic functions. *J Neurosci* 25: 11693-709

Laird JM, Roza C, De Felipe C, Hunt SP, Cervero F. 2001. Role of central and peripheral tachykinin NK1 receptors in capsaicin-induced pain and hyperalgesia in mice. *Pain* 90: 97-103

Larsson M, Broman J. 2011. Synaptic plasticity and pain: role of ionotropic glutamate receptors. *Neuroscientist* 17: 256-73

Latremoliere A, Woolf CJ. 2009. Central sensitization: a generator of pain hypersensitivity by central neural plasticity. *J Pain* 10: 895-926

Lau BK, Vaughan CW. 2014. Descending modulation of pain: the GABA disinhibition hypothesis of analgesia. *Curr Opin Neurobiol* 29: 159-64

Lautenbacher S. 2012. Experimental approaches in the study of pain in the elderly. *Pain Med* 13 Suppl 2: S44-50

Lautenbacher S, Peters JH, Heesen M, Scheel J, Kunz M. 2017. Age changes in pain perception: A systematic-review and meta-analysis of age effects on pain and tolerance thresholds. *Neurosci Biobehav Rev* 75: 104-13

Le Bars D, Dickenson AH, Besson JM. 1979a. Diffuse noxious inhibitory controls (DNIC). I. Effects on dorsal horn convergent neurones in the rat. *Pain* 6: 283-304

Le Bars D, Dickenson AH, Besson JM. 1979b. Diffuse noxious inhibitory controls (DNIC). II. Lack of effect on non-convergent neurones, supraspinal involvement and theoretical implications. *Pain* 6: 305-27

Le Pichon CE, Chesler AT. 2014. The functional and anatomical dissection of somatosensory subpopulations using mouse genetics. *Front Neuroanat* 8

Lee MC, Zambreanu L, Menon DK, Tracey I. 2008. Identifying brain activity specifically related to the maintenance and perceptual consequence of central sensitization in humans. *J Neurosci* 28: 11642-9

Lee Y, Pai M, Brederson JD, Wilcox D, Hsieh G, et al. 2011a. Monosodium iodoacetate-induced joint pain is associated with increased phosphorylation of mitogen activated protein kinases in the rat spinal cord. *Mol Pain* 7: 39

Lee YC, Lu B, Bathon JM, Haythornthwaite JA, Smith MT, et al. 2011b. Pain Sensitivity and Pain Reactivity in Osteoarthritis. *Arthrit Care Res* 63: 320-27

Leon WC, Canneva F, Partridge V, Allard S, Ferretti MT, et al. 2010. A novel transgenic rat model with a full Alzheimer's-like amyloid pathology displays pre-plaque intracellular amyloid-beta-associated cognitive impairment. *J Alzheimers Dis* 20: 113-26

Lever IJ, Bradbury EJ, Cunningham JR, Adelson DW, Jones MG, et al. 2001. Brain-derived neurotrophic factor is released in the dorsal horn by distinctive patterns of afferent fiber stimulation. *J Neurosci* 21: 4469-77

Lewis J, Dickson DW, Lin WL, Chisholm L, Corral A, et al. 2001. Enhanced neurofibrillary degeneration in transgenic mice expressing mutant tau and APP. *Science* 293: 1487-91

Li L, Rutlin M, Abraira VE, Cassidy C, Kus L, et al. 2011. The functional organization of cutaneous low-threshold mechanosensory neurons. *Cell* 147: 1615-27

Liddelow SA, Barres BA. 2017. Reactive Astrocytes: Production, Function, and Therapeutic Potential. *Immunity* 46: 957-67

Limongi F, Radaelli S, Noale M, Maggi S, Crepaldi G. 2013. Somatosensory Evoked Potentials and pain assessment in Alzheimer's disease. *Eur Geriatr Med* 4: 384-88

Linley JE, Rose K, Ooi L, Gamper N. 2010. Understanding inflammatory pain: ion channels contributing to acute and chronic nociception. *Pflugers Arch* 459: 657-69

Litwic A, Edwards MH, Dennison EM, Cooper C. 2013. Epidemiology and burden of osteoarthritis. *Br Med Bull* 105: 185-99

Llorca-Torralba M, Borges G, Neto F, Mico JA, Berrocoso E. 2016. Noradrenergic Locus Coeruleus pathways in pain modulation. *Neuroscience* 338: 93-113

Loggia ML, Chonde DB, Akeju O, Arabasz G, Catana C, et al. 2015. Evidence for brain glial activation in chronic pain patients. *Brain* 138: 604-15

Lopez OL. 2011. The growing burden of Alzheimer's disease. *Am J Manag Care* 17 Suppl 13: S339-45

Lovheim H, Karlsson S, Gustafson Y. 2008. The use of central nervous system drugs and analgesics among very old people with and without dementia. *Pharmacoepidemiol Drug Saf* 17: 912-8

Lucin KM, O'Brien CE, Bieri G, Czirr E, Mosher KI, et al. 2013. Microglial Beclin 1 Regulates Retromer Trafficking and Phagocytosis and Is Impaired in Alzheimer's Disease. *Neuron* 79: 873-86

Luo C, Kuner T, Kuner R. 2014. Synaptic plasticity in pathological pain. *Trends Neurosci* 37: 343-55

Lynch JL, Alley JF, Wellman L, Beitz AJ. 2008. Decreased spinal cord opioid receptor mRNA expression and antinociception in a Theiler's murine encephalomyelitis virus model of multiple sclerosis. *Brain Res* 1191: 180-91

Ma Y, Wang S, Tian Y, Chen L, Li G, Mao J. 2013. Disruption of persistent nociceptive behavior in rats with learning impairment. *PLoS One* 8: e74533

Magistretti PJ, Pellerin L. 1999. Cellular mechanisms of brain energy metabolism and their relevance to functional brain imaging. *Philos T Roy Soc B* 354: 1155-63

Malara A, De Biase GA, Bettarini F, Ceravolo F, Di Cello S, et al. 2016. Pain Assessment in Elderly with Behavioral and Psychological Symptoms of Dementia. *J Alzheimers Dis* 50: 1217-25

Malcangio M. 2016. Microglia and chronic pain. *Pain* 157: 1002-3

Malcangio M, Bowery NG. 1993. Gamma-aminobutyric acidB, but not gamma-aminobutyric acidA receptor activation, inhibits electrically evoked substance P-like immunoreactivity release from the rat spinal cord in vitro. *J Pharmacol Exp Ther* 266: 1490-6

Malcangio M, Bowery NG. 1996. Calcitonin gene-related peptide content, basal outflow and electrically-evoked release from monoarthritic rat spinal cord in vitro. *Pain* 66: 351-8

Malm TM, Jay TR, Landreth GE. 2015. The evolving biology of microglia in Alzheimer's disease. *Neurotherapeutics : the journal of the American Society for Experimental NeuroTherapeutics* 12: 81-93

Mann A, Illing S, Miess E, Schulz S. 2015. Different mechanisms of homologous and heterologous mu-opioid receptor phosphorylation. *Br J Pharmacol* 172: 311-6

Mantyh PW, Rogers SD, Honore P, Allen BJ, Ghilardi JR, et al. 1997. Inhibition of hyperalgesia by ablation of lamina I spinal neurons expressing the substance P receptor. *Science* 278: 275-9

Mapplebeck JC, Beggs S, Salter MW. 2016. Sex differences in pain: a tale of two immune cells. *Pain* 157 Suppl 1: S2-6

Mapplebeck JC, Beggs S, Salter MW. 2017. Molecules in pain and sex: a developing story. *Mol Brain* 10: 9

Maragakis NJ, Rothstein JD. 2006. Mechanisms of disease: astrocytes in neurodegenerative disease. *Nat Clin Pract Neuro* 2: 679-89

Marshak DR, Pesce SA, Stanley LC, Griffin WS. 1992. Increased S100 beta neurotrophic activity in Alzheimer's disease temporal lobe. *Neurobiol Aging* 13: 1-7

Masters CL, Bateman R, Blennow K, Rowe CC, Sperling RA, Cummings JL. 2015. Alzheimer's disease. *Nat Rev Dis Primers* 1: 15056

Mathieu-Kia AM, Fan LQ, Kreek MJ, Simon EJ, Hiller JM. 2001. Mu-, delta- and kappa-opioid receptor populations are differentially altered in distinct areas of postmortem brains of Alzheimer's disease patients. *Brain Res* 893: 121-34

Matsumoto S, Goto S, Hirano A. 1990. A comparative immunohistochemical study on striatal Met-enkephalin expression in Alzheimer's disease and in progressive supranuclear palsy. *Acta Neuropathol* 81: 74-7

Maurer K, Volk S, Gerbaldo H. 1997. Auguste D and Alzheimer's disease. *Lancet* 349: 1546-9

Mazzanti M, Sul JY, Haydon PG. 2001. Glutamate on demand: Astrocytes as a ready source. *Neuroscientist* 7: 396-405

McCoy ES, Taylor-Blake B, Street SE, Pribisko AL, Zheng J, Zylka MJ. 2013. Peptidergic CGRPalpha primary sensory neurons encode heat and itch and tonically suppress sensitivity to cold. *Neuron* 78: 138-51

McDougall JJ. 2006. Arthritis and pain. Neurogenic origin of joint pain. *Arthritis Res Ther* 8: 220

McGeer PL, McGeer EG. 2002. Local neuroinflammation and the progression of Alzheimer's disease. *Journal of neurovirology* 8: 529-38

McGeer PL, Rogers J, McGeer EG. 2016. Inflammation, Antiinflammatory Agents, and Alzheimer's Disease: The Last 22 Years. *J Alzheimers Dis* 54: 853-57

McKhann G, Drachman D, Folstein M, Katzman R, Price D, Stadlan EM. 1984. Clinical diagnosis of Alzheimer's disease: report of the NINCDS-ADRDA Work Group under the auspices of Department of Health and Human Services Task Force on Alzheimer's Disease. *Neurology* 34: 939-44

McKhann GM, Knopman DS, Chertkow H, Hyman BT, Jack CR, Jr., et al. 2011. The diagnosis of dementia due to Alzheimer's disease: recommendations from the National Institute on Aging-Alzheimer's Association workgroups on diagnostic guidelines for Alzheimer's disease. *Alzheimers Dement* 7: 263-9

McMahon SB, Malcangio M. 2009. Current challenges in glia-pain biology. *Neuron* 64: 46-54

Meilandt WJ, Yu GQ, Chin J, Roberson ED, Palop JJ, et al. 2008. Enkephalin elevations contribute to neuronal and behavioral impairments in a transgenic mouse model of Alzheimer's disease. *J Neurosci* 28: 5007-17

Mellone M, Kestoras D, Andrews MR, Dassie E, Crowther RA, et al. 2013. Tau pathology is present in vivo and develops in vitro in sensory neurons from human P301S tau transgenic mice: a system for screening drugs against tauopathies. *J Neurosci* 33: 18175-89

Melzack R, Katz J. 2013. Pain. *Wiley Interdiscip Rev Cogn Sci* 4: 1-15

Merighi A, Polak JM, Theodosis DT. 1991. Ultrastructural visualization of glutamate and aspartate immunoreactivities in the rat dorsal horn, with special reference to the co-localization of glutamate, substance P and calcitonin-gene related peptide. *Neuroscience* 40: 67-80

Meyer-Luehmann M, Spires-Jones TL, Prada C, Garcia-Alloza M, de Calignon A, et al. 2008. Rapid appearance and local toxicity of amyloid-beta plaques in a mouse model of Alzheimer's disease. *Nature* 451: 720-4

Millan MJ. 1999. The induction of pain: an integrative review. *Prog Neurobiol* 57: 1-164

Minett T, Classey J, Matthews FE, Fahrenhold M, Taga M, et al. 2016. Microglial immunophenotype in dementia with Alzheimer's pathology. *J Neuroinflammation* 13: 135

Mirra SS, Heyman A, McKeel D, Sumi SM, Crain BJ, et al. 1991. The Consortium to Establish a Registry for Alzheimer's Disease (CERAD). Part II. Standardization of the neuropathologic assessment of Alzheimer's disease. *Neurology* 41: 479-86

Mogil JS, Miermeister F, Seifert F, Strasburg K, Zimmermann K, et al. 2005. Variable sensitivity to noxious heat is mediated by differential expression of the CGRP gene. *Proc Natl Acad Sci U S A* 102: 12938-43

Monroe TB, Gibson SJ, Bruehl SP, Gore JC, Dietrich MS, et al. 2016. Contact heat sensitivity and reports of unpleasantness in communicative people with mild to moderate cognitive impairment in Alzheimer's disease: a cross-sectional study. *BMC Med* 14: 74

Monroe TB, Gore JC, Chen LM, Mion LC, Cowan RL. 2012. Pain in people with Alzheimer disease: potential applications for psychophysical and neurophysiological research. *J Geriatr Psychiatry Neurol* 25: 240-55

Montine TJ, Phelps CH, Beach TG, Bigio EH, Cairns NJ, et al. 2012. National Institute on Aging-Alzheimer's Association guidelines for the neuropathologic assessment of Alzheimer's disease: a practical approach. *Acta Neuropathol* 123: 1-11

Moore KA, Kohno T, Karchewski LA, Scholz J, Baba H, Woolf CJ. 2002. Partial peripheral nerve injury promotes a selective loss of GABAergic inhibition in the superficial dorsal horn of the spinal cord. *J Neurosci* 22: 6724-31

Morris GP, Clark IA, Vissel B. 2014. Inconsistencies and controversies surrounding the amyloid hypothesis of Alzheimer's disease. *Acta Neuropathol Commun* 2: 135

Morrison RS, Siu AL. 2000. A comparison of pain and its treatment in advanced dementia and cognitively intact patients with hip fracture. *J Pain Symptom Manage* 19: 240-8

Mosconi L, Mistur R, Switalski R, Tsui WH, Glodzik L, et al. 2009. FDG-PET changes in brain glucose metabolism from normal cognition to pathologically verified Alzheimer's disease. *Eur J Nucl Med Mol Imaging* 36: 811-22

Mosher KI, Wyss-Coray T. 2014. Microglial dysfunction in brain aging and Alzheimer's disease. *Biochem Pharmacol* 88: 594-604

Muhlbauer M, Metcalf JC, Jr., Robertson JT, Fridland G, Desiderio DM. 1986. Opioid peptides in the cerebrospinal fluid of Alzheimer patients. *Biomed Chromatogr* 1: 155-8

Muller R, Heinrich M, Heck S, Blohm D, Richter-Landsberg C. 1997. Expression of microtubule-associated proteins MAP2 and tau in cultured rat brain oligodendrocytes. *Cell and tissue research* 288: 239-49

Mulligan SJ, MacVicar BA. 2004. Calcium transients in astrocyte endfeet cause cerebrovascular constrictions. *Nature* 431: 195-9

Nagele RG, D'Andrea MR, Lee H, Venkataraman V, Wang HY. 2003. Astrocytes accumulate A beta 42 and give rise to astrocytic amyloid plaques in Alzheimer disease brains. *Brain Res* 971: 197-209

Negrete R, Garcia Gutierrez MS, Manzanares J, Maldonado R. 2017. Involvement of the dynorphin/KOR system on the nociceptive, emotional and cognitive manifestations of joint pain in mice. *Neuropharmacology* 116: 315-27

Neogi T. 2013. The epidemiology and impact of pain in osteoarthritis. *Osteoarthritis Cartilage* 21: 1145-53

Nichols ML, Allen BJ, Rogers SD, Ghilardi JR, Honore P, et al. 1999. Transmission of chronic nociception by spinal neurons expressing the substance P receptor. *Science* 286: 1558-61

Niciu MJ, Kelmendi B, Sanacora G. 2012. Overview of glutamatergic neurotransmission in the nervous system. *Pharmacol Biochem Behav* 100: 656-64

Nicoll JA, Weller RO. 2003. A new role for astrocytes: beta-amyloid homeostasis and degradation. *Trends in molecular medicine* 9: 281-2

Nieto FR, Clark AK, Grist J, Hathway GJ, Chapman V, Malcangio M. 2016. Neuron-immune mechanisms contribute to pain in early stages of arthritis. *J Neuroinflammation* 13: 96

Nimmerjahn A, Kirchhoff F, Helmchen F. 2005. Resting microglial cells are highly dynamic surveillants of brain parenchyma in vivo. *Science* 308: 1314-8

Njie EG, Boelen E, Stassen FR, Steinbusch HW, Borchelt DR, Streit WJ. 2012. Ex vivo cultures of microglia from young and aged rodent brain reveal age-related changes in microglial function. *Neurobiol Aging* 33: 195 e1-12

Nuesch E, Rutjes AW, Husni E, Welch V, Juni P. 2009. Oral or transdermal opioids for osteoarthritis of the knee or hip. *Cochrane Database Syst Rev*: CD003115

Nwosu LN, Mapp PI, Chapman V, Walsh DA. 2016. Relationship between structural pathology and pain behaviour in a model of osteoarthritis (OA). *Osteoarthritis Cartilage* 24: 1910-17

O'Brien RJ, Wong PC. 2011. Amyloid precursor protein processing and Alzheimer's disease. *Annu Rev Neurosci* 34: 185-204

Oakley H, Cole SL, Logan S, Maus E, Shao P, et al. 2006. Intraneuronal beta-amyloid aggregates, neurodegeneration, and neuron loss in transgenic mice with five familial Alzheimer's disease mutations: potential factors in amyloid plaque formation. *J Neurosci* 26: 10129-40

Oddo S, Caccamo A, Shepherd JD, Murphy MP, Golde TE, et al. 2003. Triple-transgenic model of Alzheimer's disease with plaques and tangles: intracellular Abeta and synaptic dysfunction. *Neuron* 39: 409-21

Ogbonna AC, Clark AK, Gentry C, Hobbs C, Malcangio M. 2013. Pain-like behaviour and spinal changes in the monosodium iodoacetate model of osteoarthritis in C57Bl/6 mice. *Eur J Pain* 17: 514-26

Ogomori K, Kitamoto T, Tateishi J, Sato Y, Suetsugu M, Abe M. 1989. Beta-protein amyloid is widely distributed in the central nervous system of patients with Alzheimer's disease. *Am J Pathol* 134: 243-51

Oh ES, Savonenko AV, King JF, Fangmark Tucker SM, Rudow GL, et al. 2009. Amyloid precursor protein increases cortical neuron size in transgenic mice. *Neurobiol Aging* 30: 1238-44

Onos KD, Sukoff Rizzo SJ, Howell GR, Sasner M. 2016. Toward more predictive genetic mouse models of Alzheimer's disease. *Brain Res Bull* 122: 1-11

Orita S, Ishikawa T, Miyagi M, Ochiai N, Inoue G, et al. 2011. Pain-related sensory innervation in monoiodoacetate-induced osteoarthritis in rat knees that gradually develops neuronal injury in addition to inflammatory pain. *BMC Musculoskelet Disord* 12: 134

Osikowicz M, Mika J, Przewlocka B. 2013. The glutamatergic system as a target for neuropathic pain relief. *Experimental Physiology* 98: 372-84

Ossipov MH, Dussor GO, Porreca F. 2010. Central modulation of pain. *J Clin Invest* 120: 3779-87

Ossipov MH, Morimura K, Porreca F. 2014. Descending pain modulation and chronification of pain. *Curr Opin Support Palliat Care* 8: 143-51

Pamplona FA, Pandolfo P, Duarte FS, Takahashi RN, Prediger RD. 2010. Altered emotionality leads to increased pain tolerance in amyloid beta (Abeta1-40) peptide-treated mice. *Behav Brain Res* 212: 96-102

Panula P, Rinne J, Kuokkanen K, Eriksson KS, Sallmen T, et al. 1998. Neuronal histamine deficit in Alzheimer's disease. *Neuroscience* 82: 993-7

Parameshwaran K, Dhanasekaran M, Suppiramaniam V. 2008. Amyloid beta peptides and glutamatergic synaptic dysregulation. *Exp Neurol* 210: 7-13

Park SM, Shin JH, Moon GJ, Cho SI, Lee YB, Gwag BJ. 2011. Effects of collagen-induced rheumatoid arthritis on amyloidosis and microvascular pathology in APP/PS1 mice. *BMC Neurosci* 12: 106

Paula-Lima AC, Brito-Moreira J, Ferreira ST. 2013. Deregulation of excitatory neurotransmission underlying synapse failure in Alzheimer's disease. *J Neurochem* 126: 191-202

Pautex S, Michon A, Guedira M, Emond H, Le Lous P, et al. 2006. Pain in severe dementia: self-assessment or observational scales? *J Am Geriatr Soc* 54: 1040-5

Peirs C, Seal RP. 2016. Neural circuits for pain: Recent advances and current views. *Science* 354: 578-84

Perl DP. 2010. Neuropathology of Alzheimer's disease. *Mt Sinai J Med* 77: 32-42

Perry EK, Tomlinson BE, Blessed G, Bergmann K, Gibson PH, Perry RH. 1978. Correlation of cholinergic abnormalities with senile plaques and mental test scores in senile dementia. *Br Med J* 2: 1457-9

Perry VH. 2004. The influence of systemic inflammation on inflammation in the brain: implications for chronic neurodegenerative disease. *Brain Behav Immun* 18: 407-13

Perry VH, Cunningham C, Holmes C. 2007. Systemic infections and inflammation affect chronic neurodegeneration. *Nat Rev Immunol* 7: 161-7

Perry VH, Nicoll JA, Holmes C. 2010. Microglia in neurodegenerative disease. *Nature reviews. Neurology* 6: 193-201

Perry VH, Teeling J. 2013. Microglia and macrophages of the central nervous system: the contribution of microglia priming and systemic inflammation to chronic neurodegeneration. *Semin Immunopathol* 35: 601-12

Pertovaara A. 2006. Noradrenergic pain modulation. *Prog Neurobiol* 80: 53-83

Pezet S, Malcangio M, McMahon SB. 2002. BDNF: a neuromodulator in nociceptive pathways? *Brain research. Brain research reviews* 40: 240-9

Pezet S, McMahon SB. 2006. Neurotrophins: mediators and modulators of pain. *Annu Rev Neurosci* 29: 507-38

Pickering G, Jourdan D, Dubray C. 2006. Acute versus chronic pain treatment in Alzheimer's disease. *Eur J Pain* 10: 379-84

Pihlaja R, Koistinaho J, Kauppinen R, Sandholm J, Tanila H, Koistinaho M. 2011. Multiple Cellular and Molecular Mechanisms Are Involved in Human A beta Clearance by Transplanted Adult Astrocytes. *Glia* 59: 1643-57

Pihlaja R, Koistinaho J, Malm T, Sikkila H, Vainio S, Koistinaho M. 2008. Transplanted astrocytes internalize deposited beta-amyloid peptides in a transgenic mouse model of Alzheimer's disease. *Glia* 56: 154-63

Pillemer L, Ecker EE. 1941. Anticomplementary factor in fresh yeast. *J Biol Chem* 137: 139-42

Pitcher T, Sousa-Valente J, Malcangio M. 2016. The Monoiodoacetate Model of Osteoarthritis Pain in the Mouse. *J Vis Exp*

Poulin SP, Dautoff R, Morris JC, Barrett LF, Dickerson BC, Alzheimer's Disease Neuroimaging I. 2011. Amygdala atrophy is prominent in early Alzheimer's disease and relates to symptom severity. *Psychiatry Res* 194: 7-13

Prince M, Comas-Herrera A, Knapp M, Guerchet M, Karagiannidou M. 2016. World Alzheimer Report 2016, London

Prince M, Knapp M, Guerchet M, McCrone P, Prina M, et al. 2014. Dementia UK: Update

Proctor WR, Hirdes JP. 2001. Pain and cognitive status among nursing home residents in Canada. *Pain Res Manag* 6: 119-25

Przewlocki R, Przewlocka B. 2001. Opioids in chronic pain. *Eur J Pharmacol* 429: 79-91

Pugh PL, Richardson JC, Bate ST, Upton N, Sunter D. 2007. Non-cognitive behaviours in an APP/PS1 transgenic model of Alzheimer's disease. *Behav Brain Res* 178: 18-28

Qiu T, Liu Q, Chen YX, Zhao YF, Li YM. 2015. Abeta42 and Abeta40: similarities and differences. *J Pept Sci* 21: 522-9

Raadsheer FC, van Heerikhuize JJ, Lucassen PJ, Hoogendijk WJ, Tilders FJ, Swaab DF. 1995. Corticotropin-releasing hormone mRNA levels in the paraventricular nucleus of patients with Alzheimer's disease and depression. *Am J Psychiatry* 152: 1372-6

Raghavendra V, Tanga RY, DeLeo JA. 2004. Complete Freunds adjuvant-induced peripheral inflammation evokes glial activation and proinflammatory cytokine expression in the CNS. *European Journal of Neuroscience* 20: 467-73

Rahman W, Bauer CS, Bannister K, Vonsy JL, Dolphin AC, Dickenson AH. 2009. Descending serotonergic facilitation and the antinociceptive effects of pregabalin in a rat model of osteoarthritic pain. *Mol Pain* 5: 45

Rainero I, Vighetti S, Bergamasco B, Pinessi L, Benedetti F. 2000. Autonomic responses and pain perception in Alzheimer's disease. *Eur J Pain* 4: 267-74

Rajkumar AP, Ballard C, Fossey J, Orrell M, Moniz-Cook E, et al. 2017. Epidemiology of Pain in People With Dementia Living in Care Homes: Longitudinal Course, Prevalence, and Treatment Implications. *J Am Med Dir Assoc*

Ramirez AI, de Hoz R, Salobrar-Garcia E, Salazar JJ, Rojas B, et al. 2017. The Role of Microglia in Retinal Neurodegeneration: Alzheimer's Disease, Parkinson, and Glaucoma. *Front Aging Neurosci* 9: 214

Randall LO, Selitto JJ. 1957. A method for measurement of analgesic activity on inflamed tissue. *Arch Int Pharmacodyn Ther* 111: 409-19

Ransohoff RM, Cardona AE. 2010. The myeloid cells of the central nervous system parenchyma. *Nature* 468: 253-62

Ransohoff RM, Perry VH. 2009. Microglial physiology: unique stimuli, specialized responses. *Annu Rev Immunol* 27: 119-45

Rapoport M, Dawson HN, Binder LI, Vitek MP, Ferreira A. 2002. Tau is essential to beta-amyloid-induced neurotoxicity. *P Natl Acad Sci USA* 99: 6364-69

Rashid MH, Theberge Y, Elmes SJ, Perkins MN, McIntosh F. 2013. Pharmacological validation of early and late phase of rat mono-iodoacetate model using the Tekscan system. *Eur J Pain* 17: 210-22

Raskin J, Cummings J, Hardy J, Schuh K, Dean RA. 2015. Neurobiology of Alzheimer's Disease: Integrated Molecular, Physiological, Anatomical, Biomarker, and Cognitive Dimensions. *Curr Alzheimer Res* 12: 712-22

Raskind MA, Peskind ER, Halter JB, Jimerson DC. 1984. Norepinephrine and MHPG levels in CSF and plasma in Alzheimer's disease. *Arch Gen Psychiatry* 41: 343-6

Reitz C, Brayne C, Mayeux R. 2011. Epidemiology of Alzheimer disease. *Nature reviews. Neurology* 7: 137-52

Rexed B. 1952. The cytoarchitectonic organization of the spinal cord in the cat. *J Comp Neurol* 96: 414-95

Ricci G, Volpi L, Pasquali L, Petrozzi L, Siciliano G. 2009. Astrocyte-neuron interactions in neurological disorders. *Journal of biological physics* 35: 317-36

Richardson JC, Kendal CE, Anderson R, Priest F, Gower E, et al. 2003. Ultrastructural and behavioural changes precede amyloid deposition in a transgenic model of Alzheimer's disease. *Neuroscience* 122: 213-28

Ridet JL, Malhotra SK, Privat A, Gage FH. 1997. Reactive astrocytes: cellular and molecular cues to biological function. *Trends in Neurosciences* 20: 570-77

Rindos AJ, Loeb GE, Levitan H. 1984. Conduction velocity changes along lumbar primary afferent fibers in cats. *Exp Neurol* 86: 208-26

Risser D, You ZB, Cairns N, Herrera-Marschitz M, Seidl R, et al. 1996. Endogenous opioids in frontal cortex of patients with Down syndrome. *Neurosci Lett* 203: 111-4

Rodriguez-Vieitez E, Saint-Aubert L, Carter SF, Almkvist O, Farid K, et al. 2016. Diverging longitudinal changes in astrocytosis and amyloid PET in autosomal dominant Alzheimer's disease. *Brain* 139: 922-36

Rodriguez JJ, Olabarria M, Chvatal A, Verkhratsky A. 2009. Astroglia in dementia and Alzheimer's disease. *Cell death and differentiation* 16: 378-85

Rombouts SA, Barkhof F, Witter MP, Scheltens P. 2000. Unbiased whole-brain analysis of gray matter loss in Alzheimer's disease. *Neurosci Lett* 285: 231-3

Rosner H, Rubin L, Kestenbaum A. 1996. Gabapentin adjunctive therapy in neuropathic pain states. *Clin J Pain* 12: 56-8

Rossi D, Volterra A. 2009. Astrocytic dysfunction: insights on the role in neurodegeneration. *Brain Res Bull* 80: 224-32

Rub U, Del Tredici K, Del Turco D, Braak H. 2002. The intralaminar nuclei assigned to the medial pain system and other components of this system are early and progressively

affected by the Alzheimer's disease-related cytoskeletal pathology. *J Chem Neuroanat* 23: 279-90

Rub U, Del Tredici K, Schultz C, Thal DR, Braak E, Braak H. 2001. The autonomic higher order processing nuclei of the lower brain stem are among the early targets of the Alzheimer's disease-related cytoskeletal pathology. *Acta Neuropathol* 101: 555-64

Rygiel K. 2016. Novel strategies for Alzheimer's disease treatment: An overview of anti-amyloid beta monoclonal antibodies. *Indian J Pharmacol* 48: 629-36

Sagar DR, Burston JJ, Hathway GJ, Woodhams SG, Pearson RG, et al. 2011. The contribution of spinal glial cells to chronic pain behaviour in the monosodium iodoacetate model of osteoarthritic pain. *Mol Pain* 7: 88

Saito Y, Murayama S. 2000. Expression of tau immunoreactivity in the spinal motor neurons of Alzheimer's disease. *Neurology* 55: 1727-9

Sala M, Braida D, Calcaterra P, Leone MP, Gori E. 1992. Dose-dependent conditioned place preference produced by etonitazene and morphine. *Eur J Pharmacol* 217: 37-41

Samarasekera N, Al-Shahi Salman R, Huitinga I, Klioueva N, McLean CA, et al. 2013. Brain banking for neurological disorders. *Lancet Neurol* 12: 1096-105

Sampson EL, White N, Lord K, Leurent B, Vickerstaff V, et al. 2015. Pain, agitation, and behavioural problems in people with dementia admitted to general hospital wards: a longitudinal cohort study. *Pain* 156: 675-83

Sandvik R, Selbaek G, Kirkevold O, Aarsland D, Husebo BS. 2016. Analgesic prescribing patterns in Norwegian nursing homes from 2000 to 2011: trend analyses of four data samples. *Age Ageing* 45: 54-60

Sandvik RK, Selbaek G, Seifert R, Aarsland D, Ballard C, et al. 2014. Impact of a stepwise protocol for treating pain on pain intensity in nursing home patients with dementia: a cluster randomized trial. *Eur J Pain* 18: 1490-500

Santacruz K, Lewis J, Spires T, Paulson J, Kotilinek L, et al. 2005. Tau suppression in a neurodegenerative mouse model improves memory function. *Science* 309: 476-81

Santello M, Volterra A. 2010. Neuroscience: Astrocytes as aide-memoires. *Nature* 463: 169-70

Saul A, Sprenger F, Bayer TA, Wirths O. 2013. Accelerated tau pathology with synaptic and neuronal loss in a novel triple transgenic mouse model of Alzheimer's disease. *Neurobiol Aging* 34: 2564-73

Scanzello CR, Goldring SR. 2012. The role of synovitis in osteoarthritis pathogenesis. *Bone* 51: 249-57

Schaible HG. 2007. Peripheral and central mechanisms of pain generation. *Handb Exp Pharmacol*: 3-28

Schaible HG. 2012. Mechanisms of chronic pain in osteoarthritis. *Curr Rheumatol Rep* 14: 549-56

Schaible HG, Ebersberger A, Natura G. 2011. Update on peripheral mechanisms of pain: beyond prostaglandins and cytokines. *Arthritis Res Ther* 13: 210

Schaible HG, Ebersberger A, Von Banchet GS. 2002. Mechanisms of pain in arthritis. *Ann N Y Acad Sci* 966: 343-54

Schaible HG, Grubb BD. 1993. Afferent and spinal mechanisms of joint pain. *Pain* 55: 5-54

Schaible HG, Richter F, Ebersberger A, Boettger MK, Vanegas H, et al. 2009. Joint pain. *Exp Brain Res* 196: 153-62

Scheff SW, Price DA, Schmitt FA, DeKosky ST, Mufson EJ. 2007. Synaptic alterations in CA1 in mild Alzheimer disease and mild cognitive impairment. *Neurology* 68: 1501-8

Scherder E, Bouma A, Slaets J, Ooms M, Ribbe M, et al. 2001. Repeated pain assessment in Alzheimer's disease. *Dement Geriatr Cogn Disord* 12: 400-7

Scherder E, Oosterman J, Swaab D, Herr K, Ooms M, et al. 2005. Recent developments in pain in dementia. *BMJ* 330: 461-4

Scherder EJ. 2000. Low use of analgesics in Alzheimer's disease: possible mechanisms. *Psychiatry* 63: 1-12

Scherder EJ, Bouma A. 2000. Acute versus chronic pain experience in Alzheimer's disease. a new questionnaire. *Dement Geriatr Cogn Disord* 11: 11-6

Scherder EJ, Sergeant JA, Swaab DF. 2003. Pain processing in dementia and its relation to neuropathology. *Lancet Neurol* 2: 677-86

Schmidt ML, Zhukareva V, Perl DP, Sheridan SK, Schuck T, et al. 2001. Spinal cord neurofibrillary pathology in Alzheimer disease and Guam Parkinsonism-dementia complex. *J Neuropathol Exp Neurol* 60: 1075-86

Scholz J, Woolf CJ. 2007. The neuropathic pain triad: neurons, immune cells and glia. *Nat Neurosci* 10: 1361-8

Schweinhardt P, Bushnell MC. 2010. Pain imaging in health and disease--how far have we come? *J Clin Invest* 120: 3788-97

Seal RP, Wang X, Guan Y, Raja SN, Woodbury CJ, et al. 2009. Injury-induced mechanical hypersensitivity requires C-low threshold mechanoreceptors. *Nature* 462: 651-5

Selkoe DJ. 2001. Alzheimer's disease: genes, proteins, and therapy. *Physiol Rev* 81: 741-66

Selkoe DJ, Hardy J. 2016. The amyloid hypothesis of Alzheimer's disease at 25 years. *EMBO Mol Med* 8: 595-608

Seltzer Z, Dubner R, Shir Y. 1990. A novel behavioral model of neuropathic pain disorders produced in rats by partial sciatic nerve injury. *Pain* 43: 205-18

Senechal Y, Kelly PH, Dev KK. 2008. Amyloid precursor protein knockout mice show age-dependent deficits in passive avoidance learning. *Behav Brain Res* 186: 126-32

Seo JS, Leem YH, Lee KW, Kim SW, Lee JK, Han PL. 2010. Severe motor neuron degeneration in the spinal cord of the Tg2576 mouse model of Alzheimer disease. *J Alzheimers Dis* 21: 263-76

Serrano-Pozo A, Frosch MP, Masliah E, Hyman BT. 2011. Neuropathological alterations in Alzheimer disease. *Cold Spring Harb Perspect Med* 1: a006189

Serrano-Pozo A, Muzikansky A, Gomez-Isla T, Growdon JH, Betensky RA, et al. 2013. Differential relationships of reactive astrocytes and microglia to fibrillar amyloid deposits in Alzheimer disease. *J Neuropathol Exp Neurol* 72: 462-71

Shega JW, Hougham GW, Stocking CB, Cox-Hayley D, Sachs GA. 2004. Pain in community-dwelling persons with dementia: frequency, intensity, and congruence between patient and caregiver report. *J Pain Symptom Manage* 28: 585-92

Sheng JG, Mrak RE, Griffin WS. 1994. S100 beta protein expression in Alzheimer disease: potential role in the pathogenesis of neuritic plaques. *Journal of neuroscience research* 39: 398-404

Shukla M, Quirion R, Ma W. 2013. Reduced expression of pain mediators and pain sensitivity in amyloid precursor protein over-expressing CRND8 transgenic mice. *Neuroscience* 250: 92-101

Sidoryk-Wegrzynowicz M, Wegrzynowicz M, Lee E, Bowman AB, Aschner M. 2011. Role of astrocytes in brain function and disease. *Toxicologic pathology* 39: 115-23

Silver J, Miller JH. 2004. Regeneration beyond the glial scar. *Nature Reviews Neuroscience* 5: 146-56

Simic G, Babic Leko M, Wray S, Harrington CR, Delalle I, et al. 2017. Monoaminergic neuropathology in Alzheimer's disease. *Prog Neurobiol* 151: 101-38

Singh SK, Srivastav S, Yadav AK, Srikrishna S, Perry G. 2016. Overview of Alzheimer's Disease and Some Therapeutic Approaches Targeting A beta by Using Several Synthetic and Herbal Compounds. *Oxid Med Cell Longev*

Sivilotti L, Woolf CJ. 1994. The contribution of GABAA and glycine receptors to central sensitization: disinhibition and touch-evoked allodynia in the spinal cord. *J Neurophysiol* 72: 169-79

Smith BH, Torrance N. 2012. Epidemiology of neuropathic pain and its impact on quality of life. *Curr Pain Headache Rep* 16: 191-8

Smith MA, Yancey DL. 2003. Sensitivity to the effects of opioids in rats with free access to exercise wheels: mu-opioid tolerance and physical dependence. *Psychopharmacology (Berl)* 168: 426-34

Smith PA. 2014. BDNF: no gain without pain? *Neuroscience* 283: 107-23

Sofat N, Ejindu V, Kiely P. 2011. What makes osteoarthritis painful? The evidence for local and central pain processing. *Rheumatology (Oxford)* 50: 2157-65

Sofroniew MV. 2005. Reactive astrocytes in neural repair and protection. *Neuroscientist* 11: 400-7

Sofroniew MV, Vinters HV. 2010. Astrocytes: biology and pathology. *Acta Neuropathol* 119: 7-35

Sorge RE, Mapplebeck JC, Rosen S, Beggs S, Taves S, et al. 2015. Different immune cells mediate mechanical pain hypersensitivity in male and female mice. *Nat Neurosci* 18: 1081-3

Sotiropoulos I, Lopes AT, Pinto V, Lopes S, Carlos S, et al. 2014. Selective impact of Tau loss on nociceptive primary afferents and pain sensation. *Exp Neurol* 261: 486-93

Spires-Jones TL, Hyman BT. 2014. The Intersection of Amyloid Beta and Tau at Synapses in Alzheimer's Disease. *Neuron* 82: 756-71

Sprouse-Blum AS, Smith G, Sugai D, Parsa FD. 2010. Understanding endorphins and their importance in pain management. *Hawaii Med J* 69: 70-1

Stagg NJ, Mata HP, Ibrahim MM, Henriksen EJ, Porreca F, et al. 2011. Regular exercise reverses sensory hypersensitivity in a rat neuropathic pain model: role of endogenous opioids. *Anesthesiology* 114: 940-8

Stamelou M, de Silva R, Arias-Carrion O, Boura E, Hollerhage M, et al. 2010. Rational therapeutic approaches to progressive supranuclear palsy. *Brain* 133: 1578-90

Staniland AA, Clark AK, Wodarski R, Sasso O, Maione F, et al. 2010. Reduced inflammatory and neuropathic pain and decreased spinal microglial response in fractalkine receptor (CX3CR1) knockout mice. *J Neurochem* 114: 1143-57

Starr CJ, Sawaki L, Wittenberg GF, Burdette JH, Oshiro Y, et al. 2009. Roles of the insular cortex in the modulation of pain: insights from brain lesions. *J Neurosci* 29: 2684-94

Stein C, Gramsch C, Herz A. 1990. Intrinsic mechanisms of antinociception in inflammation: local opioid receptors and beta-endorphin. *J Neurosci* 10: 1292-8

Stein C, Schafer M, Machelska H. 2003. Attacking pain at its source: new perspectives on opioids. *Nat Med* 9: 1003-8

Streit WJ. 2004. Microglia and Alzheimer's disease pathogenesis. *Journal of neuroscience research* 77: 1-8

Streit WJ, Mrak RE, Griffin WS. 2004. Microglia and neuroinflammation: a pathological perspective. *J Neuroinflammation* 1: 14

Streit WJ, Xue QS, Tischer J, Bechmann I. 2014. Microglial pathology. *Acta Neuropathol Commun* 2: 142

Struble RG, Powers RE, Casanova MF, Kitt CA, Brown EC, Price DL. 1987. Neuropeptidergic systems in plaques of Alzheimer's disease. *J Neuropathol Exp Neurol* 46: 567-84

Sturchler-Pierrat C, Abramowski D, Duke M, Wiederhold KH, Mistl C, et al. 1997. Two amyloid precursor protein transgenic mouse models with Alzheimer disease-like pathology. *Proc Natl Acad Sci U S A* 94: 13287-92

Suokas AK, Walsh DA, McWilliams DF, Condon L, Moreton B, et al. 2012. Quantitative sensory testing in painful osteoarthritis: a systematic review and meta-analysis. *Osteoarthritis Cartilage* 20: 1075-85

Sweitzer SM, Colburn RW, Rutkowski M, DeLeo JA. 1999. Acute peripheral inflammation induces moderate glial activation and spinal IL-1beta expression that correlates with pain behavior in the rat. *Brain Res* 829: 209-21

Takahashi RH, Milner TA, Li F, Nam EE, Edgar MA, et al. 2002. Intraneuronal Alzheimer A beta 42 accumulates in multivesicular bodies and is associated with synaptic pathology. *Am J Pathol* 161: 1869-79

Takeuchi H, Iba M, Inoue H, Higuchi M, Takao K, et al. 2011. P301S mutant human tau transgenic mice manifest early symptoms of human tauopathies with dementia and altered sensorimotor gating. *PLoS One* 6: e21050

Tanga FY, Raghavendra V, DeLeo JA. 2004. Quantitative real-time RT-PCR assessment of spinal microglial and astrocytic activation markers in a rat model of neuropathic pain. *Neurochem Int* 45: 397-407

Tanzi RE, Bertram L. 2001. New frontiers in Alzheimer's disease genetics. *Neuron* 32: 181-4

Tariot PN, Sunderland T, Weingartner H, Murphy DL, Cohen MR, Cohen RM. 1986. Naloxone and Alzheimer's disease. Cognitive and behavioral effects of a range of doses. *Arch Gen Psychiatry* 43: 727-32

Tashima R, Mikuriya S, Tomiyama D, Shiratori-Hayashi M, Yamashita T, et al. 2016. Bone marrow-derived cells in the population of spinal microglia after peripheral nerve injury. *Sci Rep* 6: 23701

Teeple E, Jay GD, Elsaid KA, Fleming BC. 2013. Animal models of osteoarthritis: challenges of model selection and analysis. *AAPS J* 15: 438-46

Teipel SJ, Meindl T, Grinberg L, Grothe M, Cantero JL, et al. 2011. The cholinergic system in mild cognitive impairment and Alzheimer's disease: an in vivo MRI and DTI study. *Hum Brain Mapp* 32: 1349-62

Teng L, Zhao J, Wang F, Ma L, Pei G. 2010. A GPCR/secretase complex regulates beta- and gamma-secretase specificity for Abeta production and contributes to AD pathogenesis. *Cell Res* 20: 138-53

Terry RD, Masliah E, Salmon DP, Butters N, DeTeresa R, et al. 1991. Physical basis of cognitive alterations in Alzheimer's disease: synapse loss is the major correlate of cognitive impairment. *Ann Neurol* 30: 572-80

Thakur M, Rahman W, Hobbs C, Dickenson AH, Bennett DL. 2012. Characterisation of a peripheral neuropathic component of the rat monoiodoacetate model of osteoarthritis. *PLoS One* 7: e33730

Thal DR, Rub U, Orantes M, Braak H. 2002. Phases of A beta-deposition in the human brain and its relevance for the development of AD. *Neurology* 58: 1791-800

Tian G, Kong Q, Lai L, Ray-Chaudhury A, Lin CL. 2010. Increased expression of cholesterol 24S-hydroxylase results in disruption of glial glutamate transporter EAAT2 association with lipid rafts: a potential role in Alzheimer's disease. *J Neurochem* 113: 978-89

Ting JT, Kelley BG, Lambert TJ, Cook DG, Sullivan JM. 2007. Amyloid precursor protein overexpression depresses excitatory transmission through both presynaptic and postsynaptic mechanisms. *Proc Natl Acad Sci U S A* 104: 353-8

Todd AJ. 2002. Anatomy of primary afferents and projection neurones in the rat spinal dorsal horn with particular emphasis on substance P and the neurokinin 1 receptor. *Exp Physiol* 87: 245-9

Todd AJ. 2010. Neuronal circuitry for pain processing in the dorsal horn. *Nat Rev Neurosci* 11: 823-36

Todd AJ. 2017. Identifying functional populations among the interneurons in laminae I-III of the spinal dorsal horn. *Molecular Pain* 13: 1-19

Todd AJ, Hughes DI, Polgar E, Nagy GG, Mackie M, et al. 2003. The expression of vesicular glutamate transporters VGLUT1 and VGLUT2 in neurochemically defined axonal populations in the rat spinal cord with emphasis on the dorsal horn. *Eur J Neurosci* 17: 13-27

Todd AJ, Spike RC, Polgar E. 1998. A quantitative study of neurons which express neurokinin-1 or somatostatin sst2a receptor in rat spinal dorsal horn. *Neuroscience* 85: 459-73

Towheed TE, Maxwell L, Judd MG, Catton M, Hochberg MC, Wells G. 2006. Acetaminophen for osteoarthritis. *Cochrane Database Syst Rev*: CD004257

Treede RD, Kenshalo DR, Gracely RH, Jones AK. 1999. The cortical representation of pain. *Pain* 79: 105-11

Tsuda M, Inoue K, Salter MW. 2005. Neuropathic pain and spinal microglia: a big problem from molecules in "small" glia. *Trends Neurosci* 28: 101-7

Tsuda M, Kohro Y, Yano T, Tsujikawa T, Kitano J, et al. 2011. JAK-STAT3 pathway regulates spinal astrocyte proliferation and neuropathic pain maintenance in rats. *Brain* 134: 1127-39

Tyan SH, Shih AY, Walsh JJ, Maruyama H, Sarsoza F, et al. 2012. Amyloid precursor protein (APP) regulates synaptic structure and function. *Mol Cell Neurosci* 51: 43-52

Ullian EM, Sapperstein SK, Christopherson KS, Barres BA. 2001. Control of synapse number by glia. *Science* 291: 657-61

van Herpen E, Rosso SM, Serverijnen LA, Yoshida H, Breedveld G, et al. 2003. Variable phenotypic expression and extensive tau pathology in two families with the novel tau mutation L315R. *Ann Neurol* 54: 573-81

Vane JR, Botting RM. 1996. Mechanism of action of anti-inflammatory drugs. *Scand J Rheumatol Suppl* 102: 9-21

Vega-Avelaira D, Moss A, Fitzgerald M. 2007. Age-related changes in the spinal cord microglial and astrocytic response profile to nerve injury. *Brain Behav Immun* 21: 617-23

Verkhratsky A, Olabarria M, Noristani HN, Yeh CY, Rodriguez JJ. 2010. Astrocytes in Alzheimer's disease. *Neurotherapeutics : the journal of the American Society for Experimental NeuroTherapeutics* 7: 399-412

Verma V, Sheikh Z, Ahmed AS. 2015. Nociception and role of immune system in pain. *Acta Neurol Belg* 115: 213-20

Viisanen H, Pertovaara A. 2007. Influence of peripheral nerve injury on response properties of locus coeruleus neurons and coeruleospinal antinociception in the rat. *Neuroscience* 146: 1785-94

Villemagne VL, Dore V, Bourgeat P, Burnham SC, Laws S, et al. 2017. Abeta-amyloid and Tau Imaging in Dementia. *Semin Nucl Med* 47: 75-88

Vincent VA, Tilders FJ, Van Dam AM. 1997. Inhibition of endotoxin-induced nitric oxide synthase production in microglial cells by the presence of astroglial cells: a role for transforming growth factor beta. *Glia* 19: 190-8

Vinegar R, Truax JF, Selph JL. 1976. Quantitative studies of the pathway to acute carrageenan inflammation. *Fed Proc* 35: 2447-56

Vonsy JL, Ghandehari J, Dickenson AH. 2009. Differential analgesic effects of morphine and gabapentin on behavioural measures of pain and disability in a model of osteoarthritis pain in rats. *Eur J Pain* 13: 786-93

Wall PD. 1979. On the relation of injury to pain. The John J. Bonica lecture. *Pain* 6: 253-64

Wang Y, Cella M, Mallinson K, Ulrich JD, Young KL, et al. 2015. TREM2 lipid sensing sustains the microglial response in an Alzheimer's disease model. *Cell* 160: 1061-71

Wang Y, Mandelkow E. 2016. Tau in physiology and pathology. *Nat Rev Neurosci* 17: 5-21

Wegiel J, Wang KC, Tarnawski M, Lach B. 2000. Microglia cells are the driving force in fibrillar plaque formation, whereas astrocytes are a leading factor in plague degradation. *Acta Neuropathol* 100: 356-64

Weibel R, Reiss D, Karchewski L, Gardon O, Matifas A, et al. 2013. Mu opioid receptors on primary afferent nav1.8 neurons contribute to opiate-induced analgesia: insight from conditional knockout mice. *PLoS One* 8: e74706

Weinreb O, Amit T, Bar-Am O, Youdim MBH. 2016. Neuroprotective effects of multifaceted hybrid agents targeting MAO, cholinesterase, iron and beta-amyloid in ageing and Alzheimer's disease. *Brit J Pharmacol* 173: 2080-94

Weisshaar CL, Winkelstein BA. 2014. Ablating spinal NK1-bearing neurons eliminates the development of pain and reduces spinal neuronal hyperexcitability and inflammation from mechanical joint injury in the rat. *J Pain* 15: 378-86

Whitehouse PJ, Price DL, Clark AW, Coyle JT, DeLong MR. 1981. Alzheimer disease: evidence for selective loss of cholinergic neurons in the nucleus basalis. *Ann Neurol* 10: 122-6

Wiesenfeld-Hallin Z, Hokfelt T, Lundberg JM, Forssmann WG, Reinecke M, et al. 1984. Immunoreactive calcitonin gene-related peptide and substance P coexist in sensory neurons to the spinal cord and interact in spinal behavioral responses of the rat. *Neurosci Lett* 52: 199-204

Willis Jr WD, Coggeshall RE. 1991. Structure of the Dorsal Horn In *Sensory Mechanisms of the Spinal Cord*, pp. 79-151. New York and London: Plenum Press

Willis WD, Westlund KN. 1997. Neuroanatomy of the pain system and of the pathways that modulate pain. *J Clin Neurophysiol* 14: 2-31

Willnow TE, Petersen CM, Nykjaer A. 2008. VPS10P-domain receptors - regulators of neuronal viability and function. *Nat Rev Neurosci* 9: 899-909

Wirths O, Weis J, Szczygielski J, Multhaup G, Bayer TA. 2006. Axonopathy in an APP/PS1 transgenic mouse model of Alzheimer's disease. *Acta Neuropathol* 111: 312-9

Woolf CJ. 2000. Pain. *Neurobiol Dis* 7: 504-10

Woolf CJ. 2010. What is this thing called pain? *J Clin Invest* 120: 3742-44

Woolf CJ. 2011. Central sensitization: implications for the diagnosis and treatment of pain. *Pain* 152: S2-15

Woolf CJ, Ma Q. 2007. Nociceptors--noxious stimulus detectors. *Neuron* 55: 353-64

Wylde V, Palmer S, Learmonth ID, Dieppe P. 2013. The association between pre-operative pain sensitisation and chronic pain after knee replacement: an exploratory study. *Osteoarthritis Cartilage* 21: 1253-6

Wyss-Coray T. 2006. Inflammation in Alzheimer disease: driving force, bystander or beneficial response? *Nat Med* 12: 1005-15

Wyss-Coray T, Loike JD, Brionne TC, Lu E, Anankov R, et al. 2003. Adult mouse astrocytes degrade amyloid-beta in vitro and in situ. *Nat Med* 9: 453-7

Xu Q, Yaksh TL. 2011. A brief comparison of the pathophysiology of inflammatory versus neuropathic pain. *Curr Opin Anaesthesiol* 24: 400-7

Yaksh TL. 1997. Pharmacology and mechanisms of opioid analgesic activity. *Acta Anaesthesiol Scand* 41: 94-111

Yang L, Wang Z, Wang B, Justice NJ, Zheng H. 2009. Amyloid precursor protein regulates Cav1.2 L-type calcium channel levels and function to influence GABAergic short-term plasticity. *J Neurosci* 29: 15660-8

Ye Z, Wimalawansa SJ, Westlund KN. 1999. Receptor for calcitonin gene-related peptide: localization in the dorsal and ventral spinal cord. *Neuroscience* 92: 1389-97

Yew DT, Li WP, Webb SE, Lai HW, Zhang L. 1999. Neurotransmitters, peptides, and neural cell adhesion molecules in the cortices of normal elderly humans and Alzheimer patients: a comparison. *Exp Gerontol* 34: 117-33

Yoshiyama Y, Higuchi M, Zhang B, Huang SM, Iwata N, et al. 2007. Synapse loss and microglial activation precede tangles in a P301S tauopathy mouse model. *Neuron* 53: 337-51

Yu DG, Liu FX, Liu M, Zhao X, Wang XQ, et al. 2013. The Inhibition of Subchondral Bone Lesions Significantly Reversed the Weight-Bearing Deficit and the Overexpression of CGRP in DRG Neurons, GFAP and Iba-1 in the Spinal Dorsal Horn in the Monosodium Iodoacetate Induced Model of Osteoarthritis Pain. *Plos One* 8

Zarow C, Lyness SA, Mortimer JA, Chui HC. 2003. Neuronal loss is greater in the locus coeruleus than nucleus basalis and substantia nigra in Alzheimer and Parkinson diseases. *Arch Neurol* 60: 337-41

Zarrindast MR, Samadi P, Haeri-Rohani A, Moazami N, Shafizadeh M. 2002. Nicotine potentiation of morphine-induced catalepsy in mice. *Pharmacol Biochem Behav* 72: 197-202

Zhang J, Shi XQ, Echeverry S, Mogil JS, De Koninck Y, Rivest S. 2007. Expression of CCR2 in both resident and bone marrow-derived microglia plays a critical role in neuropathic pain. *Journal of Neuroscience* 27: 12396-406

Zhang LP, Hoff AO, Wimalawansa SJ, Cote GJ, Gagel RF, Westlund KN. 2001. Arthritic calcitonin/alpha calcitonin gene-related peptide knockout mice have reduced nociceptive hypersensitivity. *Pain* 89: 265-73

Zhang RX, Ren K, Dubner R. 2013. Osteoarthritis pain mechanisms: basic studies in animal models. *Osteoarthritis Cartilage* 21: 1308-15

Zhang YW, Thompson R, Zhang H, Xu H. 2011. APP processing in Alzheimer's disease. *Mol Brain* 4: 3

Zhao ZQ, Lacey G, Hendry IA, Morton CR. 2004. Substance P release in the cat spinal cord upon afferent C-fibre stimulation is not attenuated by clonidine at analgesic doses. *Neurosci Lett* 361: 216-9

Zheng H, Jiang M, Trumbauer ME, Sirinathsinghji DJ, Hopkins R, et al. 1995. beta-Amyloid precursor protein-deficient mice show reactive gliosis and decreased locomotor activity. *Cell* 81: 525-31

Zheng H, Koo EH. 2011. Biology and pathophysiology of the amyloid precursor protein. *Mol Neurodegener* 6: 27

Zhou C, Luo ZD. 2014. Electrophysiological characterization of spinal neuron sensitization by elevated calcium channel alpha-2-delta-1 subunit protein. *Eur J Pain* 18: 649-58

Zhuang ZY, Wen YR, Zhang DR, Borsello T, Bonny C, et al. 2006. A peptide c-Jun N-terminal kinase (JNK) inhibitor blocks mechanical allodynia after spinal nerve ligation: respective roles of JNK activation in primary sensory neurons and spinal astrocytes for neuropathic pain development and maintenance. *J Neurosci* 26: 3551-60

Zhuo M. 2017. Ionotropic glutamate receptors contribute to pain transmission and chronic pain. *Neuropharmacology* 112: 228-34

Zuchero JB, Barres BA. 2015. Glia in mammalian development and disease. *Development* 142: 3805-9